

MECH541
KINEMATIC SYNTHESIS
Lecture Notes

Jorge Angeles

Department of Mechanical Engineering &
Centre for Intelligent Machines
McGill University, Montreal (Quebec), Canada

© September 2009

These lecture notes are not as yet in final form.

Please report corrections & suggestions to

Prof. J. Angeles

Department of Mechanical Engineering &

McGill Centre for Intelligent Machines

McGill University

817 Sherbrooke St. W.

Montreal, Quebec

CANADA H3A 2K6

FAX: (514) 398-7348

angeles@cim.mcgill.ca

Contents

1	Introduction to Kinematic Synthesis	5
1.1	The Role of Kinematic Synthesis in Mechanical Design	5
1.2	Glossary	8
1.3	Kinematic Analysis vs. Kinematic Synthesis	11
1.4	Algebraic and Computational Tools	13
1.4.1	The Two-Dimensional Representation of the Cross Product	13
1.4.2	Algebra of 2×2 Matrices	15
1.4.3	Algebra of 3×3 Matrices	16
1.4.4	Linear-Equation Solving: Determined Systems	16
1.4.5	Linear-Equation Solving: Overdetermined Systems	20
1.5	Nonlinear-equation Solving: the Determined Case	27
1.5.1	The Newton-Raphson Method	28
1.6	Overdetermined Nonlinear Systems of Equations	30
1.6.1	The Newton-Gauss Method	31
1.6.2	Convergence Criterion	32
1.7	Computer Implementation Using ODA—C-Library of Routines for Opti- mum Design	33
1.7.1	Computational Tools: Software Packages Relevant to Linkage Syn- thesis	35
2	The Qualitative Synthesis of Kinematic Chains	39
2.1	Notation	39
2.2	Background	40
2.3	Kinematic Pairs	42
2.4	Groups of Displacements	44
2.4.1	Displacement Subgroups	45
2.5	Kinematic Bonds	50
2.6	The Chebyshev-Grübler-Kutzbach-Hervé Formula	53
2.6.1	Trivial Chains	53

2.6.2	Exceptional Chains	55
2.6.3	Paradoxical Chains	59
2.7	Applications to the Qualitative Synthesis of Robotic Architectures	59
2.7.1	The Synthesis of Robotic Architectures	59
3	Function Generation	65
3.1	Introduction	65
3.2	Input-Output Functions	66
3.2.1	Planar Four-Bar Linkages	66
3.2.2	The Denavit-Hartenberg Notation	69
3.2.3	Spherical Four-Bar-Linkages	70
3.2.4	Spatial Four-Bar-Linkages	75
3.3	Exact Synthesis	78
3.3.1	Planar Linkages	78
3.3.2	Spherical Linkages	82
3.3.3	Spatial Linkages	84
3.4	Analysis of the Synthesized Linkage	85
3.4.1	Planar Linkages	85
3.4.2	Spherical Four-Bar Linkages	95
3.4.3	Spatial Four-Bar Linkages	96
3.5	Approximate Synthesis	103
3.6	Linkage Performance Evaluation	113
3.6.1	Planar Linkages: Transmission Angle and Transmission Quality . .	113
3.6.2	Spherical Linkages: Transmission Angle and Transmission Quality .	118
3.6.3	Spatial Linkages: Transmission Angle and Transmission Quality . .	118
3.7	Design Error vs. Structural Error	118
3.7.1	Minimizing the Structural Error	120
3.7.2	Introducing a Massive Number of Data Points	123
3.8	Synthesis Under Mobility Constraints	123
3.8.1	Constrained Least Squares	123
3.8.2	Introducing a Massive Number of Data Points	123
3.9	Synthesis of Complex Linkages	123
3.9.1	Synthesis of Stephenson Linkages	123
4	Motion Generation	125
5	Path Generation	127
5.1	Introduction	127
5.2	Planar Path Generation	128
5.3	Planar Path Generation With Prescribed Timing	130

5.4	Coupler Curves of Planar Four-Bar Linkages	134
5.5	The Theorem of Roberts-Chebyshev	138
A	A Summary of Dual Algebra	139
A.1	Introduction	139
A.2	Definitions	140
A.3	Fundamentals of Rigid-Body Kinematics	144
A.3.1	Finite Displacements	145
A.3.2	Velocity Analysis	153
A.3.3	The Linear Invariants of the Dual Rotation Matrix	155
A.3.4	The Dual Euler-Rodrigues Parameters of a Rigid-Body Motion . . .	160
A.4	The Dual Angular Velocity	165
A.5	Conclusions	171
	Bibliography	173
	Index	181

Chapter 1

Introduction to Kinematic Synthesis

1.1 The Role of Kinematic Synthesis in Mechanical Design

When designing a *mechanical system*, whether a *structure* or a *machine*, the first step is to produce a *conceptual design* that will meet the *design specifications*. Broadly speaking, the main *function* of a structure is *to be capable of withstanding the anticipated loads without exhibiting major deformations that would hamper the integrity of the structure or the safety of its occupants*. Likewise, the main function of a machine is *to be able to perform the intended task, usually involving finite displacements of its parts, without major deformations that would hamper the integrity of the machine or the safety of its users*.

In the above preamble we have introduced concepts of *engineering design* as pertaining to mechanical systems at large. Of these, we have focused on structures and machines. In fact, design, together with *manufacturing*, is the *raison d'être* of engineers, all disciplines known as *engineering science*, namely, mechanics, thermofluids and numerics, to name but just the major branches, playing a supporting role in the production process. For this reason it is necessary to dwell on this concept. Because of its importance, the *engineering design process* has been the subject of study over the centuries, starting with Marcus Vitruvius Polio (ca. 75 BCE–ca. 15 CE) and his 10-volume work under the title *De Architectura* (Vitruvius, 28 B.C.E.). Modern engineering design theory owes its origins, to a great extent, to Franz Reuleaux (1829–1905), who first proposed a *grammar* to describe the kinematic chain of a machine (Moon, 2003). A modern model of the design process, due to French (1992), is depicted in Fig. 1.1. In this model, four stages are distinguished: a) analysis of the problem; b) conceptual design; c) embodiment design; and d) detailing, or detailed design.

In the first stage, analysis of the problem, the *functions* required from the object under design, in our case, a machine, are clearly defined, in general, but precise terms. At this

stage, the task of the design engineer is to produce a) design requirements, in terms as general as possible, in order to avoid biasing the design team towards a specific layout of the solution, and b) *design specifications*, so as to satisfy the rather vaguely spelled-out needs of the *client*.

In the second stage, the design team produces a set of *design variants*, as rich as possible, after several sessions, structured or unstructured, which are part of the *creative* aspect of the design process.

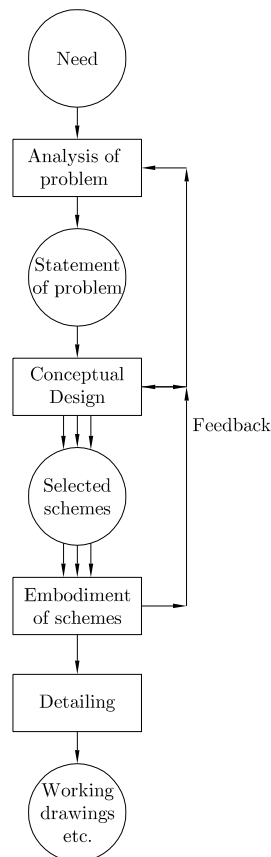


Figure 1.1: French’s model of the design process

In the third stage, the design team focuses on a reduced set of design variants, those having the highest likelihood of succeeding in satisfying the client’s demands within the resources—budget, deadlines, technology—set at the disposal of the design team. In this stage, the task of the team is to produce a preliminary model of the design solution, with a clear identification of the main parameters defining a specific design variant. At this stage, then, a *parametric model* of each of the short-listed candidate variants is produced, which is then subject to optimization with the aim of finding the specific fundamental dimensions that either maximize a profit or minimize a cost of the design solution, or even do both at the same time, in a process that is known as *multiobjective optimization*. Design optimization is thus a key activity in the embodiment stage, which makes this stage *iterative*, as optimization requires several rounds of assignment of numerical values to the

parameters of the mathematical model; evaluating the performance of the design solution thus resulting; improving this performance, when there is still room for improvement; and stopping when no more improvement is possible.

The final stage involves materials selection, manufacturing issues, and production-cost analysis. As a result of this stage, a set of manufacturing drawings is produced that is then sent out for prototype manufacturing, when the design job so requires, or directly to production.

Kinematic synthesis plays a key role in the first three stages of the foregoing design process, as pertaining to machine design. In fact, in the first stage, analysis of the problem, more than kinematic synthesis, what is required is *kinematics knowledge*, as design functions and specifications are to be understood by any engineer trained in the discipline. It is in the second and third stages where kinematic synthesis plays a fundamental role, as explained below.

As pertaining to machine design or, more specifically, to mechanism design, Denavit and Hartenberg (1964) proposed three phases of kinematic synthesis: a) *type synthesis*; b) *number synthesis*; and c) *dimensional synthesis*. Both type and number syntheses pertain to the *conceptual design* phase, as the former refers to choosing the type of mechanism to perform the required function, namely, a linkage, a cam-follower mechanism, a belt-pulley transmission, or a gear train, for example. Number synthesis refers to the numbers of links and joints in a linkage, along with the type of joints to be used—kinematic joints, or lower kinematic pairs, are studied in Ch. 2.

The conceptual phase of the design process is fundamental. Moreover, this phase is the one that has posed the major challenges to those attempting to automate the design process. In the realm of kinematic synthesis, we introduce a methodology, termed *qualitative synthesis*, in Ch. 2, in an attempt to provide a structure to the rather unstructured stage of conceptual mechanism design. Qualitative synthesis focuses on the synthesis of linkages.

Chapters 3–5 are devoted to what Denavit and Hartenberg call dimensional synthesis, as the main objective here is to find the dimensions defining the geometry of the various links and joints of the kinematic chain underlying the mechanism under design. In these chapters, we assume that a *preliminary layout* of the conceptual design—obtained as a result of the type and number syntheses of the kinematic chain at hand—is available, our main job being to contribute to the production of the embodiment of this design. The design embodiment is the realization of a kinematic chain as a table of what is known as the *Denavit-Hartenberg parameters*—to be introduced in Ch. 3—that define uniquely the kinematic chain at hand.

Going back to the more general machine-design process, *dimensioning* involves two phases: functional dimensioning and mechanical dimensioning. The former is previous to the latter, and includes the determination of the *fundamental dimensions* of the machine,

prior to the shaping of all its parts. It is the functional dimensioning where kinematic synthesis plays a major role. Mechanical dimensioning pertains to the dimensioning of the machine elements for stress, strength, heat capacity, and dynamic-response requirements.

Before we embark on the details of the course, a review of the glossary is in order.

1.2 Glossary

Some general definitions are first recalled:

- Kinematics: The branch of mechanics that studies motion, independent of its relation with forces.
- Statics: The branch of mechanics that studies the equilibrium of forces and moments acting on particles, rigid bodies, and flexible bodies.
- Kinematic constraint: The physical prevention of relative motion—rotation and translation—between two bodies in one or more directions. The term also denotes the algebraic or differential relations representing the physical constraint.
- Kinetostatics: The branch of mechanics that studies the interplay of forces and moments with motion variables under static, conservative conditions.

The concepts of *machine* and *mechanism* are frequently interchanged as if they were equivalent, but they are not. We give below some definitions from various sources, with added comments:

Machine

- Here is an account of the definitions of machine, taken from (Dudiță et al., 1987).
Different definitions of machine have been given by scholars for more than two millennia, starting with Vitruvius in 28 BCE, namely,
 - *A machine is a combination (system, assemblage) of moving material bodies* (Vitruvius, 28 B.C.E.; Hachette, 1811; Borgnis, 1818; Beck, 1859; Reuleaux, 1875; Koenigs, 1901).
 - *A machine is generally composed of three parts: a motor part, a transmission part, and an execution part* (Euler, 1753; Bogolyubov, 1976).
 - *A machine produces mechanical work, or performs productive operations, actions, or effects* (Vitruvius, 28 B.C.; Poncelet, 1824; Reuleaux, 1900; Koenigs, 1901; Bogolyubov, 1976).
 - *A machine transforms or transmits forces* (Vitruvius, 28 B.C.; Leupold, 1724; Euler, 1753; Bogolyubov, 1976; Reuleaux, 1900; Koenigs, 1901).

- *A machine is characterized by deterministic motions* (Hachette, 1811; Leupold, 1724; Reuleaux, 1875; Borgnis, 1818; Reuleaux, 1900).
- *A machine is an artifact* (Leupold, 1724).
- Some dictionary definitions:
 - *Webster’s Collegiate Dictionary* (2003, on-line):
 - (archaic): a constructed thing whether material or immaterial;
 - an assemblage of parts that transmit forces, motion, and energy one to another in a predetermined manner;
 - an instrument (as a lever) designed to transmit or modify the application of power, force, or motion;
 - a mechanically, electrically, or electronically operated device for performing a task (a calculating machine, a card-sorting machine.)

Comment: *comprehensive definitions when considered as a whole*
 - *The Concise Oxford Dictionary* (1995):
 - An *apparatus* for applying mechanical power, having several parts, each with a definite function

Comment: *leaves computers out*
 - *The Random House College Dictionary* (1979):
 - An *apparatus* consisting of interrelated parts with separate functions, used in the performance of some kind of work.

Comment: *ditto*
 - Le Petit Robert (Robert, 1994):
 - Any *system* in which a specific correspondence exists between an input form of energy or information and the corresponding ones at the output (loosely translated).

Comment: *a comprehensive definition, that includes computers*
- *An apparatus* for transformation of power, materials, and information to substitute or simplify physical or intellectual work (Frolov, 1987).

Comment: *a comprehensive definition, that includes computers.*
- *Mechanical system* that performs a specific task, such as the forming of material, and the transference and transformation of *motion* and *force* (IFTtoMM PC SoT, 2003).

Comment: *leaves computers out*

Mechanism

- A piece of machinery (Merriam Webster's Collegiate Dictionary, 2003, on-line).
Comment: too vague
- Definitions in (IFTToMM PC SoT, 2003):
 - *System* of bodies designed to convert *motions* of, and *forces* on, one or several bodies into constrained motions of, and *forces* on, other bodies.
Comment: Could be much terser and more informative.
 - *Kinematic chain* with one of its components (*link* or *joint*) connected to the *frame*.
Comment: confuses mechanism with its kinematic chain
- Structure, adaptation of parts of machine; system of mutually adapted parts working together (as) in machine (The Concise Oxford Dictionary, 1995).
- An assembly of moving parts performing a complete functional motion (Stein, 1979).
- A combination layout of pieces or elements, assembled with the goal of (producing) an operation as a unit (Loosely translated from (Robert, 1994).
Comment: In all above definitions, the concept of goal or task is present

Linkage

- Definitions in Merriam Webster's Collegiate Dictionary (2003, on-line):
 - A system of links.
Comment: concise and comprehensive
 - a system of links or bars which are jointed together and more or less constrained by having a link or links fixed and by means of which straight or nearly straight lines or other point paths may be traced.
Comment: unnecessarily cumbersome and limited to path-generating linkages
- *Kinematic chain* whose *joints* are equivalent to *lower pairs* only (IFTToMM PC on SoT, 2003).
Comment: confuses linkage with its kinematic chain.

Rigid Body

A continuum whose points remain equidistant under any possible motion.

Rigid-Body Pose

The position of one landmark point of the body and the orientation of a coordinate frame fixed to the body with respect to a reference frame.

Rigid-Body Twist

The velocity of one landmark point of the body and the angular velocity of the body.

1.3 Kinematic Analysis vs. Kinematic Synthesis

The fundamental problems in mechanism kinematics can be broadly classified into:

- (a) **Analysis:** Given a linkage, find the motion of its links, for a prescribed motion of its input joint(s).
- (b) **Synthesis:** Given a *task* to be produced by a linkage, find the linkage that *best* performs the task.

The task at hand can be one of three, in this context:

- (a) **Function generation:** the motion of the output joint(s) is prescribed as a function of the motion variable(s) of the input joint(s);
- (b) **Motion generation** (a.k.a. rigid-body guidance): the motion of the output link(s) is prescribed in terms of the motion variable(s) of the input link(s) or joint(s);
- (c) **Path generation:** the path traced by a point on a *floating link*—a link not anchored to the mechanism frame—is prescribed as a curve, possibly timed with the motion of the input joint(s).

Kinematic synthesis being a quite broad concept, it involves various aspects (Denavit and Hartenberg, 1964):

- *Type synthesis:* Given a task to be produced by a mechanism, find the type that will best perform it, e.g., a linkage, a cam mechanism, a gear train, or a combination thereof.
- *Number synthesis:* Given a task to be produced by a mechanism of a given type, find the number of links and joints that will best execute the task.
- *Dimensional synthesis:* Given a task to be produced by a mechanism, find its relevant geometric parameters.

We have, further, two types of dimensional synthesis:

1. **Exact synthesis:** Number of linkage parameters available is sufficient to produce *exactly* the prescribed motion. Problem leads to—linear or, most frequently, nonlinear—equation solving .
2. **Approximate synthesis:** Number of linkage parameters available is **not** sufficient to produce exactly the prescribed motion. Optimum dimensions are sought that *approximate* the prescribed motion with the *minimum* error. Problem leads to mathematical programming (optimization)

Furthermore, kinematic synthesis can be achieved, with a variable degree of success, via one of two classes of methods:

- Graphical: Once the problem is formulated as one of dimensional synthesis, the geometric relations of the task at hand are manipulated, by means of drafting instruments alone, including CAD software, to produce the desired linkage parameters as intersections of circles, of lines, or of circles and lines.
- Algebraic: Once the problem is formulated as one of dimensional synthesis, the geometric relations of the task at hand are manipulated, by algebraic means, supported with computer hardware and software, to produce the desired linkage parameters as the solutions to the underlying *synthesis equations*.
- Semigraphical: Purely algebraic methods entail some drawbacks, like *algebraic singularities*, which are conditions under which some solutions cannot be found for reasons other than kinematic. Semigraphical methods reduce the system of algebraic equations to a subsystem of *bivariate equations*, i.e., equations involving only two variables. The bivariate equations defining a set of contours in the plane of those two variables, the solutions to the problem at hand are found as the intersections of all those contours.

The merits of graphical methods as educational tools cannot be overstated. However, as practical means of solving engineering problems, their scope is rather limited. On the one hand, only lines and circles can be traced with standard drafting instruments—paper, pencil, ruler, square, and compass—the tracing of other geometric shapes requiring specialized instruments, for example, templates or CAD software. On the other hand, kinematic synthesis problems, as pertaining to lower-pair linkages, usually lead to *algebraic* systems of equations¹, i.e., to systems of *multivariable polynomial equations*. Each equation is a linear combination of products of integer powers of several unknowns, e.g., $x_1^{p_1} x_2^{p_2} \cdots x_n^{p_n}$. The sum of the exponents of each product, $\sum_1^n p_k$, is known as the degree of the product; the highest product-degree of the i th equation is termed the *degree* d_i of the equation. Using a suitable elimination procedure, it is conceptually possible, although not really possible all the time, to reduce the system of n equations in n unknowns to one single *monovariate polynomial equation*. According to a result due to Bezout (Salmon, 1964), the degree of the resulting monovariate polynomial, the *resolvent* or *eliminant* of the algebraic system at hand, cannot be greater than the product $P = d_1 d_2 \cdots d_n$. The number of possible solutions, thus, can be as high as P . Now, with ruler, square and compass one cannot find but the intersection of circles and lines, and hence, one cannot solve graphically but linear and quadratic equations. While some simple kinematic synthesis

¹The exception here occurs when a linkage involves at least one screw pair, to be introduced in Chapter 2, where *transcendental* equations occur.

problems lead to either linear or quadratic equations, some not so complicated problems can lead to resolvent polynomials of a degree of the order of 10. Some synthesis problems of planar four-bar linkages lead to resolvent polynomials of a degree lying in the billions! (Chen and Angeles, 2008).

Because of the above reasons, we stress in this course semigraphical methods of kinematic synthesis.

1.4 Algebraic and Computational Tools

In deriving the kinematic relations that lead to the various synthesis equations, we shall resort to the two-dimensional representation of the cross product. To do this, we introduce below a 2×2 orthogonal matrix \mathbf{E} that will prove to be extremely useful. An alternative to the use of this matrix for the same purpose is the use of *complex numbers*. The problem with complex numbers is that they are quite useful to represent two-dimensional vectors, their application to three and higher dimensions being still unknown. On the contrary, the two-dimensional representation of the cross product is just a particular case of three-dimensional vector algebra.

We will also need some quick computations with 2×2 matrices, which will be revised in this section. Methods for the numerical solution of linear systems of equations are also included.

1.4.1 The Two-Dimensional Representation of the Cross Product

The cross product occurs frequently in planar kinematics and statics, and hence, in planar *kinetostatics*. However, planar problems involve only two-dimensional vectors and 2×2 matrices, while the cross product is limited to three-dimensional spaces. Here we describe how to represent in two dimensions the cross product, without resorting to three-dimensional vectors. Let: \mathbf{r} be the position vector of a point of a rigid body under planar motion; $\boldsymbol{\omega}$ be the angular-velocity vector of the rigid body and assumed normal to the plane of motion.

Without loss of generality, assume that \mathbf{r} lies entirely in the plane of motion, which is normal to $\boldsymbol{\omega}$. Below we compute $\boldsymbol{\omega} \times \mathbf{r}$ using only two-dimensional vectors.

Let \mathbf{E} be an *orthogonal matrix* that rotates vectors in the plane through an angle of 90° counterclockwise (ccw):

$$\mathbf{E} \equiv \begin{bmatrix} 0 & -1 \\ 1 & 0 \end{bmatrix} \quad (1.1a)$$

Note that

$$\mathbf{E}^T \mathbf{E} = \mathbf{E} \mathbf{E}^T = \mathbf{1}, \quad \mathbf{1} = \begin{bmatrix} 1 & 0 \\ 0 & 1 \end{bmatrix} \quad (1.1b)$$

with $\mathbf{1}$ denoting the 2×2 *identity matrix*. Also note that \mathbf{E} is *skew-symmetric*:

$$\mathbf{E} = -\mathbf{E}^T \quad \Rightarrow \quad \mathbf{E}^2 = -\mathbf{1}, \quad \mathbf{E}^{-1} = -\mathbf{E} \quad (1.1c)$$

Therefore, \mathbf{E} rotates vectors \mathbf{r} in the plane through an angle of 90° ccw, as depicted in Fig. 1.2, i.e.,

$$\mathbf{r} = \begin{bmatrix} x \\ y \end{bmatrix} \quad \Rightarrow \quad \mathbf{E}\mathbf{r} = \begin{bmatrix} -y \\ x \end{bmatrix} \quad (1.1d)$$

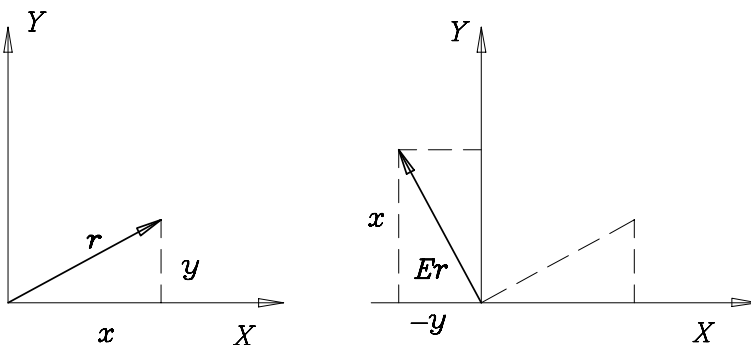


Figure 1.2: Vector \mathbf{r} and its image under \mathbf{E}

Now, for the purpose at hand, we start with the usual three-dimensional vectors \mathbf{r} and $\boldsymbol{\omega}$ and assume an *orthonormal basis* for the three-dimensional space, $\{\mathbf{i}, \mathbf{j}, \mathbf{k}\}$, with \mathbf{k} defined normal to the plane of motion and pointing toward the viewer. Thus,

$$\boldsymbol{\omega} = \omega\mathbf{k} = \begin{bmatrix} 0 \\ 0 \\ \omega \end{bmatrix}, \quad \mathbf{r} = \begin{bmatrix} x \\ y \\ 0 \end{bmatrix} \quad (1.2)$$

where $\omega > 0$ if the angular velocity is ccw; if cw, then $\omega < 0$. Therefore,

$$\boldsymbol{\omega} \times \mathbf{r} = \det \begin{bmatrix} \mathbf{i} & \mathbf{j} & \mathbf{k} \\ 0 & 0 & \omega \\ x & y & 0 \end{bmatrix} = -\omega y\mathbf{i} + \omega x\mathbf{j}$$

Then, the two-dimensional form of the foregoing product is

$$[\boldsymbol{\omega} \times \mathbf{r}]_{2D} = \omega \begin{bmatrix} -y \\ x \end{bmatrix} \equiv \omega\mathbf{E}\mathbf{r} \quad (1.3)$$

As a second use of matrix \mathbf{E} , we derive the two-dimensional form of the cross product $\mathbf{r} \times \mathbf{f}$ yielding the moment of force \mathbf{f} about the origin. We assume that \mathbf{r} and \mathbf{f} both lie in a plane normal to the unit vector \mathbf{k} .

First, we start with the usual three-dimensional representation of vectors \mathbf{r} and \mathbf{f} , and hence,

$$\mathbf{r} \times \mathbf{f} = \det \begin{bmatrix} \mathbf{i} & \mathbf{j} & \mathbf{k} \\ x & y & 0 \\ f_x & f_y & 0 \end{bmatrix} = (xf_y - yf_x)\mathbf{k}$$

Now, let

$$xf_y - yf_x \equiv n \quad (1.4)$$

which can be readily recognized as the dot product of the two-dimensional vectors \mathbf{Er} and \mathbf{f} , i.e.,

$$n = \mathbf{f}^T \mathbf{Er} \equiv (\mathbf{Er})^T \mathbf{f} = -\mathbf{r}^T \mathbf{Ef} \quad (1.5)$$

If $n > 0$, then the moment is ccw; otherwise, cw. We have thus shown that the cross product of two two-dimensional vectors reduces to a scalar, i.e., n .

Matrix \mathbf{E} also appears in the representation of the rotation of a rigid body in planar motion through an angle θ . This rotation is represented algebraically by means of a *proper orthogonal matrix* \mathbf{Q} . This matrix is proper orthogonal because it is orthogonal and its determinant is +1. Matrix \mathbf{Q} is given by

$$\mathbf{Q} = \begin{bmatrix} \cos \theta & -\sin \theta \\ \sin \theta & \cos \theta \end{bmatrix} \equiv (\cos \theta)\mathbf{1} + (\sin \theta)\mathbf{E} \quad (1.6)$$

Thus, if a vector \mathbf{r}_0 is “fixed” to a rigid body rotating about the origin through an angle θ , after the rotation, \mathbf{r}_0 becomes \mathbf{r} , which is given by

$$\mathbf{r} = \mathbf{Q}\mathbf{r}_0 = (\cos \theta)\mathbf{r}_0 + (\sin \theta)\mathbf{E}\mathbf{r}_0 \quad (1.7)$$

1.4.2 Algebra of 2×2 Matrices

A 2×2 matrix \mathbf{A} can be partitioned either columnwise or rowwise:

$$\mathbf{A} \equiv [\mathbf{a} \quad \mathbf{b}] \equiv \begin{bmatrix} \mathbf{c}^T \\ \mathbf{d}^T \end{bmatrix}$$

where \mathbf{a} , \mathbf{b} , \mathbf{c} , and \mathbf{d} are all two-dimensional column vectors. We have

Fact 1.4.1

$$\det(\mathbf{A}) = -\mathbf{a}^T \mathbf{Eb} = \mathbf{b}^T \mathbf{Ea} = -\mathbf{c}^T \mathbf{Ed} = \mathbf{d}^T \mathbf{Ec}$$

and

Fact 1.4.2

$$\mathbf{A}^{-1} = \frac{1}{\det(\mathbf{A})} \begin{bmatrix} \mathbf{b}^T \\ -\mathbf{a}^T \end{bmatrix} \mathbf{E} = \frac{1}{\det(\mathbf{A})} \mathbf{E} [-\mathbf{d} \quad \mathbf{c}]$$

Componentwise, if a_{ij} denotes the i th entry of the j th column of \mathbf{A} ,

$$\mathbf{A}^{-1} = \frac{1}{\det(\mathbf{A})} \begin{bmatrix} a_{22} & -a_{21} \\ -a_{12} & a_{11} \end{bmatrix} \quad (1.8)$$

That is, the inverse of a 2×2 nonsingular matrix is obtained upon:

- (a) exchanging the diagonal entries of the given matrix;
- (b) reversing the sign of its off-diagonal entries; and
- (c) dividing the matrix thus resulting by the determinant of the given matrix.

1.4.3 Algebra of 3×3 Matrices

A 3×3 matrix \mathbf{A} can be partitioned columnwise into three columns, each having as entries the components of a three-dimensional vector, namely,

$$\mathbf{A} = [\mathbf{a}_1 \quad \mathbf{a}_2 \quad \mathbf{a}_3]$$

its determinant being readily computed as the *mixed* vector-scalar product of its column vectors:

$$\det(\mathbf{A}) = \mathbf{a}_1 \times \mathbf{a}_2 \cdot \mathbf{a}_3$$

The inverse of \mathbf{A} can also be readily computed symbolically if we resort to the concept of *reciprocal bases*:

$$\mathbf{A}^{-1} = \frac{1}{\Delta} \begin{bmatrix} (\mathbf{a}_2 \times \mathbf{a}_3)^T \\ (\mathbf{a}_3 \times \mathbf{a}_1)^T \\ (\mathbf{a}_1 \times \mathbf{a}_2)^T \end{bmatrix} \quad (1.9a)$$

where

$$\Delta \equiv \mathbf{a}_1 \times \mathbf{a}_2 \cdot \mathbf{a}_3 \quad (1.9b)$$

The reader can verify the validity of the foregoing formula by straightforward computation of the product $\mathbf{A}\mathbf{A}^{-1}$ or, equivalently, of $\mathbf{A}^{-1}\mathbf{A}$, which should yield the 3×3 identity matrix.

1.4.4 Linear-Equation Solving: Determined Systems

Consider solving for \mathbf{x} the system below:

$$\mathbf{A}\mathbf{x} = \mathbf{b} \quad (1.10)$$

where \mathbf{A} is a $n \times n$ matrix of *known* coefficients; \mathbf{b} is the n -dimensional right-hand side *known* vector; and \mathbf{x} is the n -dimensional vector of *unknowns*.

Definition: \mathbf{A} is said to be *singular* if

$$\det(\mathbf{A}) = 0 \quad (1.11)$$

Otherwise, \mathbf{A} is *nonsingular*

Fact 1.4.3 *If \mathbf{A} is nonsingular, then eq.(1.10) has a unique solution, namely,*

$$\mathbf{x} = \mathbf{A}^{-1}\mathbf{b} \quad (1.12)$$

Caveat: Never compute—unless instructed to do so!— \mathbf{A}^{-1} explicitly. A matrix inverse is seldom needed and incurs a waste of precious CPU time! Instead, find a *good* numerical approximation to the solution, while taking into account that \mathbf{A} and \mathbf{b} are usually known only up to a certain roundoff error.

In computing the solution of system (1.10) for \mathbf{x} , we must take into account the unavoidable roundoff error of the data, \mathbf{A} and \mathbf{b} . Let:

- $\delta\mathbf{A}$ be the matrix roundoff error in \mathbf{A}
- $\delta\mathbf{b}$ be the vector roundoff-error in \mathbf{b}
- $\delta\mathbf{x}$ be the vector roundoff-error incurred when solving eq.(1.10) for \mathbf{x} , by virtue of $\delta\mathbf{A}$ and $\delta\mathbf{b}$

The *relative* roundoff errors in the data, $\epsilon_{\mathbf{A}}$ and $\epsilon_{\mathbf{b}}$, and in the computed solution, $\epsilon_{\mathbf{x}}$, are defined as

$$\epsilon_{\mathbf{x}} \equiv \frac{\|\delta\mathbf{x}\|}{\|\mathbf{x}\|}, \quad \epsilon_{\mathbf{A}} \equiv \frac{\|\delta\mathbf{A}\|}{\|\mathbf{A}\|}, \quad \epsilon_{\mathbf{b}} \equiv \frac{\|\delta\mathbf{b}\|}{\|\mathbf{b}\|} \quad (1.13)$$

where $\|\cdot\|$ denotes *any* vector or matrix norm².

The relative roundoff error in the computed solution is known to be related to the relative roundoff error in the data via the relation (Golub and Van Loan, 1983)

$$\epsilon_{\mathbf{x}} \leq \kappa(\mathbf{A})(\epsilon_{\mathbf{A}} + \epsilon_{\mathbf{b}}) \quad (1.14)$$

where $\kappa(\mathbf{A})$ is the *condition number* of matrix \mathbf{A} of eq.(1.10):

$$\kappa(\mathbf{A}) \equiv \|\mathbf{A}\|\|\mathbf{A}^{-1}\| \quad (1.15)$$

Various matrix norms are at our disposal, such as the *Euclidean norm*, a.k.a. the *2-norm*, the *Frobenius norm* and the *infinity norm*, a.k.a. the *Chebyshev norm*, denoted, respectively, by $\|\mathbf{A}\|_2$, $\|\mathbf{A}\|_F$ and $\|\mathbf{A}\|_{\infty}$. The definitions of these norms are given below:

$$\|\mathbf{A}\|_2 \equiv \max_i \{ |\lambda_i| \}_1^n \quad (1.16a)$$

$$\|\mathbf{A}\|_F \equiv \sqrt{\text{tr}(\mathbf{A}\mathbf{W}\mathbf{A}^T)} \quad (1.16b)$$

$$\|\mathbf{A}\|_{\infty} \equiv \max_i \sum_{j=1}^n |a_{ij}| \quad (1.16c)$$

where $\{ \lambda_i \}_1^n$ denotes the set of eigenvalues of \mathbf{A} , and \mathbf{W} is a *weighting* positive-definite matrix, that is defined according to the user's needs. For example, if $\mathbf{W} = (1/n)\mathbf{1}$, with $\mathbf{1}$ defined as the $n \times n$ identity matrix, then the Frobenius norm of the identity matrix is unity, regardless of the value of n , which is convenient. Not only this; with the foregoing value of \mathbf{W} , $\|\mathbf{A}\|_F$ is the rms value of the *singular values*³ of \mathbf{A} . Moreover, $\text{tr}(\cdot)$ denotes the *trace* of its $n \times n$ matrix argument (\cdot) , i.e., the sum of the diagonal entries of the matrix. Also notice that the eigenvalues of \mathbf{A} can be real or complex, and hence, $|\cdot|$ denotes the *module* of its complex argument (\cdot) . Computing the eigenvalues of arbitrary matrices is

²The matrix norm is a generalization of the vector norm, the latter being, in turn, a generalization of the module of complex numbers or the absolute value of real numbers.

³The singular values of a $m \times n$ matrix \mathbf{A} , with $m \leq n$ are the (nonnegative) eigenvalues of the product $\mathbf{A}\mathbf{A}^T$

cumbersome because of the complex nature of the eigenvalues, in general. Computing the eigenvalues of symmetric matrices, on the contrary, is much simpler, because these are known to be real. In fact, the set $\{|\lambda_i|\}_1^n$ is most conveniently computed as the square roots of the eigenvalues of $\mathbf{A}\mathbf{A}^T$, which is not only symmetric, but also positive-definite, and hence, its eigenvalues $\{\mu_i\}_1^n$ are all positive. In fact, if \mathbf{A} is singular, then $\mathbf{A}\mathbf{A}^T$ is only positive-semidefinite, meaning that some of its eigenvalues vanish, but none is negative. We thus have

$$|\lambda_i| = \sqrt{\mu_i}, \quad \mu_i \geq 0, \quad i = 1, \dots, n \quad (1.17)$$

Whenever we have chosen one specific norm to define the condition number, we indicate the condition number as κ_2 , κ_F or κ_∞ . In particular,

$$\kappa_2 = \frac{\sqrt{\mu_l}}{\sqrt{\mu_s}} \equiv \frac{|\lambda_l|}{|\lambda_s|} \quad (1.18)$$

where μ_s and μ_l denote the smallest and the largest eigenvalues of $\mathbf{A}\mathbf{A}^T$, while λ_l and λ_s denote the eigenvalues of \mathbf{A} with the largest and the smallest modules, respectively. In fact, $\{\sqrt{\mu_i}\}_1^n$ is known as the set of *singular values* of matrix \mathbf{A} . Moreover,

$$\kappa_F = \sqrt{\frac{1}{n}\text{tr}(\mathbf{A}\mathbf{A}^T)} \sqrt{\frac{1}{n}\text{tr}(\mathbf{A}^{-1}\mathbf{A}^{-T})} \quad (1.19)$$

where \mathbf{A}^{-T} denotes the inverse of the transpose of \mathbf{A} or, equivalently, the transpose of the inverse of the same matrix.

It is now apparent that κ , regardless of the matrix norm used to compute it, is bounded from below but unbounded from above:

$$1 \leq \kappa < \infty \quad (1.20)$$

Remark 1.4.1 *The condition number of a singular matrix is infinitely large.*

Remark 1.4.2 *If a matrix $\mathbf{A}\mathbf{A}^T$ has all its eigenvalues identical, then \mathbf{A} is said to be isotropic. Isotropic matrices have a $\kappa = 1$, regardless of the matrix norm used to compute κ . They are optimally conditioned.*

Methods for computing a good numerical approximation to *the* solution (1.12):

- Gaussian elimination, a.k.a. LU-decomposition: Based on the observation that a *triangular system* is readily solved by either *backward* or *forward substitution*. \mathbf{A} is decomposed into a *lower-* and an *upper-triangular* factors, \mathbf{L} and \mathbf{U} , respectively.
- Iteratively: Various types of methods, by the names Gauss-Jordan, Gauss-Seidel, successive-overrelaxation (SOR), etc. Used mainly for “large” systems (hundreds or thousands of unknowns) that we will not be handling

- Symbolically: Only possible for certain classes of \mathbf{A} matrices, like tridiagonal, and for arbitrary matrices of modest size (n is below 5 or so)

We focus here on Gaussian elimination, or LU-decomposition. We start by *decomposing* the $n \times n$ matrix \mathbf{A} in the form

$$\mathbf{A} = \mathbf{L}\mathbf{U} \quad (1.21)$$

where \mathbf{L} and \mathbf{U} take the forms

$$\mathbf{L} = \begin{bmatrix} 1 & 0 & \cdots & 0 \\ l_{21} & 1 & \cdots & 0 \\ \vdots & \vdots & \ddots & \vdots \\ l_{n1} & l_{n2} & \cdots & 1 \end{bmatrix}, \quad \mathbf{U} = \begin{bmatrix} u_{11} & u_{12} & \cdots & u_{1n} \\ 0 & u_{22} & \cdots & u_{2n} \\ \vdots & \vdots & \ddots & \vdots \\ 0 & 0 & \cdots & u_{nn} \end{bmatrix} \quad (1.22)$$

Now eq.(1.10) is rewritten as

$$\mathbf{L}\mathbf{U}\mathbf{x} = \mathbf{b} \Rightarrow \begin{cases} \mathbf{L}\mathbf{y} = \mathbf{b} \\ \mathbf{U}\mathbf{x} = \mathbf{y} \end{cases} \quad (1.23)$$

and hence, \mathbf{x} is computed in two stages: First, \mathbf{y} is computed from a lower-triangular system; then, \mathbf{x} is computed from an upper-triangular system. The lower-triangular system is solved for \mathbf{y} by *forward substitution*; the upper-triangular system is solved for \mathbf{x} by *backward substitution*.

Note that

$$\det(\mathbf{A}) = \det(\mathbf{L})\det(\mathbf{U}) \quad (1.24a)$$

But, apparently,

$$\det(\mathbf{L}) = 1, \quad \det(\mathbf{U}) = \prod_1^n u_{ii} \quad (1.24b)$$

Hence,

$$\det(\mathbf{A}) = \det(\mathbf{U}) = \prod_1^n u_{ii} \quad (1.24c)$$

Therefore, \mathbf{A} is singular iff any of the diagonal entries of \mathbf{U} vanishes.

The Case of a Positive-Definite Matrix

If \mathbf{A} is *symmetric and positive-definite*, then it admits the **Cholesky decomposition**:

$$\mathbf{A} = \mathbf{C}^T\mathbf{C} \quad (1.25a)$$

where \mathbf{C} is a *real, lower-triangular* matrix, namely,

$$\mathbf{C} = \begin{bmatrix} c_{11} & 0 & \cdots & 0 \\ c_{21} & c_{22} & \cdots & 0 \\ \vdots & \vdots & \ddots & \vdots \\ c_{n1} & c_{n2} & \cdots & c_{nn} \end{bmatrix} \quad (1.25b)$$

The solution of system (1.10) proceeds as in the general case, in two steps:

$$\mathbf{C}^T\mathbf{y} = \mathbf{b} \quad (1.26)$$

$$\mathbf{C}\mathbf{x} = \mathbf{y} \quad (1.27)$$

1.4.5 Linear-Equation Solving: Overdetermined Systems

We are now confronted with solving a system of linear equations formally identical to that given in eq.(1.10). The difference now is that matrix \mathbf{A} is no longer square, but rectangular, with n columns of dimension m , namely,

$$\mathbf{Ax} = \mathbf{b}, \quad \mathbf{A} : m \times n, \quad m > n \quad (1.28)$$

where \mathbf{b} is, obviously, m -dimensional. Now, given that we have a surplus of equations over the number of unknowns, it is not possible, in general, to find a vector \mathbf{x} that will verify all m equations, and hence, an error will be incurred, the purpose here being to find the vector \mathbf{x} that renders the error of minimum norm. That is, we cannot *actually solve* system (1.28); all we can do is find an acceptable approximation \mathbf{x} to the system. The *error vector* \mathbf{e} in this approximation is defined as

$$\mathbf{e} \equiv \mathbf{Ax} - \mathbf{b} \quad (1.29)$$

Again, we have various norms at our disposal that we can choose to minimize. All norms of \mathbf{e} can be expressed as

$$\|\mathbf{e}\|_p \equiv \left(\sum_1^m |e_k|^p \right)^{1/p} \quad (1.30)$$

with e_k being understood as the k th component of the m -dimensional vector \mathbf{e} . When $p = 2$, the foregoing norm is known as the *Euclidean norm*, which is used most frequently in mechanics. When $p \rightarrow \infty$, the *infinity norm*, also known as the *Chebyshev norm*, is obtained. This norm is, in fact, nothing but the largest absolute value of the components of the vector at hand; finding this norm, thus, incurs no computational cost. It turns out that upon seeking the value of \mathbf{x} that minimizes a norm of \mathbf{e} , the simplest is the Euclidean norm, for the minimization of its square leads to a linear system of equations whose solution can be obtained *directly*, as opposed to *iteratively*. Indeed, let us set up the minimization problem below:

$$z(\mathbf{x}) \equiv \frac{1}{2} \|\mathbf{e}\|_2^2 \quad \rightarrow \quad \min_{\mathbf{x}} \quad (1.31)$$

The *normality condition* of the minimization problem at hand is derived upon setting the *gradient* of z with respect to \mathbf{x} equal to zero, i.e.,

$$\frac{dz}{d\mathbf{x}} = \mathbf{0} \quad (1.32)$$

Now, the chain rule allows us to write

$$\frac{dz}{d\mathbf{x}} \equiv \left(\frac{d\mathbf{e}}{d\mathbf{x}} \right)^T \frac{dz}{d\mathbf{e}} \equiv \mathbf{A}^T \mathbf{e} \quad (1.33)$$

whence, the error vector of minimum Euclidean norm, or *least-square error* for brevity, represented henceforth by \mathbf{e}_0 , satisfies the normality condition

$$\mathbf{A}^T \mathbf{e}_0 = \mathbf{0}_n \quad (1.34)$$

with $\mathbf{0}_n$ denoting the n -dimensional zero vector. Now we have the first result:

Theorem 1.4.1 *The least-square error \mathbf{e}_0 of the overdetermined system of linear equations (1.10) lies in the null space of the transpose of the full-rank $m \times n$ matrix \mathbf{A} , with $m > n$.*

In order to gain insight into the above result, let $\{\mathbf{a}_i\}_1^n$ represent the n m -dimensional columns of matrix \mathbf{A} . Hence, \mathbf{A}^T can be expressed as a column array of vectors \mathbf{a}_i^T , for $i = 1, \dots, n$, eq.(1.34) thus leading to

$$\mathbf{a}_i^T \mathbf{e}_0 = 0 \quad (1.35)$$

Furthermore, if eq.(1.29) is substituted into eq.(1.33), and the product thus resulting is substituted, in turn, into the normality condition (1.32), we obtain

$$\mathbf{A}^T \mathbf{A} \mathbf{x} = \mathbf{A}^T \mathbf{b} \quad (1.36)$$

which is known as the *normal equations* of the minimization problem at hand. By virtue of the assumption on the rank of \mathbf{A} , the product $\mathbf{A}^T \mathbf{A}$ is *positive-definite* and hence, invertible. As a consequence, the value \mathbf{x}_0 of \mathbf{x} that minimizes the Euclidean norm of the approximation error of the given system is

$$\mathbf{x}_0 = (\mathbf{A}^T \mathbf{A})^{-1} \mathbf{A}^T \mathbf{b} \quad (1.37)$$

the matrix coefficient of \mathbf{b} being known as a *generalized inverse* of \mathbf{A} ; we shall refer to this generalized inverse here as \mathbf{A}^I , i.e.,

$$\mathbf{A}^I \equiv (\mathbf{A}^T \mathbf{A})^{-1} \mathbf{A}^T \quad (1.38)$$

More specifically, \mathbf{A}^I is known as the *left Moore-Penrose generalized inverse* of \mathbf{A} , because, when \mathbf{A} is multiplied by \mathbf{A}^I from the left, the product becomes

$$\mathbf{A}^I \mathbf{A} = \mathbf{1}_n \quad (1.39)$$

in which $\mathbf{1}_n$ denotes the $n \times n$ identity matrix. The error obtained with this value is known as the *least-square error* of the approximation, i.e.,

$$\mathbf{e}_0 \equiv \mathbf{b} - \mathbf{A} \mathbf{x}_0 \quad (1.40)$$

Now we have one more result:

Theorem 1.4.2 (Projection Theorem) *The least-square error is orthogonal to \mathbf{Ax}_0 , i.e.,*

$$\mathbf{e}_0^T \mathbf{Ax}_0 \equiv \mathbf{x}_0^T \mathbf{A}^T \mathbf{e}_0 = 0 \quad (1.41)$$

Proof: Readily follows from Theorem 1.4.1.

The Projection Theorem is illustrated in Fig. 1.3.

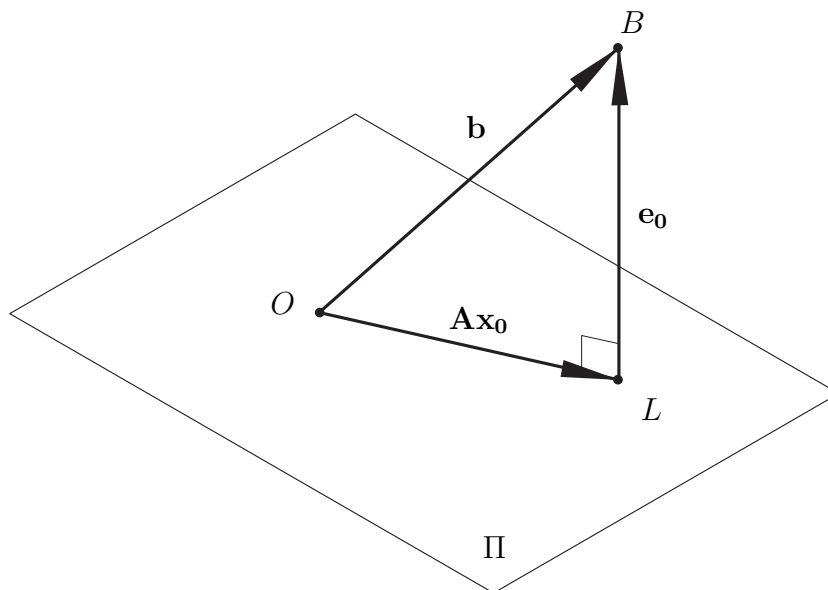


Figure 1.3: The Projection Theorem

While the formula yielding the foregoing generalized inverse is quite simple to implement, the number of floating-point operations (flops) it takes to evaluate, along with the ever-present roundoff errors in both the data and the results, renders it not only *inefficient*, but also *unreliable*, if applied verbatim. What is at stake here is the concept of condition number, introduced in Subsection 1.4.4 for square matrices. The same concept can be applied to rectangular matrices, if the matrix inverse is replaced by its left Moore-Penrose generalized inverse. In fact, the singular values of rectangular \mathbf{A} are the non-negative square roots of the non-negative eigenvalues of the $n \times n$ positive-semidefinite matrix $\mathbf{A}^T \mathbf{A}$, exactly as in the case of square matrices. If \mathbf{A} is of full rank, i.e., if its n m -dimensional columns are linearly independent, then $\mathbf{A}^T \mathbf{A}$ is positive-definite. However, note that \mathbf{AA}^T is singular, regardless of whether \mathbf{A} is of full rank or not. The foregoing statement is a result of Sylvester's Theorem (Strang, 1988):

Theorem 1.4.3 (Sylvester's Theorem) *Let $p \times q$ \mathbf{A} and $q \times r$ \mathbf{B} be two arbitrary matrices, which are thus compatible under multiplication. Then,*

$$\text{rank}(\mathbf{AB}) \leq \min\{\text{rank}(\mathbf{A}), \text{rank}(\mathbf{B})\} \quad (1.42)$$

Therefore, if \mathbf{A} is of full rank, then $\text{rank}(\mathbf{A}) = n$, and hence, $\text{rank}(\mathbf{A}\mathbf{A}^T) \leq n < m$, which means that the product $\mathbf{A}\mathbf{A}^T$ is rank-deficient, i.e., singular in this case.

Remark 1.4.3 *If the working condition number is either κ_2 or κ_F , then the condition number of $\mathbf{A}^T\mathbf{A}$ is exactly the square of the condition number of \mathbf{A} .*

As a consequence, then, even if \mathbf{A} is only slightly ill-conditioned, the product $\mathbf{A}^T\mathbf{A}$ can be catastrophically ill-conditioned, the moral being that the normal equations (1.36) are much more sensitive to data roundoff error than the original equations (1.28). Therefore, **the normal equations should be avoided**. Below we outline two procedures to calculate efficiently the least-square approximation of the overdetermined system (1.10) that do not resort to the normal equations, and hence, preserve the condition number of \mathbf{A} and do this with a low number of flops.

In figuring out a numerical method suitable to finding the *least-square approximation* of the overdetermined system of linear equations (1.28) it is convenient to resort to the geometric interpretation of the problem at hand: Let us assume that \mathbf{A} is of full rank, and hence, its n m -dimensional columns $\{\mathbf{a}_i\}_1^n$, introduced in eq.(1.35), are linearly independent. However, notice that this set cannot constitute a basis of the m -dimensional space of these vectors, or of vector \mathbf{b} for that matter, because of a deficit of $m - n$ vectors in the set. Hence, there is no guarantee that, given an arbitrary m -dimensional vector \mathbf{b} , we can find n real numbers $\{x_k\}_1^n$ that will produce \mathbf{b} as a linear combination of the given set of vectors—the columns of \mathbf{A} . Now, let us regard \mathbf{b} as the position vector of a point B in m -dimensional space, with \mathbf{l} denoting the vector spanned by the linear combination

$$\mathbf{l} \equiv \mathbf{a}_1x_1 + \mathbf{a}_2x_2 + \cdots + \mathbf{a}_nx_n \quad (1.43)$$

We can also regard \mathbf{l} as the position vector of a point L in the same space, the purpose of the numerical method sought being to find the set $\{x_i\}_1^n$ that yields a vector \mathbf{l} corresponding to a point L lying a minimum distance from B . If vector \mathbf{a}_i were represented in a basis in which only its first i components were nonzero, then the task at hand would be straightforward: it would be obvious then that we would be able to match the first n components of \mathbf{b} with a suitable choice of numbers $\{x_i\}_1^n$ —these numbers could be found by backward substitution! However the last $m - n$ components of \mathbf{b} would remain unmatched, and hence, would contain the error in the approximation.

Now, in general, the columns of \mathbf{A} most likely will be full. Nevertheless, it is always possible to find a suitable coordinate system, i.e., a suitable basis, under which the columns of \mathbf{A} will have the special structure described above.

In seeking the new coordinate system, we aim at a transformation of both all columns of \mathbf{A} and \mathbf{b} that will render \mathbf{A} in upper-triangular form, similar to the effect of the LU-decomposition applied to the solution of system (1.10). However, in seeking the suitable transformation in the case at hand, we should preserve the distances between

points in m -dimensional space; else, the Euclidean norm will not be preserved and the approximation obtained will not yield the minimum distance between points B and L . A safe numerical procedure should thus preserve the Euclidean norm of the columns of \mathbf{A} and, hence, the inner product between any two columns of this matrix. Therefore, a triangularization procedure like LU-decomposition would not work, because this does not preserve inner products. Obviously, the transformations that do preserve these inner products are orthogonal, either rotations or reflections. Examples of these methods are (a) the Gram-Schmidt orthogonalization procedure and (b) *Householder reflections*, which are outlined below⁴.

The Gram-Schmidt Orthogonalization Procedure

This procedure consists in regarding the columns of \mathbf{A} as a set of n m -dimensional vectors $\{\mathbf{a}_k\}_1^n$. From this set, a new set $\{\mathbf{e}_k\}_1^n$ is obtained that is *orthonormal*. The procedure is quite simple and works as follows: Define \mathbf{e}_1 as

$$\mathbf{e}_1 = \frac{\mathbf{a}_1}{\|\mathbf{a}_1\|} \quad (1.44)$$

Further, we define \mathbf{e}_2 as the *normal component* of \mathbf{a}_2 onto \mathbf{e}_1 , namely,

$$\mathbf{b}_2 \equiv (\mathbf{1} - \mathbf{e}_1\mathbf{e}_1^T)\mathbf{a}_2 \quad (1.45a)$$

$$\mathbf{e}_2 \equiv \frac{\mathbf{b}_2}{\|\mathbf{b}_2\|} \quad (1.45b)$$

In the next step, we define \mathbf{e}_3 as the unit vector normal to the plane defined by \mathbf{e}_1 and \mathbf{e}_2 and in the direction in which the inner product $\mathbf{e}_3^T\mathbf{a}_3$ is positive, which is possible because all vectors of the set $\{\mathbf{a}_k\}_1^m$ have been assumed to be linearly independent—remember that \mathbf{A} has been assumed to be of full rank. To this end, we subtract from \mathbf{a}_3 its projection onto the plane mentioned above, i.e.,

$$\mathbf{b}_3 = (\mathbf{1} - \mathbf{e}_1\mathbf{e}_1^T - \mathbf{e}_2\mathbf{e}_2^T)\mathbf{a}_3 \quad (1.46a)$$

$$\mathbf{e}_3 \equiv \frac{\mathbf{b}_3}{\|\mathbf{b}_3\|} \quad (1.46b)$$

and so on, until we obtain \mathbf{e}_{n-1} , the last unit vector of the orthogonal set, \mathbf{e}_n , being obtained as

$$\mathbf{b}_n = (\mathbf{1} - \mathbf{e}_1\mathbf{e}_1^T - \mathbf{e}_2\mathbf{e}_2^T - \cdots - \mathbf{e}_{n-1}\mathbf{e}_{n-1}^T)\mathbf{a}_n \quad (1.47a)$$

Finally,

$$\mathbf{e}_n \equiv \frac{\mathbf{b}_n}{\|\mathbf{b}_n\|} \quad (1.47b)$$

⁴These methods are implemented in Maple, a language for computer algebra, under the command `LeastSquares(A, B, ...)`.

In the next stage, we represent all vectors of the set $\{\mathbf{a}_k\}_1^n$ in *orthogonal coordinates*, i.e., in the base $\mathcal{O} = \{\mathbf{e}_k\}_1^n$, which are then arranged in an $m \times n$ array \mathbf{A}_o . By virtue of the form in which the set $\{\mathbf{e}_k\}_1^n$ was defined, the last $m - k$ components of vector \mathbf{a}_k vanish. We thus have, in the said orthonormal basis,

$$[\mathbf{a}_k]_{\mathcal{O}} = \begin{bmatrix} \alpha_{1k} \\ \alpha_{2k} \\ \vdots \\ \alpha_{kk} \\ 0 \\ \vdots \\ 0 \end{bmatrix}, \quad [\mathbf{b}]_{\mathcal{O}} = \begin{bmatrix} \beta_1 \\ \beta_2 \\ \vdots \\ \beta_m \end{bmatrix}$$

Therefore, eq.(1.28), when expressed in \mathcal{O} , becomes

$$\begin{bmatrix} \alpha_{11} & \alpha_{12} & \cdots & \alpha_{1n} \\ 0 & \alpha_{22} & \cdots & \alpha_{2n} \\ \vdots & \vdots & \ddots & \vdots \\ 0 & 0 & \cdots & \alpha_{nn} \\ 0 & 0 & \cdots & 0 \\ \vdots & \vdots & \ddots & \vdots \\ 0 & 0 & \cdots & 0 \end{bmatrix} \begin{bmatrix} x_1 \\ x_2 \\ \vdots \\ x_n \end{bmatrix} = \begin{bmatrix} \beta_1 \\ \beta_2 \\ \vdots \\ \beta_n \\ \beta_{n+1} \\ \vdots \\ \beta_m \end{bmatrix} \quad (1.48)$$

whence \mathbf{x} can be computed by back-substitution. It is apparent, then, that the last $m - n$ equations of the foregoing system are incompatible: their left-hand sides are zero, while their right-hand sides are not necessarily so. What the right-hand sides of these equations represent, then, is the approximation error in orthogonal coordinates. Its Euclidean norm is, then,

$$\|\mathbf{e}_0\| \equiv \sqrt{\beta_{n+1}^2 + \cdots + \beta_m^2} \quad (1.49)$$

Householder Reflections

The second method discussed here is based on the application of a chain of n transformations $\{\mathbf{H}_k\}_1^n$, known as *Householder reflections*, to both sides of eq.(1.10). The purpose of these reflections is, again, to obtain a representation of matrix \mathbf{A} in upper-triangular form (Golub and Van Loan, 1989). The algorithm proceeds as follows: We assume that we have applied reflections $\mathbf{H}_1, \mathbf{H}_2, \dots, \mathbf{H}_{k-1}$, in this order, to \mathbf{A} that have rendered it in *upper-trapezoidal form*, i.e.,

$$\mathbf{A}_{i-1} \equiv \mathbf{H}_{i-1} \dots \mathbf{H}_2 \mathbf{H}_1 \mathbf{A}$$

$$= \begin{bmatrix} a_{11}^* & a_{12}^* & \cdots & a_{1,i-1}^* & a_{1i}^* & \cdots & a_{1n}^* \\ 0 & a_{22}^* & \cdots & a_{2,i-1}^* & a_{2i}^* & \cdots & a_{2n}^* \\ 0 & 0 & \cdots & a_{3,i-1}^* & a_{3i}^* & \cdots & a_{3n}^* \\ \vdots & \vdots & \ddots & \vdots & \vdots & \ddots & \vdots \\ 0 & 0 & \cdots & a_{i-1,i-1}^* & a_{i-1,i}^* & \cdots & a_{i-1,n}^* \\ 0 & 0 & \cdots & 0 & a_{i,i}^* & \cdots & a_{i,n}^* \\ \vdots & \vdots & \ddots & \vdots & \vdots & \ddots & \vdots \\ 0 & 0 & \cdots & 0 & a_{m,i}^* & \cdots & a_{mn}^* \end{bmatrix} \quad (1.50)$$

The next Householder reflection, \mathbf{H}_i , is determined so as to render the last $m - i$ components of the i th column of $\mathbf{H}_i \mathbf{A}_{i-1}$ equal to zero, while leaving its first $i - 1$ columns unchanged. We do this by setting

$$\alpha_i = \text{sgn}(a_{ii}^*) \sqrt{(a_{ii}^*)^2 + (a_{i+1,i}^*)^2 + \cdots + (a_{mi}^*)^2} \quad (1.51a)$$

$$\mathbf{u}_i = [0 \quad 0 \quad \cdots \quad 0 \quad a_{ii}^* + \alpha_i \quad a_{i+1,i}^* \quad \cdots \quad a_{mi}^*]^T \quad (1.51b)$$

$$\mathbf{H}_i = \mathbf{1} - \frac{\mathbf{u}_i \mathbf{u}_i^T}{\|\mathbf{u}_i\|^2/2} \quad (1.51c)$$

where $\text{sgn}(x)$, the *signum function* of x , is defined as $+1$ if $x > 0$, as -1 if $x < 0$, and is left undefined when $x = 0$. As the reader can readily verify,

$$\frac{1}{2} \|\mathbf{u}_i\|^2 = \alpha_i (\mathbf{u}_i)_i = \alpha_i (a_{ii}^* + \alpha_i) \equiv \gamma_i \quad (1.52)$$

and hence, the denominator appearing in the expression for \mathbf{H}_i is calculated with one single addition and a single multiplication. Notice that \mathbf{H}_i reflects vectors in m -dimensional space onto a hyperplane of unit normal $\mathbf{u}_i/\|\mathbf{u}_i\|$.

It is important to realize that

- (a) α_i is defined with the sign of a_{ii}^* because the denominator γ_i appearing in eq.(1.52) is proportional to the sum of a_{ii}^* and α_i , thereby guaranteeing that the absolute value of this sum will always be greater than the absolute value of each of its terms. If this provision were not made, then the resulting sum could be of a negligibly small absolute value, which would thus render γ_i a small positive number. Such a small number would thus introduce unnecessarily an inadmissibly large roundoff-error amplification upon dividing the product $\mathbf{u}_i \mathbf{u}_i^T$ by γ_i ;
- (b) an arbitrary vector \mathbf{v} is transformed by \mathbf{H}_i with unusually few flops, namely,

$$\mathbf{H}_i \mathbf{v} = \mathbf{v} - \frac{1}{\gamma_i} (\mathbf{v}^T \mathbf{u}_i) \mathbf{u}_i$$

Upon application of the n Householder reflections thus defined, the system at hand becomes

$$\mathbf{H} \mathbf{A} \mathbf{x} = \mathbf{H} \mathbf{b} \quad (1.53)$$

with \mathbf{H} defined as

$$\mathbf{H} \equiv \mathbf{H}_n \dots \mathbf{H}_2 \mathbf{H}_1 \quad (1.54)$$

Similar to that in equation (1.48), the matrix coefficient of \mathbf{x} in eq.(1.53), i.e., \mathbf{HA} , is in upper-triangular form. That is, we have

$$\mathbf{HA} = \begin{bmatrix} \mathbf{U} \\ \mathbf{O}_{m'n} \end{bmatrix}, \quad \mathbf{Hb} = \begin{bmatrix} \mathbf{b}_U \\ \mathbf{b}_L \end{bmatrix} \quad (1.55)$$

with \mathbf{U} a $n \times n$ upper-triangular matrix identical to that appearing in eq.(1.22), $\mathbf{O}_{m'n}$ denoting the $(m - n) \times n$ zero matrix, $m' \equiv m - n$, and \mathbf{b}_U and \mathbf{b}_L being n - and m' -dimensional vectors. The unknown \mathbf{x} can thus be calculated from eq.(1.53) by back-substitution.

Note that the last m' components of the left-hand side of eq.(1.53) are zero, while the corresponding components of the right-hand side of the same equation are not necessarily so. This apparent contradiction can be resolved by recalling that the overdetermined system at hand, in general, has no solution. The lower part of \mathbf{b} , \mathbf{b}_L , is then nothing but an m' -dimensional array containing the nonzero components of the approximation error in the new coordinates. That is, the least-square error, \mathbf{e}_0 , in these coordinates takes the form

$$\mathbf{e}_0 = \begin{bmatrix} \mathbf{0}_n \\ \mathbf{b}_L \end{bmatrix} \quad (1.56a)$$

Therefore,

$$\|\mathbf{e}_0\| = \|\mathbf{b}_L\| \quad (1.56b)$$

1.5 Nonlinear-equation Solving: the Determined Case

Definition 1.5.1 A system of algebraic equations containing some that are not linear is termed *nonlinear*. If the number of equations is identical to the number of unknowns, the system is *determined*.

Example: Find the intersection of the circle and the hyperbola depicted in Fig. 1.4.

Solution: The equations of the circle and the hyperbola are

$$\begin{aligned} \phi_1(x, y) &\equiv x^2 + y^2 - 4 = 0 \\ \phi_2(x, y) &\equiv x^2 - y^2 - 1 = 0 \end{aligned}$$

The solution to a nonlinear system of equations, when one exists at all, is usually *multiple*: The circle and the hyperbola of Fig. 1.4 intersect at four points $\{P_i\}_1^4$, of coordinates (x_i, y_i) , as displayed in Table 1.1. The problem may have **no real solution**, e.g., the circle and the hyperbola of Fig. 1.5 do not intersect. The system of equations from which

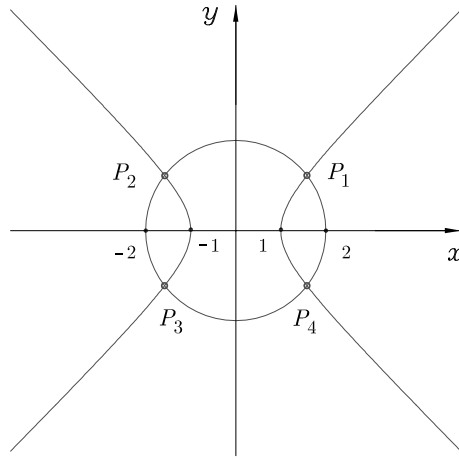


Figure 1.4: Intersection of a circle and a hyperbola

P_i	x_i	y_i
1	$\sqrt{5/2}$	$\sqrt{3/2}$
2	$\sqrt{5/2}$	$-\sqrt{3/2}$
3	$-\sqrt{5/2}$	$\sqrt{3/2}$
4	$-\sqrt{5/2}$	$-\sqrt{3/2}$

Table 1.1: The four intersection points of the circle and the hyperbola of Fig. 1.4

the coordinates of the intersection points are to be computed is given below:

$$\begin{aligned}\phi_1(x, y) &\equiv x^2 + y^2 - 1 = 0 \\ \phi_2(x, y) &\equiv x^2 - y^2 - 16 = 0\end{aligned}$$

This system of equations admits no real solution!

In general, a determined nonlinear system of equations takes the form

$$\boldsymbol{\phi}(\mathbf{x}) = \mathbf{0} \tag{1.57}$$

where \mathbf{x} and $\boldsymbol{\phi}$ are both n -dimensional vectors:

$$\mathbf{x} \equiv \begin{bmatrix} x_1 \\ x_2 \\ \vdots \\ x_n \end{bmatrix}, \quad \boldsymbol{\phi} \equiv \begin{bmatrix} \phi_1(x_1, x_2, \dots, x_n) \\ \phi_2(x_1, x_2, \dots, x_n) \\ \vdots \\ \phi_n(x_1, x_2, \dots, x_n) \end{bmatrix} \tag{1.58}$$

1.5.1 The Newton-Raphson Method

We outline below the method of solution of determined nonlinear systems using the Newton-Raphson method. This is an *iterative method*, whereby a sequence of approx-

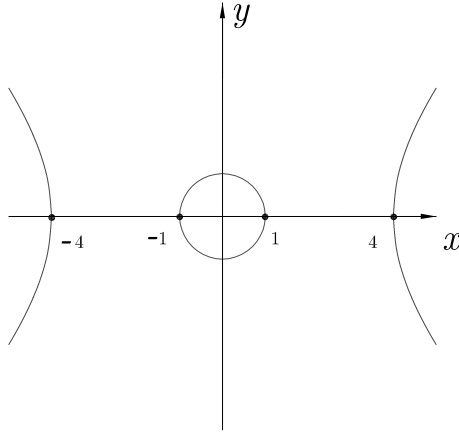


Figure 1.5: A circle and a hyperbola that do not intersect

imations is obtained that, if converging, it approaches the solution in a finite number of iterations within a prescribed *tolerance*.

A value \mathbf{x}^0 of \mathbf{x} is given as an *initial guess*:

$$\mathbf{x}^0 \equiv [p_1 \quad p_2 \quad \dots \quad p_n]^T$$

and ϕ is evaluated at \mathbf{x}^0 :

$$\phi^0 \equiv \phi(\mathbf{x}^0)$$

If the value \mathbf{x}^0 was chosen randomly, most likely it will not verify the given system of equations, i.e.,

$$\phi^0 \neq \mathbf{0}$$

Next, we look for a “small” increment $\Delta\mathbf{x}$ of \mathbf{x} (the increment is small if its norm—any norm—is small):

$$\Delta\mathbf{x} \equiv [\Delta x_1 \quad \Delta x_2 \quad \dots \quad \Delta x_n]^T$$

Now, $\phi(\mathbf{x}^0 + \Delta\mathbf{x})$ is evaluated up to its linear approximation (all quadratic and higher-order terms are dropped from its series expansion):

$$\phi(\mathbf{x}^0 + \Delta\mathbf{x}) \approx \phi(\mathbf{x}^0) + \left. \frac{\partial\phi}{\partial\mathbf{x}} \right|_{\mathbf{x}=\mathbf{x}^0} \Delta\mathbf{x} \quad (1.59)$$

The *Jacobian matrix* of ϕ with respect to \mathbf{x} is defined as the matrix of partial derivatives of the components of ϕ with respect to all the components of \mathbf{x} :

$$\Phi \equiv \frac{\partial\phi}{\partial\mathbf{x}} = \begin{bmatrix} \partial\phi_1/\partial x_1 & \partial\phi_1/\partial x_2 & \dots & \partial\phi_1/\partial x_n \\ \partial\phi_2/\partial x_1 & \partial\phi_2/\partial x_2 & \dots & \partial\phi_2/\partial x_n \\ \vdots & \vdots & \ddots & \vdots \\ \partial\phi_n/\partial x_1 & \partial\phi_n/\partial x_2 & \dots & \partial\phi_n/\partial x_n \end{bmatrix} \quad (1.60)$$

In the next step, we find $\Delta\mathbf{x}$ that renders zero the linear approximation of $\phi(\mathbf{x}_0 + \Delta\mathbf{x})$:

$$\phi_0 + \Phi(\mathbf{x}^0)\Delta\mathbf{x} = \mathbf{0}$$

or

$$\Phi(\mathbf{x}^0)\Delta\mathbf{x} = -\phi^0 \quad (1.61)$$

whence $\Delta\mathbf{x}$ can be found using Gaussian elimination:

$$\Delta\mathbf{x} = -\Phi_0^{-1}\phi^0, \quad \Phi_0 \equiv \Phi(\mathbf{x}^0) \quad (1.62)$$

Next, \mathbf{x} is updated:

$$\mathbf{x} \leftarrow \mathbf{x}^0 + \Delta\mathbf{x} \quad (1.63)$$

the procedure stopping when

$$\|\Delta\mathbf{x}\| \leq \epsilon_x \quad (1.64)$$

for a prescribed tolerance ϵ_x .

Remarks:

- Use the maximum norm to test convergence in eq.(1.64), for it costs virtually nothing;
- no guarantee that the Newton-Raphson method will converge at all;
- whether the Newton-Raphson method converges is dependent upon the initial guess, \mathbf{x}^0 ;
- the boundary between regions of convergence and divergence is a *fractal* (Mandelbrot, 1983; Gleick, 1988);
- when the Newton-Raphson method converges, it does so *quadratically*: At every iteration, *two* decimal places of accuracy are gained (Dahlquist and Björck, 1974).

1.6 Overdetermined Nonlinear Systems of Equations

A system of nonlinear equations of the form

$$\phi(\mathbf{x}) = \mathbf{0} \quad (1.65)$$

where \mathbf{x} is a n -dimensional vector and ϕ is a q -dimensional vector, is *overdetermined* if $q > n$. Just as in the linear case, in general, no vector \mathbf{x} can be found that verifies *all* the q scalar equations of the system. However, approximations can be found that minimize the least-square error of the approximation, as described in the balance of this Section. The method of solution adopted here is the overdetermined counterpart of the Newton-Raphson method.

1.6.1 The Newton-Gauss Method

Problem: Find an *approximate solution* to system (1.65) that verifies those equations with the *least-square error*:

$$f(\mathbf{x}) = \frac{1}{2} \boldsymbol{\phi}^T \mathbf{W} \boldsymbol{\phi} \quad \rightarrow \quad \min_{\mathbf{x}} \quad (1.66)$$

where \mathbf{W} is a $q \times q$ positive-definite *weighting matrix*.

Solution: We follow a procedure similar to Newton-Raphson's, which is known as the *Newton-Gauss method*, as described below:

First, an initial guess \mathbf{x}^0 of \mathbf{x} is given; then, we produce the sequence

$$\mathbf{x}^1, \mathbf{x}^2, \dots, \quad (1.67)$$

such that

$$\mathbf{x}^{k+1} = \mathbf{x}^k + \Delta \mathbf{x}^k \quad (1.68)$$

Calculation of $\Delta \mathbf{x}^k$:

- Factor \mathbf{W} into its two Cholesky factors:

$$\mathbf{W} = \mathbf{V}^T \mathbf{V} \quad (1.69)$$

which is possible because \mathbf{W} is assumed positive-definite.

- Compute $\Delta \mathbf{x}^k$ as the *least-square solution* of the unconstrained overdetermined linear system

$$\mathbf{V} \boldsymbol{\Phi}(\mathbf{x}^k) \Delta \mathbf{x}^k = -\mathbf{V} \boldsymbol{\phi}(\Delta \mathbf{x}^k) \quad (1.70)$$

with $\boldsymbol{\Phi}(\mathbf{x})$ defined as the $q \times n$ Jacobian matrix of the vector function $\boldsymbol{\phi}(\mathbf{x})$, i.e.,

$$\boldsymbol{\Phi}(\mathbf{x}) = \frac{\partial \boldsymbol{\phi}(\mathbf{x})}{\partial \mathbf{x}} \quad (1.71)$$

Drop superscripts for the sake of notation-simplicity and recall eq.(1.37):

$$\Delta \mathbf{x} = -(\boldsymbol{\Phi}^T \mathbf{W} \boldsymbol{\Phi})^{-1} \boldsymbol{\Phi}^T \mathbf{W} \boldsymbol{\phi} \quad (1.72)$$

This procedure is iterative, stopping when a *convergence criterion is met*.

The Damping Factor

When implementing the Newton-Gauss method, the objective function f may increase upon correcting \mathbf{x}^k according to eq.(1.68), i.e.

$$f(\mathbf{x}^{k+1}) > f(\mathbf{x}^k) \quad (1.73)$$

This increase gives rise to oscillations and sometimes even leads to divergence. One way to cope with this situation is by introducing *damping*. Instead of using the whole increment $\Delta \mathbf{x}^k$, we use a fraction of it, i.e.

$$\mathbf{x}^{k+1} = \mathbf{x}^k + \alpha \Delta \mathbf{x}^k, \quad 0 < \alpha < 1 \quad (1.74)$$

where α is known as the *damping factor*.

1.6.2 Convergence Criterion

Calculate first $\nabla f(\mathbf{x})$:

$$\nabla f(\mathbf{x}) \equiv \frac{\partial f}{\partial \mathbf{x}} = \left(\frac{\partial \phi}{\partial \mathbf{x}} \right)^T \frac{\partial f}{\partial \phi} \quad (1.75)$$

$$\frac{\partial \phi}{\partial \mathbf{x}} \equiv \Phi, \quad \frac{\partial f}{\partial \phi} = \mathbf{W}\phi \quad (1.76)$$

Hence, the condition for a stationary point is

$$\Phi^T \mathbf{W}\phi = \mathbf{0} \quad (1.77)$$

which is the *normality condition* of eq.(1.66).

It is thus apparent that, at a stationary point of f , $\phi(\mathbf{x})$ **need not vanish**, as is the case of unconstrained optimization; however, $\phi(\mathbf{x})$ **must lie in the null space of $\Phi^T \mathbf{W}$** . Moreover, from eqs.(1.72) and (1.77) follows that, at a stationary point, $\Delta \mathbf{x}$ vanishes. Hence, the convergence criterion is

$$\|\Delta \mathbf{x}\| < \epsilon \quad (1.78)$$

where ϵ is a prescribed tolerance.

Remarks:

- The normality condition (1.77) alone does not guarantee a minimum, but only a *stationary point*.
- However, as it turns out, if the procedure converges, then it does so, to a second-order approximation, to a minimum, and neither to a maximum nor a saddle point, as we prove below.

The sequence $f(\mathbf{x}^0), f(\mathbf{x}^1), \dots, f(\mathbf{x}^k), f(\mathbf{x}^{k+1}), \dots$, obtained from the sequence of \mathbf{x} values, evolves, to a first order, as $\Delta f(\mathbf{x})$, given by

$$\Delta f = \left(\frac{\partial f}{\partial \mathbf{x}} \right)^T \Delta \mathbf{x} \quad (1.79)$$

i.e.,

$$\Delta f = \phi^T \mathbf{W}\Phi \Delta \mathbf{x} \quad (1.80)$$

Upon plugging expression (1.72) of $\Delta \mathbf{x}$ into eq. (1.80), we obtain

$$\Delta f = -\phi^T \underbrace{\mathbf{W}\Phi(\Phi^T \mathbf{W}\Phi)^{-1}\Phi^T \mathbf{W}}_{\mathbf{M}} \phi = -\phi^T \mathbf{M}\phi \quad (1.81)$$

where, apparently, \mathbf{M} is a $q \times q$ positive-definite matrix. As a consequence, $\phi^T \mathbf{M}\phi$ becomes a positive-definite quadratic expression of ϕ ; hence, Δf is negative definite. Thus, the

second-order approximation of $f(\mathbf{x})$ is negative-definite, and hence, the sequence of f values *decreases monotonically*. That is, in the neighbourhood of a stationary point the first-order approximation of $\phi(\mathbf{x})$ is good enough, and hence, if the procedure **converges**, it does so to a **minimum**.

The reader may wonder whether the Newton-Raphson method can be used to solve nonlinear least-square problems. Although the answer is *yes*, the Newton-Raphson method is not advisable in this case, as made apparent below.

Recall ∇f from eqs.(1.66) and (1.67):

$$\begin{aligned} \nabla f(\mathbf{x}) &= \frac{\partial f}{\partial \mathbf{x}} = \underbrace{\Phi^T(\mathbf{x})}_{n \times q} \underbrace{\mathbf{W}}_{q \times q} \underbrace{\phi(\mathbf{x})}_{q\text{-dim}} \\ \nabla f(\mathbf{x}) = \mathbf{0} &\Rightarrow \underbrace{\Phi^T(\mathbf{x})\mathbf{W}\phi(\mathbf{x})}_{\equiv \psi(\mathbf{x}) \in \mathbb{R}^n} = \mathbf{0} \end{aligned} \quad \text{(NC)}$$

thereby obtaining a determined system of n equations in n unknowns. This system can be solved using Newton-Raphson method, which requires $\nabla\psi(\mathbf{x})$:

$$\nabla\psi(\mathbf{x}) = \frac{\partial\psi}{\partial \mathbf{x}} = \frac{\partial}{\partial \mathbf{x}} \left[\underbrace{\Phi^T(\mathbf{x})}_{(\partial\phi/\partial\mathbf{x})^T} \mathbf{W}\phi(\mathbf{x}) \right]$$

That is, $\nabla\psi(\mathbf{x})$ involves second-order derivatives of ψ with respect to \mathbf{x} :

$$\frac{\partial^2\phi_i}{\partial x_j \partial x_i}, \quad i = 1, \dots, n$$

In summary, the Newton-Raphson method is too cumbersome and prone to ill-conditioning, for it is based on the normality conditions of the least-square problem at hand.

1.7 Computer Implementation Using ODA—C-Library of Routines for Optimum Design

ODA is a C library of subroutines for optimization problems, that implements the *Orthogonal-Decomposition Algorithm* (Teng and Angeles, 2001). The source file of this package, implemented in C, consists of a number of subroutines designed and classified based on their application. At the beginning of each subroutine a detailed description of the purpose and usage of the subroutine is included. Moreover, data validation has been considered in the software. In order to solve a problem, the user simply calls one corresponding C subroutine.

Since the solutions for linear problems are *direct*—as opposed to *iterative*—the use of ODA to solve linear problems requires only information on the problem parameters, such as matrices \mathbf{A} , \mathbf{C} , and \mathbf{W} , as well as vectors \mathbf{b} and \mathbf{d} , as applicable. For nonlinear

problems, the solution is iterative, and hence, the user is required to provide functions describing $\phi(\mathbf{x})$, $\mathbf{h}(\mathbf{x})$, $\Phi(\mathbf{x})$, $\mathbf{J}(\mathbf{x})$, as needed. These functions are provided via subroutines in forms that can be called by the package. In addition to this information, the user is also required to provide an initial guess \mathbf{x}_0 of \mathbf{x} , so that the iterative procedure can be started.

1. **Unconstrained linear problems:** Subroutine `MNSLS` is used to find the minimum-norm solution of an underdetermined linear system, while subroutine `LSSLS` is used to find the least-square approximation of an overdetermined linear system. `LSSLS` can also handle determined systems, i.e., systems of as many equations as unknowns.
2. **Unconstrained nonlinear problems:** Subroutine `LSSNLS` is used to solve this type of problems. Since the nonlinear functions and their associated gradient matrices are problem-dependent, the user is required to provide two subroutines that are used to evaluate the foregoing items, namely,
 - `FUNPHI`: This subroutine is used to evaluate the q -dimensional vector function $\phi(\mathbf{x})$ in terms of the given n -dimensional vector \mathbf{x} .
 - `DPHIDX`: This subroutine is used to evaluate the $q \times n$ gradient matrix Φ of the vector-function $\phi(\mathbf{x})$ with respect to \mathbf{x} , at the current value of \mathbf{x} .
 Moreover, an initial guess of \mathbf{x} is required when calling this subroutine.
3. **Constrained linear problems:** Subroutine `LSSCLS` is used to solve this type of problems.
4. **Constrained nonlinear problems:** Subroutine `LSSCNL` is used for solving this type of problems. Before calling `LSSCNL`, the user is required to provide four problem-dependent subroutines: Two of these are `FUNPHI` and `DPHIDX`, already described in item 2 above. The other two are used to evaluate the left-hand sides of the constraint equations and their gradient matrix, as listed below:
 - `FUNH`: This subroutine is used to evaluate the l -dimensional constraint function \mathbf{h} in terms of the given n -dimensional vector \mathbf{x} .
 - `DHDX`: This subroutine is used to evaluate the $l \times n$ gradient matrix \mathbf{J} of the vector-function $\mathbf{h}(\mathbf{x})$ in terms of the given n -dimensional vector \mathbf{x} . Moreover, an initial guess of \mathbf{x} is required when calling `LSSCNL`.
5. **Constrained problems with arbitrary objective function:** Subroutine `ARBITRARY` is used for solving this type of problems. Before calling `ARBITRARY`, the user is required to provide four problem-dependent subroutines: Two of these are `FUNPHI` and `DPHIDX`, as described in item 2 above. The other two subroutines are used to

evaluate the left-hand sides of the constraint equations and their gradient matrix, as listed below:

- **phi**: Subroutine used to evaluate the objective function $\phi(\mathbf{x})$ in terms of the given n -dimensional vector \mathbf{x} .
- **h**: Subroutine used to evaluate the l -dimensional constraint function \mathbf{h} in terms of the given n -dimensional vector \mathbf{x} .
- **J**: Subroutine used to evaluate the $l \times n$ gradient matrix \mathbf{J} of the vector-function $\mathbf{h}(\mathbf{x})$ at the current value of \mathbf{x} .
- **gradient**: Subroutine used to evaluate the n -dimensional gradient ∇f of the objective function $f(\mathbf{x})$ at the current value of vector \mathbf{x} .
- **Hessian**: Subroutine used to evaluate the $n \times n$ Hessian matrix $\nabla \nabla f$ of the objective function $f(\mathbf{x})$ at the current value of vector \mathbf{x} . Moreover, an initial guess of \mathbf{x} is required when calling **ARBITRARY**.

1.7.1 Computational Tools: Software Packages Relevant to Linkage Synthesis

Several software packages of interest to kinematic synthesis are currently available, either commercially or semi-commercially. A list, with some features, follows:

- **LINCAGES**: Commercially available from *MINNT* (Minnesota Technology Transfer, a spinoff of the U. of Minnesota.) Handles only exact synthesis of planar four and six-bar linkages. Runs on Windows.
- **SAM**: More general than LINCAGES, SAM provides static analysis. Runs only on Windows and is commercially available from *Artas Engineering Software*, of RJ Neuen, The Netherlands:

www.artas.nl

- **WORKING MODEL**: Commercially available from *MSC.Software* (USA). Mostly for kinematic and dynamic analyses of two-dimensional and three-dimensional mechanisms. Runs only on Windows.
- **PRO/ENGINEER**: Comprehensive package for mechanical design and analysis at large. Its **PRO/MECHANICA** module provides motion analysis, simulation, and animation of fairly complex mechanisms. Runs on Windows and Unix. Vendor: *Parametric Technology, Inc.* (USA):

<http://www.ptc.com/>

- UNIGRAPHICS: High-end, comprehensive package with modules for finite-element analysis, CAD/CAM, and CAE (Computer-Aided Engineering). Vendor: *Siemens PLM Software*

<http://www.plm/automation.siemens.com>

- CATIA: The most widespread CAE package, in CAD, CAE, CAM. Vendor: *Dassault Systèmes*

<http://www.3ds.com/contact/>

- ADAMS, a general tool for mechanism and multibody-system analysis, produced by *MSC.ADAMS Software*. No synthesis features are supported.
- AUTOCAD: Comprehensive package for mechanical design and geometric analysis. To be used as a CAD support for linkage synthesis. No special features for linkage synthesis available. Runs mostly on Windows. Old versions run also on Unix. Vendor: *Autodesk, Inc.* with

www.autodesk.com

- MATLAB: General-purpose numerical analysis package with excellent routines for equation-solving and optimization. To be used as a support for linkage synthesis. A few Matlab routines are specifically geared to linkage analysis. Package is produced by *The MathWorks* with

www.mathworks.com

- MACSYMA, MAPLE, and MATHEMATICA: commercial packages for symbolic computations. MAPLE

www.maplesoft.com

and MATHEMATICA

www.wolfram.com/mathematica4/isp

provide for numerical computations

- M□BILE : Excellent object-oriented modeller and simulator of mechanical systems composed mostly of rigid bodies. No synthesis capabilities. Semicommercial. Available from the University of Duisburg-Essen. For information, contact: Martin Tändl: m.taendl@uni-duisburg.de
- HERON: A software package still in its beta-phase, intended for analysis and synthesis of linkages. It features both kinematics and dynamics analyses. Information is available at URL:

<http://www.heron-technologies.com/>

Chapter 2

The Qualitative Synthesis of Kinematic Chains

li·ai·son 1: a binding or thickening agent used in cooking

2 a) a close bond or connection : INTERRELATIONSHIP

b): an illicit sexual relationship : AFFAIR

Merriam Webster's Collegiate Dictionary, Tenth Edition (C)1997,
1996 Zane Publishing, Inc.

*Qui pourrait ne pas frémir en songeant aux malheurs
que peut causer une seule liaison dangereuse!*

Lettre CLXXV. Madame DE VOLANGES
à Madame DE ROSEMONDE (de Laclos, 1782).

The fundamental concepts of motion representation and groups of displacements, as pertaining to rigid bodies, are recalled. These concepts are then applied to: a) the classification of kinematic chains according to their mobility; b) the determination of the degree of freedom of kinematic chains; and c) the qualitative synthesis of multiloop chains occurring in various types of machines, including parallel robots.

2.1 Notation

In following the notation introduced in Ch. 1, we will denote with lower-case boldfaces all vectors; with upper-case boldfaces all matrices. Additionally, sets will be denoted with calligraphic fonts, e.g., \mathcal{A} , \mathcal{B} , etc., while lower kinematic pairs (LKP), to be introduced in Section 2.3, are denoted with *sans-serif* upper cases: R, P, H, C, E, and S.

2.2 Background

The notion of *rigid body* is fundamental in the study of kinematic chains. A rigid body is a geometric concept that stems from the more general concept of *continuum*: *A rigid body \mathcal{B} is an unbounded continuum of points such that, under any possible transformation, two arbitrary points of \mathcal{B} remain equidistant.*

A rigid body \mathcal{B} is thus a set of points that fills continuously the three-dimensional Euclidean space \mathcal{E} . That is, between any two distinct points of \mathcal{B} we can always find an infinite, nondenumerable set of points of \mathcal{B} . A rigid body, as any set of points, is capable of undergoing transformations. In the case at hand, these transformations preserve the distance between any two points of \mathcal{B} ; as a consequence, the same transformation preserves the angle between any two lines of the body. Any such transformation is called an *isometry*—from Greek *isos* for “equal” and *metron* for “measure.” We must, however, distinguish between two kinds of isometries, as described below: Choose any four points O , A , B , and C of the body, not lying in a plane. If, when the last three points, as viewed from O , lie in the ccw order A , B , C , the trihedron defined by segments OA , OB and OC is said to be *right-handed*; otherwise, it is *left-handed*. If a “hand” can be attributed to a set, we refer to this feature as the *chirality*—Greek: *chéir* = hand. It is apparent that under any *physically possible* motion of \mathcal{B} , a right-handed (left-handed) trihedron remains right-handed (left-handed). Isometries that do not preserve the hand of the trihedron are *reflections*, examples of which are the two shoes, or the two gloves, or the two eyes, etc., of the same individual. One is a reflection, or a mirror-image, of the other. A hand-preserving isometry of \mathcal{B} is implicit in a *displacement* of \mathcal{B} from a reference *pose*—both position and orientation—to its current pose. To simplify matters, we will denote body and pose with the same calligraphic letter, while distinguishing among various poses of the same body by subscripts, whenever needed. Thus, \mathcal{B}_0 denotes a reference pose of \mathcal{B} , while its current pose can be represented by \mathcal{B} , as long as no confusion arises. Chirality-preserving isometries are involved in *rigid-body motions*.

Rigid-body pose and displacement are thus two abstract concepts. To quantify the pose we resort to *coordinate frames*. A coordinate frame is attached to a rigid body \mathcal{B} . The *orientation* of \mathcal{B} with respect to a reference frame is thus given by the orientation of the body-frame with respect to that of the reference frame. The position of \mathcal{B} , in turn, is given by that of the origin of the body-frame in the reference frame. The body-pose thus comprises both body-position and body-orientation. Body-position is thus defined by the *position vector* \mathbf{o}_B of the origin O_B of the body-frame, while body-orientation by the *rotation matrix* \mathbf{Q} carrying the reference frame into an attitude coincident with that of the body-frame.

According to Euler’s Theorem (Angeles, 2007), the displacement of a rigid body about a fixed point O , called a *pure rotation*, is fully characterized by an axis passing through

O and parallel to the unit vector \mathbf{e} and an angle ϕ , as depicted in Fig. 2.1.

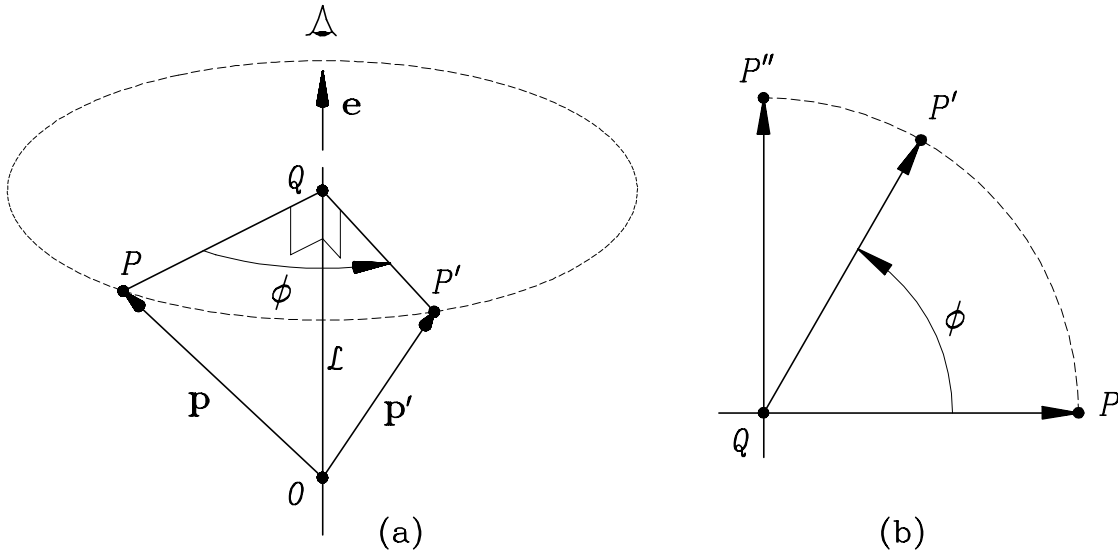


Figure 2.1: Rotation of a rigid body about a line

The foregoing motion is represented algebraically by a rotation matrix, i.e., a 3×3 *proper orthogonal* matrix \mathbf{Q} —a matrix is said to be proper-orthogonal if and only if its inverse equals its transpose and its determinant is $+1$; if the said determinant is -1 , the matrix is said to be *improper-orthogonal*—that adopts any of the equivalent forms given below:

$$\mathbf{Q} = e^{\phi \mathbf{E}} \quad (2.1a)$$

$$\mathbf{Q} = \mathbf{e}\mathbf{e}^T + \cos \phi (\mathbf{1} - \mathbf{e}\mathbf{e}^T) + \sin \phi \mathbf{E} \quad (2.1b)$$

$$\mathbf{Q} = \mathbf{1} + \sin \phi \mathbf{E} + (1 - \cos \phi) \mathbf{E}^2 \quad (2.1c)$$

In the above expressions we have resorted to the matrix exponential in the first representation of \mathbf{Q} . Moreover, we introduced matrices $\mathbf{1}$, $\mathbf{e}\mathbf{e}^T$, and \mathbf{E} , that will be described presently. Matrix $\mathbf{1}$ denotes the 3×3 *identity matrix*, while $\mathbf{e}\mathbf{e}^T$ is a *symmetric, rank-one matrix*; finally, \mathbf{E} denotes the *cross-product matrix* (CPM) of the unit vector \mathbf{e} , the CPM being defined as: Given any three-dimensional vector \mathbf{a} , the cross-product matrix \mathbf{A} of \mathbf{a} is given by

$$\mathbf{A} \equiv \frac{\partial(\mathbf{a} \times \mathbf{v})}{\partial \mathbf{v}} \quad (2.1d)$$

for any three-dimensional vector \mathbf{v} . More concretely, if \mathbf{e} has components $[e_1 \ e_2 \ e_3]^T$ in a given coordinate frame, then, in the same frame,

$$\mathbf{e}\mathbf{e}^T = \begin{bmatrix} e_1^2 & e_1 e_2 & e_1 e_3 \\ e_1 e_2 & e_2^2 & e_2 e_3 \\ e_1 e_3 & e_2 e_3 & e_3^2 \end{bmatrix}, \quad \mathbf{E} = \begin{bmatrix} 0 & -e_3 & e_2 \\ e_3 & 0 & -e_1 \\ -e_2 & e_1 & 0 \end{bmatrix} \quad (2.2a)$$

Now, given a rigid body in two poses, \mathcal{B}_1 and \mathcal{B}_2 , characterized by the position vectors \mathbf{o}_1 and \mathbf{o}_2 , and the rotation matrices \mathbf{Q}_1 and \mathbf{Q}_2 , the displacement of the body from \mathcal{B}_1 to \mathcal{B}_2 is *represented* by a) the vector difference $\mathbf{u} = \mathbf{o}_2 - \mathbf{o}_1$ and b) the matrix product $\mathbf{Q} = \mathbf{Q}_1^T \mathbf{Q}_2$. Special cases of displacements are the pure rotation, as introduced above, for which $\mathbf{u} = \mathbf{0}$, and the *pure translation*, for which $\mathbf{Q} = \mathbf{1}$.

The concepts, and to a great extent the notation and nomenclature that follow, are taken from (Hervé, 1978; 1999).

2.3 Kinematic Pairs

The kinematics of machines is studied via their underlying *kinematic chains*. A kinematic chain is the result of the coupling of rigid bodies, called *links*. Upon coupling *two* links, a kinematic pair is obtained. When the coupling takes place in such a way that the two links share a common surface, a *lower kinematic pair* results; when the coupling takes place along a common line or a common point of the two links, an *upper kinematic pair* is obtained.

If every link of a chain is coupled to at most two other links, then the chain is said to be *simple*. If all the links of a simple kinematic chain are coupled to two other links, then a *closed kinematic chain* is obtained. Moreover, this chain constitutes a *single loop*. If a simple chain has a link coupled to only one other link, then it has necessarily a second link coupled to only one other link, an *open chain* thus resulting. A multiloop chain can have open *subchains*. Single-loop kinematic chains are present in single-degree-of-freedom mechanisms, but a single-loop chain may have a degree of freedom (dof) greater than or less than unity. Simple kinematic chains of the open type are present in robotic manipulators of the *serial* type. Multiloop kinematic chains occur in both single-degree-of-freedom machines, e.g., in automobile suspensions, and in multi-dof robotic manipulators of the *parallel* type, paradigms of which are flight simulators. We shall elaborate on these concepts in this course.

Lower kinematic pairs deserve special attention for various reasons: One is that they model fairly well the mechanical couplings in a variety of machines; one more is that they are known to occur in exactly six types, to be described presently. Higher kinematic pairs occur in cam-follower mechanisms and in gears, in which contact occurs along common lines or common points of the coupled bodies.

The six lower kinematic pairs, displayed in Fig. 2.2, are listed below:

- (i) The *revolute pair* R allows a relative rotation through an angle ϕ about one axis \mathcal{A} passing through a point A of position vector \mathbf{a} and parallel to the unit vector \mathbf{e} ;
- (ii) The *prismatic pair* P allows a relative translation u in the direction of a unit vector \mathbf{e} ;

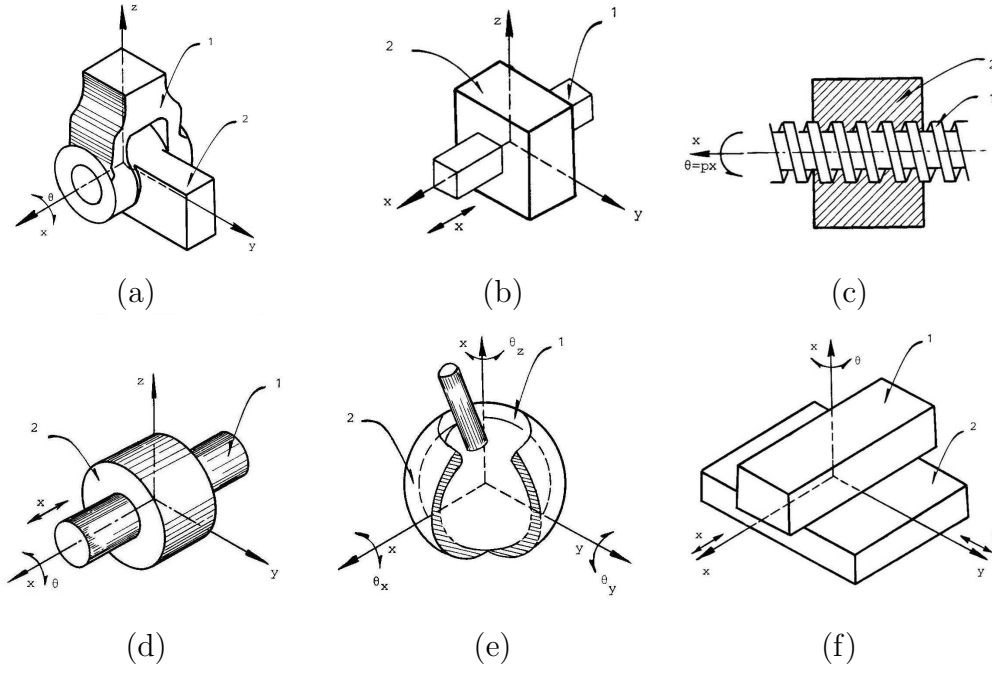


Figure 2.2: The six lower kinematic pairs: (a) revolute (R); (b) prismatic (P); (c) screw (H); (d) cylindrical (C); (e) spherical (S); and (f) planar (E)

- (iii) The *screw pair* H allows both a relative rotation through an angle ϕ about an axis \mathcal{A} passing through a point A of position vector \mathbf{a} and parallel to the unit vector \mathbf{e} , and a relative translation u in the direction of \mathbf{e} . However, the rotation and the translation are not independent, for they are related by the *pitch* p of the pair: $u = p\phi$;
- (iv) The *cylindrical pair* C allows both a relative rotation through an angle ϕ about an axis \mathcal{A} passing through a point A of position vector \mathbf{a} and parallel to the unit vector \mathbf{e} , and a relative translation in the direction of \mathbf{e} , rotation and translation being independent;
- (v) The *planar pair* E allows two independent translations t_u and t_v in the directions of the *distinct* unit vectors \mathbf{u} and \mathbf{v} , respectively, and a rotation ϕ about an axis normal to the plane of these two vectors; and
- (vi) The *spherical pair* S, allowing one independent rotation about each of three non-coplanar axes concurrent at a point O . The relative motion allowed by S is thus characterized by point O , and is associated with an axis parallel to the unit vector \mathbf{e} and with the angle of rotation ϕ about this axis, as per Euler's Theorem.

Remark 2.3.1 While the R, H, and C pairs are characterized by an axis, the P pair is characterized by a direction alone; not by an axis!

The Π Kinematic Pair

Besides the six LKPs, the Π -joint will be introduced in this chapter. This joint is a *parallelogram four-bar linkage*, which couples two links, one of the four that is considered arbitrarily *fixed* and its opposite counterpart. The latter moves under *pure translation*, all its points describing circles of variable location and radius identical to the length of the two other links of the parallelogram.

In the standard terminology, the linkage is composed of: a) one fixed link, labelled 1; b) one input link, labelled 2; c) one coupler link, labelled 3; and d) one output link, labelled 4. In a parallelogram, the opposite links move with a relative pure translation, each point of one link describing a circular trajectory onto the other link. The linkage thus provides a kinematic pair of the coupler link with respect to the fixed link. Hervé and Sparacino (1992) termed this coupling a Π kinematic pair, a.k.a. a Π -joint. At about the same time, Wohlhart (1991, 1992) and Dietmaier (1992) reported work on the use of the same type of joints in mechanisms.

Note that the Π pair does not belong to the class of lower kinematic pairs. It couples two links while allowing a relative translation along a circular trajectory. The interest of this pair lies in its ability to generate pure translations when combined with other Π -joints or with lower kinematic pairs, as discussed below.

2.4 Groups of Displacements

In the sequel, we shall resort to the algebraic concept of *group*. A group is a set \mathcal{G} of elements related by a *binary operation* \star with four properties:

P1 if a and $b \in \mathcal{G}$, then $a \star b \in \mathcal{G}$;

P2 if a , b , and $c \in \mathcal{G}$, then $a \star (b \star c) = (a \star b) \star c$;

P3 \mathcal{G} contains an element ι^1 called the *identity* of \mathcal{G} under \star , such that $a \star \iota = \iota \star a = a$;
and

P4 for every $a \in \mathcal{G}$, there exists an element a^{-1} , called the *inverse of a under \star* such that $a \star a^{-1} = a^{-1} \star a = \iota$.

If the elements of a set \mathcal{D} are the displacements undergone by a rigid body, then we can define a binary operation \odot —read “o-dot”—of displacements as the *composition* of displacements: As the body undergoes first a displacement d_a and then a displacement d_b , taking the body, successively, from pose \mathcal{B}_0 to pose \mathcal{B}_a , and then to pose \mathcal{B}_b , it is intuitively apparent that the composition of the two displacements, $d_a \odot d_b$, is in turn a rigid-body displacement. Hence,

¹ ι is the Greek letter *iota*.

- (a) $d_a \odot d_b \in \mathcal{D}$;
- (b) given d_a and d_b as introduced above, we define a third displacement d_c carrying \mathcal{B} from pose \mathcal{B}_b to pose \mathcal{B}_c . Then, $d_a \odot (d_b \odot d_c) = (d_a \odot d_b) \odot d_c$;
- (c) under no motion, any pose \mathcal{B} of a rigid body is preserved, the motion undergone by the body then being represented by a displacement ι that can be defined as the *identity element* of \mathcal{D} , such that, for any displacement d , $d \odot \iota = \iota \odot d = d$; and
- (d) for any displacement d carrying the body from pose \mathcal{B}_0 to pose \mathcal{B} , the *inverse displacement* d^{-1} is defined as that bringing back the body from \mathcal{B} to \mathcal{B}_0 , and hence, $d \odot d^{-1} = d^{-1} \odot d = \iota$.

From the foregoing discussion it is apparent that the set of rigid-body displacements \mathcal{D} has the algebraic structure of a group. Henceforth, we refer to the set of displacements of a rigid body as *group* \mathcal{D} . The interest in studying rigid-body displacements as algebraic groups lies in that, on the one hand, \mathcal{D} includes interesting and practical subgroups that find relevant applications in the design of production-automation and prosthetic devices. On the other hand, the same subgroups can be *combined* to produce novel mechanical layouts that would be insurmountably difficult to produce by sheer intuition. The combination of subgroups, in general, can take place via the standard set operations of *union* and *intersection*. As we shall see, however, the set defined as that comprising the elements of two displacement subgroups is not necessarily a subgroup, and hence, one cannot speak of the union of displacement subgroups. On the contrary, the intersection of two displacement subgroups is always a subgroup itself, and hence, the *intersection of displacement subgroups* is a valid group operation.

Rather than the union of groups, what we have is the *product* of groups. Let \mathcal{G}_1 and \mathcal{G}_2 be two groups defined over the same binary operation \star ; if $g_1 \in \mathcal{G}_1$ and $g_2 \in \mathcal{G}_2$, then the product of these two groups, represented by $\mathcal{G}_1 \bullet \mathcal{G}_2$, is the *set* of elements of the form $g_1 \star g_2$, where the order is important, for commutativity is not to be taken for granted in group theory.

The intersection of the two foregoing groups, represented by the usual set-theoretic symbol \cap , i.e., $\mathcal{G}_1 \cap \mathcal{G}_2$, is the group of elements g belonging to both \mathcal{G}_1 and \mathcal{G}_2 , and hence, the order is not important.

2.4.1 Displacement Subgroups

A *subgroup* \mathcal{G}_s of a given group \mathcal{G} is a set of objects such that: (a) they all belong to \mathcal{G} , although some objects, or elements, of \mathcal{G} may not belong to \mathcal{G}_s , and (b) \mathcal{G}_s has the algebraic structure of a group. Therefore, a subgroup \mathcal{D}_s of the group of rigid-body displacements \mathcal{D} is itself a group of displacements, but may lack some rigid-body displacements. If \mathcal{D}

includes elements not included in \mathcal{D}_s , then the latter is said to be a *proper subset* of the former.

The six lower kinematic pairs can be regarded as *generators* of displacement subgroups. We thus have:

- (i) The revolute pair \mathcal{R} of axis \mathcal{A} generates the subgroup $\mathcal{R}(\mathcal{A})$ of rotations about \mathcal{A} . Each element of this subgroup is characterized by the angle ϕ of the corresponding rotation;
- (ii) the prismatic pair in the direction \mathbf{e} generates the subgroup $\mathcal{P}(\mathbf{e})$ of translations along \mathbf{e} . Each element of $\mathcal{P}(\mathbf{e})$ is characterized by the translation u along \mathbf{e} ;
- (iii) the screw pair of axis \mathcal{A} and pitch p generates the subgroup $\mathcal{H}(\mathcal{A}, p)$ of rotations ϕ about \mathcal{A} and translations u along the direction of the same axis, translations and rotations being related by the pitch p in the form $u = p\phi$, as described when the screw pair was introduced. Each element of $\mathcal{H}(\mathcal{A}, p)$ can thus be characterized either by u or by ϕ ;
- (iv) the cylindrical pair of axis \mathcal{A} generates the subgroup $\mathcal{C}(\mathcal{A})$ of independent rotations about and translations along \mathcal{A} . Each element of $\mathcal{C}(\mathcal{A})$ is thus characterized by both the displacement u and the rotation ϕ ;
- (v) the planar pair generates the subgroup $\mathcal{F}(\mathbf{u}, \mathbf{v})$ of two independent translations in the directions of the *distinct* unit vectors \mathbf{u} and \mathbf{v} , and one rotation about an axis normal to both \mathbf{u} and \mathbf{v} . Each element of $\mathcal{F}(\mathbf{u}, \mathbf{v})$ is thus characterized by the two translations t_u, t_v and the rotation ϕ ;
- (vi) the spherical pair generates the subgroup $\mathcal{S}(O)$ of rotations about point O . Each element of $\mathcal{S}(O)$, a rotation about O , is characterized by the axis of rotation passing through O in the direction of a unit vector \mathbf{e} and through an angle ϕ . Alternatively, each rotation about O can be characterized by the independent rotations about three designated axes, e.g., the well-known Euler angles.

Besides the six foregoing subgroups, we can define six more, namely,

- (vii) The *identity subgroup* \mathcal{I} , whose single element is the identity displacement ι introduced above;
- (viii) the *planar-translation subgroup* $\mathcal{T}_2(\mathbf{u}, \mathbf{v})$ of translations in the directions of the two distinct unit vectors \mathbf{u} and \mathbf{v} . Each element of this group is thus characterized by two translations, t_u and t_v ;
- (ix) the *translation subgroup* \mathcal{T}_3 of translations in \mathcal{E} , each element of which is characterized by three independent translations t_u, t_v , and t_w ;

- (x) the subgroup $\mathcal{Y}(\mathbf{e}, p)$ of motions allowed by a screw of pitch p and axis parallel to \mathbf{e} undergoing arbitrary translations in a direction normal to \mathbf{e} . Each element of this subgroup is thus characterized by the two independent translations t_u, t_v of the axis, and either the rotation ϕ about this axis or the translation $t_w = p\phi$ along the axis. Faute-de-mieux, we shall call this subgroup the *translating-screw group*;
- (xi) the subgroup $\mathcal{X}(\mathbf{e}) = \mathcal{F}(\mathbf{e}) \bullet \mathcal{P}(\mathbf{e})$, resulting of the product of the planar subgroup of plane normal to \mathbf{e} and the prismatic subgroup of direction \mathbf{e} . Each element of this subgroup is thus characterized by the two translations t_u, t_v and the angle ϕ of the planar subgroup plus the translation t_w in the direction of \mathbf{e} . Moreover, note that $\mathcal{F}(\mathbf{e}) \bullet \mathcal{P}(\mathbf{e}) = \mathcal{P}(\mathbf{e}) \bullet \mathcal{F}(\mathbf{e})$. This subgroup, named after the German mathematician and minerologist Arthur Moritz Schönflies (1853–1928), is known as the *Schönflies subgroup*, and is generated most commonly by what is known as SCARA systems, for *Selective-Compliance Assembly Robot Arm*;
- (xii) the group \mathcal{D} itself. Each element of this subgroup is characterized by three independent translations and three independent rotations.

It is thus apparent that each subgroup includes a set of displacements with a specific *degree of freedom*. We shall need below an extension of the concept of dof, for which reason we term the dof of each subgroup its *dimension*, and denote the dimension of any subgroup \mathcal{G}_s by $\dim[\mathcal{G}_s]$. Thus,

$$\dim[\mathcal{I}] = 0 \tag{2.3a}$$

$$\dim[\mathcal{R}(\mathcal{A})] = \dim[\mathcal{P}(\mathbf{e})] = \dim[\mathcal{H}(\mathcal{A}, p)] = 1 \tag{2.3b}$$

$$\dim[\mathcal{T}_2(\mathbf{u}, \mathbf{v})] = \dim[\mathcal{C}(\mathcal{A})] = 2 \tag{2.3c}$$

$$\dim[\mathcal{T}_3] = \dim[\mathcal{F}(\mathbf{e})] = \dim[\mathcal{S}(O)] = \dim[\mathcal{Y}(\mathbf{e}, p)] = 3 \tag{2.3d}$$

$$\dim[\mathcal{X}(\mathbf{e})] = 4 \tag{2.3e}$$

$$\dim[\mathcal{D}] = 6 \tag{2.3f}$$

The foregoing list of *twelve* displacement subgroups is *exhaustive*, none of which is of dimension five. The reader may wonder whether displacement products are missing from the list that might be subgroups. However, any displacement product not appearing in the above list *is not a subgroup*. As a matter of fact, any set of displacements including rotations about *two axes*, and no more than two, fails to have a group structure. Consider, for example, the set of rotations \mathcal{W} produced by a (two-dof) *pitch-roll wrist* (PRW), as depicted in Fig. 2.3. With reference to this figure, frame \mathcal{F}_0 , serving as the *reference frame*, is defined with X_0 along the roll axis, passing through the *operation point* P , while Z_0 is defined along the pitch axis.

Now we introduce a first rotation \mathbf{Q}_1 (not a coordinate transformation!): Define \mathcal{F}_1 with X_1 along the displaced roll axis, passing through P in the displaced pose of the end-

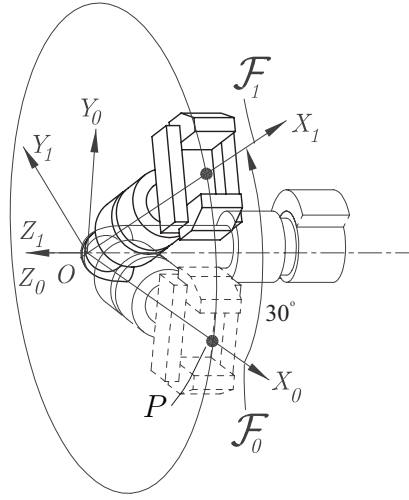


Figure 2.3: A pitch-roll wrist producing a first rotation

effector (EE), and making an angle of 30° with X_0 , Z_1 coinciding with Z_0 . Matrix \mathbf{Q}_1 , rotating \mathcal{F}_0 into \mathcal{F}_1 as depicted in Fig. 2.3, is obtained, in \mathcal{F}_0 -coordinates, upon assigning to its first column the \mathcal{F}_0 -components of the unit vector \mathbf{i}_1 , parallel to X_1 , its second column being given by the \mathcal{F}_0 -components of the unit vector \mathbf{j}_1 , parallel to Y_1 ; its third column follows the same pattern². The rotation \mathbf{Q}_1 carrying \mathcal{F}_0 into \mathcal{F}_1 as depicted in Fig. 2.3 is, hence, a simple rotation through an angle of 30° about Z_0 . Hence,

$$\mathbf{Q}_1 = \begin{bmatrix} \sqrt{3}/2 & -1/2 & 0 \\ 1/2 & \sqrt{3}/2 & 0 \\ 0 & 0 & 1 \end{bmatrix} \quad (2.4)$$

Next, we introduce a second rotation \mathbf{Q}_2 : Define a new frame \mathcal{F}_2 with X_2 along the displaced roll axis, passing through P in the displaced pose of the EE, and making an angle of 60° with X_0 , Z_2 lying in the X_0 - Y_0 plane, and making an angle of -30° with X_0 . Hence, in \mathcal{F}_0 -coordinates as well,

$$\mathbf{Q}_2 = \begin{bmatrix} 1/2 & 0 & \sqrt{3}/2 \\ \sqrt{3}/2 & 0 & -1/2 \\ 0 & 1 & 0 \end{bmatrix} \quad (2.5a)$$

Moreover, let $\mathbf{Q}_3 = \mathbf{Q}_2\mathbf{Q}_1$, a third rotation obtained as the product of the first two, namely,

$$\mathbf{Q}_3 = \begin{bmatrix} \sqrt{3}/4 & -1/4 & \sqrt{3}/2 \\ 3/4 & -\sqrt{3}/4 & -1/2 \\ 1/2 & \sqrt{3}/2 & 0 \end{bmatrix} \quad (2.5b)$$

which yields a third attitude of the EE, as depicted in Fig. 2.5.

²The matrix transforming \mathcal{F}_0 -coordinates into \mathcal{F}_1 -coordinates is \mathbf{Q}_1^T .

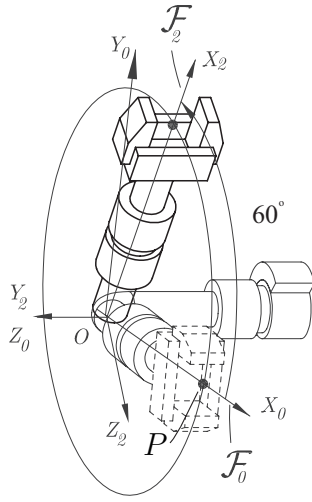


Figure 2.4: A pitch-roll wrist producing a second rotation

We note that, in an arbitrary configuration, the roll axis remains normal to Z_0 . Hence, any rotation produced by the PRW takes the EE to a pose in which the roll axis is normal to Z_0 , i.e., the set of possible displaced configurations of the roll axis is a pencil of lines passing through the origin and normal to Z_0 . The roll axis in the displaced pose of the EE thus lies in the X_0 - Y_0 plane. Any EE pose whereby the roll axis lies outside of the X_0 - Y_0 plane is attained by a rotation *outside* of \mathcal{W} .

As it turns out, the roll axis is carried by \mathbf{Q}_3 into a configuration parallel to \mathbf{i}_3 , the image of \mathbf{i}_0 under \mathbf{Q}_3 , as depicted in Fig. 2.5, i.e.,

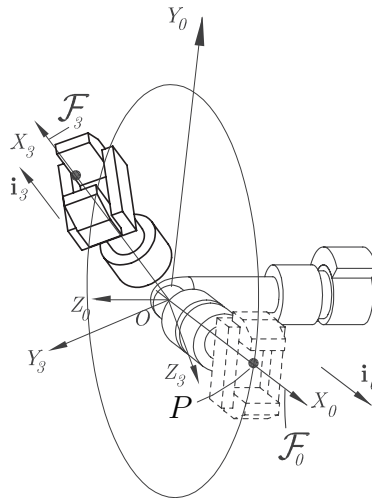


Figure 2.5: The EE of a pitch-roll wrist undergoing a third, unfeasible, rotation

$$\mathbf{i}_3 = \mathbf{Q}_3 \mathbf{i}_0 = [\sqrt{3}/4 \quad 3/4 \quad 1/2]^T \quad (2.6)$$

which, apparently, is not normal to Z_0 and, hence, \mathbf{Q}_3 lies outside of the set \mathcal{W} of feasible rotations produced by the PRW. Hence, the set of rotations produced by a PRW does not have the algebraic structure of a group.

2.5 Kinematic Bonds

Displacement subgroups can be combined to produce new sets of displacements that may or may not be displacement subgroups themselves. To combine subgroups, we resort to the group operations of product (\bullet) and intersection (\cap).

Now we introduce the concept of *kinematic bond*, which is a generalization of kinematic pair, as first proposed by Hervé (1978), who called this concept *liaison cinématique* in French. This concept has been termed *kinematic liaison* (Angeles, 1982) or *mechanical connection* (Hervé, 1999) in English. Since “liaison” in English is usually applied to human relations, the term “bond” seems more appropriate, and is thus adopted here.

We illustrate the concept with an example: Let us assume three links, numbered from 1 to 3, and coupled by two kinematic pairs generating the two subgroups \mathcal{G}_1 and \mathcal{G}_2 , where these two subgroups are instanced by specific displacement subgroups below. We then have

$$\mathcal{G}_1 \bullet \mathcal{G}_2 = \mathcal{R}(\mathcal{A}) \bullet \mathcal{P}(\mathbf{e}) = \mathcal{C}(\mathcal{A}), \quad \text{for } \mathbf{e} \parallel \mathcal{A} \quad (2.7a)$$

$$\mathcal{G}_1 \bullet \mathcal{G}_2 = \mathcal{R}(\mathcal{A}) \bullet \mathcal{T}_2(\mathbf{u}, \mathbf{v}) = \mathcal{F}(\mathbf{e}), \quad \text{for } \mathbf{e}, \mathcal{A} \perp \mathbf{u}, \mathbf{v} \quad (2.7b)$$

$$\mathcal{G}_1 \bullet \mathcal{G}_2 = \mathcal{R}(\mathcal{A}) \bullet \mathcal{R}(\mathcal{B}) = \mathcal{L}(1, 3) \quad (2.7c)$$

$$\mathcal{G}_1 \cap \mathcal{G}_2 = \mathcal{R}(\mathcal{A}) \cap \mathcal{C}(\mathcal{A}) = \mathcal{R}(\mathcal{A}) \quad (2.7d)$$

$$\mathcal{G}_1 \cap \mathcal{G}_2 = \mathcal{R}(\mathcal{A}) \cap \mathcal{S}(O) = \mathcal{R}(\mathcal{A}), \quad \text{for } O \in \mathcal{A} \quad (2.7e)$$

$$\mathcal{G}_1 \cap \mathcal{G}_2 = \mathcal{R}(\mathcal{A}) \cap \mathcal{P}(\mathbf{e}) = \mathcal{I}, \quad \text{for any } \mathcal{A}, \mathbf{e} \quad (2.7f)$$

All of the above examples, except for the third one, amount to a displacement subgroup. This is why no subgroup symbol is attached to that set. Instead, we have used the symbol $\mathcal{L}(1, 3)$ to denote the kinematic bond between the first and third links of the chain. In general, a kinematic bond between links i and n of a kinematic chain, when no ambiguity is possible, is denoted by $\mathcal{L}(i, n)$. When the chain connecting these two links is not unique, such as in a closed chain, where these two links can be regarded as connected by two possible *paths*, a subscript will be used, e.g., $\mathcal{L}_I(i, j)$, $\mathcal{L}_{II}(i, j)$, etc. A kinematic bond is, thus, a set of displacements, as stemming from a binary operation of displacement subgroups, although the bond itself need not be a subgroup. Obviously, the 12 subgroups described above are themselves special cases of kinematic bonds.

The kinematic bond between links i and n can be conceptualized as the product of the various subgroups associated with the kinematic pairs between the i th and the n th links. To keep the discussion general enough, we shall denote the subgroup associated

with the kinematic pair coupling links i and $i + 1$ as $\mathcal{L}(i, i + 1)$, with a similar notation for all other kinematic-pair subgroups. Thus,

$$\mathcal{L}(i, n) = \mathcal{L}(i, i + 1) \bullet \mathcal{L}(i + 1, i + 2) \bullet \cdots \bullet \mathcal{L}(n - 1, n) \quad (2.8)$$

For example, in a six-axis serial manipulator, we can set $i = 1$, $n = 7$, all six kinematic pairs in-between being revolutes of skew axes $\mathcal{R}(\mathcal{A}_1)$, $\mathcal{R}(\mathcal{A}_2)$, \dots , $\mathcal{R}(\mathcal{A}_6)$. Then,

$$\mathcal{L}(1, 7) = \mathcal{D}$$

That is, the manipulator is a generator of the general six-dimensional group of rigid-body displacements \mathcal{D} .

As an example of group-intersection, let us consider the *Sarrus mechanism*, depicted in Fig. 2.6.

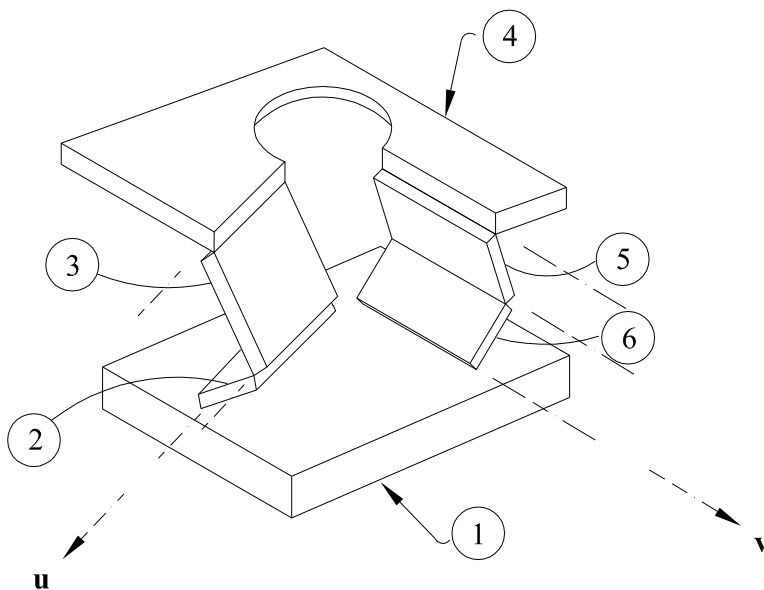


Figure 2.6: The Sarrus mechanism

A less common realization of the Sarrus mechanism is depicted in Fig. 2.5. This is a IIIIII closed kinematic chain, modelled as a *compliant mechanism*, which bears a

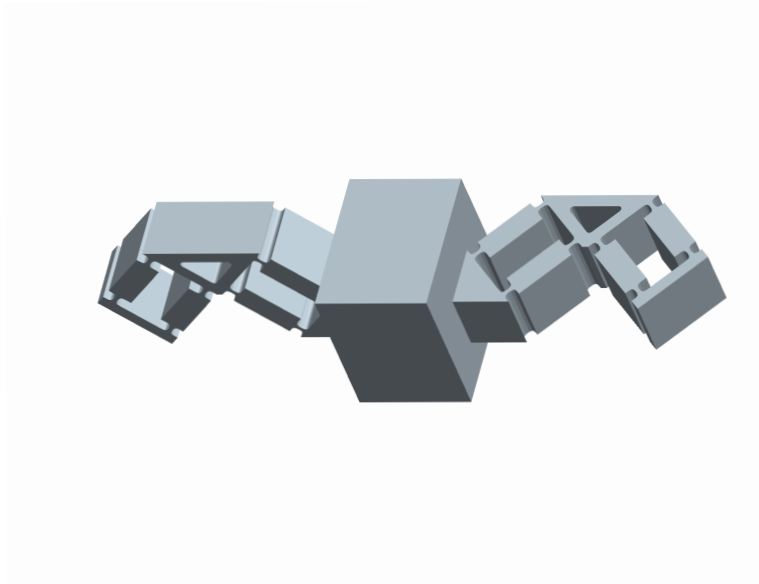


Figure 2.7: An alternative realization of the Sarrus mechanism

monolithic structure, made of a polymer. The R joints of the mechanism are realized by removing material at the joint locations, so as to render these areas much more compliant than the other areas. The mechanism is designed so as to serve as a uniaxial accelerometer.

In the Sarrus mechanism, we have six links, coupled by six revolute pairs. Moreover, the revolute pairs occur in two triplets, each on one leg of the mechanism. The axes of the three revolute pairs of each leg are parallel to each other. The bond $\mathcal{L}(1, 4)$, apparently, is not unique, for it can be defined by traversing any of the two legs. Let the leg of links 1, 2, 3 and 4, coupled by revolutes of axes parallel to the unit vector \mathbf{u} , be labelled I ; the other leg, of links 4, 5, 6 and 1, coupled by revolutes of axes parallel to the unit vector \mathbf{v} , is labelled II . It is apparent that, upon traversing leg I , we obtain

$$\mathcal{L}_I(1, 4) = \mathcal{F}(\mathbf{u})$$

Moreover, upon traversing leg II ,

$$\mathcal{L}_{II}(1, 4) = \mathcal{F}(\mathbf{v})$$

That is, leg I is a generator of the planar subgroup \mathcal{F} of plane normal to vector \mathbf{u} , while leg II is that of the subgroup \mathcal{F} of plane normal to vector \mathbf{v} . Therefore, the intersection $\mathcal{L}_I(1, 4) \cap \mathcal{L}_{II}(1, 4)$ is the set of displacements common to the two \mathcal{F} -subgroups, namely, the prismatic subgroup of translations in the direction $\mathbf{w} = \mathbf{v} \times \mathbf{u}$, i.e.,

$$\mathcal{L}_I(1, 4) \cap \mathcal{L}_{II}(1, 4) = \mathcal{P}(\mathbf{w})$$

The Sarrus mechanism is thus a revolute realization of the prismatic joint.

2.6 The Chebyshev-Grübler-Kutzbach-Hervé Formula

Finding the degree of freedom (dof) f of a given kinematic chain has been an elusive task for over a century. Here we adopt the methodology proposed by Hervé (1978), based on the concept of *groups of displacements*.

Essentially, Hervé considers whether the *topology* of a kinematic chain suffices to predict its dof or not. The topology of a kinematic chain pertains to the numbers of links and joints as well as their layouts, regardless of the values of the geometric parameters of the chain, such as distances and angles between pair axes and the like. According to Hervé (1978), kinematic chains can be classified, with regard to their mobility, as:

- (a) *Trivial*, when all the possible kinematic bonds between any pair of links is a subset of a particular subgroup of \mathcal{D} , including \mathcal{D} itself, but excluding \mathcal{I} . If the common subgroup of interest is \mathcal{D} itself, the chain is trivial if the product of the subgroups of all the foregoing kinematic pairs yields \mathcal{D} . The dof of a trivial kinematic chain can be determined with the aid of the formula derived below, which takes into account only the topology of the chain;
- (b) *exceptional*, when a kinematic bond can be identified in the chain that is a subgroup \mathcal{D}_s of \mathcal{D} , and this subset is the *intersection* of a number of bonds of \mathcal{D} . The dof of the chain is, then, the dimension of the intersection.
- (c) *paradoxical*, when the topology of the kinematic chain alone does not suffice to determine the chain dof. In this case, special relations among the various geometric parameters of the chain yield a mobility that would be absent under general values of those parameters, for the same topology.

2.6.1 Trivial Chains

Regarding trivial chains, let \mathcal{G}_m be the subgroup of the *least dimension* d_m , containing all possible bonds between any pair of links of the chain. \mathcal{G}_m can thus be thought of as a kind of *least common multiple* of all possible bonds of the chain. Moreover, let d_i be the dimension of the subgroup associated with the i th kinematic pair, and $r_i \equiv d_m - d_i$ be its degree of constraint, termed its *restriction* for brevity. In determining the dof of a chain, we are interested in the *relative* motion capability of the chain, and hence, we consider arbitrarily one link *fixed*. It is immaterial which specific link is the designated fixed one. If the chain is composed of l links and p kinematic pairs, then its dof f is given by the difference between its total dof before coupling and the sum of its restrictions, i.e.,

$$f = d_m(l - 1) - \sum_{i=1}^p r_i \quad (2.9)$$

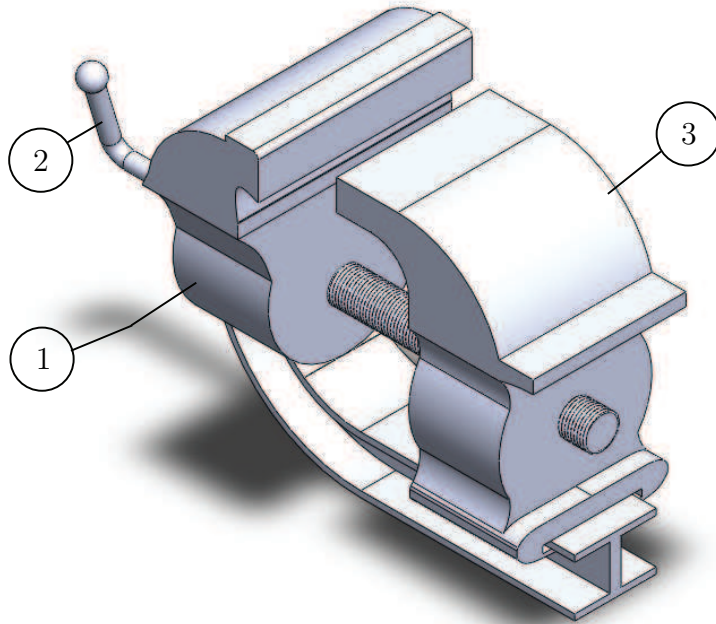


Figure 2.8: The well-known vise mechanism

The above relation can be termed a *generalized Chebyshev-Grübler-Kutzbach* (CGK) formula in that it generalizes the concept involved in parameter d_m above. Conventional CGK formulas usually consider that d_m can attain one of two possible values, 3 for planar and spherical chains and 6 for spatial chains. In the generalized formula, d_m can attain any of the values 2, 3, 4, or 6. Moreover, rather than considering only three subgroups of displacements, we consider all 12 described above, none of which is of dimension five.

As an example of the application of the above formula, we consider the *vise mechanism*, displayed in Fig. 2.6.1. In that figure, we distinguish three links and three LKPs. The links are the frame 1, the crank 2 and the slider 3, which define three bonds, namely,

$$\mathcal{L}(1, 2) = \mathcal{R}(\mathcal{A}), \quad \mathcal{L}(2, 3) = \mathcal{H}(\mathcal{A}), \quad \mathcal{L}(3, 1) = \mathcal{P}(\mathbf{a})$$

in which \mathcal{A} is the common axis of the R and the H pairs, while \mathbf{a} is the unit vector parallel to \mathcal{A} . In this case, it is apparent that all three bonds lie in the \mathcal{C} subgroup, and hence, $d_m = 2$. Moreover, if we number the three joints in the order R, H, P, and notice that the dimension d_i associated with each of the three joints is unity, then $r_i = 1$, for $i = 1, 2, 3$. Application of the generalized CGK formula (2.9) yields

$$f = 2(3 - 1) - 3 \times 1 = 4 - 3 = 1$$

which is indeed the correct value of the vise dof.

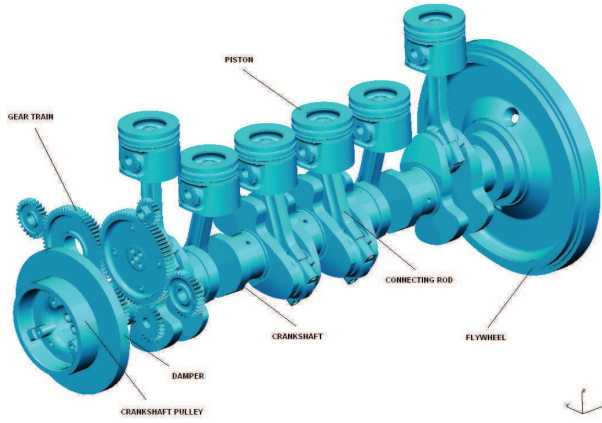


Figure 2.9: The slider-crank mechanism as a key component of an internal combustion engine: a power-generation system with six cylinders in line (courtesy of MMM International Motores, Campinas, Brazil)

2.6.2 Exceptional Chains

The Sarrus mechanism of Figs. 2.6 and 2.5 is an example of an exceptional chain. Indeed, all its links undergo motions of either one of two planar subgroups, $\mathcal{F}(\mathbf{u})$ and $\mathcal{F}(\mathbf{v})$. Moreover, the product of these two subgroups does not yield the group \mathcal{D} —notice that the linkage has two sets of R pairs, each parallel to a distinct unit vector, \mathbf{u} or \mathbf{v} . The dof of this mechanism can still be found, but not with the aid of the CGK formula of eq.(2.9), for all its kinematic bonds do not belong to the same subgroup of \mathcal{D} . This dof is found, rather, as the dimension of the intersection of the two foregoing subgroups, i.e.,

$$f = \dim[\mathcal{F}(\mathbf{u}) \cap \mathcal{F}(\mathbf{v})] = \dim[\mathcal{P}(\mathbf{u} \times \mathbf{v})] = 1$$

Another example of exceptional chain is the familiar slider-crank mechanism of internal combustion engines and compressors, as shown in Fig. 2.6.2. It is customary to represent this mechanism as a planar RRRP mechanism. However, a close look at the coupling of the piston with its chamber reveals that this coupling is not via a prismatic, but rather via a cylindrical pair. It is thus apparent that the displacements of all the links lie not in one single subgroup of \mathcal{D} , but rather in a subset that can be decomposed into two kinematic bonds, which happen to be subgroups of \mathcal{D} , the $\mathcal{F}(\mathbf{e})$ subgroup of motions generated by the RRR subchain and the $\mathcal{C}(\mathcal{A})$ subgroup of the piston-chamber coupling \mathcal{C} . Here, \mathcal{A} is the axis of the cylindrical chamber and \mathbf{e} is the unit vector parallel to the axes of the three R pairs. Apparently, the product of these two subgroups does not generate all of \mathcal{D} , for it is short of rotations about an axis normal to both \mathbf{e} and \mathcal{A} . Nevertheless, the dof of this chain can be determined as the dimension of the intersection of the two subgroups, i.e.,

$$f = \dim[\mathcal{F}(\mathbf{e}) \cap \mathcal{C}(\mathcal{A})] = \dim[\mathcal{P}(\mathbf{u})] = 1, \quad \mathbf{u} \parallel \mathcal{A}$$

Now, why would such a simple planar mechanism—the slider-crank—as portrayed in elementary books on mechanisms, be built with a spatial structure? The answer to this question lies in the *assemblability* of the mechanism: a planar RRRP mechanism requires a highly accurate machining of the crankshaft, connecting rod, piston and chamber, in order to guarantee that the axes of the three R pairs are indeed parallel and that the axis of the cylindrical chamber is normal to the three R axes, which is by no means a simple task!

One more example of exceptional chain is the parallel robot of Fig. 2.10, consisting of four identical limbs that couple a base $A_I A_{II} A_{III} A_{IV}$ with a moving plate $D_I D_{II} D_{III} D_{IV}$. Each limb, moreover, is a PRIIR chain (Altuzarra et al., 2009).

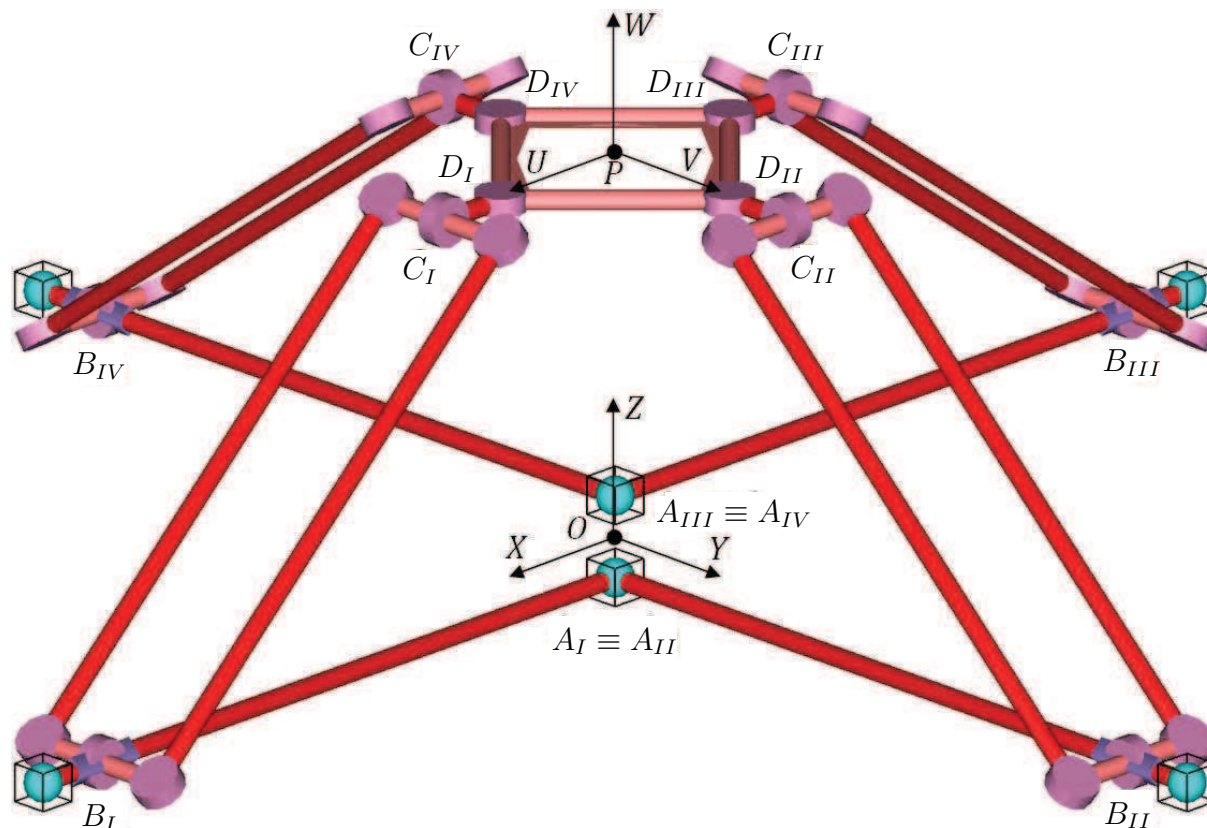


Figure 2.10: The Schönflies-motion generator developed at the University of the Basque Country, in Bilbao, Spain

The kinematic chain thus contains five joints per limb and 18 links: the base plate, the mobile plate and four intermediate links per limb. If the CGK formula is applied for the general kinematic chain, with $d_m = 6$, $l = 18$, $r_i = 5$, for $i = 1, \dots, 18$, the dof f thus resulting turns out to be

$$f = 6(18 - 1) - 20 \times 5 = 102 - 100 = 2$$

which is not what the authors claim, namely, four. In order to elucidate the apparent contradiction, we conduct below a group-theoretic analysis of the chain mobility: first,

let $\mathcal{R}(P, \mathbf{e})$ denote the subgroup generated by a R joint of axis passing through point P and parallel to the unit vector \mathbf{e} ; then, let \mathcal{L}_J denote the kinematic bond of the J th limb, which is the product of five simple bonds, each with a dimension equal to one, namely,

1. Either the prismatic subgroup $\mathcal{P}(\mathbf{i})$ of displacements parallel to \mathbf{i} , for $J = I, III$, or its counterpart $\mathcal{P}(\mathbf{j})$ of displacements parallel to \mathbf{j} , for $J = II, IV$;
2. the rotation subgroup $\mathcal{R}(B_J, \mathbf{j})$, of axis of rotation passing through point B_J and parallel either to \mathbf{j} , for $J = I, III$, or its counterpart $\mathcal{R}(B_J, \mathbf{i})$, for $J = II, IV$;
3. the subset of displacements $\mathcal{D}_{\Pi}(\mathbf{n}_J)$ associated with the Π -joint, characterized by translations along circles of radius $\overline{B_J C_J}$ lying in the plane of the J th parallelogram, of normal \mathbf{n}_J ;
4. the rotation subgroup $\mathcal{R}(C_J, \mathbf{j})$, of axis of rotation passing through point C_J and parallel either to \mathbf{j} , for $J = I, III$, or its counterpart $\mathcal{R}(C_J, \mathbf{i})$, for $J = II, IV$;
5. the rotation subgroup $\mathcal{R}(D_J, \mathbf{k})$ of axis of rotation passing through D_J and parallel to \mathbf{k} .

Therefore,

$$\mathcal{L}_J = \underbrace{\mathcal{P}(\mathbf{i}) \bullet \mathcal{R}(B_J, \mathbf{j}) \bullet \mathcal{D}_{\Pi}(\mathbf{J}) \bullet \mathcal{R}(C_J, \mathbf{j})}_{\mathcal{X}(\mathbf{j})} \bullet \mathcal{R}(D_J, \mathbf{k}) = \mathcal{X}(\mathbf{j}) \bullet \mathcal{R}(D_J, \mathbf{k}), \quad J = I, III$$

Likewise,

$$\mathcal{L}_J = \mathcal{X}(\mathbf{i}) \bullet \mathcal{R}(D_J, \mathbf{k}), \quad J = II, IV$$

Notice that none of the four bonds derived above is a subgroup of \mathcal{D} , which disqualifies the multiloop kinematic chain from being trivial. However, notice also that

$$\mathcal{X}(\mathbf{j}) \bullet \mathcal{R}(D_J, \mathbf{k}) = \mathcal{X}(\mathbf{k}) \bullet \mathcal{R}(C_J, \mathbf{j}), \quad J = I, III$$

and

$$\mathcal{X}(\mathbf{i}) \bullet \mathcal{R}(D_J, \mathbf{k}) = \mathcal{X}(\mathbf{k}) \bullet \mathcal{R}(C_J, \mathbf{i}), \quad J = II, IV$$

Therefore,

$$\mathcal{L}_J \cap \mathcal{L}_K = \mathcal{X}(\mathbf{k}), \quad J, K = I, \dots, IV, \quad J \neq K$$

thereby proving that, indeed, the intersection of all limb bonds is a subgroup of \mathcal{D} , namely, the Schönflies subgroup $\mathcal{X}(\mathbf{k})$. The dof f of the robot at hand is, thus,

$$f = \dim[\mathcal{X}(\mathbf{k})] = 4$$

and, according to Hervé's classification, the multiloop chain can be considered exceptional.

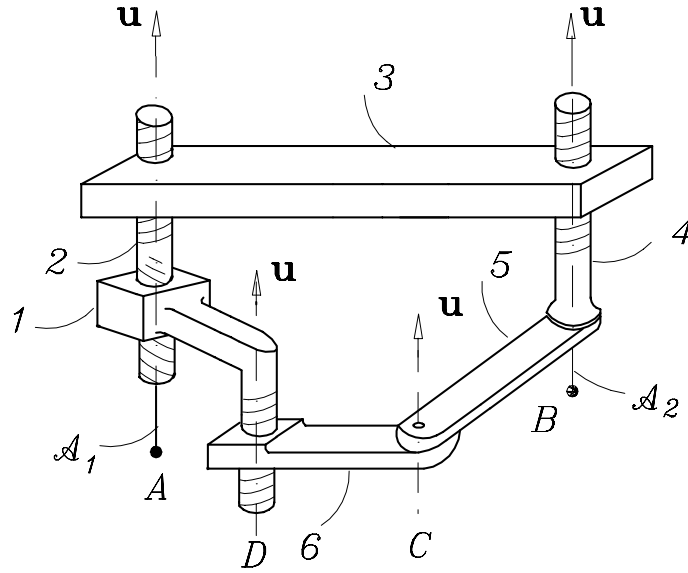


Figure 2.11: The HHHRRH mechanism

While the generalized CGK formula is more broadly applicable and less error-prone than its conventional counterpart, it is not error-free. Indeed, let us consider the HHHRRH closed chain of Fig. 2.11, first proposed by Hervé (1978). The four H pairs of this figure have distinct pitches.

It is apparent that all links move in parallel planes, and that these planes also translate along their common normal direction. The displacement subgroup containing all possible kinematic bonds of the mechanism under study, of minimum dimension, is thus the Schönflies subgroup $\mathcal{X}(\mathbf{u})$, and hence, $d_m = 4$. Since we have six links and six joints, each of restriction $r_i = d_m - f_i$, for $f_i = 1$ and $i = 1, \dots, 6$, the dof of the mechanism is obtained from the CGK formula as

$$f = 4(6 - 1) - 6 \times 3 = 2$$

However, the above result is wrong, for it predicts a too large dof. Indeed, the mechanism has one idle dof, as can be readily shown by means of a bond analysis: Let us compute $\dim[\mathcal{L}(1, 5)]$:

$$\mathcal{L}(1, 5) = \underbrace{\mathcal{L}(1, 2) \bullet \mathcal{L}(2, 3)}_{\mathcal{C}(\mathcal{A}_1)} \bullet \underbrace{\mathcal{L}(3, 4) \bullet \mathcal{L}(4, 5)}_{\mathcal{C}(\mathcal{A}_2)}$$

where \mathcal{A}_1 and \mathcal{A}_2 are axes parallel to vector \mathbf{u} and pass through points A and B , respectively, of Fig. 2.11. Now we find the above-mentioned idle dof. To this end, we compute $\dim[\mathcal{L}(1, 5)]$, which may appear to be the sum of the dimensions of the two subgroups, $\mathcal{C}(\mathcal{A}_1)$ and $\mathcal{C}(\mathcal{A}_2)$. However, notice that these two subgroups include a common translation along \mathbf{u} , and hence, in computing the said dimension, care should be taken in not

counting this translation twice. What this means is that the dimension of the intersection of the above two factors must be subtracted from the sum of their dimensions, i.e.,

$$\dim[\mathcal{L}(1, 5)] = \dim[\mathcal{C}(\mathcal{A}_1)] + \dim[\mathcal{C}(\mathcal{A}_2)] - \dim[\mathcal{C}(\mathcal{A}_1) \cap \mathcal{C}(\mathcal{A}_2)] = 2 + 2 - 1 = 3$$

We have thus shown that the chain entails one idle dof. In order to obtain the correct dof of the chain from the generalized CGK formula, then, the total number m of idle dof must be subtracted from the dof predicted by that formula, i.e.,

$$f = d_m(n - 1) - \sum_{i=1}^p r_i - m \quad (2.10)$$

which can be fairly called the *Chebyshev-Grübler-Kutzbach-Hervé* formula. In the case at hand, $m = 1$, and hence, the dof of the chain of Fig. 2.11 is unity.

2.6.3 Paradoxical Chains

Examples of paradoxical chains are well documented in the literature (Bricard, 1927; Angeles, 1982). These include the *Bennett mechanism* and the *Bricard mechanism*, among others.

2.7 Applications to the Qualitative Synthesis of Robotic Architectures

The foregoing concepts are now applied to the *qualitative* synthesis of parallel robotic architectures. By qualitative we mean the determination of the topology of the kinematic chain, not including the corresponding dimensions. These dimensions are found at a later stage, by means of methods of *quantitative synthesis*, which Denavit and Hartenberg (1964) term dimensional synthesis, the subject of Chs. 3–5. The full determination of the kinematic chain, including dimensions, yields what is known as the *architecture* of the robotic system at hand.

2.7.1 The Synthesis of Robotic Architectures

The first robotic architecture with II-joints was proposed by Clavel in what he called the *Delta Robot* (Clavel, 1988). The kinematic chain of this robot is displayed in Fig. 2.12. Delta is a generator of the $\mathcal{T}_3(\mathbf{u})$ displacement subgroup; it is thus capable of three-dof translations.

The kinematic chain of the Delta robot is composed of two triangular plates, the top (\mathcal{A}) and the bottom (\mathcal{B}) plates. The top plate supports the three (direct-drive) motors, the bottom plate the gripper, and hence, constitutes the moving-platform (MP) of the

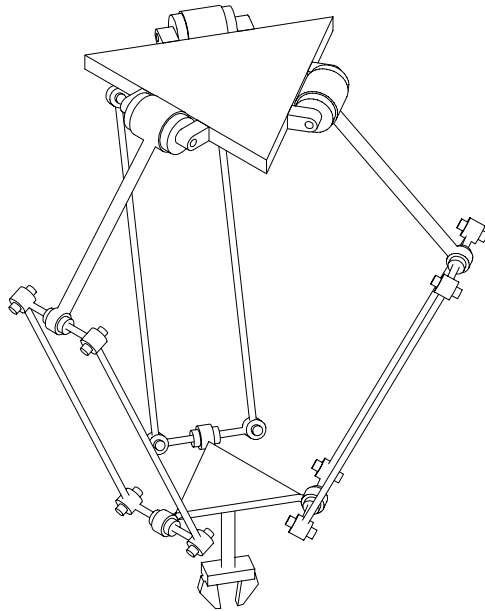


Figure 2.12: Kinematic chain of the Clavel Delta robot

robot. The MP is capable of translating in 3D space with respect to the upper plate, which is considered fixed. The two plates are coupled by means of three legs, each with a RRIIR chain.

To be true, the Π -joints of the actual Delta are not composed of R joints, but rather of *orientable pin joints*, equivalent to S joints. The reason is that providing parallelism between any pair of R axes is physically impossible. To allow for *assemblability*, then, a margin of manoeuvre must be provided.

While Clavel did not cite any group-theoretical reasoning behind his ingenious design, an analysis in this framework will readily explain the principle of operation of the robot. This analysis is conducted on the ideal kinematic chain displayed in Fig. 2.12.

The i th leg is a generator of the Schönflies $\mathcal{X}(\mathbf{e}_i)$ subgroup, with \mathbf{e}_i denoting the unit vector parallel to the axis of the i th motor. That is, the i th leg generates a Schönflies subgroup of displacements comprising translations in 3D space and one rotation about an axis parallel to \mathbf{e}_i . The subset of EE displacements is thus the intersection of the three subgroups $\mathcal{X}(\mathbf{e}_i)$, for $i = 1, 2, 3$, i.e., the subgroup \mathcal{T}_3 . Therefore, the EE is capable of pure translations in 3D space. This kinematic chain is, thus, of the exceptional type.

One second applications example is the microfinger of Japan's Mechanical Engineering Laboratory (MEL) at Tsukuba (Arai et al., 1996), as displayed in Fig. 2.13. In the MEL design, the authors use a structure consisting of two plates that translate with respect to each other by means of three legs coupling the plates. The i th leg entails a RIIIR chain, shown in Fig. 2.14, that generates the Schönflies subgroup in the direction of a unit vector \mathbf{e}_i , for $i = 1, 2, 3$. The three unit vectors, moreover, are coplanar and make angles of 120° pairwise. The motion of the moving plate is thus the result of the intersection of these

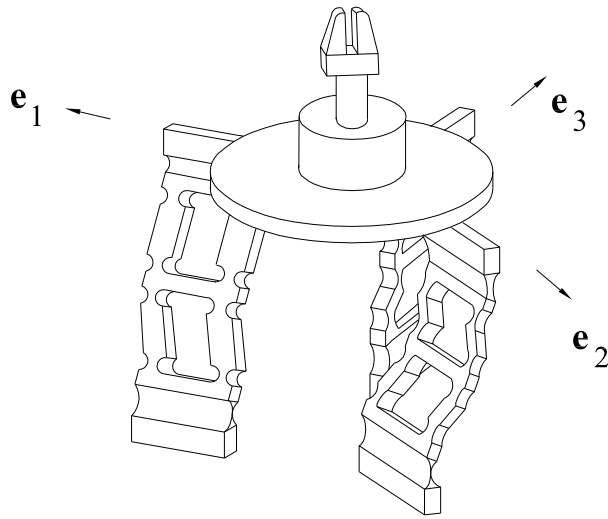


Figure 2.13: The MEL microfinger

three subgroups, which is, in turn, the \mathcal{T}_3 subgroup. Moreover, the kinematic chain of each leg is made of an elastic material in one single piece, in order to allow for micrometric displacements.

Another example is the Y-Tristar robot, developed at Ecole Centrale de Paris by Hervé and Sparacino (1992). One more application of the same concepts is the four-dof SCARA-motion generator proposed by Angeles et al., (2000), and displayed in Fig. 2.15. This robot entails a kinematic chain of the RIIRII type with two vertical revolute and two Π -pairs lying in distinct, vertical planes. The Schönflies subgroup generated by this device is of vertical axis. While Delta and Y-Tristar are made up of Schönflies motion generators, the product of all these is the translation subgroup \mathcal{T}_3 . A Schönflies motion generator with parallel architecture is possible, as shown in Fig. 2.16. This architecture is the result of coupling two identical Schönflies motion generators of the type displayed in Fig. 2.15, each generating the same Schönflies subgroup. As a result, the two-legged parallel robot generates the intersection of two identical subgroups, which is the same subgroup. Yet another application of the Π pair is found in the four-degree-of-freedom parallel robot patented by Company et al. (2001), and now marketed by Adept Technology, Inc. under the trade mark Quattro s650. A photograph of this robot is displayed in Fig. 2.17.

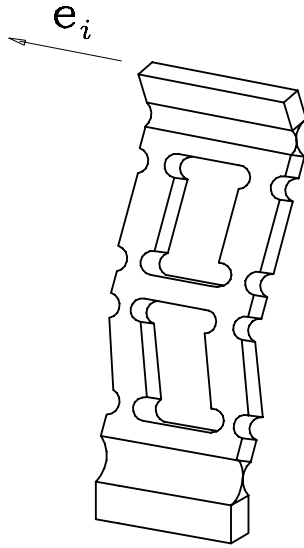


Figure 2.14: The i th leg of the MEL microfinger

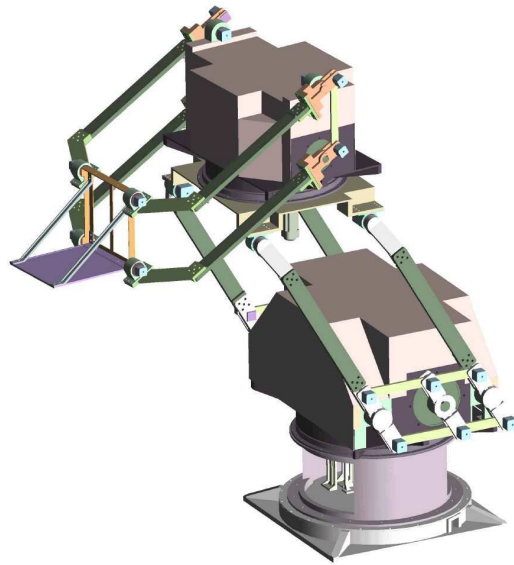


Figure 2.15: A serial-parallel Schönflies-motion generator with a RIIRII architecture

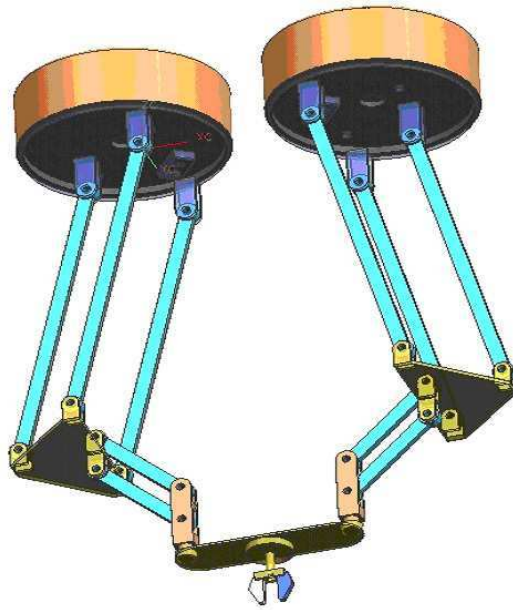


Figure 2.16: A parallel Schönflies-motion generator composed of two RIIRII legs



Figure 2.17: Adept Technology's Quattro robot, a parallel Schönflies-motion generator

Chapter 3

Function Generation

3.1 Introduction

Linkages are the most common means of producing a large variety of motions of a rigid body, termed the *output link*, about an axis fixed to the machine frame. In the best known applications, motion is produced by a motor, usually running at a constant rpm, and coupled by means of a speed reducer—gear train, harmonic drive, or similar—to the *input link*. Under these conditions, the input link moves at a constant speed as well. Other applications of linkages involve alternative forms of actuation, such as motors under computer control, whose motion is all but uniform, and dictated by unpredictable changes in the environment, that are detected by means of sensors sending their signals to the computer generating the signals fed into the motor. Such applications fall in the realm of mechatronic systems.

In one more class of applications, the linkage is driven by a human actuator. Examples of this class are numerous, and sometimes taken for granted, e.g., when cutting a paper sheet with scissors, when pedalling a bicycle, etc. In the case of scissors, the two links of this instrument form what is known as a *dyad*, with the two links coupled by a R pair. This dyad is coupled to a second one, formed by the two proximal phalanges of the thumb and the index finger, thereby forming a four-bar linkage. Likewise, in the case of a bicycle, the frame and one of the two pedals form a dyad, which couples with a second dyad, that formed by the calf and the thigh of a human user, thereby forming, again, a four-bar linkage.

One more application of the concepts studied in this chapter involves *parameter identification*, whereby a linkage exists but is not accessible for measurements, and we want to know its dimensions. Take the case of the subtalar and ankle-joint complex, which is known to entail a closed kinematic chain, i.e., a linkage, but its joints are not readily accessible for measurement. We can cite here a case in which a series of experiments was conducted, measuring input and output angles, from which linkage dimensions were

estimated by fitting the measurements to a linkage kinematic model (Wright et al, 1964).

3.2 Input-Output Functions

3.2.1 Planar Four-Bar Linkages

The classical problem of function generation was first formulated algebraically by Freudenstein in a seminal paper that has been recognized as the origin of modern kinematics (Freudenstein, 1955). In that paper, Freudenstein set to finding the link lengths $\{a_i\}_1^4$ of the planar four-bar linkage displayed in Fig. 3.1 so as to obtain a prescribed relation between the angles ψ and ϕ .

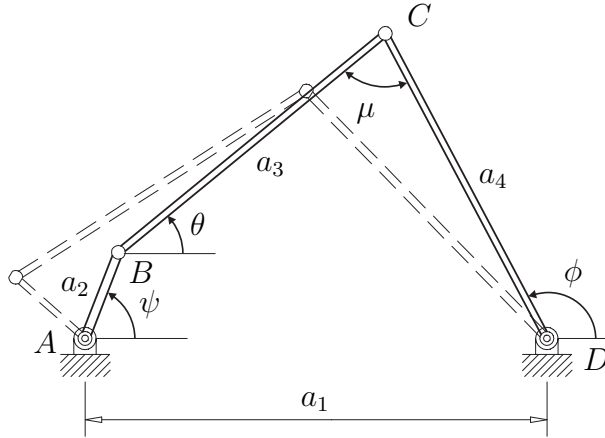


Figure 3.1: A four-bar linkage for function generation

In Fig. 3.1, ψ denotes the *input angle* of the linkage; ϕ the *output angle*; θ the *coupler angle*; and μ the *transmission angle*, which will be studied in Section 3.6. We state below the *function-generation problem* associated with the linkage of Fig. 3.1:

Find $\{a_k\}_1^4$ so that the linkage will produce the set of input-output pairs $\{\psi_k, \phi_k\}_1^m$.

Implicit in the foregoing statement is an algebraic relation between the two angles, ψ and ϕ , known as the *input-output equation* (IOE), which is assumed to be available in the form of an *implicit function*, namely,

$$F(\psi, \phi) = 0 \quad (3.1)$$

In formulating the input-output equation, we introduce four two-dimensional vectors:

$$\mathbf{r}_1 \equiv \overrightarrow{AB} = a_2 \begin{bmatrix} \cos \psi \\ \sin \psi \end{bmatrix}, \quad \mathbf{r}_2 \equiv \overrightarrow{BC} = a_3 \begin{bmatrix} \cos \theta \\ \sin \theta \end{bmatrix}, \quad (3.2a)$$

$$\mathbf{r}_3 \equiv \overrightarrow{AD} = a_1 \begin{bmatrix} 1 \\ 0 \end{bmatrix}, \quad \mathbf{r}_4 \equiv \overrightarrow{DC} = a_4 \begin{bmatrix} \cos \phi \\ \sin \phi \end{bmatrix} \quad (3.2b)$$

From Fig. 3.1 follows that

$$\mathbf{r}_1 + \mathbf{r}_2 = \mathbf{r}_3 + \mathbf{r}_4 \quad (3.3)$$

Obviously, we need a *scalar* relation between the input and output angles, but we have derived above a vector equation. Note, however, that the angles of interest appear in \mathbf{r}_1 and \mathbf{r}_4 ; \mathbf{r}_3 remains constant throughout the linkage motion; and \mathbf{r}_2 contains an *unwanted unknown*, θ . This is eliminated below: From eq.(3.3),

$$\mathbf{r}_2 = \mathbf{r}_3 + \mathbf{r}_4 - \mathbf{r}_1 \quad (3.4)$$

Now, the right-hand side of the above equation is independent of this angle. If we take the *Euclidean norm*, a.k.a. the *magnitude*, of both sides of eq.(3.4), then angle θ is eliminated, for the magnitude of \mathbf{r}_2 is independent of this angle; in fact, this magnitude is nothing but the link length a_3 . We thus have

$$\|\mathbf{r}_2\|^2 = \|\mathbf{r}_3 + \mathbf{r}_4 - \mathbf{r}_1\|^2 \quad (3.5)$$

Upon expansion,

$$\|\mathbf{r}_2\|^2 = \|\mathbf{r}_3\|^2 + \|\mathbf{r}_4\|^2 + \|\mathbf{r}_1\|^2 + 2\mathbf{r}_3^T \mathbf{r}_4 - 2\mathbf{r}_3^T \mathbf{r}_1 - 2\mathbf{r}_4^T \mathbf{r}_1 \quad (3.6)$$

where

$$\begin{aligned} \|\mathbf{r}_1\|^2 &= a_2^2, & \|\mathbf{r}_2\|^2 &= a_3^2, & \|\mathbf{r}_3\|^2 &= a_1^2, & \|\mathbf{r}_4\|^2 &= a_4^2 \\ \mathbf{r}_3^T \mathbf{r}_4 &= a_1 a_4 \cos \phi, & \mathbf{r}_3^T \mathbf{r}_1 &= a_1 a_2 \cos \psi, & \mathbf{r}_4^T \mathbf{r}_1 &= a_2 a_4 \cos(\phi - \psi) \end{aligned}$$

Plugging the foregoing expressions into eq.(3.6) yields

$$a_3^2 = a_1^2 + a_4^2 + a_2^2 + 2a_1 a_4 \cos \phi - 2a_1 a_2 \cos \psi - 2a_2 a_4 \cos(\phi - \psi) \quad (3.7)$$

which is already a scalar relation between the input and the output angles, with the link lengths as parameters. However, this relation is not yet in the most suitable form for our purposes. Indeed, it is apparent that a scaling of the link lengths by the same factor does not change the input-output relation, and hence, the above equation cannot yield all four link lengths. This means that we can only obtain the relative values of the link lengths for a set of prescribed input-output angles. One more remark is in order: the link lengths appear as unknowns when a pair of input-output angles is given; moreover, these unknowns appear quadratically in that equation. Thus, simply dividing the two sides of the equation by any link length will still yield a quadratic equation in the link-length ratios. What Freudenstein cleverly realized was that by means of a suitable *nonlinear mapping* from link lengths into nondimensional parameters, a linear equation in these parameters can be produced. To this end, both sides of eq.(3.7) are divided by $2a_2 a_4$. Once this is done, the definitions below are introduced:

$$k_1 \equiv \frac{a_1^2 + a_2^2 - a_3^2 + a_4^2}{2a_2 a_4}, \quad k_2 \equiv \frac{a_1}{a_2}, \quad k_3 \equiv \frac{a_1}{a_4} \quad (3.8)$$

which are the *Freudenstein parameters* of the linkage at hand. The inverse relations are readily derived, if in terms of one of the link lengths, say a_1 :

$$a_2 = \frac{1}{k_2}a_1, \quad a_4 = \frac{1}{k_3}a_1, \quad a_3 = \sqrt{a_1^2 + a_2^2 + a_4^2 - 2k_1a_2a_4} \quad (3.9)$$

The IOE (3.7) then becomes

$$k_1 + k_2 \cos \phi - k_3 \cos \psi = \cos(\phi - \psi) \quad (3.10)$$

thereby obtaining the *Freudenstein equation*. Notice that, upon writing this equation in homogeneous form, we obtain $F(\psi, \phi)$ of eq.(3.1), namely,

$$F(\psi, \phi) \equiv k_1 + k_2 \cos \phi - k_3 \cos \psi - \cos(\phi - \psi) = 0 \quad (3.11)$$

If we now write eq.(3.10) for $\{\psi_k, \phi_k\}_1^m$, we obtain m linear equations in the three Freudenstein parameters, arrayed in vector \mathbf{k} , namely,

$$\mathbf{S}\mathbf{k} = \mathbf{b} \quad (3.12)$$

where \mathbf{S} is the $m \times 3$ *synthesis matrix*; \mathbf{k} is the 3-dimensional vector of unknown Freudenstein parameters; and \mathbf{b} is an m -dimensional vector of known components, i.e.,

$$\mathbf{S} \equiv \begin{bmatrix} 1 & \cos \phi_1 & -\cos \psi_1 \\ 1 & \cos \phi_2 & -\cos \psi_2 \\ \vdots & \vdots & \vdots \\ 1 & \cos \phi_m & -\cos \psi_m \end{bmatrix}, \quad \mathbf{k} \equiv \begin{bmatrix} k_1 \\ k_2 \\ k_3 \end{bmatrix}, \quad \mathbf{b} \equiv \begin{bmatrix} \cos(\phi_1 - \psi_1) \\ \cos(\phi_2 - \psi_2) \\ \vdots \\ \cos(\phi_m - \psi_m) \end{bmatrix} \quad (3.13)$$

Three cases arise:

$m < 3$: Case $m = 1$ reduces to the synthesis of a quadrilateron with two given angles, which admits infinitely many solutions. Case $m = 2$ seldom occurs in practice without additional conditions, that render the problem more complex, e.g., in the synthesis of quick-return mechanisms;

$m = 3$: The number of equations coincides with the number of unknowns, and hence, the problem admits one *unique* solution—unless the synthesis matrix is **singular**. We are in the case of *exact synthesis*;

$m > 3$: The number of equations exceeds the number of unknowns, which leads to an over-determined system of equations. Hence, no solution is possible, in general, but an optimum solution can be found that best approximates the synthesis equations in the least-square sense. Problem falls in the category of *approximate synthesis*.

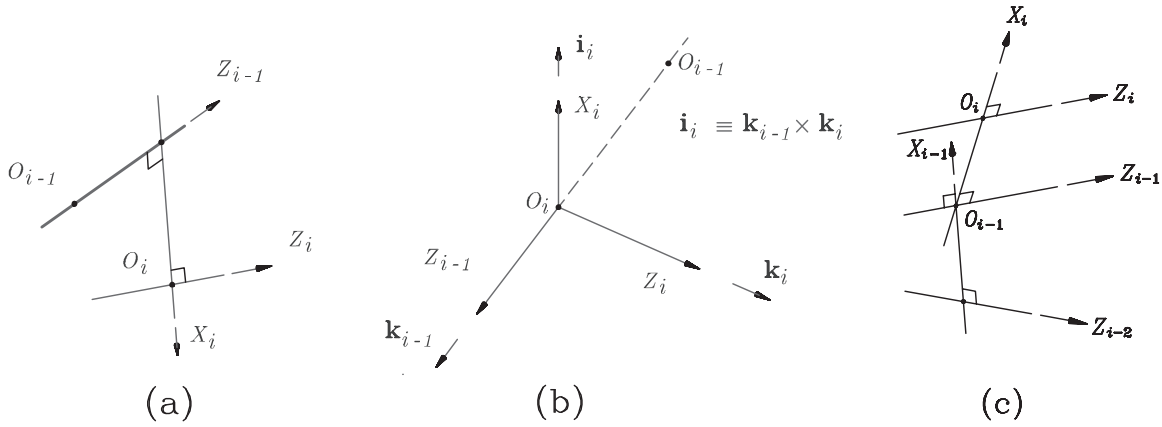


Figure 3.2: Definition of X_i when Z_{i-1} and Z_i : (a) are skew; (b) intersect; and (c) are parallel.

3.2.2 The Denavit-Hartenberg Notation

Prior to deriving the I/O equations of spherical and spatial linkages, we introduce the *Denavit-Hartenberg (DH) notation*, which is extremely useful in the analysis of kinematic chains in three dimensions.

In order to uniquely describe the *architecture* of a kinematic chain, i.e., the relative location and orientation of its neighbouring-pair axes, the Denavit-Hartenberg notation (Denavit and Hartenberg, 1964) is introduced. To this end, we assume a *simple kinematic chain*, open or closed, with links numbered $1, \dots, n$, the i th pair being defined as that coupling the $(i-1)$ st link with the i th link. Next, a coordinate frame \mathcal{F}_i is defined with origin O_i and axes X_i, Y_i, Z_i . This frame is attached to the $(i-1)$ st link—**not** to the i th link!—for $i = 1, \dots, n$. This is done by following the rules given below:

1. Z_i is the axis of the i th pair. Notice that there are two possibilities of defining the positive direction of this axis, since each pair axis is only a line, not a directed segment. Moreover, the Z_i axis of a prismatic pair can be located arbitrarily, since only its direction is defined by the axis of this pair.
2. X_i is defined as the common perpendicular to Z_{i-1} and Z_i , directed from the former to the latter, as shown in Fig. 3.2a. Notice that if these two axes intersect, the positive direction of X_i is undefined and hence, can be freely assigned. Henceforth, we will follow the *right-hand* rule in this case. This means that if unit vectors $\mathbf{i}_i, \mathbf{k}_{i-1}$, and \mathbf{k}_i are attached to axes X_i, Z_{i-1} , and Z_i , respectively, as indicated in Fig. 3.2b, then \mathbf{i}_i is defined as $\mathbf{k}_{i-1} \times \mathbf{k}_i$. Moreover, if Z_{i-1} and Z_i are parallel, the location of X_i is undefined. In order to define it uniquely, we will specify X_i as passing through the origin of the $(i-1)$ st frame, as shown in Fig. 3.2c.
3. The *distance* between Z_i and Z_{i+1} is defined as a_i , which is thus *nonnegative*.

4. The Z_i -coordinate of the intersection O'_i of Z_i with X_{i+1} is denoted by b_i . Since this quantity is a coordinate, it can be either positive or negative. Its absolute value is the distance between X_i and X_{i+1} , also called the *offset* between successive common perpendiculars.
5. The angle between Z_i and Z_{i+1} is defined as α_i and is measured about the positive direction of X_{i+1} . This item is known as the *twist angle* between successive pair axes.
6. The angle between X_i and X_{i+1} is defined as θ_i and is measured about the positive direction of Z_i .

3.2.3 Spherical Four-Bar-Linkages

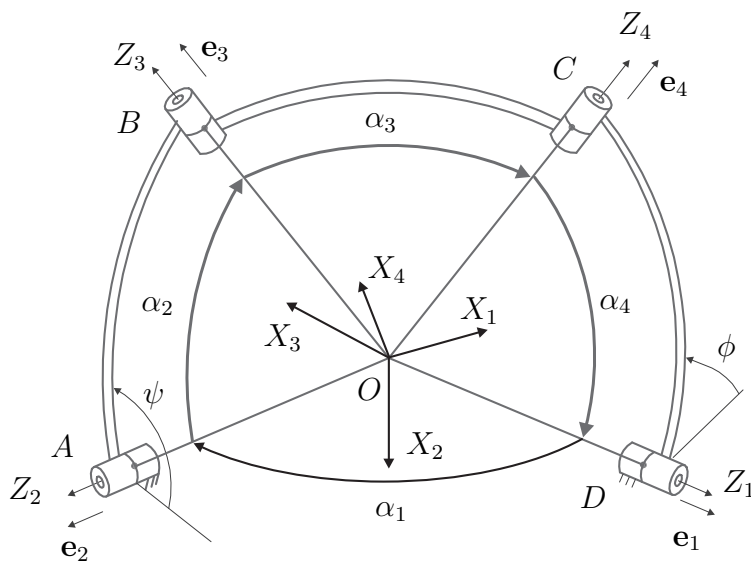


Figure 3.3: A spherical four-bar linkage for function generation

A spherical four-bar linkage for function generation is depicted in Fig. 3.3. In this case, we are interested in deriving a relation between the input angle ψ and the output angle ϕ , that should include the *linkage dimensions* $\{\alpha_i\}_1^4$ as parameters. To this end, we introduce the unit vectors $\{\mathbf{e}_i\}_1^4$, directed along the concurrent axes of the four revolute, as depicted in Fig. 3.3. Notice that, in order to bring the notation adopted for planar four-bar linkages, as proposed by Freudenstein and displayed in Fig. 3.1, in line with the Denavit-Hartenberg notation, we have placed Z_1 along the axis of the output joint and Z_2 along that of the input joint.

Deriving the desired relation is now a simple matter, for we have one geometric relation at our disposal, namely,

$$\mathbf{e}_3 \cdot \mathbf{e}_4 = \cos \alpha_3 \quad (3.14)$$

Now, in order to perform the foregoing dot product, we need expressions for its two factors that satisfy two conditions: (i) the expressions should give the two unit vectors \mathbf{e}_3 and \mathbf{e}_4 in the same coordinate frame; and (ii) the expressions should involve the input and output angles. Apparently, if we choose \mathcal{F}_2 , the coordinate frame fixed to the mechanism frame, to represent the two unit vectors in question, we will have the desired expressions.

Under the Denavit-Hartenberg notation, the Z_i -axis is defined as the axis of the i th revolute, while X_i is defined as the common perpendicular to Z_{i-1} and Z_i , directed from the former to the latter, according to the *right-hand rule*. These axes are illustrated in Fig. 3.3.

Now, the matrix rotating \mathcal{F}_i into \mathcal{F}_{i+1} is denoted \mathbf{Q}_i . This matrix is given as (Denavit and Hartenberg, 1964; Angeles, 2007):

$$\mathbf{Q}_i \equiv [\mathbf{Q}_i]_i \equiv \begin{bmatrix} \cos \theta_i & -\lambda_i \sin \theta_i & \mu_i \sin \theta_i \\ \sin \theta_i & \lambda_i \cos \theta_i & -\mu_i \cos \theta_i \\ 0 & \mu_i & \lambda_i \end{bmatrix} \quad (3.15)$$

where $\lambda_i \equiv \cos \alpha_i$ and $\mu_i \equiv \sin \alpha_i$, while θ_i was already defined in Subsection 3.2.2. Apparently, vector \mathbf{e}_i in \mathcal{F}_i , denoted $[\mathbf{e}_i]_i$, is given by

$$[\mathbf{e}_i]_i = \begin{bmatrix} 0 \\ 0 \\ 1 \end{bmatrix} \quad (3.16)$$

Moreover, \mathbf{Q}_i can be regarded as the matrix transforming \mathcal{F}_{i+1} -coordinates into \mathcal{F}_i -coordinates, i.e., for *any* three-dimensional vector \mathbf{v} ,

$$[\mathbf{v}]_i = \mathbf{Q}_i [\mathbf{v}]_{i+1} \quad (3.17)$$

Likewise,

$$[\mathbf{v}]_{i+1} = [\mathbf{Q}_i^T]_i [\mathbf{v}]_i \quad (3.18)$$

More specifically, we represent the foregoing transformations in the abbreviated form:

$$\mathbf{Q}_1: \mathcal{F}_1 \rightarrow \mathcal{F}_2, \quad \mathbf{Q}_2: \mathcal{F}_2 \rightarrow \mathcal{F}_3, \quad \mathbf{Q}_3: \mathcal{F}_3 \rightarrow \mathcal{F}_4, \quad \mathbf{Q}_4: \mathcal{F}_4 \rightarrow \mathcal{F}_1 \quad (3.19a)$$

$$\mathbf{Q}_1: [\cdot]_2 \rightarrow [\cdot]_1, \quad \mathbf{Q}_2: [\cdot]_3 \rightarrow [\cdot]_2, \quad \mathbf{Q}_3: [\cdot]_4 \rightarrow [\cdot]_3, \quad \mathbf{Q}_4: [\cdot]_1 \rightarrow [\cdot]_4 \quad (3.19b)$$

$$\mathbf{Q}_1^T: \mathcal{F}_2 \rightarrow \mathcal{F}_1, \quad \mathbf{Q}_2^T: \mathcal{F}_3 \rightarrow \mathcal{F}_2, \quad \mathbf{Q}_3^T: \mathcal{F}_4 \rightarrow \mathcal{F}_3, \quad \mathbf{Q}_4^T: \mathcal{F}_1 \rightarrow \mathcal{F}_4 \quad (3.19c)$$

$$\mathbf{Q}_1^T: [\cdot]_1 \rightarrow [\cdot]_2, \quad \mathbf{Q}_2^T: [\cdot]_2 \rightarrow [\cdot]_3, \quad \mathbf{Q}_3^T: [\cdot]_3 \rightarrow [\cdot]_4, \quad \mathbf{Q}_4^T: [\cdot]_4 \rightarrow [\cdot]_1 \quad (3.19d)$$

In particular, given expression (3.16) for $[\mathbf{e}_i]_i$, it is apparent that the third column of \mathbf{Q}_i^T or, equivalently, the third row of \mathbf{Q}_i , is $[\mathbf{e}_i]_{i+1}$. By the same token, the third column of \mathbf{Q}_i is $[\mathbf{e}_{i+1}]_i$, i.e.,

$$[\mathbf{e}_i]_{i+1} = \begin{bmatrix} 0 \\ \mu_i \\ \lambda_i \end{bmatrix}, \quad [\mathbf{e}_{i+1}]_i = \begin{bmatrix} \mu_i \sin \theta_i \\ -\mu_i \cos \theta_i \\ \lambda_i \end{bmatrix} \quad (3.20)$$

The vector representations required are derived below. We do this by recalling that $[\mathbf{e}_3]_2$ is the third column of \mathbf{Q}_2 , while $[\mathbf{e}_4]_1$ is the third row of \mathbf{Q}_4 .

$$[\mathbf{e}_3]_2 = \begin{bmatrix} \mu_2 \sin \theta_2 \\ -\mu_2 \cos \theta_2 \\ \lambda_2 \end{bmatrix} \quad (3.21)$$

$$[\mathbf{e}_4]_2 = \mathbf{Q}_1^T [\mathbf{e}_4]_1 \equiv \begin{bmatrix} \cos \theta_1 & \sin \theta_1 & 0 \\ -\lambda_1 \sin \theta_1 & \lambda_1 \cos \theta_1 & \mu_1 \\ \mu_1 \sin \theta_1 & -\mu_1 \cos \theta_1 & \lambda_1 \end{bmatrix} \begin{bmatrix} 0 \\ \mu_4 \\ \lambda_4 \end{bmatrix} \quad (3.22)$$

$$= \begin{bmatrix} \mu_4 \sin \theta_1 \\ \mu_4 \lambda_1 \cos \theta_1 + \lambda_4 \mu_1 \\ -\mu_4 \mu_1 \cos \theta_1 + \lambda_4 \lambda_1 \end{bmatrix} \quad (3.23)$$

which are the expressions sought. Hence,

$$[\mathbf{e}_3^T]_2 [\mathbf{e}_4]_2 = \mu_2 \mu_4 \sin \theta_1 \sin \theta_2 - \mu_2 \cos \theta_2 (\mu_4 \lambda_1 \cos \theta_1 + \lambda_4 \mu_1) + \lambda_2 (-\mu_4 \mu_1 \cos \theta_1 + \lambda_4 \lambda_1) \quad (3.24)$$

Upon substituting the above expression into eq.(3.14), we obtain

$$\lambda_4 \lambda_1 \lambda_2 - \lambda_3 - \lambda_4 \mu_1 \mu_2 \cos \theta_2 - \mu_4 \lambda_1 \mu_2 \cos \theta_1 \cos \theta_2 - \mu_4 \mu_1 \lambda_2 \cos \theta_1 + \mu_2 \mu_4 \sin \theta_1 \sin \theta_2 = 0 \quad (3.25)$$

which is a form of the input-output equation sought. This equation can be simplified upon realizing that the last coefficient of its left-hand side cannot vanish, least one of the input and output links, or even both, shrinks to one point on the sphere—a consequence of at least one of α_2 and α_4 vanishing or equating π . In this light, we can safely divide both sides of the above equation by $\mu_2 \mu_4$. Moreover, in order to render the same equation terser, we introduce the *Freudenstein parameters for the spherical linkage* below:

$$k_1 \equiv \frac{\lambda_4 \lambda_1 \lambda_2 - \lambda_3}{\mu_2 \mu_4}, \quad k_2 = \frac{\lambda_4 \mu_1}{\mu_4}, \quad k_3 = \lambda_1, \quad k_4 = \frac{\mu_1 \lambda_2 \lambda_4}{\mu_2 \mu_4} \quad (3.26)$$

Upon dividing both sides of eq.(3.25) by $\mu_2 \mu_4$, and introducing definitions (3.26) in the equation thus resulting, the same equation becomes

$$k_1 - k_2 \cos \theta_2 - k_3 \cos \theta_1 \cos \theta_2 - k_4 \cos \theta_1 + \sin \theta_1 \sin \theta_2 = 0 \quad (3.27)$$

This equation, however, involves a relation between angles θ_1 and θ_2 of the DH notation, which are different from, although related to, the input and the output angles ψ and ϕ . To better understand the relation between the two pairs of angles, we sketch these in Fig. 3.4. From this figure, it is apparent that

$$\theta_2 = \psi + \pi, \quad \theta_1 = 2\pi - \phi \quad \text{or} \quad \theta_1 = -\phi \quad (3.28)$$

Hence,

$$\cos \theta_2 = -\cos \psi, \quad \sin \theta_2 = -\sin \psi, \quad \cos \theta_1 = \cos \phi, \quad \sin \theta_1 = -\sin \phi \quad (3.29)$$

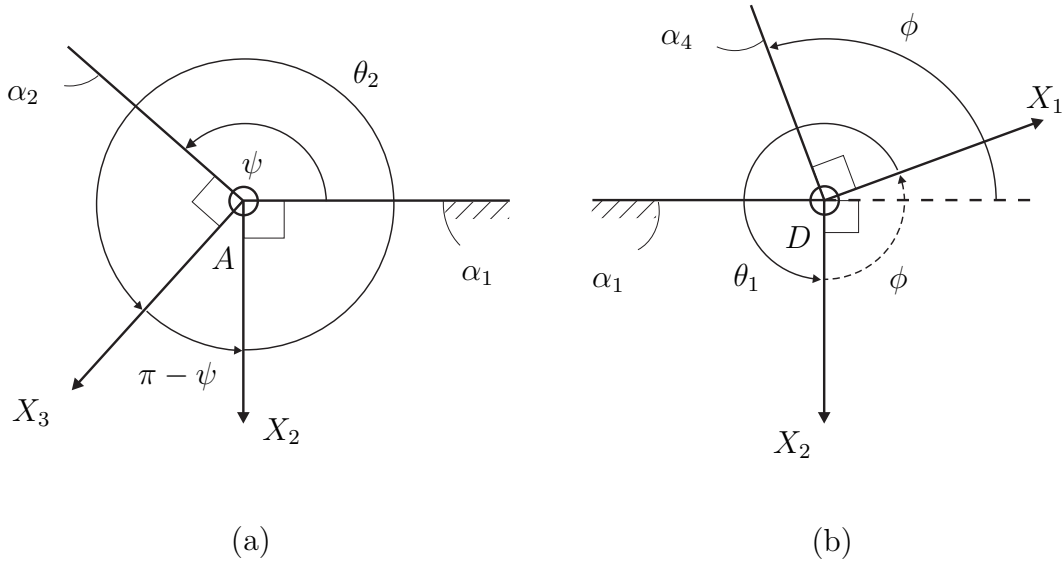


Figure 3.4: Relation between input and output angles with their counterparts in the DH notation: (a) ψ and θ_2 ; and (b) ϕ and θ_1

Substitution of relations (3.29) into eq.(3.27) leads to

$$F(\psi, \phi) \equiv k_1 + k_2 \cos \psi + k_3 \cos \psi \cos \phi - k_4 \cos \phi + \sin \psi \sin \phi = 0 \quad (3.30)$$

which is the *input-output equation for spherical linkages* written in terms of the input and output angles ψ and ϕ , respectively.

Either eq.(3.27) or eq.(3.30) can be used to find the output angle ϕ for a given linkage and a given value of the input angle ψ , which constitutes the *analysis problem*. The same equation is to be used for synthesis, as described below.

In a synthesis problem, we aim at calculating the set of unknown linkage angles $\{\alpha_i\}_1^4$, for a *given* set of pairs $\{(\psi_i, \phi_i)\}_1^m$ of I/O angle values that the linkage is to meet. In order to obtain the synthesis equations allowing us to compute the set of Freudenstein parameters leading to the desired linkage, we proceed as in the planar case and write eq.(3.30) for the given set of pairs of angle values, thus obtaining the *synthesis equations* in the form of eq.(3.12), as derived for planar four-bar linkages. Obviously, the synthesis matrix \mathbf{S} and vectors \mathbf{b} and \mathbf{k} now change to

$$\mathbf{S} \equiv \begin{bmatrix} 1 & \cos \psi_1 & \cos \psi_1 \cos \phi_1 & -\cos \phi_1 \\ 1 & \cos \psi_2 & \cos \psi_2 \cos \phi_2 & -\cos \phi_2 \\ \vdots & \vdots & \vdots & \\ 1 & \cos \psi_m & \cos \psi_m \cos \phi_m & -\cos \phi_m \end{bmatrix}, \quad \mathbf{k} \equiv \begin{bmatrix} k_1 \\ k_2 \\ k_3 \\ k_4 \end{bmatrix}, \quad \mathbf{b} \equiv \begin{bmatrix} -\sin \psi_1 \sin \phi_1 \\ -\sin \psi_2 \sin \phi_2 \\ \vdots \\ -\sin \psi_m \sin \phi_m \end{bmatrix} \quad (3.31)$$

Similar to the planar case, we have exact synthesis when the number m of given pairs of input-output angular values equals the number of Freudenstein parameters at hand, which in this case happens when $m = 4$. When $m > 4$, then we have a problem of

approximate synthesis.

However, eq.(3.30) only provides values for the linkage parameters $\{k_i\}_1^4$. Hence, we need a means to convert the latter into the former.

Notice that the relations between the two sets, $\{\alpha_i\}_1^4$ and $\{k_i\}_1^4$, are nonlinear, and hence, solving eqs.(3.26) for the former needs careful planning. For starters, the foregoing equations are rewritten explicitly in terms of the linkage dimensions $\{\alpha_i\}_1^4$, and reordered conveniently:

$$c\alpha_1 - k_3 = 0 \quad (3.32a)$$

$$c\alpha_4 s\alpha_1 - k_2 s\alpha_4 = 0 \quad (3.32b)$$

$$c\alpha_2 c\alpha_4 s\alpha_1 - k_4 s\alpha_2 s\alpha_4 = 0 \quad (3.32c)$$

$$c\alpha_1 c\alpha_2 c\alpha_4 - c\alpha_3 - k_1 s\alpha_2 s\alpha_4 = 0 \quad (3.32d)$$

In a semigraphical method, based on *contour-intersection* and favoured in this course, all but two of the unknowns are first eliminated from the set of nonlinear equations, thereby ending up with a reduced number of equations in the two remaining unknowns. Each of these equations is then plotted in the plane of the two unknowns, which yields one contour per bivariate equation, in that plane. All real solutions are then found *by inspection*, at the intersections of all the contours. Notice that, if the reduced system comprises more than two bivariate equations, then the system entails algebraic redundancy, which is convenient, as this adds *robustness* to the system.

In the particular case at hand, the transformation sought can be most readily found by noticing the structure of eqs.(3.32a–d): the first equation involves one single unknown, α_1 ; the second only *one new* unknown, α_4 ; the third only *one new* unknown, α_2 ; and the fourth only one new unknown as well, α_3 . Hence, we devise the *algorithm* below:

- i) From eq.(3.32a), compute $\alpha_1 = \cos^{-1}(k_3) \Rightarrow$ two possible values of α_1 ;
- ii) From eq.(3.32b), compute $\alpha_4 = \tan^{-1}(\sin \alpha_1/k_2) \Rightarrow$ two possible values of α_4 for each value of $\sin \alpha_1$;
- iii) From eq.(3.32b), $\cos \alpha_4 \sin \alpha_1 = k_2 \sin \alpha_4$, which, upon substitution into eq.(3.32c), leads to $(k_2 \cos \alpha_2 - k_4 \sin \alpha_2) \sin \alpha_4 = 0$. However, $\sin \alpha_4 \neq 0$ for a physically meaningful linkage, and hence, the two sides of the foregoing equation can be divided by $\sin \alpha_4$, which then leads to $\alpha_2 = \tan^{-1}(k_2/k_4)$, thereby obtaining two values of α_2 , *independent* of all other α_i values;
- iv) From eq.(3.32a), $\cos \alpha_1 = k_3$, eq.(3.32b) leading to $\sin \alpha_4 = \cos \alpha_4 \sin \alpha_1/k_2$; moreover, eq.(3.32c) leads to $\cos \alpha_2 \cos \alpha_4 = k_4 \sin \alpha_2 \sin \alpha_4/\sin \alpha_1$. If the three foregoing expressions are substituted into eq.(3.32d), then $\cos \alpha_3 = (k_3 k_4 - k_1 \sin \alpha_1) \sin \alpha_2 \cos \alpha_4/k_2$, whence, $\alpha_3 = \cos^{-1}[(k_3 k_4 - k_1 \sin \alpha_1) \sin \alpha_2 \cos \alpha_4/k_2] \Rightarrow$ two values of α_3 are obtained for each possible combination of values of $\sin \alpha_1$, $\sin \alpha_2$ and $\cos \alpha_4$.

In summary, then, we have: four possible combinations of values of α_1 and α_4 ; two possible values of α_2 ; and 16 values¹ of α_3 . Hence, we end up with up to $4 \times 2 \times 16 = 128$ sets of $\{\alpha_i\}_1^4$ values for one single set $\{k_i\}_1^4$. However, some of the 128 sets of linkage dimensions found above may be complex, and hence, uninteresting. The problem may also not admit any single real solution, for example, if $|k_3| > 1$. As well, α_3 becomes complex when $|(k_3k_4 - k_1 \sin \alpha_1) \sin \alpha_2 \cos \alpha_4 / k_2| > 1$. That is, for a feasible linkage, two conditions must be obeyed by the Freudenstein parameters $\{k_i\}_1^4$:

$$|k_3| \leq 1 \quad \text{and} \quad \left| \frac{(k_3k_4 - k_1 \sin \alpha_1) \sin \alpha_2 \cos \alpha_4}{k_2} \right| \leq 1 \quad (3.33)$$

Note that the semigraphical method *filters* all complex solutions and is guaranteed to yield all real solutions. In order to implement the semigraphical method, first four pairs of values (α_1, α_4) are computed from eqs.(3.32a & b). Each of these pairs is then substituted into eqs.(3.32c & d), thereby obtaining four pairs of contours in the α_3 - α_4 plane. The intersections of each pair of contours, which can be estimated by inspection, yield one subset of real solutions. Each of these estimates of α_3 and α_4 values can then be used as an *initial guess* for a Newton-Raphson solution of the two equations. Due to the proximity of each estimate from the pair of real roots, the Newton-Raphson method should converge in a pair of iterations for a reasonable tolerance. If each pair of contours is plotted inside a square of side π centred at the origin of the α_2 - α_3 plane, *all real roots* of the problem have been computed.

Finally, notice that any *spherical triangle* and, in fact, any *spherical polygon* defined on the surface of the unit sphere, has an *antipodal* counterpart. In this light, then, even if we end up with a full set of feasible linkage dimensions, only 64 four-bar linkages defined by this set are distinct.

3.2.4 Spatial Four-Bar-Linkages

The analysis of spatial four-bar linkages relies heavily on the algebra of *dual numbers*, which is extensively discussed in Appendix A. What we should recall now is (a) the usual representation of dual quantities, by means of a “hat” (^) on top of the variable in question and (b) the definition of the *dual unit*, ϵ , via its two properties

$$\epsilon \neq 0, \quad \epsilon^2 = 0 \quad (3.34)$$

A general layout of a spatial four-bar linkage is included in Fig. 3.5, in which we use the Denavit-Hartenberg notation, introduced in Subsection 3.2.2. Similar to that subsection, we have laid the output axis along Z_1 , in order to comply both with the DH notation and with the notation adopted in Figs. 3.1 and 3.3. In this case, ψ and ϕ denote the input

¹Two possible values of each of $\sin \alpha_1, \sin \alpha_2$ and $\cos \alpha_4$, which yields eight possible values of $\cos \alpha_3$, but the latter yields, in turn, two possible values of α_3 .

and the output angles, as in Subsection 3.2.3, their relations with angles θ_1 and θ_2 of the DH notation being exactly as in the spherical case, namely,

$$\psi = \theta_2 - \pi, \quad \phi = 2\pi - \theta_1 \quad (3.35)$$

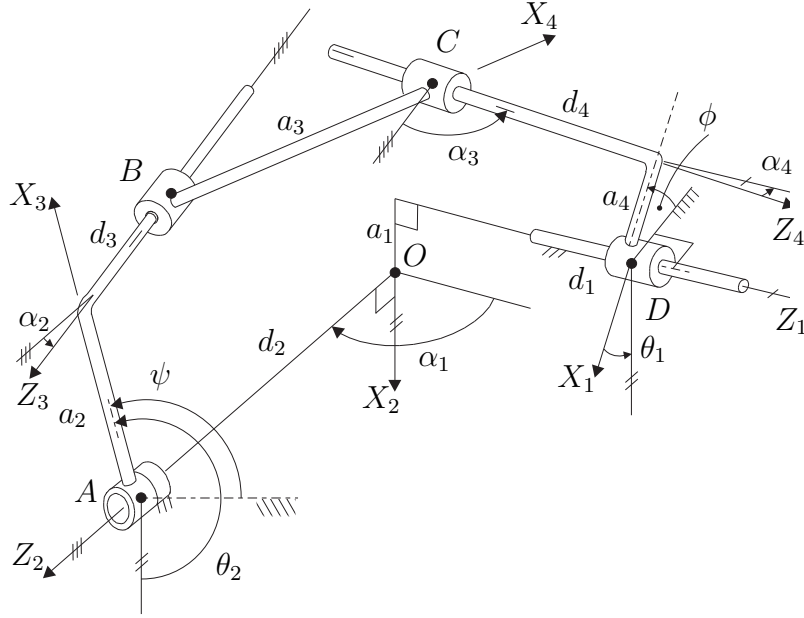


Figure 3.5: A RCCC linkage for function generation

The I/O equation of the RCCC linkage is most readily derived by resorting to the *Principle of Transference* (Dimentberg, 1965; Rico Martínez and Duffy, 1995), which is cited below:

The kinematics and statics relations of spatial linkages and cam mechanisms can be derived upon replacing the real variables occurring in the corresponding relations for spherical linkages by dual numbers.

Put quite simply, the I/O equation of the RCCC linkage can be derived from that of the spherical RRRR linkage upon “putting hats” on the variables and the (Freudenstein) parameters occurring in eq.(3.30), thereby obtaining

$$\hat{F}(\psi, \hat{\phi}) \equiv \hat{k}_1 + \hat{k}_2 \cos \psi + \hat{k}_3 \cos \psi \cos \hat{\phi} - \hat{k}_4 \cos \hat{\phi} - \hat{k}_5 \sin \psi \sin \hat{\phi} = 0 \quad (3.36)$$

where ψ hasn’t been “hatted” for the reasons given below: *dualization* of an angular displacement θ about an axis \mathcal{A} is an operation by which a sliding d_o is introduced along the same axis; the dual angle $\hat{\theta}$ is then represented as

$$\hat{\theta} = \theta + \epsilon d_o \quad (3.37)$$

the variable θ then being referred to as the *primal part* of $\hat{\theta}$, d_o being the *dual part*. Notice that the latter being a sliding, its units are those of length; the dual unit ϵ can then be thought of as “having units of length-inverse.” The *dualization operation* then,

can be kinematically interpreted as the replacement of a R joint of axis \mathcal{A} by a C joint of the same axis. Hence, the RCCC linkage of Fig. 3.5 is obtained by replacing all R joints of the spherical linkage of Fig. 3.3, but that associated with the input angle ψ , with a C joint, which explains why this variable need not be dualized. In this light, then, the dual quantities appearing in eq.(3.36) are to be interpreted as

$$\hat{\phi} = \phi + \epsilon\phi_o, \quad \hat{F}(\psi, \hat{\phi}) = F(\psi, \phi) + \epsilon F_o(\psi, \phi_o), \quad \hat{k}_i \equiv k_i + \epsilon k_{oi}, \quad i = 1, \dots, 4 \quad (3.38)$$

Consistently, then, k_i is dimensionless, while k_{oi} , for $i = 1, \dots, 4$, has units of length. Moreover, if the angle of rotation θ_i , associated with the i th R joint of Fig. 3.3, of the DH notation, for $i = 1, 3, 4$, is dualized, the *dual angles* thus resulting become, in the notation of Fig. 3.5,

$$\hat{\theta}_1 = \theta_1 + \epsilon d_1 = -\phi + \epsilon d_1, \quad \hat{\theta}_2 = \theta_2 = \psi + \pi, \quad \hat{\theta}_3 = \theta_3 + \epsilon d_3, \quad \hat{\theta}_4 = \theta_4 + \epsilon d_4 \quad (3.39)$$

where

$$-\infty < d_i < \infty, \quad i = 1, 3, 4$$

which is an unbounded real number, with units of length. Notice that d_i is not a “length,” properly speaking, because a length is positive, while d_i can be negative, exactly the same as a joint angle.

Now, in order to derive the trigonometric functions of the dual input and output angles, we recall from the Appendix, that a dual function $\hat{f}(\hat{x})$, of the dual variable $\hat{x} \equiv x + \epsilon x_o$ is defined as

$$\hat{f}(\hat{x}) = \hat{f}(x + \epsilon x_o) \equiv f(x) + \epsilon x_o \frac{df(x)}{dx}$$

whence,

$$\cos \hat{\phi} \equiv \cos(\phi) - \epsilon d_1 \sin \phi, \quad \sin \hat{\phi} \equiv \sin \phi + \epsilon d_1 \cos \phi \quad (3.40)$$

Further, the synthesis equations for the spatial four-bar linkage can be readily set up by dualizing those derived for the spherical case, with the synthesis matrix \mathbf{S} and the right-hand side \mathbf{b} of eq.(3.31) substituted by their “hatted” counterparts, namely,

$$\hat{\mathbf{S}}\hat{\mathbf{k}} = \hat{\mathbf{b}} \quad (3.41)$$

where, as usual,

$$\hat{\mathbf{S}} = \mathbf{S} + \mathbf{S}_o, \quad \hat{\mathbf{k}} = \mathbf{k} + \mathbf{k}_o, \quad \hat{\mathbf{b}} = \mathbf{b} + \mathbf{b}_o \quad (3.42)$$

the primal and dual parts of vector $\hat{\mathbf{k}}$ having been displayed componentwise in eq.(3.38). The primal and dual parts of \mathbf{S} and \mathbf{b} are derived below: Upon dualizing \mathbf{S} of eq.(3.31) componentwise, the relation below is obtained:

$$\hat{\mathbf{S}} = \begin{bmatrix} 1 & c\psi_1 & c\psi_1(c\phi_1 - \epsilon u_1 s\phi_1) & -c\phi_1 + \epsilon u_1 s\phi_1 \\ 1 & c\psi_2 & c\psi_2(c\phi_2 - \epsilon u_2 s\phi_2) & -c\phi_2 + \epsilon u_2 s\phi_2 \\ \vdots & \vdots & \vdots & \\ 1 & c\psi_m & c\psi_m(c\phi_m - \epsilon u_m s\phi_m) & -c\phi_m + \epsilon u_m s\phi_m \end{bmatrix} \quad (3.43)$$

or

$$\hat{\mathbf{S}} = \underbrace{\begin{bmatrix} 1 & c\psi_1 & c\psi_1c\phi_1 & -c\phi_1 \\ 1 & c\psi_2 & c\psi_2c\phi_2 & -c\phi_2 \\ \vdots & \vdots & \vdots & \\ 1 & c\psi_m & c\psi_m c\phi_m & -c\phi_m \end{bmatrix}}_{\mathbf{S}} + \epsilon \underbrace{\begin{bmatrix} 0 & 0 & -u_1c\psi_1s\phi_1 & u_1s\phi_1 \\ 0 & 0 & -u_2c\psi_2s\phi_2 & u_2s\phi_2 \\ \vdots & \vdots & \vdots & \\ 0 & 0 & -u_m c\psi_m s\phi_m & u_m s\phi_m \end{bmatrix}}_{\mathbf{S}_o} \quad (3.44)$$

where the definition $u_i \equiv (d_1)_i$ has been introduced. Likewise,

$$\hat{\mathbf{k}} = \underbrace{\begin{bmatrix} k_1 \\ k_2 \\ k_3 \\ k_4 \end{bmatrix}}_{\mathbf{k}} + \epsilon \underbrace{\begin{bmatrix} k_{o1} \\ k_{o2} \\ k_{o3} \\ k_{o4} \end{bmatrix}}_{\mathbf{k}_o}, \quad \hat{\mathbf{b}} = \underbrace{\begin{bmatrix} s\psi_1s\phi_1 \\ s\psi_2s\phi_2 \\ \vdots \\ s\psi_ms\phi_m \end{bmatrix}}_{\mathbf{b}} + \epsilon \underbrace{\begin{bmatrix} u_1s\psi_1c\phi_1 \\ u_2s\psi_2c\phi_2 \\ \vdots \\ u_ms\psi_m c\phi_m \end{bmatrix}}_{\mathbf{b}_o} \quad (3.45)$$

Now, upon equating the primal and the dual parts of eq.(3.41), two real vector equations are obtained, namely,

$$\mathbf{S}\mathbf{k} = \mathbf{b}, \quad \mathbf{S}\mathbf{k}_o + \mathbf{S}_o\mathbf{k} = \mathbf{b}_o \quad (3.46)$$

As the reader can readily verify, the first of the two foregoing equations is identical to that derived for spherical linkages in eq.(3.31). That is, the problem of synthesis of a spatial function generator has been *decoupled* into two, the synthesis procedure then being straightforward:

1. Synthesize first a spherical linkage for the angular input-output data given at the outset;
2. Substitute vector \mathbf{k} obtained from step 1 along with the additional data $\{(d_1)_i\}_1^m$, with $u_i \leftarrow (d_1)_i$, for $i = 1, \dots, m$, and solve the second vector equation of (3.46) for \mathbf{k}_o , thereby completing the synthesis problem.

Remark 3.2.1 *Given that the output involves a sliding variable d_1 , besides the angle ϕ , two sets of data-points must be given: $\{\psi_i, \phi_i\}_1^m$ and $\{\psi_i, (d_1)_i\}_1^m$.*

3.3 Exact Synthesis

3.3.1 Planar Linkages

We have $m = 3$ in this case, and hence, the synthesis equations look like

$$\begin{bmatrix} 1 & c\phi_1 & -c\psi_1 \\ 1 & c\phi_2 & -c\psi_2 \\ 1 & c\phi_3 & -c\psi_3 \end{bmatrix} \begin{bmatrix} k_1 \\ k_2 \\ k_3 \end{bmatrix} = \begin{bmatrix} c(\phi_1 - \psi_1) \\ c(\phi_2 - \psi_2) \\ c(\phi_3 - \psi_3) \end{bmatrix} \quad (3.47a)$$

where

$$c(\cdot) \equiv \cos(\cdot) \quad \text{and} \quad s(\cdot) \equiv \sin(\cdot) \quad (3.47b)$$

Solving *numerically* for $\{k_i\}_1^3$ is straightforward, if Gaussian elimination, or LU-decomposition, is applied—as, implemented, e.g., in Matlab. Given the simple structure of the system at hand, however, a solution in *closed form* is also possible: To this end, subtract the first equation from the second and third equations:

$$\begin{bmatrix} 1 & c\phi_1 & -c\psi_1 \\ 0 & c\phi_2 - c\phi_1 & -c\psi_2 + c\psi_1 \\ 0 & c\phi_3 - c\phi_1 & -c\psi_3 + c\psi_1 \end{bmatrix} \begin{bmatrix} k_1 \\ k_2 \\ k_3 \end{bmatrix} = \begin{bmatrix} c(\phi_1 - \psi_1) \\ c(\phi_2 - \psi_2) - c(\phi_1 - \psi_1) \\ c(\phi_3 - \psi_3) - c(\phi_1 - \psi_1) \end{bmatrix} \quad (3.48)$$

Note that the second and third equations are free of k_1 , and hence, one can solve them first for k_2 and k_3 :

$$\begin{bmatrix} c\phi_2 - c\phi_1 & -c\psi_2 + c\psi_1 \\ c\phi_3 - c\phi_1 & -c\psi_3 + c\psi_1 \end{bmatrix} \begin{bmatrix} k_2 \\ k_3 \end{bmatrix} = \begin{bmatrix} c(\phi_2 - \psi_2) - c(\phi_1 - \psi_1) \\ c(\phi_3 - \psi_3) - c(\phi_1 - \psi_1) \end{bmatrix} \quad (3.49)$$

The above 2×2 system can be solved for k_2 and k_3 if we recall expression (1.8):

$$\begin{bmatrix} k_2 \\ k_3 \end{bmatrix} = \frac{1}{\Delta} \begin{bmatrix} -c\psi_3 + c\psi_1 & c\psi_2 - c\psi_1 \\ -c\phi_3 + c\phi_1 & c\phi_2 - c\phi_1 \end{bmatrix} \begin{bmatrix} c(\phi_2 - \psi_2) - c(\phi_1 - \psi_1) \\ c(\phi_3 - \psi_3) - c(\phi_1 - \psi_1) \end{bmatrix} \quad (3.50a)$$

where

$$\begin{aligned} \Delta &\equiv \det \begin{bmatrix} c\phi_2 - c\phi_1 & -c\psi_2 + c\psi_1 \\ c\phi_3 - c\phi_1 & -c\psi_3 + c\psi_1 \end{bmatrix} \\ &= (c\phi_2 - c\phi_1)(-c\psi_3 + c\psi_1) + (c\psi_2 - c\psi_1)(c\phi_3 - c\phi_1) \end{aligned} \quad (3.50b)$$

With k_2 and k_3 obtained from eqs.(3.50a & b), k_1 is derived from the first of eqs.(3.48). The final result is

$$k_i = \frac{N_i}{\Delta}, \quad i = 1, 2, 3 \quad (3.51)$$

with numerators N_i calculated sequentially:

$$\begin{aligned} N_2 &= (-c\psi_3 + c\psi_1)[c(\phi_2 - \psi_2) - c(\phi_1 - \psi_1)] \\ &\quad + (c\psi_2 - c\psi_1)[c(\phi_3 - \psi_3) - c(\phi_1 - \psi_1)] \end{aligned} \quad (3.52a)$$

$$\begin{aligned} N_3 &= (-c\phi_3 + c\phi_1)[c(\phi_2 - \psi_2) - c(\phi_1 - \psi_1)] \\ &\quad + (c\phi_2 - c\phi_1)[c(\phi_3 - \psi_3) - c(\phi_1 - \psi_1)] \end{aligned} \quad (3.52b)$$

$$N_1 = c(\phi_1 - \psi_1)\Delta - c\phi_2 N_2 + c\psi_1 N_3 \quad (3.52c)$$

The foregoing problem is therefore quite simple to solve. We just showed how to solve it in closed form. However, the solution obtained must be correctly interpreted. Indeed, upon looking at definitions (3.8), it is apparent that, all link lengths being positive, k_2 and k_3 should be positive as well, while k_1 is capable of taking any finite positive or negative real values. However, nothing in the above formulation prevents k_2 and k_3 from turning

out to be negative or zero. Negative values of these parameters are not to be discarded, for they have a geometric interpretation: Notice that, in eq.(3.10), if ϕ is changed to $\phi + \pi$, then the sign of the second term of the left-hand side of that equation is reversed. Ditto the third term if ψ is changed to $\psi + \pi$. The conclusion then follows:

A negative k_2 (k_3) indicates that the input (output) angle ψ (ϕ) should not be measured as indicated in Fig. 3.1, but all the way down to the extension of link O_1O_2 (O_4O_3).

If the solution to the synthesis problem leads to $k_2 = 0$, then $a_2 \rightarrow \infty$, which means that the input link is of infinite length. The interpretation now is that the first joint of the linkage is of the P type, i.e., we end up with a PRRR linkage. Likewise, if $k_3 = 0$, then $a_4 \rightarrow \infty$, and we end up with a RRRP linkage.

Finally, even in the presence of nonzero values of the Freudenstein parameters, nothing guarantees that the link lengths derived from them will yield a feasible linkage. Indeed, for a linkage to be possible, the link lengths must satisfy the *feasibility condition* :

Any link length must be smaller than the sum of the three other link lengths.

Bloch Synthesis

A special kind of linkage synthesis occurs when input-output relations are not specified at three distinct values of the input and output angles, but rather at one single value of the input and output angles, to which *velocity and acceleration conditions* are adjoined. The problem thus arising is known as *Bloch synthesis*. Besides its special nature, this problem becomes relevant because of its revelation: the simultaneous vanishing of velocity and acceleration of the output link, i.e., *second-order rest* of the output link, cannot be obtained with a planar four-bar linkage whose input link turns at a constant angular velocity. As a matter of fact, second-order rest cannot be obtained with any linkage, but good approximations can be obtained with six-bar linkages producing short-duration *dwell*. The foregoing claim will be made clear in the sequel.

The problem at hand then can be stated as: *Synthesize a four-bar linkage that meets conditions on position, velocity and acceleration at a given position of the input link.*

In order to formulate this problem, we differentiate both sides of the Freudenstein equation, eq.(3.10), with respect to time. After rearrangement of terms and a reversal of signs, this gives

$$\dot{\phi}s\phi k_2 - \dot{\psi}s\psi k_3 = (\dot{\phi} - \dot{\psi})s(\phi - \psi) \quad (3.53a)$$

$$\begin{aligned} (\ddot{\phi}s\phi + \dot{\phi}^2c\phi)k_2 - (\ddot{\psi}s\psi + \dot{\psi}^2c\psi)k_3 &= (\ddot{\phi} - \ddot{\psi})s(\phi - \psi) \\ &+ (\dot{\phi} - \dot{\psi})^2c(\phi - \psi) \end{aligned} \quad (3.53b)$$

Next, we write eqs.(3.10) and (3.53a & b) at $\psi = \psi_1$, and cast them in vector form:

$$\mathbf{A}\mathbf{k} = \mathbf{b} \quad (3.54a)$$

where \mathbf{A} and \mathbf{b} are given below:

$$\mathbf{A} \equiv \begin{bmatrix} 1 & c\phi_1 & -c\psi_1 \\ 0 & \dot{\phi}_1 s\phi_1 & -\dot{\psi}_1 s\psi_1 \\ 0 & \ddot{\phi}_1 s\phi_1 + \dot{\phi}_1^2 c\phi_1 & -\ddot{\psi}_1 s\psi_1 - \dot{\psi}_1^2 c\psi_1 \end{bmatrix} \quad (3.54b)$$

$$\mathbf{b} \equiv \begin{bmatrix} c(\phi_1 - \psi_1) \\ (\dot{\phi}_1 - \dot{\psi}_1)s(\phi_1 - \psi_1) \\ [(\ddot{\phi}_1 - \ddot{\psi}_1)s(\phi_1 - \psi_1) + (\dot{\phi}_1 - \dot{\psi}_1)^2 c(\phi_1 - \psi_1)] \end{bmatrix} \quad (3.54c)$$

Again, the second and third equations are free of k_1 , and hence, we can decouple them from the first equation to solve for k_2 and k_3 , namely,

$$\begin{bmatrix} \dot{\phi}_1 s\phi_1 & -\dot{\psi}_1 s\psi_1 \\ \ddot{\phi}_1 s\phi_1 + \dot{\phi}_1^2 c\phi_1 & -(\ddot{\psi}_1 s\psi_1 + \dot{\psi}_1^2 c\psi_1) \end{bmatrix} \begin{bmatrix} k_2 \\ k_3 \end{bmatrix} = \begin{bmatrix} (\dot{\phi}_1 - \dot{\psi}_1)s(\phi_1 - \psi_1) \\ (\ddot{\phi}_1 - \ddot{\psi}_1)s(\phi_1 - \psi_1) \\ + (\dot{\phi}_1 - \dot{\psi}_1)^2 c(\phi_1 - \psi_1) \end{bmatrix} \quad (3.55)$$

In solving the above system, we shall need the determinant Δ of the above 2×2 matrix, which is computed below:

$$\begin{aligned} \Delta &\equiv \det \begin{bmatrix} \dot{\phi}_1 s\phi_1 & -\dot{\psi}_1 s\psi_1 \\ \ddot{\phi}_1 s\phi_1 + \dot{\phi}_1^2 c\phi_1 & -\ddot{\psi}_1 s\psi_1 - \dot{\psi}_1^2 c\psi_1 \end{bmatrix} \\ &= -\dot{\phi}_1 s\phi_1(\ddot{\psi}_1 s\psi_1 + \dot{\psi}_1^2 c\psi_1) + \dot{\psi}_1 s\psi_1(\ddot{\phi}_1 s\phi_1 + \dot{\phi}_1^2 c\phi_1) \end{aligned} \quad (3.56)$$

It is thus apparent that, if $\dot{\phi}_1 = 0$ and $\dot{\psi}_1 = 0$, then $\Delta = 0$, and the above 2×2 matrix is singular. A close look at \mathbf{A} of eq.(3.54a) will reveal that, under these conditions, \mathbf{A} is indeed singular. As a consequence, **a four-bar linkage cannot produce zero velocity and zero acceleration concurrently at the output link when its input link turns at a constant rpm.**

Now we recall expression (1.8) to invert the 2×2 matrix coefficient of vector $[k_2, k_3]^T$, thus obtaining

$$\begin{aligned} \begin{bmatrix} k_2 \\ k_3 \end{bmatrix} &= \frac{1}{\Delta} \begin{bmatrix} -(\ddot{\psi}_1 s\psi_1 + \dot{\psi}_1^2 c\psi_1) & \dot{\psi}_1 s\psi_1 \\ -(\ddot{\phi}_1 s\phi_1 + \dot{\phi}_1^2 c\phi_1) & \dot{\phi}_1 s\phi_1 \end{bmatrix} \\ &\times \begin{bmatrix} (\dot{\phi}_1 - \dot{\psi}_1)s(\phi_1 - \psi_1) \\ [(\ddot{\phi}_1 - \ddot{\psi}_1)s(\phi_1 - \psi_1) + (\dot{\phi}_1 - \dot{\psi}_1)^2 c(\phi_1 - \psi_1)] \end{bmatrix} \end{aligned} \quad (3.57)$$

Hence,

$$k_2 = \frac{N_2}{\Delta}, \quad k_3 = \frac{N_3}{\Delta} \quad (3.58a)$$

with

$$\begin{aligned} N_2 &\equiv -(\ddot{\psi}_1 s\psi_1 + \dot{\psi}_1^2 c\psi_1)(\dot{\phi}_1 - \dot{\psi}_1)s(\phi_1 - \psi_1) + \dot{\psi}_1 s\psi_1[(\ddot{\phi}_1 - \ddot{\psi}_1)s(\phi_1 - \psi_1) \\ &\quad + (\dot{\phi}_1 - \dot{\psi}_1)^2 c(\phi_1 - \psi_1)] \end{aligned} \quad (3.58b)$$

$$\begin{aligned} N_3 &\equiv -(\ddot{\phi}_1 s\phi_1 + \dot{\phi}_1^2 c\phi_1)(\dot{\phi}_1 - \dot{\psi}_1)s(\phi_1 - \psi_1) + \dot{\phi}_1 s\phi_1[(\ddot{\phi}_1 - \ddot{\psi}_1)s(\phi_1 - \psi_1) \\ &\quad + (\dot{\phi}_1 - \dot{\psi}_1)^2 c(\phi_1 - \psi_1)] \end{aligned} \quad (3.58c)$$

Once k_2 and k_3 are known, we can calculate k_1 from the first of eqs.(3.54a). After simplifications,

$$k_1 = \frac{c(\phi_1 - \psi_1)\Delta - N_2c\phi_1 + N_3c\psi_1}{\Delta} \quad (3.58d)$$

thereby completing the solution of the problem at hand.

3.3.2 Spherical Linkages

In this case, the synthesis matrix of eq.(3.31) becomes of 4×4 , while vector \mathbf{b} of the same equation becomes four-dimensional, the synthesis equations thus taking the form

$$\begin{bmatrix} 1 & \cos \psi_1 & \cos \psi_1 \cos \phi_1 & -\cos \phi_1 \\ 1 & \cos \psi_2 & \cos \psi_2 \cos \phi_2 & -\cos \phi_2 \\ 1 & \cos \psi_3 & \cos \psi_3 \cos \phi_3 & -\cos \phi_3 \\ 1 & \cos \psi_4 & \cos \psi_4 \cos \phi_4 & -\cos \phi_4 \end{bmatrix} \begin{bmatrix} k_1 \\ k_2 \\ k_3 \\ k_4 \end{bmatrix} = \begin{bmatrix} -\sin \psi_1 \sin \phi_1 \\ -\sin \psi_2 \sin \phi_2 \\ -\sin \psi_3 \sin \phi_3 \\ -\sin \psi_4 \sin \phi_4 \end{bmatrix} \quad (3.59)$$

The structure of the synthesis matrix is strikingly similar to that of the planar case, with the entries of its first column being all 1s. Hence, similar to the planar case of Subsection 3.3.1, the equations can be reduced by *elementary operations on the synthesis matrix* to a subsystems of three equations in three unknowns. This is readily done upon subtracting the first equation from the remaining three, which is equivalent to subtracting the first row of the synthesis matrix from its remaining three rows, and subtracting the first component of vector \mathbf{b} from its remaining three components, namely,

$$\begin{bmatrix} 1 & c\psi_1 & c\psi_1c\phi_1 & -c\phi_1 \\ 0 & c\psi_2 - c\psi_1 & c\psi_2c\phi_2 - c\psi_1c\phi_1 & -c\phi_2 + c\phi_1 \\ 0 & c\psi_3 - c\psi_1 & c\psi_3c\phi_3 - c\psi_1c\phi_1 & -c\phi_3 + c\phi_1 \\ 0 & c\psi_4 - c\psi_1 & c\psi_4c\phi_4 - c\psi_1c\phi_1 & -c\phi_4 + c\phi_1 \end{bmatrix} \begin{bmatrix} k_1 \\ k_2 \\ k_3 \\ k_4 \end{bmatrix} = \begin{bmatrix} -s\psi_1s\phi_1 \\ -s\psi_2s\phi_2 + s\psi_1s\phi_1 \\ -s\psi_3s\phi_3 + s\psi_1s\phi_1 \\ -s\psi_4s\phi_4 + s\psi_1s\phi_1 \end{bmatrix} \quad (3.60)$$

The foregoing system can be now cast in a more suitable block-form:

$$\begin{bmatrix} 1 & \mathbf{a}^T \\ \mathbf{0}_3 & \mathbf{A}_3 \end{bmatrix} \mathbf{k} = \begin{bmatrix} b_1 \\ \mathbf{b}_3 \end{bmatrix} \quad (3.61a)$$

with blocks defined as

$$\mathbf{a} \equiv \begin{bmatrix} c\psi_1 \\ c\psi_1c\phi_1 \\ -c\phi_1 \end{bmatrix}, \quad \mathbf{A}_3 \equiv \begin{bmatrix} c\psi_2 - c\psi_1 & c\psi_2c\phi_2 - c\psi_1c\phi_1 & -c\phi_2 + c\phi_1 \\ c\psi_3 - c\psi_1 & c\psi_3c\phi_3 - c\psi_1c\phi_1 & -c\phi_3 + c\phi_1 \\ c\psi_4 - c\psi_1 & c\psi_4c\phi_4 - c\psi_1c\phi_1 & -c\phi_4 + c\phi_1 \end{bmatrix}, \quad (3.61b)$$

$$b_1 \equiv -s\psi_1s\phi_1, \quad \mathbf{b}_3 \equiv \begin{bmatrix} -s\psi_2s\phi_2 + s\psi_1s\phi_1 \\ -s\psi_3s\phi_3 + s\psi_1s\phi_1 \\ -s\psi_4s\phi_4 + s\psi_1s\phi_1 \end{bmatrix} \quad (3.61c)$$

and $\mathbf{0}_3$ is the three-dimensional zero vector. We can thus identify in the above system a reduced system of three equations in three unknowns that has been decoupled from the

original system of four equations, namely,

$$\mathbf{A}_3 \mathbf{k}_3 = \mathbf{b}_3, \quad \mathbf{k}_3 \equiv \begin{bmatrix} k_2 \\ k_3 \\ k_4 \end{bmatrix} \quad (3.62)$$

Further, \mathbf{A}_3 is partitioned columnwise as done in Subsection 1.4.3:

$$\mathbf{A}_3 = [\mathbf{c}_1 \quad \mathbf{c}_2 \quad \mathbf{c}_3] \quad (3.63)$$

Therefore, the inverse of \mathbf{A}_3 can be computed in this case symbolically, as per eq.(1.9a):

$$\mathbf{A}_3^{-1} = \frac{1}{\Delta} \begin{bmatrix} (\mathbf{c}_2 \times \mathbf{c}_3)^T \\ (\mathbf{c}_3 \times \mathbf{c}_1)^T \\ (\mathbf{c}_1 \times \mathbf{c}_2)^T \end{bmatrix} \quad (3.64a)$$

where

$$\Delta \equiv \mathbf{c}_1 \times \mathbf{c}_2 \cdot \mathbf{c}_3 \quad (3.64b)$$

and hence,

$$\mathbf{k}_3 = \frac{1}{\Delta} \begin{bmatrix} (\mathbf{c}_2 \times \mathbf{c}_3)^T \mathbf{b}_3 \\ (\mathbf{c}_3 \times \mathbf{c}_1)^T \mathbf{b}_3 \\ (\mathbf{c}_1 \times \mathbf{c}_2)^T \mathbf{b}_3 \end{bmatrix} \quad (3.64c)$$

thereby computing k_2 , k_3 and k_4 . The remaining unknown, k_1 , is computed from the first equation of the array (3.60):

$$k_1 + k_2 c \psi_1 + k_3 c \psi_1 c \phi_1 - k_4 c \phi_1 = -s \psi_1 s \phi_1$$

whence,

$$k_1 = -s \psi_1 s \phi_1 - k_2 c \psi_1 - k_3 c \psi_1 c \phi_1 + k_4 c \phi_1 \quad (3.64d)$$

all unknowns having thus been found.

Remark 3.3.1 *The foregoing closed-form solution of the exact synthesis problem at hand is apparently elegant and gives some insight into the relations among the variables involved, e.g., the problem has no solution when the three columns of \mathbf{A}_3 , or its three rows for that matter, are coplanar. Moreover, the numerical evaluation of the Freudenstein parameters is exactly that obtained with Cramer's rule, which is notorious for being inefficient and prone to roundoff-error amplification. In our case, the dimension of the problem at hand being modest, it should be safe, in general, to use the above formulas.*

Remark 3.3.2 *Given that $k_3 = \lambda_1 = \cos \alpha_1$, the computed k_3 must be smaller than unity in absolute value, and hence, any solution with $|k_3| > 1$ must be rejected. By the same token, $c \alpha_3 = (k_3 k_4 - k_1 s \alpha_1) s \alpha_2 c \alpha_4 / k_2$, and hence, the absolute value of the foregoing difference must be smaller than unity.*

3.3.3 Spatial Linkages

The two synthesis matrices, \mathbf{S} and \mathbf{S}_o , of eq.(3.44) become now of 4×4 , while vectors \mathbf{b} and \mathbf{b}_o of eq.(3.45) become four-dimensional. As a matter of fact, \mathbf{S} , \mathbf{k} and \mathbf{b} are exactly the same as their counterparts in the spherical case, the first synthesis equation of eq.(3.46) thus being identical to eq.(3.59), which is reproduced below for quick reference:

$$\begin{bmatrix} 1 & c\psi_1 & c\psi_1c\phi_1 & -c\phi_1 \\ 1 & c\psi_2 & c\psi_2c\phi_2 & -c\phi_2 \\ 1 & c\psi_3 & c\psi_3c\phi_3 & -c\phi_3 \\ 1 & c\psi_4 & c\psi_4c\phi_4 & -c\phi_4 \end{bmatrix} \begin{bmatrix} k_1 \\ k_2 \\ k_3 \\ k_4 \end{bmatrix} = \begin{bmatrix} -s\psi_1s\phi_1 \\ -s\psi_2s\phi_2 \\ -s\psi_3s\phi_3 \\ -s\psi_4s\phi_4 \end{bmatrix} \quad (3.65)$$

The second synthesis equation of the same eq.(3.46) is rewritten below in the standard form in which the left-hand side includes the term in the unknown, namely,

$$\begin{bmatrix} 1 & c\psi_1 & c\psi_1c\phi_1 & -c\phi_1 \\ 1 & c\psi_2 & c\psi_2c\phi_2 & -c\phi_2 \\ 1 & c\psi_3 & c\psi_3c\phi_3 & -c\phi_3 \\ 1 & c\psi_4 & c\psi_4c\phi_4 & -c\phi_4 \end{bmatrix} \begin{bmatrix} k_{1o} \\ k_{2o} \\ k_{3o} \\ k_{4o} \end{bmatrix} = \begin{bmatrix} u_1s\psi_1c\phi_1 \\ u_2s\psi_2c\phi_2 \\ u_3s\psi_3c\phi_3 \\ u_4s\psi_4c\phi_4 \end{bmatrix} - \begin{bmatrix} 0 & 0 & -u_1c\psi_1s\phi_1 & u_1s\phi_1 \\ 0 & 0 & -u_2c\psi_2s\phi_2 & u_2s\phi_2 \\ 0 & 0 & -u_3c\psi_3s\phi_3 & u_3s\phi_3 \\ 0 & 0 & -u_4c\psi_4s\phi_4 & u_4s\phi_4 \end{bmatrix} \begin{bmatrix} k_1 \\ k_2 \\ k_3 \\ k_4 \end{bmatrix} \quad (3.66)$$

Upon expansion, the right-hand side becomes

$$\mathbf{b}_o - \mathbf{S}_o\mathbf{k} = \begin{bmatrix} u_1[s\psi_1c\phi_1 - s\phi_1(k_3c\psi_1 - k_4)] \\ u_2[s\psi_2c\phi_2 - s\phi_2(k_3c\psi_2 - k_4)] \\ u_3[s\psi_3c\phi_3 - s\phi_3(k_3c\psi_3 - k_4)] \\ u_4[s\psi_4c\phi_4 - s\phi_4(k_3c\psi_4 - k_4)] \end{bmatrix} \equiv \begin{bmatrix} (b_1)_o \\ (\mathbf{b}_3)_o \end{bmatrix} - \begin{bmatrix} \mathbf{s}_1^T \\ \mathbf{S}_3 \end{bmatrix}_o \mathbf{k}$$

Again, as in the spherical case, the system (3.65) can be solved in closed form upon reducing it to a system of three equations in three unknowns, which is done by subtracting the first equation from the other three, thereby ending up with a new system of equations, similar to that of eq.(3.61a), namely,

$$\begin{bmatrix} 1 & \mathbf{a}^T \\ \mathbf{0}_3 & \mathbf{A}_3 \end{bmatrix} \mathbf{k}_o \equiv \begin{bmatrix} (b_1)_o - (\mathbf{s}_1^T)_o\mathbf{k} \\ (\mathbf{b}_3)_o - (\mathbf{S}_3)_o\mathbf{k} \end{bmatrix} \quad (3.67a)$$

with the above partitioning of \mathbf{b} and \mathbf{S} , and other blocks defined as

$$\mathbf{a} \equiv \begin{bmatrix} c\psi_1 \\ c\psi_1c\phi_1 \\ -c\phi_1 \end{bmatrix}, \quad \mathbf{A}_3 \equiv \begin{bmatrix} c\psi_2 - c\psi_1 & c\psi_2c\phi_2 - c\psi_1c\phi_1 & -c\phi_2 + c\phi_1 \\ c\psi_3 - c\psi_1 & c\psi_3c\phi_3 - c\psi_1c\phi_1 & -c\phi_3 + c\phi_1 \\ c\psi_4 - c\psi_1 & c\psi_4c\phi_4 - c\psi_1c\phi_1 & -c\phi_4 + c\phi_1 \end{bmatrix}, \quad (3.67b)$$

$$(b_1)_o \equiv u_1s\psi_1s\phi_1, \quad (\mathbf{b}_3)_o \equiv \begin{bmatrix} u_2[s\psi_2c\phi_2 - s\phi_2(k_3c\psi_2 - k_4)] - (b_1)_o + (\mathbf{s}_1^T)_o\mathbf{k} \\ u_3[s\psi_3c\phi_3 - s\phi_3(k_3c\psi_3 - k_4)] - (b_1)_o + (\mathbf{s}_1^T)_o\mathbf{k} \\ u_4[s\psi_4c\phi_4 - s\phi_4(k_3c\psi_4 - k_4)] - (b_1)_o + (\mathbf{s}_1^T)_o\mathbf{k} \end{bmatrix} \quad (3.67c)$$

Now, upon comparison of eq.(3.67a) with its spherical counterpart, eq.(3.60), it is apparent that the matrix coefficient of \mathbf{k}_o is the same in the two cases. The foregoing vector,

then, can be computed using exactly the same procedure as that outlined in Section 3.3.2 for spherical function-generator synthesis. The procedure needn't be repeated here.

Again, it is noteworthy that the foregoing computations lead to the solution of a system of three equations in three unknowns, which can be solved symbolically by means of reciprocal bases. Remarks 3.3.1 and 3.3.2 apply in this case as well.

3.4 Analysis of the Synthesized Linkage

After a linkage is synthesized, its performance should be evaluated, which is done by means of analysis. The first step in analyzing a linkage synthesized for function generation is to produce its link lengths, for all we have is its Freudenstein parameters. Below we derive analysis algorithms for planar, spherical and spatial four-bar linkages.

3.4.1 Planar Linkages

We start by recalling the inverse relations of eqs.(3.11), which we reproduce below for quick reference:

$$a_2 = \frac{1}{k_2}a_1, \quad a_4 = \frac{1}{k_3}a_1, \quad a_3 = \sqrt{a_1^2 + a_2^2 + a_4^2 - 2k_1a_2a_4} \quad (3.68)$$

Two remarks are in order:

- (i) The link lengths are given in terms of a_1 , which is thus the link length that determines the scale of the linkage, but any other length can be used for the same purpose; and
- (ii) all lengths are positive. However, negative signs for k_2 and k_3 can occur, that hence lead to negative values of a_2 or, correspondingly, a_4 . As we saw in Subsection 3.3.1, negative values of any of these variables, or of both for that matter, bear a straightforward interpretation.

We now proceed to derive an algorithm for the fast and reliable computation of the output values of ϕ corresponding to a) a given linkage of feasible link lengths $\{a_i\}_1^4$ and b) a given input value ψ . We can do this in several ways. We start by recalling the IO equation of the planar four-bar linkage in homogeneous form, eq.(3.11):

$$k_1 + k_2 \cos \phi - k_3 \cos \psi - \cos(\phi - \psi) = 0$$

Upon expansion of the fourth term in the left-hand side, the foregoing equation can be rewritten as

$$A(\psi) \cos \phi + B(\psi) \sin \phi + C(\psi) = 0 \quad (3.69a)$$

with coefficients defined as

$$A(\psi) = k_2 - \cos \psi, \quad B(\psi) = -\sin \psi, \quad C(\psi) = k_1 - k_3 \cos \psi \quad (3.69b)$$

One approach to solving this equation for ϕ consists in transforming it into an algebraic equation², which is done by means of the tan-half identities, which are recalled below, as applied to angle ϕ :

$$\cos \phi \equiv \frac{1 - T^2}{1 + T^2}, \quad \sin \phi \equiv \frac{2T}{1 + T^2}, \quad T \equiv \tan \left(\frac{\phi}{2} \right) \quad (3.70)$$

Upon substitution of the foregoing identities into eq.(3.69a), a quadratic equation in T is obtained:

$$D(\psi)T^2 + 2E(\psi)T + F(\psi) = 0 \quad (3.71a)$$

whose coefficients are given below:

$$D(\psi) \equiv k_1 - k_2 + (1 - k_3) \cos \psi \quad (3.71b)$$

$$E(\psi) \equiv -\sin \psi \quad (3.71c)$$

$$F(\psi) \equiv k_1 + k_2 - (1 + k_3) \cos \psi \quad (3.71d)$$

Now, ϕ can be readily computed once the two roots of eq.(3.71a) are available. Here, a caveat is in order: Rather than naively use the standard form of the solution of the quadratic equation, we follow here a *robust* approach, as suggested by Forsythe (1970): In order to avoid *catastrophic cancellations* when $B^2 \gg AC$, that would lead to an erroneous zero root, we first compute the root with the *largest* absolute value, namely,

$$T_1 = \frac{-E - \operatorname{sgn}(E)\sqrt{E^2 - DF}}{D}, \quad \phi_1 = 2 \tan^{-1}(T_1) \quad (3.72a)$$

where $\operatorname{sgn}(\cdot)$ is the well-known signum function introduced in Section 1.4 when we studied Householder reflections. In the case at hand, $B = 0$ indicates that $\sin \psi$, and hence, $E(\psi)$, vanishes in the quadratic equation, the two roots of the equation then being symmetric; therefore, the above formula is to be skipped in favour of the simpler

$$T_{1,2} = \pm \frac{\sqrt{-DF}}{D} \quad (3.72b)$$

In case $B(\psi) \neq 0$, the second root is computed as

$$T_2 = \frac{F}{DT_1}, \quad \phi_2 = 2 \tan^{-1}(T_2) \quad (3.72c)$$

Thus, cancellations are avoided upon computing T_1 ; then, T_2 is computed safely because the denominator appearing in eq.(3.72c) has the largest possible absolute value. However,

²That is, a *polynomial equation*.

notice that the quadratic equation can degenerate into a linear equation under two cases: (a) $F = 0$ or (b) $D = 0$. The first case simply means that one root is zero, the second being computed from the linear equation derived upon dividing the two sides of that quadratic by T . The second case is a bit more elusive, but it can be handled as the limiting case $D \rightarrow 0$. To this end, let us divide both sides of eq.(3.71a) by T^2 :

$$D(\psi) + \frac{2E(\psi)}{T} + \frac{F(\psi)}{T^2} = 0$$

Now, upon taking the limit of both sides of the above equation when $D \rightarrow 0$, we obtain

$$\lim_{D(\psi) \rightarrow 0} T \rightarrow \infty$$

and hence,

$$\lim_{D(\psi) \rightarrow 0} \phi = \pi \tag{3.73}$$

In any event, the two possible solutions of the quadratic equation obtained above lead to one of three possible cases:

1. The two roots $\{T_i\}_1^2$ are real and distinct: the corresponding angles $\{\phi_i\}_1^2$ provide the two *conjugate* postures of the linkage. As the linkage moves, the two conjugate postures generate, correspondingly, two *conjugate branches* of the linkage motion;
2. The two roots $\{T_i\}_1^2$ are real and identical: the corresponding single value of $\phi_1 = \phi_2$ indicates the merging of the two branches. This indicates that the output link reached one extreme position, which is known as a *deadpoint*.
3. The two roots are complex conjugate: this indicates two possibilities:
 - (a) The link lengths are unfeasible: they do not define a quadrilateral; or
 - (b) The linkage is feasible, but its input link does not move through a full turn, i.e., it is a *rocker*, the given value of ψ lying outside of its range of motion.

Because of the *two conjugate branches* of the planar four-bar linkage, the linkage is said to be *bimodal*.

It is apparent that the quadratic-equation approach to the input-output analysis of the four-bar linkage must be handled with care, especially when writing code to implement it. As an alternative, we can pursue a more geometric, straightforward approach, free of the *singularity* $T \rightarrow \infty$ of the transformation (3.70), as described below: We go back to eq.(3.69a), and rewrite it in a slightly different form

$$\mathcal{L} : \quad A(\psi)u + B(\psi)v + C(\psi) = 0 \tag{3.74a}$$

where

$$u \equiv \cos \phi, \quad v \equiv \sin \phi \tag{3.74b}$$

and hence, u and v are subject to the constraint

$$\mathcal{C}: \quad u^2 + v^2 = 1 \quad (3.74c)$$

The input-output equation thus defines a line \mathcal{L} in the u - v plane, while the constraint (3.74c) defines a unit circle \mathcal{C} centred at the origin of the same plane. The circle is fixed, but the location of the line in the u - v plane depends on both the linkage parameters k_1 , k_2 , k_3 and the input angle ψ . Therefore, depending upon the linkage at hand and the position of its input link, the line may intersect the circle or may not. If it does, then, additionally, the line either intersects the circle at two distinct points or, as a special case, at one single point, in which case the line is tangent to the circle, the two intersection points thus merging into a single one. In the absence of intersections, either the linkage is unfeasible or its input link is a rocker, the given input angle lying outside of its mobility range. In the case of two distinct intersections, these determine the two conjugate postures of the linkage. In the case of tangency, the linkage is at a deadpoint. Figure 3.6 depicts the case of two distinct intersection points.

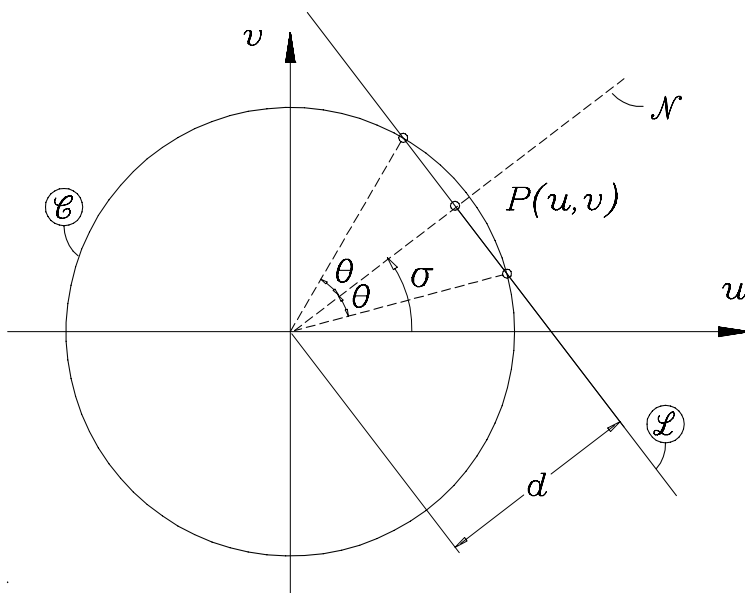


Figure 3.6: Line and circle in the u - v plane

Let the distance of the line to the origin be denoted by d . Apparently, we have the three cases below:

$d < 1$: \mathcal{L} intersects \mathcal{C} at two distinct points;

$d = 1$: \mathcal{L} is tangent to \mathcal{C} ;

$d > 1$: \mathcal{L} does not intersect \mathcal{C} .

The distance d can be readily found to be

$$d = \frac{|C(\psi)|}{S(\psi)} \quad (3.75a)$$

where $C(\psi)$ was defined in eq.(3.69b) and

$$S(\psi) \equiv \sqrt{A(\psi)^2 + B(\psi)^2} = \sqrt{(k_2 - \cos \psi)^2 + \sin^2 \psi} \quad (3.75b)$$

An interesting *singularity* occurs whereby the foregoing calculations break down: If coefficients $A(\psi)$, $B(\psi)$, and $C(\psi)$ in eq.(3.74a) all vanish, then the line \mathcal{L} disappears and *any* value of ϕ satisfies the input-output equation for the given value of ψ . The vanishing of these three coefficients is written below:

$$k_2 - \cos \psi = 0 \quad (3.76a)$$

$$\sin \psi = 0 \quad (3.76b)$$

$$k_1 - k_3 \cos \psi = 0 \quad (3.76c)$$

The second equation leads to $\psi = 0$ or π . For $\psi = 0$, the first equation yields $k_2 = 1$ and the third equation $k_1 = k_3$. Now, $k_2 = 1$ means $a_2 = a_1$, which, together with $k_1 = k_3$, means $a_4 = a_3$, the result being a set of linkage postures whereby joint centres B and D coincide, the coupler and the output links thus being free to turn about joint centre D as one single rigid-body.

For $\psi = \pi$, the first equation yields $k_2 = -1$, which leads to $a_2 = -a_1$, i.e., a “negative” link length. As we saw in Subsection 3.3.1, a negative a_2 means that the input angle should be measured “all the way down to the extension of the input link,” and we fall into the case $\psi = 0$.

Notice that this pathological case, or singularity, is not apparent from the quadratic equation.

Furthermore, in order to compute the two conjugate values ϕ_1 and ϕ_2 , we calculate first the intersection of \mathcal{L} with its normal \mathcal{N} from the origin. The intersection point has coordinates (\bar{u}, \bar{v}) , given below:

$$\bar{u} = \frac{C(\psi)(k_2 - \cos \psi)}{S(\psi)^2}, \quad \bar{v} = \frac{-C(\psi) \sin \psi}{S(\psi)^2} \quad (3.77a)$$

Now, the angle σ that \mathcal{N} makes with the u axis, when $d > 0$, and angle θ , half the angle subtended by the chord defined by the intersections of \mathcal{L} with \mathcal{C} , are given by

$$\sigma = \arctan\left(\frac{\bar{v}}{\bar{u}}\right) \quad (3.77b)$$

$$\theta = \arccos(d) \quad (3.77c)$$

When $d = 0$, σ cannot be calculated from the above expression, but rather as $\arctan(-1/m)$, where m is the slope of \mathcal{L} . Nevertheless, in this case σ is not needed, for the two conjugate

values of the output angle can be calculated directly. Thus,

$$\phi_1 = \sigma + \theta, \quad \phi_2 = \sigma - \theta, \quad \text{for } d > 0 \quad (3.77d)$$

$$\phi_2 = \arctan\left(\frac{k_2 - \cos\psi}{\sin\psi}\right), \quad \phi_1 = \phi_2 + \pi, \quad \text{for } d = 0 \quad (3.77e)$$

We thus have devised the algorithm below for computing the two conjugate values of the output angle, in Maple code:

Algorithm pl4bar-io(k,input)

This algorithm computes the intersection of one line L and the unit circle centred at the origin of the $\cos(\phi)$ - $\sin(\phi)$ plane. The intersection points, when they exist, are returned in array out, with out[1] and out[2] denoting the two conjugate values of the output angle phi

```

read k[1], k[2], k[3], input;
> pl4bar-io:=proc(k,input) #Use this
> procedure only if are sure that your linkage is feasible
> local dpoint,feasible,pathos,D_d,N_d,d,u,v,sigma,theta; global
> out;
> dpoint:=false; #we assume that we are not in the presence of a
> deadpoint
> feasible:=true; #we assume that current psi-value is feasible
> pathos:=false; #we assume that we are not in the presence of
> pathological case whereby linkage becomes a one-dof open chain if
> k[2]=1 and psi=0 then pathos:=true; print(patholo=pathos); return;
> fi;
> #if k[2]=1, then a[1]=a[2]
> D_d:=k[2]*(k[2]-2*cos(input))+1: N_d:=-k[1]+k[3]*cos(input):
> d:=abs(N_d)/sqrt(D_d): #print(dd=d); #distance of line L to origin
> if d>1.0 then feasible:=false; print(feas=feasible); return; fi;
> if d=1.0 then dpoint:=true; print(dead=dpoint); theta=0; fi;
> u:=(N_d/D_d^2)*(k[2]-cos(input)): v:=-(N_d/D_d^2)*sin(input):
> #coordinates of intersection of line L and its normal N
> passing through the origin sigma:=arctan(v,u): #print(sig=sigma);
> #angle that normal makes with u-axis if dpoint=false then
> theta:=arccos(d); fi; #print(th=theta); #(1/2)angle subtended by
> secant to circle out[1]:=sigma-theta: out[2]:=sigma+theta: if v<0
> and u>0 then out[1]:=sigma+theta: out[2]:=sigma-theta: fi: #Note:
> this line does not appear in the Lecture Notes, but it is needed
> #print(out1=out[1]); print(out2=out[2]);
> end proc;

```

Various issues stem from the foregoing discussion, namely,

- (a) Linkage feasibility: For the four link lengths to yield a *feasible linkage*, they must define a quadrilateral. The condition on four given side lengths to close a quadrilateral, as given in Subsection 3.3.1, is that every length be smaller than the sum

of the remaining three. When four link lengths are given as candidates to define a planar four-bar linkage, these lengths must first and foremost be capable of defining a quadrilateral. If they do, the lengths are said to be *feasible*; otherwise, they are *unfeasible*.

- (b) **Link mobility:** A link may or may not be capable of a full turn; if capable, it is called a *crank*; otherwise, it is called a *rocker*. This gives rise to various types of linkages, depending on the type of its input and output links, namely, *double crank*, *crank-rocker*, *rocker-crank*, or *double rocker*. Double-crank linkages are known as *drag-link* mechanisms. This variety of linkage type leads, in turn, to what is known as *Grashof mechanisms*.

A major fundamental result in linkage theory is the *Grashof classification* of planar four-bar linkages. This classification looks at the mobility of three links with respect to the remaining one. Obviously, which of the four links is considered the “remaining one” is immaterial. According to Grashof’s classification, a linkage is termed *Grashof* if *at least one* of its links is capable of a full turn with respect to any other link. Otherwise, the linkage is termed *non-Grashof*. Now we have the main result—for a proof, see, e.g., (Waldron and Kinzel, 1999)—below:

A planar four-bar linkage is Grashof if and only if the sum of the lengths of its shortest and longest links is smaller than or equal to the sum of the two other link lengths.

In linkage synthesis, we are interested in meeting mobility conditions either on the input or on the output links, or even on both. We derive below these conditions in terms of the Freudenstein parameters.

Mobility of the Input and Output Links

The condition under which the input link is a crank is quite useful because four-bar linkages are frequently driven at a constant angular velocity, and hence, the input link would better be capable of a full turn. To find this condition, we recall eq.(3.71a), whose discriminant is a function not only of constants k_1 , k_2 and k_3 , but also of ψ and, hence, it is not only linkage- but also posture-dependent. In the discussion below, we assume that the linkage parameters are fixed, and hence, the linkage discriminant Δ will be regarded as a function of ψ only. This is given by

$$\Delta(\psi) \equiv E^2(\psi) - D(\psi)F(\psi) \tag{3.78a}$$

Upon expansion, the above discriminant becomes

$$\Delta(\psi) \equiv -k_3^2 \cos^2 \psi + 2(k_1 k_3 - k_2) \cos \psi + (1 - k_1^2 + k_2^2) \tag{3.78b}$$

which is, clearly, a parabola in $\cos\psi$ with concavity downward. For the input link to be a crank, then, the discriminant $\Delta(\psi)$ should attain nonnegative values in the range $-1 \leq \cos\psi \leq +1$. Moreover, by virtue of the parabolic shape of the $\Delta(\cos\psi)$ vs. $\cos\psi$ plot, Δ is nonnegative for *any* value of ψ if and only if $\Delta(\cos\psi) \geq 0$ when $\cos\psi = \pm 1$. Let Δ_1 and Δ_2 denote the values that Δ attains when $\cos\psi$ equals $+1$ and -1 , respectively, which are given below:

$$\Delta_1 = -k_3^2 + 2(k_1k_3 - k_2) + 1 - k_1^2 + k_2^2, \quad \Delta_2 = -k_3^2 - 2(k_1k_3 - k_2) + 1 - k_1^2 + k_2^2$$

The necessary and sufficient conditions for a nonnegative linkage discriminant, for any value of ψ , are now derived. Note first that Δ_1 and Δ_2 can be expressed as differences of squares, namely,

$$\Delta_1 = (1 - k_2)^2 - (k_1 - k_3)^2, \quad \Delta_2 = (1 + k_2)^2 - (k_1 + k_3)^2$$

Now, clearly, Δ_1 and Δ_2 are nonnegative if and only if the relations below hold:

$$(k_1 - k_3)^2 - (1 - k_2)^2 \leq 0 \quad \text{and} \quad (k_1 + k_3)^2 - (1 + k_2)^2 \leq 0 \quad (3.79)$$

Upon factoring of their left-hand sides, the foregoing inequalities become

$$(k_1 - k_3 - 1 + k_2)(k_1 - k_3 + 1 - k_2) \leq 0 \quad (3.80a)$$

$$(k_1 + k_3 - 1 - k_2)(k_1 + k_3 + 1 + k_2) \leq 0 \quad (3.80b)$$

Each of the above inequalities holds if its two left-hand side factors have opposite signs, the first inequality thus leading to

$$k_1 - k_3 - 1 + k_2 \geq 0 \quad \& \quad k_1 - k_3 + 1 - k_2 \leq 0 \quad (3.80c)$$

or

$$k_1 - k_3 - 1 + k_2 \leq 0 \quad \& \quad k_1 - k_3 + 1 - k_2 \geq 0 \quad (3.80d)$$

The second inequality, likewise, leads to

$$k_1 + k_3 - 1 - k_2 \geq 0 \quad \& \quad k_1 + k_3 + 1 + k_2 \leq 0 \quad (3.80e)$$

or

$$k_1 + k_3 - 1 - k_2 \leq 0 \quad \& \quad k_1 + k_3 + 1 + k_2 \geq 0 \quad (3.80f)$$

Thus, the region of the \mathbf{k} -space containing input cranks is the *intersection* of two subregions, that defined by the four inequalities (3.80c & d) and that defined by (3.80e & f). Moreover, the subregion represented by each quadruplet is the *union* of the intersections of the regions defined by each pair of linear inequalities. Each of these, furthermore, divides the \mathbf{k} -space into two halves, one on each side of the plane obtained when turning the inequality sign of each relation into an equality sign. As the reader can readily notice, inequalities (3.80c & d) lead to the same pair of planes; likewise inequalities (3.80e & f) lead to a second pair of planes, namely,

$$\begin{aligned}
k_1 + k_2 - k_3 - 1 &= 0, & k_1 - k_2 - k_3 + 1 &= 0 \\
k_1 - k_2 + k_3 - 1 &= 0, & k_1 + k_2 + k_3 + 1 &= 0
\end{aligned}$$

In summary, then, the two original quadratic inequalities of eq.(3.79) represent a region of the \mathbf{k} -space bounded by four planes, as displayed in Fig. 3.7. Hence, the region containing input cranks comprises a regular tetrahedron with its centroid located at the origin of the above space and two open convexes. Thus, all points within that region represent linkages whose input link is a crank.

It is noteworthy that the k_1 -axis represents linkages for which $a_2, a_4 \rightarrow \infty$, i.e., the k_1 -axis represents, actually, all PRRP linkages. However, as the reader is invited to verify, the origin does not represent a feasible linkage.

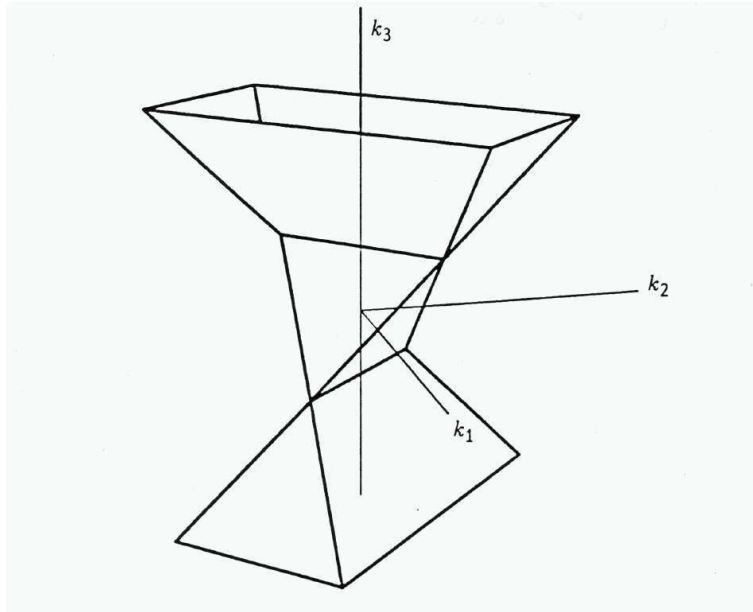


Figure 3.7: Region comprising planar four-bar linkages with an input crank

Now, in order to analyze the mobility of the output link, we simply exchange the roles of k_2 and k_3 in the foregoing results, which is apparent from the definitions of the linkage parameters $\{k_i\}_1^3$, as given in eqs.(3.68) and the Freudenstein equation (3.10). Actually, then, the region containing output cranks can be obtained by mapping that containing input cranks by means of a linear transformation:

$$k_1 = k_1, \quad k_2 = -k_3, \quad k_3 = -k_2$$

The above transformation can be represented in matrix form as a *reflection* \mathbf{R} about a plane of unit normal $[0, \sqrt{2}/2, \sqrt{2}/2]^T$, given by (Angeles, 2007)

$$\mathbf{R} = \begin{bmatrix} 1 & 0 & 0 \\ 0 & 0 & -1 \\ 0 & -1 & 0 \end{bmatrix}$$

As the reader can readily verify, $\mathbf{R}\mathbf{R}^T = \mathbf{1}$, with $\mathbf{1}$ denoting the 3×3 identity matrix and $\det(\mathbf{R}) = -1$, which verifies that \mathbf{R} is a reflection.

By means of the foregoing exchange in eqs.(3.80a & b), the inequalities leading to an output crank are obtained as

$$(k_1 - k_2)^2 < (1 - k_3)^2 \quad (3.81a)$$

$$(k_1 + k_2)^2 < (1 + k_3)^2 \quad (3.81b)$$

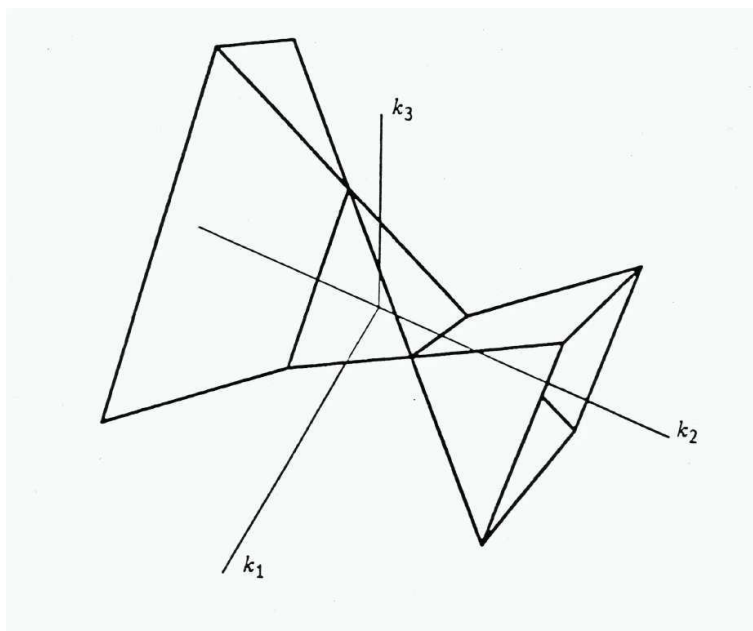


Figure 3.8: Region comprising four-bar linkages with an output crank

The mobility region represented by the two foregoing inequalities comprises all four-bar linkages with an output crank. This region is, then, the mirror image of that of Fig. 3.7 when reflected about a plane Π passing through the k_1 axis and intersecting the k_2 - k_3 plane along a line passing through the origin and contained in the third and fourth quadrants of this plane. The foregoing region is represented in Fig. 3.8. Note that this region comprises a tetrahedron identical to that of Fig. 3.7 and, hence, the tetrahedron is common to both mobility regions. Thus, any point within this region represents a double-crank four-bar linkage, except for the origin, which does not represent a four-bar linkage.

Furthermore, the central tetrahedron of Figs. 3.7 and 3.8 can be shown to have axes of length $2\sqrt{2}$.

All linkages outside of the two foregoing regions are either of the rocker-rocker type or unfeasible.

3.4.2 Spherical Four-Bar Linkages

The analysis of the spherical four-bar linkage parallels that of its planar counterpart. Indeed, upon introduction of the tan-half identities of eq.(3.70) into the I/O equation of the spherical linkage, eq.(3.27), we obtain, again, a quadratic equation in T of the form of eq.(3.71a), namely,

$$D(\psi)T^2 + 2E(\psi)T + F(\psi) = 0 \quad (3.82a)$$

but now with coefficients that are given below:

$$D(\psi) \equiv k_1 + (k_2 - k_3) \cos \psi + k_4 \quad (3.82b)$$

$$E(\psi) \equiv \sin \psi \quad (3.82c)$$

$$F(\psi) \equiv k_1 + (k_2 + k_3) \cos \psi - k_4 \quad (3.82d)$$

Similar to the planar case, rather than attempting a solution of the quadratic equation as such, we cast the input-output equation (3.27) in the same form as we did for the planar case:

$$\mathcal{L}: \quad A(\psi)u + B(\psi)v + C(\psi) = 0 \quad (3.83a)$$

with coefficients given below:

$$A(\psi) = k_3 \cos \psi - k_4, \quad B(\psi) = \sin \psi, \quad C(\psi) = k_1 + k_2 \cos \psi \quad (3.83b)$$

which is, again, the equation of a line \mathcal{L} in the u - v plane, with u and v subject to the constraint

$$\mathcal{C}: \quad u^2 + v^2 = 1 \quad (3.83c)$$

The two conjugate values of ϕ for a given value of ψ can thus be computed as the intersection of the line \mathcal{L} with the circle \mathcal{C} , in exactly the same way as in the planar case. As in the planar case, an interesting singularity occurs when coefficients $A(\psi)$, $B(\psi)$, and $C(\psi)$ of the line equation (3.83a) all vanish. In this case, we have the conditions

$$k_3 \cos \psi - k_4 = 0, \quad \sin \psi = 0, \quad k_1 + k_2 \cos \psi = 0 \quad (3.84)$$

The second of the foregoing equations leads to $\psi = 0$ or π . If $\psi = 0$, then the first equation implies $k_3 = k_4$, and hence,

$$\cos \alpha_1 \sin \alpha_2 - \sin \alpha_1 \cos \alpha_2 = 0$$

whence,

$$\alpha_2 = \alpha_1 \quad \text{or} \quad \alpha_2 = \alpha_1 + \pi$$

If $\alpha_2 = \alpha_1$, then the third equation leads to $\cos \alpha_4 = \cos \alpha_3$, and hence, $\alpha_4 = \pm \alpha_3$. If $\psi = \pi$, a similar reasoning to that introduced for the planar case leads exactly to the same result as for $\psi = 0$.

As a consequence, then, the singularity under study leads to a set of postures of the spherical linkage under which the joint axes OA and OD coincide, the coupler and the output links then being free to move as a single rigid body.

Mobility of the Input and Output Links

This analysis is conducted in the space of the four Freudenstein parameters $\{k_i\}_1^4$, with results similar to the planar case. Obviously, in this case the visualization is more challenging.

3.4.3 Spatial Four-Bar Linkages

The analysis of the spatial four-bar linkage parallels that of its planar and spherical counterparts. There are, however, a few remarkable differences, as described below.

For starters, we cast the input-output equation (3.36) in the form

$$\hat{A}\hat{u} + \hat{B}\hat{v} + \hat{C} = 0 \quad (3.85a)$$

where

$$\hat{u} = u - \epsilon d_1 v, \quad \hat{v} = v + \epsilon d_1 u, \quad u \equiv \cos \phi, \quad v \equiv \sin \phi \quad (3.85b)$$

with d_1 denoting the translation of the output cylindrical pair, while ϵ is the dual unit, which has the properties $\epsilon \neq 0$ and $\epsilon^2 = 0$. Moreover,

$$\hat{A} = A(\psi) + \epsilon A_o(\psi), \quad \hat{B} = B(\psi) + \epsilon B_o(\psi), \quad \hat{C} = C(\psi) + \epsilon C_o(\psi) \quad (3.85c)$$

whose primal parts $A(\psi)$, $B(\psi)$ and $C(\psi)$ are identical to those of the spherical linkage, as displayed in eqs.(3.83b), their dual parts $A_o(\psi)$, $B_o(\psi)$ and $C_o(\psi)$ being obtained with the aid of computer algebra and the rules of operations with dual numbers, namely,

$$A_o = a_{\max}(k_{3o}c\psi - \lambda k_3 s\psi - k_{4o}) \quad (3.86a)$$

$$B_o = a_{\max}(s\psi + \lambda c\psi) \quad (3.86b)$$

$$C_o = a_{\max}(k_{1o} + k_{2o}c\psi - \lambda k_2 s\psi) \quad (3.86c)$$

in which the Freudenstein parameters are now dual numbers: $\hat{k}_i = k_i + \epsilon k_{io}$, while λ is defined as the ratio

$$\lambda \equiv d_1/a_{\max} \quad (3.86d)$$

with $a_{\max} = \max_i\{a_i\}$, and $r_i = a_i/a_{\max}$, for $i = 1, \dots, 4$, where we have taken into account that a_i is a distance, in following the Denavit-Hartenberg notation (Denavit and Hartenberg, 1964), recalled in Subsection 3.2.2, and hence, non-negative. Moreover,

$$k_{1o} \equiv -r_1 s\alpha_1 c\alpha_2 c\alpha_4 - r_2 c\alpha_1 s\alpha_2 c\alpha_4 + r_3 s\alpha_3 - r_4 c\alpha_1 c\alpha_2 s\alpha_4 \quad (3.86e)$$

$$k_{2o} \equiv r_1 c\alpha_1 s\alpha_2 c\alpha_4 + r_2 s\alpha_1 c\alpha_2 c\alpha_4 - r_4 s\alpha_1 s\alpha_2 s\alpha_4 \quad (3.86f)$$

$$k_{3o} \equiv -r_1 s\alpha_1 s\alpha_2 s\alpha_4 + r_2 c\alpha_1 c\alpha_2 s\alpha_4 + r_4 c\alpha_1 s\alpha_2 c\alpha_4 \quad (3.86g)$$

$$k_{4o} \equiv r_1 c\alpha_1 c\alpha_2 s\alpha_4 - r_2 s\alpha_1 s\alpha_2 s\alpha_4 + r_4 s\alpha_1 c\alpha_2 c\alpha_4 \quad (3.86h)$$

Once we have obtained the input-output equation in terms of dual angles, it is possible to analyze the RCCC linkage, which allows us, in turn, to compute all the joint rotations and translations. The input-output equation above can be generally written as

$$\hat{\mathcal{L}} : \quad \hat{A}\hat{u} + \hat{B}\hat{v} + \hat{C} = 0 \quad (3.87a)$$

and

$$\hat{\mathcal{C}} : \quad \hat{u}^2 + \hat{v}^2 = 1 \quad (3.87b)$$

where

$$\hat{u} = \cos \hat{\phi}, \quad \hat{v} = \sin \hat{\phi} \quad (3.87c)$$

Equations (3.87a–c) represent a *dual line* $\hat{\mathcal{L}}$ and a *dual unit circle* $\hat{\mathcal{C}}$ in the dual \hat{u} - \hat{v} plane, respectively. Now, it is possible to decompose the equation of the “line” $\hat{\mathcal{L}}$ into two real equations, one for its primal, and one for its dual part, namely,

$$\mathcal{P} : \quad Au + Bv + C = 0 \quad (3.88a)$$

$$\mathcal{H} : \quad (A_o + Bd_1)u + (B_o - Ad_1)v + C_o = 0 \quad (3.88b)$$

For the circle $\hat{\mathcal{C}}$, the dual part vanishes identically, the primal part leading to a *real circle*, namely,

$$\mathcal{C} : \quad u^2 + v^2 = 1 \quad (3.88c)$$

Equation (3.88a) represents a plane \mathcal{P} parallel to the d_1 -axis in the (u, v, d_1) -space, while eq.(3.88b) represents a hyperbolic paraboloid \mathcal{H} in the same space. Moreover, eq.(3.88c) represents a cylinder \mathcal{C} of unit radius and axis parallel to the d_1 -axis, all foregoing items being shown in Figs. 3.9a & b.

The three-dimensional interpretation of eqs.(3.88a–c) is illustrated in Figs. 3.9(a) and (b), whereby line \mathcal{L}_i , for $i = 1, 2$, is defined by the intersection of the plane of eq.(3.88a) with the cylinder (3.88c). Moreover, each line \mathcal{L}_i intersects the paraboloid (3.88b) at one single point, as illustrated in Fig. 3.9b, and as made apparent below.

The system of equations (3.88a–c) should be solved for u, v and d_1 in order to calculate the two conjugate output angles and their corresponding output translations. The intersections \mathcal{L}_1 and \mathcal{L}_2 of the plane \mathcal{P} and the cylinder intersect the u - v plane at points P_1 and P_2 , as shown in Fig. 3.9a, while \mathcal{L}_1 and \mathcal{L}_2 intersect the hyperbolic paraboloid \mathcal{H} at points I_1 and I_2 , as depicted in Fig. 3.9b. The intersection points P_1 and P_2 thus yield the two conjugate output angles ϕ_1 and ϕ_2 . Once the two conjugate solutions u and v are known, via the coordinates of P_1 and P_2 , the unique value of d_1 corresponding to each solution, and defining the intersection points I_1 and I_2 , is determined from eq.(3.88b), namely,

$$d_1(\psi) = \frac{A_o u + B_o v + C_o}{Av - Bu}, \quad Av \neq Bu \quad (3.89)$$

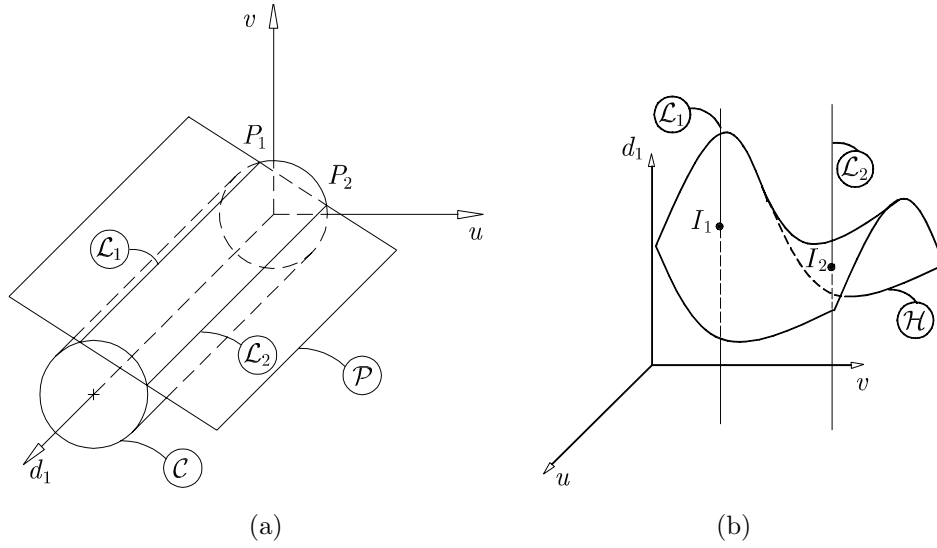


Figure 3.9: Intersections of (a) \mathcal{P} and \mathcal{C} ; and (b) \mathcal{L}_i and \mathcal{H} , for $i = 1, 2$

where we have dispensed with the argument ψ in coefficients A , B , A_o , B_o and C_o for simplicity.

Note that the denominator of eq.(3.89) vanishes if $Av = Bu$; then, as can be readily verified, the numerator of d_1 in the above expression vanishes as well, and d_1 is indeterminate. In this case, the surface \mathcal{H} disappears for all values of the output translations d_1 and we are left with the plane \mathcal{P} and the cylinder \mathcal{C} , which means that d_1 is free to take any value. That is, the motion of this linkage in the plane normal to its joint axes is independent of the translations along these axes. We are here in the presence of a parametric singularity producing a degeneracy of the linkage, similar to those described for the planar and spherical linkages in Subsections 3.4.1 and 3.4.2. Under this singularity, all joint axes are parallel ($\alpha_i = 0, i = 1, \dots, 4$) and, hence, the coupler and the output links can freely slide along their cylindrical-joint axes.

Canonical Equation of the Hyperbolic Paraboloid \mathcal{H}

In order to gain insight into the problem geometry, we derive below the canonical equation of \mathcal{H} . To this end, we let

$$\mathbf{x} \equiv [u \quad v \quad d_1]^T, \quad Q(\mathbf{x}) \equiv A_o u + B d_1 u + B_o v - A d_1 v + C_o$$

the Hessian matrix \mathbf{H} of $Q(\mathbf{x})$ then being evaluated as

$$\mathbf{H} \equiv \frac{\partial^2 Q}{\partial \mathbf{x}^2} = \begin{bmatrix} 0 & 0 & B \\ 0 & 0 & -A \\ B & -A & 0 \end{bmatrix} \quad (3.90)$$

whose eigenvalues are readily computed as

$$\lambda_1 = -\sqrt{A^2 + B^2}, \quad \lambda_2 = 0, \quad \lambda_3 = \sqrt{A^2 + B^2}$$

The corresponding non-normalized eigenvectors \mathbf{e}_i , for $i = 1, 2, 3$, are

$$\mathbf{e}_1 = \begin{bmatrix} B \\ -A \\ \sqrt{A^2 + B^2} \end{bmatrix}, \quad \mathbf{e}_2 = \begin{bmatrix} A \\ B \\ 0 \end{bmatrix}, \quad \mathbf{e}_3 = \begin{bmatrix} -B \\ A \\ \sqrt{A^2 + B^2} \end{bmatrix}$$

and hence, the canonical equation of the surface \mathcal{H} is of the form:

$$\zeta = \frac{\xi^2}{K} - \frac{\eta^2}{K}, \quad K = \frac{2(A_o A + B_o B)}{A^2 + B^2}$$

where

$$\begin{aligned} \xi &= \frac{-\sqrt{2}}{2\sqrt{A^2 + B^2}} \left[Bu + Av + d_1 + \frac{A_o B - B_o A}{4(A_o A + B_o B)} \right] \\ \eta &= \frac{\sqrt{2}}{4\sqrt{A^2 + B^2}} \left(Bu - Av + d_1 + \frac{A_o B - B_o A}{A_o A + B_o B} \right) \\ \zeta &= \frac{1}{\sqrt{A^2 + B^2}} \left[Au + Bv + \frac{(A^2 + B^2)C_o A}{A_o A + B_o B} \right] \end{aligned}$$

which proves that \mathcal{H} is indeed a hyperbolic paraboloid.

The Case of d_1 Acting as Input

We include here a case that has been overlooked in the literature. In this case we regard the translational displacement of the output C joint of a RCCC linkage as input, the two outputs being angles ψ and ϕ . The problem no longer leads to a quadratic equation, but rather to a system of one quartic and one quadratic equations in two variables, as described presently.

Equations (3.88a & b) are both linear in u and v , which allows us to solve for these variables in terms of d_1 , namely,

$$u = u(p, q) = \frac{-BC_o + CB_o - CAd_1}{-AB_o + BA_o + B^2 d_1 + A^2 d_1} \quad (3.91a)$$

$$v = v(p, q) = \frac{-CA_o - AC_o + CBd_1}{-AB_o + BA_o + B^2 d_1 + A^2 d_1} \quad (3.91b)$$

where, in light of eqs.(3.86a-c), with $p = \cos \psi$ and $q = \sin \psi$, u and v become functions of p and q . The latter, moreover, are subject to

$$p^2 + q^2 = 1 \quad (3.92)$$

Substituting the values of u and v given above into eq.(3.88c) produces an equation free of u and v or, correspondingly, free of ϕ , namely,

$$f(p, q) = 0 \quad (3.93)$$

From eq.(3.69b) and eqs.(3.86a–c), both u and v , as given by eqs.(3.91a & b), are rational functions in these variables, with both numerator and denominator quadratic in p and q . Hence, u^2 and v^2 are rational functions with both numerator and denominator quartic in p and q . Therefore, $f(p, q) = 0$ leads, after clearing denominators, to a quartic equation in p and q .

The system of polynomial equations (3.92) and (3.93) apparently has a Bezout number of $4 \times 2 = 8$.

Numerical Examples

The foregoing algorithm is validated with two numerical examples. All numerical and symbolic calculations were completed with the aid of Maple 9.0.

Example 1: The Yang and Freudenstein Linkage

The first example is taken from (Yang and Freudenstein, 1964), with data as listed in Table 3.1. The output displacements, which vary with the input angle, are recorded in Table 3.2. For conciseness, we list only the results for $0 \leq \psi \leq \pi$. Our results match those reported by Yan and Freudenstein, considering the difference of input and output angles in both works, as explained in Subsections 3.2.4. It is noteworthy that only two displacement equations need be solved in our method, as compared with the system of six equations in six unknowns formulated by Yang and Freudenstein, within a purely numerical approach.

Table 3.1: D-H parameters of a RCCC mechanism

Link	1	2	3	4
a_i [in]	5	2	4	3
α_i [deg]	60	30	55	45
d_i [in]	0	variable	variable	variable

Example 2: Prescribing d_1 as Input

In the second example, we try to find the rotations, ψ and ϕ , for a given d_1 , and given dimensions of a RCCC linkage. The dimensions are the same as those in Example 1, with $d_1 = 1.0$. In this example, eq.(3.93) takes the form:

$$A_0 p^4 + A_1(q) p^3 + A_2(q) p^2 + A_3(q) p + A_4(q) = 0 \quad (3.94)$$

Table 3.2: RCCC displacements

ψ [deg]	Branch 1		Branch 2	
	ϕ [deg]	d_1 [in]	ϕ [deg]	d_1 [in]
0	83.70015289	-0.1731633183	-83.70015289	0.1731633183
20	68.59658457	0.01107737578	-105.3298310	0.8429100445
40	64.21379652	-0.5291731100	235.9479009	1.085719194
60	67.55907283	-1.262205018	223.0109192	0.9378806915
80	75.72376603	-1.888758476	214.5328380	0.6631677103
100	87.21970033	-2.259417488	209.1315343	0.3676536240
120	101.1949772	-2.248309766	206.1460158	0.08437533590
140	116.6745934	-1.770565950	205.6297490	-0.1502382358
160	131.8997404	-0.9205435228	208.4003706	-0.2203697101
180	144.2093802	-0.1150813726	215.7906198	0.1150813650

where coefficients $A_i(q)$, for $i = 0, \dots, 4$, are given below:

$$\begin{aligned}
A_0 &= 0.09209746694 \\
A_1(q) &= -0.06765823468q - 0.0073324502 \\
A_2(q) &= -0.1754806581q^2 + 0.01487658368q - 0.1902460942 \\
A_3(q) &= 0.1353164694q^3 + 0.1202907568q^2 + 0.2424947249q + 0.04203177757 \\
A_4(q) &= -0.015625q^4 - 0.0811898817q^3 - 0.020697377q^2 - 0.1362382267q \\
&\quad + 0.0484753242
\end{aligned}$$

Equation (3.94) represents a curve in the p - q plane, whose intersections with the circle of eq.(3.92) yield all real roots of the system at hand. Note, moreover, that all such roots are bound to lie on the above circle. The four real solutions of the foregoing system are given by the four intersections depicted in Fig. 3.10. The solutions are listed in Table 3.3, including the corresponding angles of rotation³.

Mobility of the Input and Output Links

In this case, the mobility analysis applies *only to the input ψ and the output ϕ* , as this analysis decides whether a joint is fully rotatable—can sweep an angle of 2π —or not. This analysis thus reduces to that of the spherical mechanism whose I/O equation is the primal part of the dual equation of this linkage.

³In this table only p and q are given with 10 digits; all other values are given with only four, for the sake of economy of space.

Table 3.3: Possible values of ψ and ϕ

	$[p, q]$	$\psi[\text{deg}]$	$\phi[\text{deg}]$
1	$[0.6047587377, -0.7964087325]$	-52.78	$[-65.68, -227.07]$
2	$[-0.9289796338, -0.3701308418]$	-158.27	$[-130.66, -207.99]$
3	$[0.5819053587, 0.8132565115]$	54.41	$[66.04, 226.10]$
4	$[0.8869350365, 0.4618941881]$	27.50	$[65.79, -113.02]$

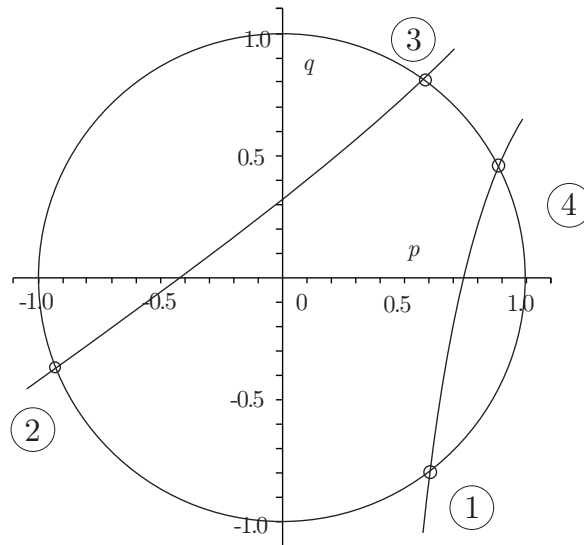


Figure 3.10: The case of an input translation

3.5 Approximate Synthesis

In general, \mathbf{k} is a n -dimensional vector of Freudenstein parameters. For planar linkages $n = 3$; for spherical linkages, $n = 4$, while for spatial linkages of the RCCC type⁴, $n = 8$. For spatial linkages of the RSSR type, moreover, $n = 6$. For $m > n$, no set of values $\{k_i\}_1^n$ can verify all m synthesis equations. We thus have an *error vector* \mathbf{e} :

$$\mathbf{e} \equiv \mathbf{S}\mathbf{k} - \mathbf{b} \quad (3.95)$$

This error vector is termed the *design-error vector*. A positive scalar derived from this vector will be termed a *design error*.

The *design error* e_d adopted here is the rms value of the components of vector \mathbf{e} , i.e.,

$$e_d \equiv \sqrt{\frac{1}{m} \sum_1^m e_i^2} \quad (3.96a)$$

where e_i is the i th component of vector \mathbf{e} , i.e., the *residual* of the i th synthesis equation. Hence, the design error is proportional to the Euclidean norm of the design-error vector:

$$e_d \equiv \sqrt{\frac{1}{m}} \|\mathbf{e}\| \quad (3.96b)$$

It is apparent that, for fixed m , if we minimize $\|\mathbf{e}\|$, we minimize e_d . The value \mathbf{k}_0 of \mathbf{k} that minimizes $\|\mathbf{e}\|$ was derived in Subsection 1.4, and is given in eq.(1.37)⁵. In our case, this equation leads to

$$\mathbf{k}_0 = \mathbf{S}^I \mathbf{b} \quad (3.97a)$$

which is the *least-square approximation* of the given overdetermined system of linear equations, \mathbf{S}^I being the left Moore-Penrose generalized inverse of \mathbf{S} , as introduced in eq.(1.38), and is given by

$$\mathbf{S}^I = (\mathbf{S}\mathbf{S}^T)^{-1} \mathbf{S}^T \quad (3.97b)$$

Hence,

$$\mathbf{e}_0 \equiv \mathbf{S}\mathbf{k}_0 - \mathbf{b} \quad (3.98)$$

is the *least-square error vector*, and

$$e_{d0} \equiv \sqrt{\frac{1}{m}} \|\mathbf{e}_0\| \quad (3.99)$$

is the *least-square design error* of the approximation to the overdetermined system of synthesis equations.

⁴For this type of linkage, two input-output relations are available: the input is the same in both, but the prescribed output comprises both the rotation and the translation of the C joint.

⁵ \mathbf{k}_0 shouldn't be mistaken by \mathbf{k}_o , the dual part of $\hat{\mathbf{k}}$.

Remark 3.5.1 Expression (3.97a) for \mathbf{k}_0 can be derived upon multiplying both sides of eq.(3.12) by \mathbf{S}^T :

$$(\mathbf{S}^T \mathbf{S})\mathbf{k} = \mathbf{S}^T \mathbf{b} \quad (3.100)$$

where $\mathbf{S}^T \mathbf{S}$ is a $n \times n$ matrix. If this matrix is nonsingular, then

$$\mathbf{k} \equiv \mathbf{k}_0 = (\mathbf{S}^T \mathbf{S})^{-1} \mathbf{S}^T \mathbf{b}$$

Remark 3.5.2 The least-square approximation \mathbf{k}_0 can be thought of as being derived upon “inverting” the rectangular \mathbf{S} matrix in the original overdetermined system, eq.(3.12), with the “inverse” of \mathbf{S} understood in the generalized sense.

Remark 3.5.3 \mathbf{k}_0 minimizes the Euclidean norm of \mathbf{e} , which is proportional to the design error.

Remark 3.5.4 The least-square error of the approximation of the overdetermined system of synthesis equations does not measure the positioning error, a.k.a. the structural error, but rather the design error \mathbf{e} defined above. The structural error produced by the synthesized linkage must be measured with respect to the task, not with respect to the synthesis equations. That is, if we let $\bar{\phi}_i$ denote the prescribed value of the output angle, corresponding to the ψ_i value, with ϕ_i denoting the generated value of the output angle, then the structural error is the vector \mathbf{s} given by

$$\mathbf{s} \equiv [\phi_1 - \bar{\phi}_1 \quad \phi_2 - \bar{\phi}_2 \quad \cdots \quad \phi_m - \bar{\phi}_m]^T \quad (3.101)$$

Computing the least-square approximation \mathbf{k}_0 *verbatim* as appearing in eq.(3.97a) is not advisable because of Remark 1.4.3 and the discussion in the paragraph below this remark. This is, if $\kappa(\mathbf{S})$ is moderately large, say, of the order of 1000, $\kappa(\mathbf{S}^T \mathbf{S})$ is inadmissibly large, of the order of 10^6 .

Alternatives to the solution of eq.(3.12) in the presence of a rectangular \mathbf{S} exist (Golub and Van Loan, 1983), as outlined in Subsection 1.4.5 and implemented in scientific software. The two methods outlined in Subsection 1.4.5 fall into what is called the *QR decomposition*: \mathbf{S} is factored into an orthogonal matrix \mathbf{Q} and an upper-triangular matrix \mathbf{R} .

Maple uses Householder reflections to find numerically the least-square approximation of an overdetermined system of linear equations; it uses Gram-Schmidt orthogonalization to do the same if data are given *symbolically*.

In any event, the original system (3.12) is transformed into the form

$$\mathbf{T}\mathbf{k} = \mathbf{c} \quad (3.102)$$

where \mathbf{T} and \mathbf{c} are the transforms of \mathbf{S} and \mathbf{b} of eq.(3.95), respectively, with \mathbf{T} of the form

$$\mathbf{T} = \begin{bmatrix} \mathbf{U} \\ \mathbf{O} \end{bmatrix} \quad (3.103)$$

while \mathbf{U} and \mathbf{O} are

$$\mathbf{U} = \begin{bmatrix} u_{11} & u_{12} & \cdots & u_{1n} \\ 0 & u_{22} & \cdots & u_{2n} \\ \vdots & \vdots & \ddots & \vdots \\ 0 & 0 & \cdots & u_{nn} \end{bmatrix}, \quad \mathbf{O}: \quad (m-n) \times n \text{ zero matrix} \quad (3.104)$$

In order to solve eq.(3.102) for \mathbf{k} , we partition vector \mathbf{c} into a n -dimensional upper part \mathbf{c}_U and a $(m-n)$ -dimensional lower part \mathbf{c}_L :

$$\mathbf{c} = \begin{bmatrix} \mathbf{c}_U \\ \mathbf{c}_L \end{bmatrix} \quad (3.105)$$

where, in general, $\mathbf{c}_L \neq \mathbf{0}$.

System (3.102) thus takes the form

$$\begin{bmatrix} \mathbf{U} \\ \mathbf{O} \end{bmatrix} \mathbf{k} = \begin{bmatrix} \mathbf{c}_U \\ \mathbf{c}_L \end{bmatrix} \quad \Rightarrow \quad \begin{cases} \mathbf{U}\mathbf{k} = \mathbf{c}_U \\ \mathbf{O}\mathbf{k} = \mathbf{c}_L \neq \mathbf{0} \end{cases} \quad (3.106)$$

Remark 3.5.5 *If \mathbf{S} is of full rank, then so is \mathbf{T} and hence, \mathbf{U} is nonsingular.*

Remark 3.5.6 *If \mathbf{U} is nonsingular, then none of its diagonal entries vanishes, for $\det(\mathbf{U}) = u_{11}u_{22} \cdots u_{nn}$.*

Remark 3.5.7 *If \mathbf{U} is nonsingular, then k_1, k_2, \dots, k_n can be computed from the first of eqs.(3.106) by backward substitution.*

Remark 3.5.8 *The second of eqs.(3.106) is a contradiction: its RHS is zero, but its LHS is not! Hence, \mathbf{c}_L is the error vector, and thus, the error in the approximation of the synthesis equations is*

$$e_{d0} = \sqrt{\frac{1}{m-n}} \|\mathbf{c}_L\| \quad (3.107)$$

Example: Synthesis of a Planar Four-Bar Linkage for 10 Data Points

In this example, taken from (Kimbrell, 1991), we show the effect of roundoff-error amplification. The input-output pairs are given in Table 3.4.

The synthesis matrix \mathbf{S} and vector \mathbf{b} of eq.(3.12) become of 10×3 and 10-dimensional, respectively, i.e.,

Table 3.4: Prescribed input-output values for function generation with 10 data points

j	1	2	3	4	5	6	7	8	9	10
ψ_j (deg)	60.0	55.0	50.0	45.0	40.0	35.0	30.0	25.0	20.0	15.0
ϕ_j (deg)	130.0	114.3	99.4	85.7	73.0	61.6	51.5	42.9	35.6	30.0

$$\mathbf{S} = \begin{bmatrix} 1 & -.6427876100 & -.5000000002 \\ 1 & -.4115143586 & -.5735764363 \\ 1 & -.1633259618 & -.6427876097 \\ 1 & .07497872679 & -.7071067812 \\ 1 & .2923717047 & -.7660444431 \\ 1 & .4756242093 & -.8191520443 \\ 1 & .6225146366 & -.8660254038 \\ 1 & .7325428988 & -.9063077870 \\ 1 & .8131007611 & -.9396926208 \\ 1 & .8660254038 & -.9659258263 \end{bmatrix}, \quad \mathbf{b} = \begin{bmatrix} .3420201428 \\ .5105429183 \\ .6507742176 \\ .7581343362 \\ .8386705679 \\ .8941542369 \\ .9304175680 \\ .9515944039 \\ .9631625668 \\ .9659258263 \end{bmatrix}$$

We end up then with a system of 10 linear equations in three unknowns, the three Freudenstein parameters of the planar four-bar linkage. Prior to solving the linear least-square problem thus resulting, it is convenient to estimate the expected accuracy of the results, in light of the precision with which the data are given. Here, a word of caution is in order: although matrix \mathbf{S} and vector \mathbf{b} exhibit 10 digits of precision, the data points, in degrees, are given with only four digits.

In order to have an idea of the expected accuracy of the ensuing results, we compute the condition number of the synthesis matrix, based on the 2-norm. To this end, we first compute the eigenvalues $\{\lambda_k\}_1^3$ of matrix $\mathbf{S}^T\mathbf{S}$, which is displayed below:

$$\mathbf{P} \equiv \mathbf{S}^T\mathbf{S} = \begin{bmatrix} 10.0 & 2.659530410 & -7.686618952 \\ 2.659530410 & 3.261793180 & -2.807787492 \\ -7.686618952 & -2.807787492 & 6.137428730 \end{bmatrix}$$

its eigenvalues being

$$\lambda_1 = 0.0005198886261, \quad \lambda_2 = 2.342915975, \quad \lambda_3 = 17.05578605$$

Hence, the condition number of the synthesis matrix is

$$\kappa(\mathbf{S}) = \sqrt{\frac{\lambda_3}{\lambda_1}} = 181.1259647$$

which means that the roundoff error is expected to be amplified by a factor of less than 200. Since the data are given with four digits of precision, we can guarantee that the

results will be accurate to at least two digits. This is fair enough, for the conventional machine tools that are used to cut links for linkages are capable of accuracies that do not go much farther than these two digits anyway.

If we compute the least-square approximation of the original overdetermined system of equations using all 10 digits of matrix \mathbf{S} and vector \mathbf{b} , then the result obtained by Maple, using Householder reflections, is

$$k_1 = 2.797688253, \quad k_2 = 1.316326216, \quad k_3 = 3.079675927$$

which yield the link lengths

$$a_2 = 0.7596901041a_1, \quad a_3 = 0.5498233725a_1, \quad a_4 = 0.3247094901a_1$$

and the linkage shown in Fig. 3.11, displayed in its two conjugate postures.

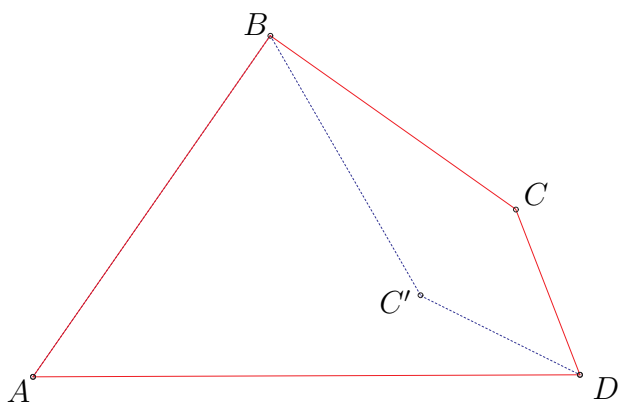


Figure 3.11: Four-bar linkage minimizing the design error for 10 prescribed input-output values in its two conjugate postures

The *least-square error vector* obtained with the foregoing values of \mathbf{k}_0 is computed as

$$\mathbf{e}_0 = \mathbf{S}\mathbf{k}_0 - \mathbf{b} = \begin{bmatrix} -.0697119642 \\ .0209713473 \\ .0476537376 \\ .0394093512 \\ .0152944049 \\ -.0068878011 \\ -.0196254330 \\ -.0192249971 \\ -.0108827912 \\ .0030041453 \end{bmatrix}$$

which yields $e_{d0} = .03207352463$ or 3.2%.

Shown in Fig. 3.12 is the input-output function ϕ vs. ψ of the synthesized linkage, as well as the set of prescribed values, indicated as small circles.

Now we obtain the least-square approximation of the original overdetermined system, again with Householder reflections, as implemented by Maple, but using only four digits. \mathbf{S} and \mathbf{b} are thus rounded off to

$$\mathbf{S} = \begin{bmatrix} 1.0 & -0.6428 & -0.5000 \\ 1.0 & -0.4115 & -0.5736 \\ 1.0 & -0.1633 & -0.6428 \\ 1.0 & 0.07498 & -0.7071 \\ 1.0 & 0.2924 & -.7660 \\ 1.0 & 0.4756 & -0.8192 \\ 1.0 & 0.6225 & -0.8660 \\ 1.0 & 0.7325 & -0.9063 \\ 1.0 & 0.8131 & -0.9397 \\ 1.0 & 0.8660 & -0.9659 \end{bmatrix}, \quad \mathbf{b} = \begin{bmatrix} 0.3420 \\ 0.5105 \\ 0.6508 \\ 0.7581 \\ 0.8387 \\ 0.8942 \\ 0.9304 \\ 0.9516 \\ 0.9632 \\ 0.9659 \end{bmatrix}$$

which yields

$$k_1 = 2.800, \quad k_2 = 1.317, \quad k_3 = 3.082$$

and hence the link lengths

$$a_2 = .7593a_1, \quad a_3 = .5500a_1, \quad a_4 = .3245a_1$$

The *least-square error vector* obtained with the foregoing values of \mathbf{k} is computed as

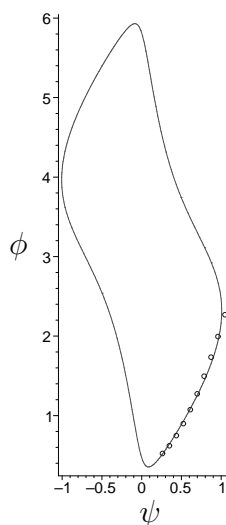


Figure 3.12: The generated I/O function and the prescribed values

$$\mathbf{e}_0 = \mathbf{S}\mathbf{k}_0 - \mathbf{b} = \begin{bmatrix} .06970 \\ .02100 \\ -.04770 \\ .03934 \\ -.01512 \\ -.006694 \\ -.01973 \\ -.01919 \\ -.01081 \\ -.002968 \end{bmatrix}$$

which yields $e_{d0} = .03206$ or, again, 3.2%.

Let us now find a solution of the normal equations (3.100), using only four digits of matrix \mathbf{P} and vector $\mathbf{S}^T\mathbf{b}$, namely⁶,

$$\mathbf{P} = \begin{bmatrix} 10.0 & 2.660 & -7.687 \\ 2.660 & 3.262 & -2.808 \\ 7.687 & 2.808 & 6.137 \end{bmatrix}, \quad \mathbf{S}^T\mathbf{b} = \begin{bmatrix} 7.805 \\ 3.086 \\ -6.298 \end{bmatrix}$$

Below is the solution of the normal equations obtained using LU decomposition, as implemented by Maple:

$$k_1 = -41.93, \quad k_2 = -18.07, \quad k_3 = -61.82$$

which bear no resemblance to the values computed with Householder reflections. These values lead to the link lengths below:

$$a_2 = -0.05533a_1, \quad a_3 = 1.038a_1, \quad a_4 = -0.01618a_1$$

and to the linkage shown in Figs. 3.13, where a provision is made to account for the negative signs of a_3 and a_4 , as outlined at the end of Subsection 3.3.1. It is noteworthy that the roundoff error incurred upon chopping the data and the numerical results after the fourth digit resulted in quite a different solution linkage when using the normal equations. However, the same chopping led only to mild differences in the results when using Householder reflections.

The *least-square error vector* obtained with the foregoing values of \mathbf{k} is computed as

⁶For the record, $\mathbf{S}^T\mathbf{b}$ with 10 digits is $\mathbf{S}^T\mathbf{b} = \begin{bmatrix} 7.805396785 & 3.087045313 & -6.299436319 \end{bmatrix}^T$.



Figure 3.13: Four-bar linkage minimizing the design error for 10 prescribed input-output values, as computed with only four digits and the normal equations

$$\mathbf{e}_0 = \mathbf{S}\mathbf{k}_0 - \mathbf{b} = \begin{bmatrix} 0.2580 \\ 0.4595 \\ 0.1092 \\ -0.3281 \\ -0.6987 \\ -0.7742 \\ -0.5704 \\ -0.0916 \\ 0.5068 \\ 1.164 \end{bmatrix}$$

which yields $e_{d0} = .5861$ or 59%, a huge error!

The solution reported by Kimbrell (1991) has erroneous values for the (1, 1) and (3, 3) entries of \mathbf{P} . For this reason, those results cannot be used for comparison with ours.

The Approximate Synthesis of Spherical Linkages

This case parallels that of planar linkages, with the provision that, as in the case of exact synthesis of spherical linkages, nothing guarantees that the computed least-square approximation complies with the two conditions (3.33). The first of these conditions, $|k_3| \leq 1$ can be enforced in the least-square solution by adding one more equation, $k_3 = 0$, to the synthesis equations. Compliance with this condition, however, will invariably lead to a larger value of e_{d0} . Enforcing the second condition of eq.(3.33), however, calls for techniques for solving problems of *constrained least squares* with nonlinear equality constraints, which fall outside of the scope of this course, and will not be further discussed. The reader is referred to the literature on engineering optimization whenever confronted with this problem.

Adjoining the above equation, $k_3 = 0$, to the synthesis equation, then, leads to the *augmented synthesis equations*

$$\mathbf{S}_a \mathbf{k} = \mathbf{b}_a \tag{3.108a}$$

where

$$\mathbf{S}_a = \begin{bmatrix} \mathbf{S} \\ \mathbf{u}^T \end{bmatrix}, \quad \mathbf{b}_a = \begin{bmatrix} \mathbf{b} \\ 0 \end{bmatrix} \tag{3.108b}$$

with $\mathbf{u} = [0, 0, 1, 0]^T$, and hence, \mathbf{S}_a now becomes of $(m + 1) \times 4$, while \mathbf{b}_a is now $(m + 1)$ -dimensional.

But least-square approximations allow for more flexibility, if we introduce *weights* in eq.(3.108a), by means of a $(m + 1) \times (m + 1)$ constant matrix \mathbf{V}_a :

$$\mathbf{V}_a \mathbf{S}_a \mathbf{k} = \mathbf{V}_a \mathbf{b}_a \quad (3.109a)$$

with

$$\mathbf{V}_a = \begin{bmatrix} \mathbf{V} & \mathbf{0}_m \\ \mathbf{0}_m^T & v \end{bmatrix} \quad (3.109b)$$

in which \mathbf{V} is a $m \times m$ block, $\mathbf{0}_m$ is the m -dimensional zero matrix, and v is a scalar. Both \mathbf{V} and v are assigned by the user under the only constraint of avoiding the introduction of large roundoff-error amplification. We will describe presently how to prescribe \mathbf{V} and v .

Notice that the least-square approximation \mathbf{k}_0 of eq.(3.109a) now becomes, symbolically,

$$\begin{aligned} \mathbf{k}_0 &= [(\mathbf{V}_a \mathbf{S}_a)^T (\mathbf{V}_a \mathbf{S}_a)]^{-1} (\mathbf{V}_a \mathbf{S}_a^T) \mathbf{V}_a \mathbf{b}_a \\ &= (\mathbf{S}_a^T \mathbf{W}_a \mathbf{S}_a)^{-1} \mathbf{S}_a^T \mathbf{W}_a \mathbf{b}_a, \quad \mathbf{W}_a \equiv \mathbf{V}_a^T \mathbf{V}_a \end{aligned} \quad (3.110)$$

in which the symmetric and positive-definite \mathbf{W}_a is termed a *weighting matrix*.

Also notice that

$$\mathbf{W}_a = \begin{bmatrix} \mathbf{V}^T & \mathbf{0}_m \\ \mathbf{0}_m^T & v_{m+1} \end{bmatrix} \begin{bmatrix} \mathbf{V} & \mathbf{0}_m \\ \mathbf{0}_m^T & v_{m+1} \end{bmatrix} = \begin{bmatrix} \mathbf{W} & \mathbf{0}_m \\ \mathbf{0}_m^T & w_{m+1} \end{bmatrix} \quad (3.111a)$$

with

$$\mathbf{W} = \mathbf{V}^T \mathbf{V}, \quad w_{m+1} \equiv v_{m+1}^2 \quad (3.111b)$$

Since no constraint is imposed on \mathbf{V} , besides robustness to round-off error amplification, \mathbf{V} can be freely chosen as *symmetric and positive-definite*, and hence, nonsingular, whence

$$\mathbf{V}^2 = \mathbf{W} \quad \Rightarrow \quad \mathbf{V} = \sqrt{\mathbf{W}} \quad (3.112a)$$

where $\sqrt{\mathbf{W}}$ denotes the *the positive-definite square root of \mathbf{W}* . Now, the simplest matrices to square-root are diagonal matrices, \mathbf{W} then being chosen as

$$\mathbf{W} = \text{diag}(w_1, w_2, \dots, w_m) \quad (3.112b)$$

Now, the error vector in the approximation of eqs.(3.109a) is

$$\mathbf{e}_a = \mathbf{V}_a (\mathbf{S}_a \mathbf{k} - \mathbf{b}_a) = \begin{bmatrix} \mathbf{V} & \mathbf{0}_m \\ \mathbf{0}_m^T & v_{m+1} \end{bmatrix} \begin{bmatrix} \mathbf{S} \mathbf{k} - \mathbf{b} \\ k_3 \end{bmatrix} \quad (3.113a)$$

whose Euclidean norm is

$$\begin{aligned}
\|\mathbf{e}_a\|^2 &= [\mathbf{k}^T \mathbf{S}^T - \mathbf{b}^T \quad k_3] \begin{bmatrix} \mathbf{V}^2 & \mathbf{0}_m \\ \mathbf{0}_m^T & v_{m+1}^2 \end{bmatrix} \begin{bmatrix} \mathbf{S}\mathbf{k} - \mathbf{b} \\ k_3 \end{bmatrix} \\
&= (\mathbf{k}^T \mathbf{S}^T - \mathbf{b}^T) \mathbf{W} (\mathbf{S}\mathbf{k} - \mathbf{b}) + w_{m+1} k_3^2 \\
&= \sum_{i=1}^m w_i e_i^2 + w_{m+1} k_3^2
\end{aligned} \tag{3.113b}$$

which thus yields a *weighted error-norm*. In order to avoid large roundoff-error amplification, we choose the weighting factors $\{w_i\}_1^{m+1}$ as

$$\sum_{i=1}^{m+1} w_i = 1, \quad 0 \leq w_i \leq 1, \quad i = 1, \dots, m \tag{3.114}$$

so that $\|\mathbf{e}_a\|^2$ becomes a *convex combination* of all $m + 1$ errors. If no preference is given to the set $\{e_i\}_1^m$, then the first m weights can be chosen all equal, while w_{m+1} is to be chosen so as to enforce $|k_3|$ to be smaller than unity but, if w_{m+1} is chosen unnecessarily large, then $|k_3|$ will be “too small” at the expense of a “large” design error. The best compromise is to be chosen by trial and error.

The Approximate Synthesis of Spatial Linkages

The synthesis equations (3.41) for the spatial four-bar linkage are reproduced below for quick reference:

$$\hat{\mathbf{S}}\hat{\mathbf{k}} = \hat{\mathbf{b}} \tag{3.115}$$

These equations can be shown to admit the least-square solution

$$\hat{\mathbf{k}}_0 = \hat{\mathbf{S}}^I \hat{\mathbf{b}}, \quad \hat{\mathbf{S}}^I = (\hat{\mathbf{S}}^T \hat{\mathbf{S}})^{-1} \hat{\mathbf{S}}^T \tag{3.116}$$

The inverse of the dual square matrix in the foregoing relations is computed using eq. (A.13) of the Appendix:

$$(\hat{\mathbf{S}}^T \hat{\mathbf{S}})^{-1} = (\mathbf{S}^T \mathbf{S})^{-1} - \epsilon (\mathbf{S}^T \mathbf{S})^{-1} (\mathbf{S}^T \mathbf{S}_o + \mathbf{S}_o^T) (\mathbf{S}^T \mathbf{S})^{-1} \tag{3.117}$$

Upon substitution of expression (3.117) in eq.(3.116), and expansion of the expression thus resulting, the least-square approximation $\hat{\mathbf{k}}_0$ is obtained as

$$\hat{\mathbf{k}}_0 = \underbrace{(\mathbf{S}^T \mathbf{S})^{-1} \mathbf{S}^T \mathbf{b}}_{\mathbf{k}_0} + \epsilon \underbrace{(\mathbf{S}^T \mathbf{S})^{-1} [\mathbf{S}_o^T \mathbf{b} + \mathbf{S}^T \mathbf{b}_o - (\mathbf{S}^T \mathbf{S}_o + \mathbf{S}_o^T \mathbf{S}) (\mathbf{S}^T \mathbf{S})^{-1} \mathbf{S}^T \mathbf{b}]}_{\mathbf{k}_{o0}} \tag{3.118}$$

While the above expressions for the least-square approximation of the primal part of $\hat{\mathbf{k}}$, \mathbf{k}_0 , and its dual counterpart \mathbf{k}_{o0} are theoretically sound, they are not appropriate for computations verbatim, given the large amount of floating-point operations involved, and their need of the inverse $(\mathbf{S}^T \mathbf{S})^{-1}$, which, as we saw in Remark 1.4.3, is not advisable

to compute verbatim because of the large condition number of the matrix product. An efficient, reliable computational scheme is outlined below:

We recall the synthesis equations (3.46), which lead to

$$\mathbf{S}\mathbf{k} = \mathbf{b} \quad (3.119a)$$

$$\mathbf{S}\mathbf{k}_o = \mathbf{b}_o - \mathbf{S}_o\mathbf{k} \quad (3.119b)$$

where the primal parts of the dual Freudenstein parameters, arrayed in vector \mathbf{k} , are first computed, using an orthogonalization method, from eq.(3.119a). The dual parts of the same parameters, arrayed in vector \mathbf{k}_o , are next computed likewise from eq.(3.119b). If, for example, the least-square approximation \mathbf{k}_0 to eq.(3.119a) is computed with Householder reflections, which yield a transformed matrix \mathbf{T} in upper-triangular form, then the same transformed matrix is used to compute the least-square approximation \mathbf{k}_{o0} to eq.(3.119b).

Again, nothing guarantees that k_1 and k_3 , as per Remark 3.3.2, will comply with the conditions therein, and yield a feasible linkage—these conditions were imposed on spherical linkages, but since the primal equations of spatial linkages are identical to those of the former, the conditions at stake apply to the latter as well. The first condition, $|k_3| \leq 1$, can be enforced via a *weighted least-square approach*, as introduced in connection with spherical linkages.

3.6 Linkage Performance Evaluation

3.6.1 Planar Linkages: Transmission Angle and Transmission Quality

A variable of merit which is used to assess the linkage performance is the *transmission angle* μ , illustrated in Fig. 3.1. The transmission angle is thus the angle between the axes of the output and the coupler links.

The relevance of this angle is apparent from a kinetostatic analysis: From Fig. 3.14, the force transmitted by the linkage to the frame has a magnitude $|F_{41}|$ given by

$$|F_{41}| = |F_{14}| = |F_{34}| \quad (3.120)$$

where, from the static equilibrium of link 1,

$$|F_{34}| = |F_{32}| = \left| \frac{\tau_\psi}{a_2 \sin(\psi - \theta)} \right| \quad (3.121)$$

and τ_ψ is the *applied torque* that balances statically the *load torque* τ_ϕ .

The magnitude of the radial component of F_{14} , denoted by $|F_{14}|_r$, is derived upon substitution of eq.(3.121) into eq.(3.120), thus obtaining

$$|F_{14}|_r \equiv |F_{14}| \cos \mu = \left| \frac{\tau_\psi \cos \mu}{a_2 \sin(\psi - \theta)} \right| \quad (3.122)$$

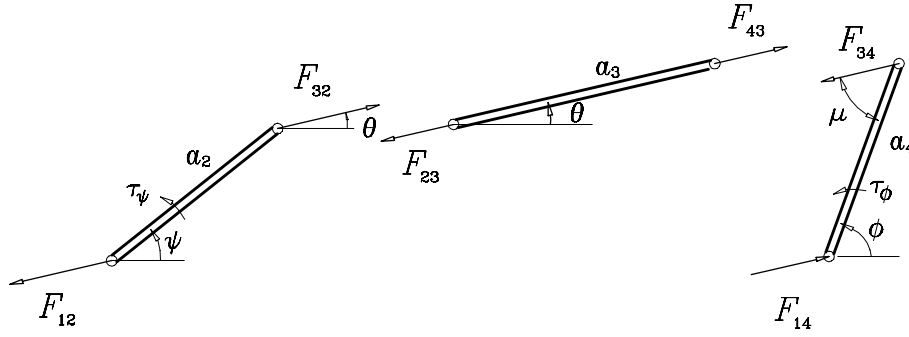


Figure 3.14: A static analysis of the four-bar linkage

from which it is clear that $|F_{14}|_r$ is proportional to the magnitude of the applied moment and to the cosine of the transmission angle. Since this is a nonworking force, one is interested in keeping it as low as possible. However, it cannot be made zero by simply making zero the applied torque because, then, no useful force would be transmitted! Thus, the only possible way of keeping that force as small as possible is by keeping $|\cos \mu|$ as small as possible, i.e., by keeping $|\mu|$ as close as possible to 90° .

Clearly, the transmission angle is posture-dependent and, hence, cannot be maintained at a fixed value for all the linkage postures. In practice, a minimum allowable value on the transmission angle or, rather, on its absolute value, is prescribed. This is commonly accepted as 45° , i.e., a specification when designing four-bar linkages is

$$|\mu| \geq 45^\circ \quad (3.123)$$

If one is interested in evaluating the overall performance of a four-bar linkage whose input link is capable of moving between ψ_1 and ψ_2 , then a merit function of the linkage considering *all possible postures* is needed. This is the *transmission quality* of the linkage, which is defined as

$$Q \equiv \sqrt{\frac{1}{\Delta\psi} \int_{\psi_1}^{\psi_2} \sin^2 \mu d\psi}, \quad \Delta\psi \equiv \psi_2 - \psi_1 \quad (3.124)$$

From the foregoing definition, note that

$$0 < Q < 1 \quad (3.125)$$

Evaluating Q as given above is rather difficult because an expression for $\sin \mu$ is not readily derivable. However, an expression for $\cos \mu$ can be readily derived. Indeed, from Fig. 3.1 and the “cosine law”, two expressions for $\overline{O_2O_4}$ can be derived:

$$\overline{O_2O_4}^2 = a_3^2 + a_4^2 - 2a_3a_4 \cos \mu \quad (3.126a)$$

$$\overline{O_2O_4}^2 = a_1^2 + a_2^2 - 2a_1a_2 \cos \psi \quad (3.126b)$$

Upon equating the two right-hand sides of the foregoing equations, an expression for $\cos \mu$ is derived, namely

$$\cos \mu = \frac{a_3^2 + a_4^2 - a_1^2 - a_2^2 + 2a_1a_2 \cos \psi}{2a_3a_4} \quad (3.127)$$

If now relations (3.68) are recalled, an expression for $\cos \mu$ in terms of the linkage parameters $\{k_i\}_1^3$ is obtained:

$$\cos \mu = \operatorname{sgn}(k_2k_3)(c_1 + c_2 \cos \psi) \quad (3.128a)$$

where coefficients c_1 and c_2 are defined as

$$c_1 \equiv \frac{k_2 - k_1k_3}{\sqrt{D}}, \quad c_2 = \frac{k_3^2}{\sqrt{D}} \quad (3.128b)$$

$$D \equiv k_2^2 + k_3^2 + k_2^2k_3^2 - 2k_1k_2k_3 \quad (3.128c)$$

Now the transmission quality Q can be written as $Q = \sqrt{1 - \delta^2}$ where δ is the integral of $\cos^2 \mu$ over the full mobility interval of the input link, i.e.,

$$\delta \equiv \sqrt{\frac{1}{\Delta\psi} \int_{\psi_1}^{\psi_2} \cos^2 \mu d\psi}, \quad \Delta\psi \equiv \psi_2 - \psi_1 \quad (3.129)$$

and, by virtue of the relation between the transmission quality Q and δ , namely,

$$Q^2 + \delta^2 = 1 \quad (3.130)$$

it is reasonable to call δ the *transmission defect* of the linkage. Hence, maximizing Q is equivalent to minimizing δ . Note that δ^2 can be written as

$$\delta^2 \equiv \frac{1}{\Delta\psi} \left[c_1^2 \Delta\psi + 2c_1c_2(\sin \psi_2 - \sin \psi_1) + \frac{1}{2}c_2^2 \Delta\psi + \frac{c_2^2}{4}(\sin 2\psi_2 - \sin 2\psi_1) \right] \quad (3.131)$$

If, in particular, the input link is a crank, then,

$$\delta^2 = c_1^2 + \frac{1}{2}c_2^2 \quad (3.132)$$

In synthesizing a four-bar linkage for function generation, the location of the zeros of the dials of the ψ and ϕ values is normally immaterial. What matters is the *incremental values* of these angles from those zeros. We can thus introduce parameters α and β denoting the location of the zeros on the ψ and the ϕ dials, respectively, so that now

$$\psi_i = \alpha + \Delta\psi_i, \quad \phi_i = \beta + \Delta\phi_i, \quad \text{for } i = 1, 2, \dots, m \quad (3.133)$$

We can thus regard the least-square approximation \mathbf{k}_0 as a function of α and β , i.e.,

$$\mathbf{k}_0 = \mathbf{k}_0(\alpha, \beta) \quad (3.134)$$

It is apparent, then, that the two new parameters can be used to optimize the linkage performance, e.g., by minimizing its defect δ .

As it turns out, the transmission angle plays an important role not only in the force-transmission characteristics of the linkage, but also in the *sensitivity* of its positioning accuracy to changes in the nondimensional parameters \mathbf{k} . Indeed, if we make abstraction of the parameters α and β , for simplicity, we can calculate the sensitivity of the synthesized angle ϕ_i to changes in \mathbf{k} from the input-output equation (3.11) written for the m prescribed input-output pairs. We display below the i th component of this vector equation:

$$F_i(\psi_i, \phi_i, \mathbf{k}) = k_1 + k_2 \cos \phi_i - k_3 \cos \psi_i - \cos(\psi_i - \phi_i) = 0, \quad i = 1, 2, \dots, m \quad (3.135)$$

where ϕ_i is one of the two values of ϕ that verify the above equation for $\psi = \psi_i$, namely, the one lying closest to $\bar{\phi}_i$, as introduced in eq.(3.101). The sensitivity of interest is, apparently, $\partial\phi_i/\partial\mathbf{k}$, which is computed below:

$$\frac{dF_i}{d\mathbf{k}} = \frac{\partial F_i}{\partial \phi_i} \frac{\partial \phi_i}{\partial \mathbf{k}} + \frac{\partial F_i}{\partial \mathbf{k}} = \mathbf{0}$$

whence,

$$\frac{\partial \phi_i}{\partial \mathbf{k}} = - \frac{\partial F_i / \partial \mathbf{k}}{\partial F_i / \partial \phi_i} \quad (3.136)$$

Now, we calculate $\partial F_i / \partial \phi_i$ from eq.(3.135):

$$\frac{\partial F_i}{\partial \phi_i} = -k_2 \sin \phi - \sin(\psi_i - \phi_i) = - \frac{a_1 \sin \phi_i - a_2 \sin(\phi_i - \psi_i)}{a_2} \quad (3.137)$$

A pertinent relation among the variables and parameters involved in eq.(3.137) is displayed in Fig. 3.15. From this figure,

$$a_1 \sin \phi_i - a_2 \sin(\phi_i - \psi_i) = a_3 \sin \mu_i \quad (3.138)$$

Upon substitution of eq.(3.138) into eq.(3.137), we obtain

$$\frac{\partial F_i}{\partial \phi_i} = - \frac{a_3}{a_2} \sin \mu_i \quad (3.139a)$$

which, when substituted into eq.(3.136), yields

$$\frac{\partial \phi_i}{\partial \mathbf{k}} = \frac{a_2}{a_3 \sin \mu_i} \frac{\partial F_i}{\partial \mathbf{k}} \quad (3.139b)$$

Furthermore,

$$\frac{\partial F_i}{\partial \mathbf{k}} = \begin{bmatrix} 1 \\ \cos \phi_i \\ -\cos \psi_i \end{bmatrix} \quad (3.139c)$$

and hence,

$$\frac{\partial \phi_i}{\partial \mathbf{k}} = \frac{a_2}{a_3 \sin \mu_i} \begin{bmatrix} 1 \\ \cos \phi_i \\ -\cos \psi_i \end{bmatrix} \quad (3.139d)$$

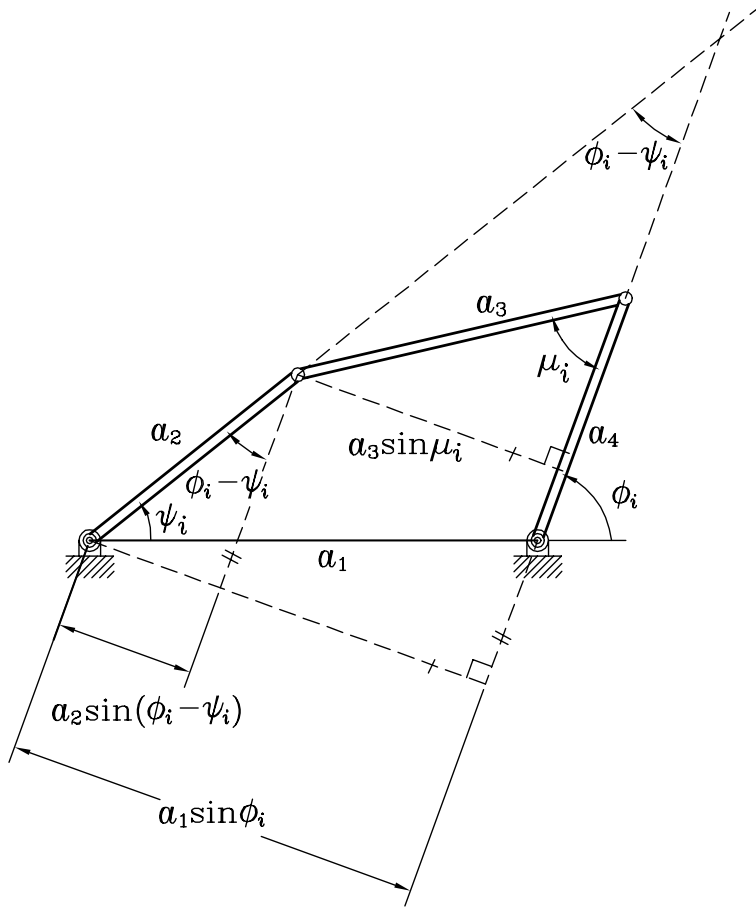


Figure 3.15: Relation between the transmission angle and the parameters and variables of a four-bar linkage

It is now apparent that the larger $|\sin \mu_i|$, the less sensitive the positioning accuracy of the linkage is to changes in the linkage dimensions.

An interesting relation between the linkage discriminant defined in eq.(3.78a) and the transmission angle is now derived. From the expression for $\cos \mu$ obtained in eqs.(3.128a), an expression for $\sin^2 \mu$ is readily obtained, in terms of the Freudenstein parameters, as

$$\sin^2 \mu = \frac{k_3^2}{k_2^2 + k_3^2 + k_2^2 k_3^2 - 2k_1 k_2 k_3} \Delta(\psi) \quad (3.140a)$$

where $\Delta(\psi)$ is the linkage discriminant of eq.(3.78a), reproduced below for quick reference:

$$\Delta(\psi) \equiv -k_3^2 \cos^2 \psi + 2(k_1 k_3 - k_2) \cos \psi + (1 - k_1^2 + k_2^2) \geq 0 \quad (3.140b)$$

which is nonnegative at feasible postures.

Apparently, then, for a given linkage, the square of the sine of the transmission angle is proportional to the discriminant. Hence, both vanish at dead points of the input link, which occur when this is a rocker.

3.6.2 Spherical Linkages: Transmission Angle and Transmission Quality

3.6.3 Spatial Linkages: Transmission Angle and Transmission Quality

3.7 Design Error vs. Structural Error

In this section we establish the relation between the design error and the structural error. In doing this, we build upon the analysis proposed by Tinubu and Gupta (1984).

The structural error was introduced in eq.(3.101); this definition is reproduced below for quick reference:

$$\mathbf{s} \equiv [\phi_1 - \bar{\phi}_1 \quad \phi_2 - \bar{\phi}_2 \quad \cdots \quad \phi_m - \bar{\phi}_m]^T \quad (3.141)$$

where, it is recalled, ϕ_i denotes the *generated* value, $\bar{\phi}_i$ the *prescribed* value of the output angle for a given value ψ_i of the input angle. In the ensuing discussion we assume that the synthesis equations are cast in the general form

$$\mathbf{S}\mathbf{k} = \mathbf{b} \quad (3.142)$$

regardless of the type of linkage, planar, spherical or spatial. In this context, \mathbf{S} is a $m \times n$ matrix, while \mathbf{k} and \mathbf{b} are n - and m -dimensional vectors, respectively. Obviously, $n = 3, 4$ or 8 , depending on the type of linkage, planar, spherical or spatial⁷. In the case of spatial linkages, a second equation of the same gestalt as that of eq.(3.142), involving a second vector of Freudenstein parameters—the dual part of the dual vector $\hat{\mathbf{k}}$ —occurs, as per eqs.(3.119a & b).

In minimizing the structural error, we aim at minimizing the *root-mean square* (rms) value of the components of vector \mathbf{s} over \mathbf{k} :

$$z \equiv \frac{1}{2m} \|\mathbf{s}\|^2 \quad \rightarrow \quad \min_{\mathbf{k}} \quad (3.143)$$

where $\|\mathbf{s}\|$ is the Euclidean norm of \mathbf{s} . In fact, we aim at minimizing the square of one-half the rms value of the structural error at the m prescribed points. The positive scalar z can be fairly called the square of the *positioning error*.

The above function attains a *stationary* value with respect to \mathbf{k} when its *gradient* vanishes, i.e.,

$$\nabla z \equiv \frac{\partial z}{\partial \mathbf{k}} = \left(\frac{\partial \mathbf{s}}{\partial \mathbf{k}} \right)^T \frac{\partial z}{\partial \mathbf{s}} = \mathbf{0}_n \quad (3.144)$$

with $\mathbf{0}_n$ denoting the n -dimensional zero vector. The above equation is the *normality condition* of the minimization problem at hand. Apparently,

$$\frac{\partial z}{\partial \mathbf{s}} = \frac{1}{m} \mathbf{s} \quad (3.145)$$

⁷See footnote 4 of this chapter.

Now, in order to compute $\partial \mathbf{s} / \partial \mathbf{k}$, we recall the definition of \mathbf{s} , eq.(3.141), whence,

$$\frac{\partial \mathbf{s}}{\partial \mathbf{k}} = \frac{\partial \boldsymbol{\phi}}{\partial \mathbf{k}} \quad (3.146)$$

where $\boldsymbol{\phi}$ is the m -dimensional vector whose i th component is the i th *generated* value of the output angle, in the same way that $\bar{\boldsymbol{\phi}}$ denotes the m -dimensional vector whose i th component is the i th *prescribed* value of the output angle, i.e.,

$$\boldsymbol{\phi} \equiv \begin{bmatrix} \phi_1 \\ \phi_2 \\ \vdots \\ \phi_m \end{bmatrix}, \quad \bar{\boldsymbol{\phi}} = \begin{bmatrix} \bar{\phi}_1 \\ \bar{\phi}_2 \\ \vdots \\ \bar{\phi}_m \end{bmatrix} \quad (3.147)$$

the i th row of matrix $\partial \boldsymbol{\phi} / \partial \mathbf{k}$, for the *planar case*, being displayed in eq.(3.139d) as a column array.

Now, in order to compute $\partial \boldsymbol{\phi} / \partial \mathbf{k}$, we need an equation relating the array $\boldsymbol{\phi}$ of *generated values* of the output angle with vector \mathbf{k} . One candidate would be the m synthesis equations (3.142), which define the *design error* \mathbf{e} :

$$\mathbf{e} \equiv \mathbf{e}(\boldsymbol{\phi}, \mathbf{k}) = \mathbf{S}\mathbf{k} - \mathbf{b} \quad (3.148)$$

The above expression is, in general, different from zero, when evaluated at the *prescribed* values $\bar{\phi}_i$ of the output angle, for $i = 1, \dots, m$, and hence, does not define an implicit equation in $\boldsymbol{\phi}$ and \mathbf{k} . As a matter of fact, the problem of approximate synthesis consists in minimizing the Euclidean norm of the nonzero vector \mathbf{e} .

However, when the above vector is evaluated at the *generated* values ϕ_i of the output angle, for $i = 1, \dots, m$, then it does vanish. Indeed, the i th component of \mathbf{e} as defined in eq.(3.148) is nothing but the input-output function $F(\psi, \phi) = 0$ evaluated at ψ_i for a given linkage defined by \mathbf{k} . In our case, \mathbf{k} is the *current value*, within an iterative process to be formulated in Subsection 3.7.1, of the unknown vector of linkage parameters, the Freudenstein parameters. Upon solving the input-output equation for ϕ , two values of ϕ_i are obtained, as found in Section 3.4, and hence, the function does vanish at these two values. We will assume that, of these two values, ϕ_i is chosen as the one closer to $\bar{\phi}_i$. We thus have

$$F(\psi_i, \phi_i) \equiv \mathbf{s}_i^T \mathbf{k} - b_i = 0 \quad (3.149)$$

in which \mathbf{s}_i^T denotes the i th row of \mathbf{S} and b_i the i th component of \mathbf{b} .

To avoid confusion, let us distinguish between the design error \mathbf{e} when evaluated at $\boldsymbol{\phi}$ and when evaluated at $\bar{\boldsymbol{\phi}}$, by denoting the latter by $\bar{\mathbf{e}}$, i.e.,

$$\bar{\mathbf{e}} \equiv \mathbf{e}(\bar{\boldsymbol{\phi}}, \mathbf{k}) = \bar{\mathbf{S}}\mathbf{k} - \bar{\mathbf{b}} \neq \mathbf{0} \quad (3.150)$$

where $\bar{\mathbf{S}}$ and $\bar{\mathbf{b}}$ denote \mathbf{S} and \mathbf{b} , respectively, when evaluated at the prescribed values of the input angle, $\{\psi_i\}_1^m$ and at the generated $\bar{\boldsymbol{\phi}}$.

Moreover, when we evaluate $\bar{\mathbf{e}}$ at the *generated* value $\bar{\boldsymbol{\phi}}$, we obtain

$$\bar{\mathbf{e}} \equiv \mathbf{e}(\bar{\boldsymbol{\phi}}, \mathbf{k}) = \mathbf{S}\mathbf{k} - \mathbf{b} = \mathbf{0}_m \quad (3.151)$$

which is an *implicit* vector function of $\boldsymbol{\phi}$ and \mathbf{k} , and hence, allows for the evaluation of $\partial\boldsymbol{\phi}/\partial\mathbf{k}$. Upon differentiation of eq.(3.151) with respect to \mathbf{k} , we obtain

$$\frac{d\bar{\mathbf{e}}}{d\mathbf{k}} = \frac{\partial\bar{\mathbf{e}}}{\partial\mathbf{k}} + \frac{\partial\bar{\mathbf{e}}}{\partial\bar{\boldsymbol{\phi}}} \frac{\partial\bar{\boldsymbol{\phi}}}{\partial\mathbf{k}} = \mathbf{0}_{mn} \quad (3.152)$$

where $\mathbf{0}_{mn}$ is the $m \times n$ zero matrix. Moreover, the $m \times m$ matrix $\partial\bar{\mathbf{e}}/\partial\bar{\boldsymbol{\phi}}$ is computed from the input-output equation (3.149). Since e_k is influenced only by ϕ_k , and not by ϕ_j , for $j \neq k$, $\partial\bar{\mathbf{e}}/\partial\bar{\boldsymbol{\phi}}$ is diagonal, i.e.,

$$\frac{\partial\bar{\mathbf{e}}}{\partial\bar{\boldsymbol{\phi}}} = \text{diag} [\partial e_1/\partial\phi_1 \quad \partial e_2/\partial\phi_2 \quad \cdots \quad \partial e_m/\partial\phi_m] \equiv \mathbf{D} \quad (3.153a)$$

Under the assumption that none of the diagonal elements of \mathbf{D} vanishes, this matrix is nonsingular, and hence, the matrix $\partial\boldsymbol{\phi}/\partial\mathbf{k}$ sought can be solved for from eq.(3.152). Furthermore, it is apparent from eq.(3.151) that $\partial\bar{\mathbf{e}}/\partial\mathbf{k}$ is nothing but the synthesis matrix \mathbf{S} , i.e.,

$$\frac{\partial\bar{\mathbf{e}}}{\partial\mathbf{k}} = \mathbf{S} \quad (3.153b)$$

Hence, $\partial\boldsymbol{\phi}/\partial\mathbf{k}$, as computed from eq.(3.152), is

$$\frac{\partial\boldsymbol{\phi}}{\partial\mathbf{k}} = -\mathbf{D}^{-1}\mathbf{S} \quad (3.154)$$

Therefore, the normality condition (3.144) leads to

$$\mathbf{S}^T\mathbf{D}^{-1}\mathbf{s} = \mathbf{0}_n \quad (3.155)$$

where $\mathbf{0}_n$ denotes the n -dimensional zero vector. The normality condition thus states that, for \mathbf{k} to produce a stationary value of the positioning error—proportional to the square of the rms value of the structural error \mathbf{s} —the structural error \mathbf{s} must lie in the null space of the matrix product $\mathbf{S}^T\mathbf{D}^{-1}$. That is, the structural error of minimum norm need not vanish and, in general, it won't, but must verify eq.(3.155).

Now, contrary to the minimization of the design error, the minimization of the positioning error thus leads to a *nonlinear least-square problem*, which must be solved *iteratively*, as described in Subsection 3.7.1.

3.7.1 Minimizing the Structural Error

The approach followed here is similar to the Newton-Gauss method used to solve nonlinear least-square problems, as outlined in Subsection 1.6.1: for starters, a sequence $\mathbf{s}^0, \mathbf{s}^1, \dots, \mathbf{s}^i, \mathbf{s}^{i+1}$ of structural-error vector values is generated, which, upon convergence,

should verify the normality condition. For a given \mathbf{s}^i , an improved vector value \mathbf{s}^{i+1} is obtained from the *first-order approximation* of \mathbf{s} :

$$\mathbf{s}^{i+1} \approx \mathbf{s}^i + \left. \frac{\partial \mathbf{s}}{\partial \mathbf{k}} \right|_{\mathbf{k}=\mathbf{k}^i} \Delta \mathbf{k}^i = \mathbf{s}^i - \mathbf{D}_i^{-1} \mathbf{S}_i \Delta \mathbf{k}^i \quad (3.156)$$

where $\mathbf{D}_i \equiv \mathbf{D}|_{\mathbf{k}=\mathbf{k}^i}$ and $\mathbf{S}_i \equiv \mathbf{S}|_{\mathbf{k}=\mathbf{k}^i}$. Hence,

$$\mathbf{D}_i^{-1} \mathbf{S}_i \Delta \mathbf{k}^i = \mathbf{s}^i - \mathbf{s}^{i+1} \quad (3.157)$$

Upon solving for $\Delta \mathbf{k}^i$, the above equation allows the updating of \mathbf{k} as $\mathbf{k}^{i+1} = \mathbf{k}^i + \Delta \mathbf{k}^i$. However, in eq.(3.157) we don't know \mathbf{s}^{i+1} . Moreover, upon convergence, \mathbf{s} needn't vanish, and most likely it won't. We can thus assume that $\mathbf{s}^{i+1} \neq \mathbf{0}_m$, but, if \mathbf{k}^{i+1} is an improvement over \mathbf{k}^i , then the corresponding structural error \mathbf{s}^{i+1} will be "close" to verifying the normality condition (3.155). In fact, let us assume that \mathbf{s}^{i+1} does verify the normality condition. Further, let us multiply both sides of eq.(3.157) from the left by $\mathbf{S}_i^T \mathbf{D}_i^{-1}$, which yields

$$\mathbf{S}_i^T \mathbf{D}_i^{-1} \mathbf{D}_i^{-1} \mathbf{S}_i \Delta \mathbf{k}^i = \mathbf{S}_i^T \mathbf{D}_i^{-1} \mathbf{s}^i \quad (3.158)$$

where the term linear in \mathbf{s}^{i+1} has been dropped because it has been assumed to verify the normality conditions. In eq.(3.158) the coefficient of $\Delta \mathbf{k}^i$ is a square $n \times n$ matrix, which allows for the computation of $\Delta \mathbf{k}^i$ in the form

$$\Delta \mathbf{k}^i = (\mathbf{S}_i^T \mathbf{D}_i^{-2} \mathbf{S}_i)^{-1} \mathbf{S}_i^T \mathbf{D}_i^{-1} \mathbf{s}^i \quad (3.159)$$

thereby showing that the correction $\Delta \mathbf{k}^i$ can be computed with the numerical values available at the i th iteration. In fact, the expression for $\Delta \mathbf{k}^i$ given in eq.(3.159) should be regarded as a *formula*, not as an algorithm. Indeed, the verbatim inversion of the matrix in parentheses in the foregoing equation is *to be avoided* due to its high *condition number*⁸. As a matter of fact, the condition number, in either the Euclidean or the Frobenius norm, of the same $n \times n$ matrix is exactly the square of the same norm of the $m \times n$ matrix $\mathbf{D}_i^{-1} \mathbf{S}_i$. Hence, a formulation is sought that will allow the computation of $\Delta \mathbf{k}^i$ from a system of equations involving the foregoing rectangular matrix. If we recall Subsection 1.4.5, the right-hand side of eq.(3.159) is the *least-square approximation* of the *overdetermined system*

$$(\mathbf{D}_i^{-1} \mathbf{S}_i) \Delta \mathbf{k}^i = \mathbf{s}^i \quad (3.160)$$

which is identical to eq.(3.157) when the term \mathbf{s}^{i+1} is dropped. Notice, however, that this term couldn't simply be dropped from the above-mentioned equation on the basis that the said term vanishes, because the structural error is not expected to vanish at the optimum solution. The computation of $\Delta \mathbf{k}^i$ from eq.(3.160) now should be pursued via an orthogonalization procedure, as studied in Subsection 1.4.5. With $\Delta \mathbf{k}^i$ calculated, the

⁸See the definition of this concept in Section 1.4.4.

i th iteration is complete, as a new, improved value \mathbf{k}^{i+1} of the design parameter vector \mathbf{k} is available. Now the new structural-error vector value \mathbf{s}^{i+1} can be computed, and then the normality condition verified. If the condition is not verified, a new iteration is in order; if the same condition is verified, then the procedure stops. An alternative convergence criterion, equivalent to the latter, is to verify whether $\|\Delta\mathbf{k}^i\| < \epsilon$, for a prescribed tolerance ϵ . The equivalence of the two criteria should be apparent from the relation between $\Delta\mathbf{k}^i$ and the product of the last three factors of the right-hand side of eq.(3.159).

Branch-switching Detection

In the foregoing analysis an implicit assumption was adopted: all generated values $\{\phi_i\}_1^m$ lie on the same linkage branch. However, all four-bar linkages studied in this chapter, planar, spherical and spatial, were shown in Section 3.4 to be *bimodal*, i.e., they all entail two solution branches of their input-output equation. This means that, within an iteration loop, the occurrence of branch-switching should be monitored. Below we explain a simple means of doing this, as applicable to planar linkages. The two branches of a typical planar four-bar linkage are apparent in Fig. 3.13. In this figure, the transmission angle is $\mu = \angle BCD$ in one branch, in the second being $\mu' = \angle BC'D$. The qualitative difference between the two branches lies in the sign of the transmission angle, for, in the first branch, we have $\sin \mu > 0$; in the second, $\sin \mu' < 0$. Moreover, $\sin \mu$ vanishes at *dead points*, when the input angle reaches either a maximum or a minimum—linkages of this kind have an input rocker. Hence, a simple way of deciding whether all values $\{\phi_i\}_1^m$ lie in the same branch relies on the computation of $\sin \mu$ with the correct sign. This is most simply done by means of the 2D version of the cross product⁹ of vectors $\overrightarrow{CB} = \mathbf{b} - \mathbf{c}$ and $\overrightarrow{CD} = \mathbf{d} - \mathbf{c}$, in this order, where \mathbf{b} , \mathbf{c} and \mathbf{d} are the position vectors of points B , C and D , respectively, in the given coordinate frame. The product at stake is given by

$$p \equiv (\mathbf{b} - \mathbf{c})^T \mathbf{E}(\mathbf{d} - \mathbf{c}) = \|\mathbf{b} - \mathbf{c}\| \|\mathbf{d} - \mathbf{c}\| \sin \mu = a_3 a_4 \sin \mu \quad (3.161)$$

with \mathbf{E} introduced in eq.(1.1a). Given that the link lengths are positive, we have the relation

$$\text{sgn}(\sin \mu) = \text{sgn}(p) \quad (3.162)$$

which now can be used to monitor branch-switching.

⁹See Subsection 1.4.1.

3.7.2 Introducing a Massive Number of Data Points

3.8 Synthesis Under Mobility Constraints

3.8.1 Constrained Least Squares

3.8.2 Introducing a Massive Number of Data Points

3.9 Synthesis of Complex Linkages

3.9.1 Synthesis of Stephenson Linkages

Chapter 4

Motion Generation

This chapter has not been updated. It will be based, to a large extent, on

1. Chen, C., Bai, S.P. and Angeles, J., 2008, “A comprehensive solution of the classic Burmester problem,” *CSME Transactions*, Vol. 32, No. 2, pp. 137–154.
2. Chiang, C.H., 1988, *Kinematics of Spherical Mechanisms*, Cambridge University Press, Cambridge.
3. McCarthy, J.M., 2000, *Geometric Design of Linkages*, Springer, New York.

Chapter 5

Path Generation

Disclaimer: This chapter is still at a very preliminary state. It should be taken with a grain of salt!

5.1 Introduction

A recurrent problem in mechanical engineering design is the tracing of a continuous path by means of a mechanism. Examples abound in practice: cranes to upload and download containers from ships; guiding of laser beams to cut a profile from a metal plate; and so on. While the foregoing operations can be realized by means of robots, these become impractical when the operation involves endless repetitions through the same path. A single-dof linkage is the solution here not only because of its low cost in terms of production, maintenance and servicing, but also because of repeatability. A robot cannot compete with a linkage in terms of repeatability. Other applications include the synthesis of *dwell* in production lines. For example, the gluing of labels or the filling of a bottle, presented to the pertinent mechanism of a packaging system, calls for contact of a mechanism link with the bottle during a finite amount of time. From the results of Subsection 3.3.1, it is apparent that a four-bar linkage cannot produce dwell, which requires that output velocity and acceleration *vanish simultaneously* during a finite time interval. This then calls for a multiloop linkage, e.g., a six-bar linkage with two kinematic loops. The synthesis of a dwell mechanism then requires the addition of an extra triad¹ to a four-bar linkage. The triad can be of two types, RRR or RPR, with the extreme R joints coupled to the machine frame and to the coupler link of the four-bar linkage, at a designated point P . For triads of the first type, dwell is obtained by choosing the point P so that it traces, during a certain finite interval, a coupler curve (CC) that *locally* approximates a circle of radius r to a third order, meaning that the curvature of the CC is $1/r$ at the linkage posture at

¹Similar to a dyad, a tryad is a two-link chain, with two LKPs at its free ends and one third pair coupling both.

which the curvature becomes *stationary* with respect to the input angle of the four-bar linkage. Points of the coupler curve with the stationarity property are known (Denavit and Hartenberg, 1964) to lie on a *cubic curve* fixed to the coupler link, this curve being quite appropriately known as the *cubic of stationary curvature*. For triads of the second type, P is chosen so that its coupler curve *locally* approximates a line segment to a second order, meaning that the curvature of the CC traced by P vanishes at a given posture of the linkage. It is known (Denavit and Hartenberg, 1964) that the locus of points of the coupler link with a vanishing curvature is a circle, which is rightfully known as the *inflection circle*. Both loci are unique at a given linkage posture, meaning that these loci, fixed on the coupler link, change as the linkage moves from posture to posture.

The balance of the chapter discusses the methodology behind the synthesis of planar, spherical and spatial four-bar linkages with the property that one point, the planar case, or one line, the case of the spherical and the spatial cases, of their coupler link, will visit a discrete set of points or, correspondingly, lines.

5.2 Planar Path Generation

The problem to be solved here is formulated as:

Problem 5.2.1 (Path generation) *Synthesize a planar four-bar linkage, as shown in Fig. 5.1, whose coupler point R will attain a set of positions $\{R_j\}_0^m$, as the linkage is driven by its input link.*

In the problem statement above, the input link is to be decided by the designer. It could be any one of the two links pinned to the machine frame, BA or B^*A^* . Before the assignment of the driving function to one of the two foregoing links, it is futile to speak of the transmission angle² in this case, although it is common in the literature to find synthesis problems in which the transmission angle is to be optimized at this stage.

The general method of linkage synthesis for path generation is based on the synthesis equations derived for motion generation (Chen et al., 2008), which stem from Fig. 5.2, and recalled below for quick reference: for dyad BA_0 ,

$$\mathbf{b}^T(\mathbf{1} - \mathbf{Q}_j)\mathbf{a}_0 + \mathbf{r}_j^T \mathbf{Q}_j \mathbf{a}_0 - \mathbf{r}_j^T \mathbf{b} + \frac{1}{2} \mathbf{r}_j^T \mathbf{r}_j = 0, \text{ for } j = 1, \dots, m \quad (5.1a)$$

while, for dyad $B^*A_0^*$,

$$(\mathbf{b}^*)^T(\mathbf{1} - \mathbf{Q}_j)\mathbf{a}_0^* + \mathbf{r}_j^T \mathbf{Q}_j \mathbf{a}_0^* - \mathbf{r}_j^T \mathbf{b}^* + \frac{1}{2} \mathbf{r}_j^T \mathbf{r}_j = 0, \text{ for } j = 1, \dots, m \quad (5.1b)$$

If matrix \mathbf{Q}_j in the above equations is substituted by the expression given in eq.(1.6), with ϕ_j in lieu of θ , eq.(5.1a) becomes

$$(\mathbf{b} + \mathbf{r}_j)^T (c_j \mathbf{1} + s_j \mathbf{E}) \mathbf{a}_0 + \mathbf{r}_j^T \left(\mathbf{b} + \frac{1}{2} \mathbf{r}_j \right) = 0, \text{ for } j = 1, \dots, m$$

²This concept is defined in Section 3.2.1.

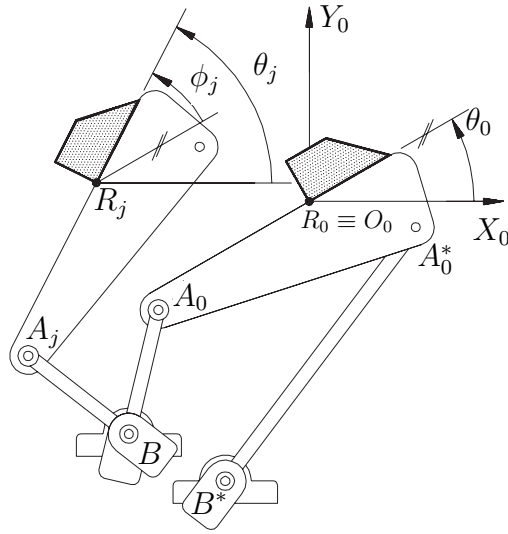


Figure 5.1: A planar four-bar linkage whose point R is to visit a set of positions $\{R_j\}_0^m$

with a similar expression for eq.(5.1b) and the definitions: $c_j \equiv \cos \phi_j$ and $s_j \equiv \sin \phi_j$. If now the tan-half identities of eq.(3.70) are introduced in the above equation, a set of polynomial equations is obtained upon clearing denominators: for dyad BA_0 ,

$$(\mathbf{b} + \mathbf{r}_j)^T [(1 - T_j^2)\mathbf{1} + 2T_j\mathbf{E}]\mathbf{a}_0 + \mathbf{r}_j^T \left(\mathbf{b} + \frac{1}{2}\mathbf{r}_j \right) (1 + T_j^2) = 0, \text{ for } j = 1, \dots, m \quad (5.2a)$$

while, for dyad $B^*A_0^*$,

$$(\mathbf{b}^* + \mathbf{r}_j)^T [(1 - T_j^2)\mathbf{1} + 2T_j\mathbf{E}]\mathbf{a}_0^* + \mathbf{r}_j^T \left(\mathbf{b}^* + \frac{1}{2}\mathbf{r}_j \right) (1 + T_j^2) = 0, \text{ for } j = 1, \dots, m \quad (5.2b)$$

In summary, then, the problem involves $8 + m$ unknowns, the two components of the four position vectors \mathbf{a}_0 , \mathbf{b} , \mathbf{a}_0^* and \mathbf{b}^* , plus the m angles of orientation of the coupler link, $\{\theta_j\}_1^m$. The number of equations is $2m$, i.e., m equations for each set of eqs. (5.2a & b). The maximum number of points that can be visited with a planar four-bar linkage is obtained by equating the number of equations with that of unknowns, namely,

$$8 + m = 2m, \quad \Rightarrow \quad m_{\max} = 8 \quad (5.3)$$

and, if the reference location R_0 is considered, the total number of points in the plane that can be visited with a planar four-bar linkage is nine.

It should be apparent now that each of equations (5.2a & b) is *quartic* in the $8 + m$ unknowns, \mathbf{a}_0 , \mathbf{b} , \mathbf{a}_0^* and \mathbf{b}^* , $\{T_j\}_1^m$. The *Bezout number* N_B of the system of equations (Salmon, 1964), for the maximum number of prescribed points, is, then,

$$N_B = 4^{2m_{\max}} = 4^{16} = 2^{32} = 4294967296 \quad (5.4)$$

which is about 4.3 billion! As a matter of fact, because of a concept from *algebraic geometry* known as *circularity*, the actual number of expected roots drops dramatically. An interesting case is $m = 4$, which leads to eight equations in 12 unknowns, thereby allowing for the free choice of four of these unknowns. Morgan and Wampler (1990) solved an instance of this problem in which they specified the two fixed joint centres B and B^* . In this case the problem is reduced to our quartic equations in four unknowns, with a Bezout number of $4^4 = 256$. They showed that this problem admits, in fact, up to 36 nonzero real solutions only.

The algebraic complexity of this problem reduces when the prescribed points are to be visited at prescribed values of the input angle, a problem known as *path generation with prescribed timing*. This problem is the subject of Section 5.3.

5.3 Planar Path Generation With Prescribed Timing

If the problem of path generation calls for a *synchronization* of the points $\{R_j\}_0^m$ with the values of the input angle, that will be assumed to be that of \overline{BA} with X_0 , as per Fig. 5.1, $\{\psi_j\}_0^m$, then we have a problem of path generation with prescribed timing. This is the case in which one may need, for example, to have points $\{R_j\}_0^m$ laid down on a line with equal spacing between consecutive points, for equal increments of the input angle.

The data are thus given as $\{R_j, \psi_j\}_0^m$. As \mathbf{Q}_j is unknown, the synthesis equations are derived now upon elimination of this matrix from eqs.(5.1a & b), as described below. Notice, however, that the set of values of the input angle, $\{\psi_j\}_0^m$, are now given.

Elimination of \mathbf{Q}_j

Since the input link BA undergoes rotations about B , we can write

$$\mathbf{a}_j - \mathbf{b} = \mathbf{R}_j(\mathbf{a}_0 - \mathbf{b}), \quad \text{for } j = 1, \dots, m \quad (5.5)$$

where \mathbf{R}_j is the rotation matrix carrying $\overline{BA_0}$ into $\overline{BA_j}$ through angle $\beta_j = \psi_j - \psi_0$. Since timing is prescribed, introduction of matrices \mathbf{R}_j does not introduce additional unknowns. Moreover, matrix \mathbf{R}_j can be represented using eq.(1.6), with θ replaced by β_j , namely,

$$\mathbf{R}_j = \cos \beta_j \mathbf{1} + \sin \beta_j \mathbf{E}, \quad \text{for } j = 1, \dots, m$$

where $\mathbf{1}$ is the 2×2 identity matrix and \mathbf{E} is the 90° -ccw rotation matrix introduced in eq.(1.1a). Referring to Fig. 5.2, we can write

$$\mathbf{a}_j - \mathbf{r}_j = \overrightarrow{R_j A_j} = \mathbf{Q}_j \overrightarrow{R_0 A_0} = \mathbf{Q}_j \mathbf{a}_0, \quad \text{for } j = 1, \dots, m$$

Upon substituting eq.(5.5) into the above equation, we obtain

$$\mathbf{Q}_j \mathbf{a}_0 = \mathbf{R}_j \mathbf{a}_0 + (\mathbf{1} - \mathbf{R}_j) \mathbf{b} - \mathbf{r}_j, \quad j = 1, \dots, m \quad (5.6)$$

Now, if we substitute eq.(1.6) into the above equation, with ϕ_j in lieu of θ , we end up with

$$c\phi_j \mathbf{a}_0 + s\phi_j \mathbf{Ea}_0 = \mathbf{R}_j \mathbf{a}_0 + (\mathbf{1} - \mathbf{R}_j) \mathbf{b} - \mathbf{r}_j, \quad j = 1, \dots, m$$

which can be cast in the form

$$\begin{bmatrix} \mathbf{a}_0 & \mathbf{Ea}_0 \end{bmatrix} \begin{bmatrix} c\phi_j \\ s\phi_j \end{bmatrix} = \underbrace{\mathbf{R}_j \mathbf{a}_0 + (\mathbf{1} - \mathbf{R}_j) \mathbf{b} - \mathbf{r}_j}_{\mathbf{c}_j}, \quad j = 1, \dots, m$$

Consequently, we can readily solve the above equation for $c\phi_j$ and $s\phi_j$ as

$$\begin{bmatrix} c\phi_j \\ s\phi_j \end{bmatrix} = \begin{bmatrix} \mathbf{a}_0 & \mathbf{Ea}_0 \end{bmatrix}^{-1} \mathbf{c}_j = \frac{1}{\|\mathbf{a}_0\|^2} \begin{bmatrix} \mathbf{a}_0^T \mathbf{E}^T \\ -\mathbf{a}_0^T \end{bmatrix} \mathbf{E} \mathbf{c}_j = \frac{1}{\|\mathbf{a}_0\|^2} \begin{bmatrix} \mathbf{a}_0^T \mathbf{c}_j \\ -\mathbf{a}_0^T \mathbf{E} \mathbf{c}_j \end{bmatrix},$$

$$j = 1, \dots, m$$

where we have recalled the formula for the inverse of a 2×2 matrix given in Fact 1.4.2.

The Equation for the BA_0R Dyad

When the expression for $\mathbf{Q}_j \mathbf{a}_0$ of eq.(5.6) is substituted into the synthesis equations (5.1a), we obtain

$$\mathbf{b}^T \mathbf{a}_0 - \mathbf{b}^T \mathbf{R}_j \mathbf{a}_0 - \mathbf{b}^T (\mathbf{1} - \mathbf{R}_j) \mathbf{b} + \mathbf{r}_j^T \mathbf{R}_j \mathbf{a}_0 + \mathbf{r}_j^T \mathbf{R}_j \mathbf{b} - \mathbf{r}_j^T \mathbf{b} - \frac{1}{2} \mathbf{r}_j^T \mathbf{r}_j = 0, \quad j = 1, \dots, m$$

which simplifies to

$$\mathbf{b}^T (\mathbf{1} - \mathbf{R}_j) \mathbf{b} + \mathbf{b}^T (\mathbf{R}_j - \mathbf{1}) \mathbf{a}_0 + \mathbf{r}_j^T (\mathbf{R}_j - \mathbf{1}) \mathbf{b} - \mathbf{r}_j^T \mathbf{R}_j \mathbf{a}_0 + \frac{1}{2} \mathbf{r}_j^T \mathbf{r}_j = 0, \quad (5.7)$$

thereby deriving the m synthesis equations for the left-hand dyad of Fig. 5.2 for the problem at hand. Apparently, these equations are quadratic in \mathbf{b} and linear in \mathbf{a}_0 , their degree being two.

The Equation for the $B^*A_0^*R$ Dyad

Vector $\mathbf{Q}_j \mathbf{a}_0^*$ appearing in eq.(5.1b) can be derived by mimicking eq.(5.6), which yields

$$\mathbf{Q}_j \mathbf{a}_0^* = \begin{bmatrix} \mathbf{a}_0^* & \mathbf{Ea}_0^* \end{bmatrix} \begin{bmatrix} c\phi_j \\ s\phi_j \end{bmatrix} = \frac{1}{\|\mathbf{a}_0\|^2} [(\mathbf{a}_0^T \mathbf{c}_j) \mathbf{a}_0^* - (\mathbf{a}_0^T \mathbf{E} \mathbf{c}_j) \mathbf{Ea}_0^*], \quad \text{for } j = 1, \dots, m$$

or

$$\mathbf{Q}_j \mathbf{a}_0^* = \frac{1}{\|\mathbf{a}_0\|^2} [(\mathbf{a}_0^T \mathbf{c}_j) \mathbf{1} - (\mathbf{a}_0^T \mathbf{E} \mathbf{c}_j) \mathbf{E}] \mathbf{a}_0^*, \quad j = 1, \dots, m$$

Substituting the above expression into eq.(5.1b), we obtain, after clearing the denominator,

$$\begin{aligned} (\mathbf{b}^*)^T [(\|\mathbf{a}_0\|^2 - \mathbf{a}_0^T \mathbf{c}_j) \mathbf{1} + (\mathbf{a}_0^T \mathbf{E} \mathbf{c}_j) \mathbf{E}] \mathbf{a}_0^* + \mathbf{r}_j^T [(\mathbf{a}_0^T \mathbf{c}_j) \mathbf{1} - (\mathbf{a}_0^T \mathbf{E} \mathbf{c}_j) \mathbf{E}] \mathbf{a}_0^* \\ - \|\mathbf{a}_0\|^2 \mathbf{r}_j^T \mathbf{b}^* + \frac{1}{2} \|\mathbf{a}_0\|^2 \|\mathbf{r}_j\|^2 = 0 \quad j = 1, \dots, m \end{aligned} \quad (5.8)$$

which are the synthesis equations for the right-hand dyad of Fig. 5.2 for the problem at hand. Apparently, these m equations are all *cubic*.

Remarks

- We have $2m$ equations, (5.7 & 5.8), to solve for eight unknowns—the components of \mathbf{a}_0 , \mathbf{b} , \mathbf{a}_0^* , \mathbf{b}^* . Therefore, to have a determined system of equations, we must have $m = 4$, which implies that up to *five points* can be visited in a plane using a four-bar linkage, with prescribed timing.
- Since the system of eqs.(5.7 & 5.8) involves four *quadratic* and four *cubic* equations in the unknowns $\{\mathbf{a}_0, \mathbf{b}\}$, the *Bezout number* N_B of the system, which gives an upper bound for the number of roots to expect, thus being $N_B = 2^4 \times 3^4 = 1296$
- Equations (5.7) are linear in \mathbf{a}_0 and quadratic in \mathbf{b} . Consequently, we can eliminate \mathbf{a}_0 by casting the said system in the form

$$\mathbf{B}\mathbf{x} = \mathbf{0} \tag{5.9}$$

in which $\mathbf{x} = [\mathbf{a}_0^T \ 1]^T$ and \mathbf{B} is a 4×3 matrix function of \mathbf{b} of the form

$$\mathbf{B} = \begin{bmatrix} \mathbf{b}^T(\mathbf{R}_1 - \mathbf{1}) - \mathbf{r}_1^T \mathbf{R}_1 & \mathbf{b}^T(\mathbf{1} - \mathbf{R}_1)\mathbf{b} + \mathbf{r}_1^T(\mathbf{R}_1 - \mathbf{1})\mathbf{b} + (1/2)\mathbf{r}_1^T \mathbf{r}_1 \\ \mathbf{b}^T(\mathbf{R}_2 - \mathbf{1}) - \mathbf{r}_2^T \mathbf{R}_2 & \mathbf{b}^T(\mathbf{1} - \mathbf{R}_2)\mathbf{b} + \mathbf{r}_2^T(\mathbf{R}_2 - \mathbf{1})\mathbf{b} + (1/2)\mathbf{r}_2^T \mathbf{r}_2 \\ \mathbf{b}^T(\mathbf{R}_3 - \mathbf{1}) - \mathbf{r}_3^T \mathbf{R}_3 & \mathbf{b}^T(\mathbf{1} - \mathbf{R}_3)\mathbf{b} + \mathbf{r}_3^T(\mathbf{R}_3 - \mathbf{1})\mathbf{b} + (1/2)\mathbf{r}_3^T \mathbf{r}_3 \\ \mathbf{b}^T(\mathbf{R}_4 - \mathbf{1}) - \mathbf{r}_4^T \mathbf{R}_4 & \mathbf{b}^T(\mathbf{1} - \mathbf{R}_4)\mathbf{b} + \mathbf{r}_4^T(\mathbf{R}_4 - \mathbf{1})\mathbf{b} + (1/2)\mathbf{r}_4^T \mathbf{r}_4 \end{bmatrix}$$

For the 4×3 matrix \mathbf{B} to have a nontrivial null space, which is needed in light of the form of \mathbf{x} , \mathbf{B} must be rank-deficient. This means that every 3×3 submatrix of \mathbf{B} must be singular. We can thus derive four bivariate polynomial equations in the Cartesian coordinates u and v of B , the components of \mathbf{b} , namely,

$$\Delta_j(u, v) = \det(\mathbf{B}_j), \quad \text{for } j = 1, \dots, 4 \tag{5.10}$$

where Δ_j is the determinant of the j th 3×3 submatrix \mathbf{B}_j , obtained by deleting the j th row of \mathbf{B} . Notice that Δ_j can be computed by the cofactors of the third column of its corresponding matrix. Moreover, this column is quadratic in \mathbf{b} , the corresponding cofactors being determinants of 2×2 matrices whose entries are linear in \mathbf{b} . Such a determinant is expanded in Fact 1.4.1, Subsection 1.4.2, in which it is apparent that this determinant is a bilinear expression of its rows or, correspondingly, of its columns. Hence, each 2×2 cofactor is quadratic in \mathbf{b} , the result being that Δ_j is quartic in \mathbf{b} . Therefore, the Bezout number of any pair of those equations is $N_B = 4^2 = 16$.

Moreover, each eq.(5.10) defines a *contour* in the u - v plane. The real solutions of system (5.9) can be visually estimated by plotting the m contours in the same figure. Notice that, at the outset, we do not have bounds for the location of B in the u - v

plane. However, we always have a region available of this plane in which we can anchor the revolute center B . Our first attempt of finding real solutions for B is thus this region.

Once \mathbf{b} is known, we can solve for \mathbf{a}_0 from eq.(5.9) using a least-square approximation. To this end, we rewrite eq.(5.9) in the form

$$\mathbf{M}\mathbf{a}_0 = \mathbf{n}$$

where

$$\mathbf{M} = \begin{bmatrix} \mathbf{b}^T(\mathbf{R}_1 - \mathbf{1}) - \mathbf{r}_1^T \mathbf{R}_1 \\ \mathbf{b}^T(\mathbf{R}_2 - \mathbf{1}) - \mathbf{r}_2^T \mathbf{R}_2 \\ \mathbf{b}^T(\mathbf{R}_3 - \mathbf{1}) - \mathbf{r}_3^T \mathbf{R}_3 \\ \mathbf{b}^T(\mathbf{R}_4 - \mathbf{1}) - \mathbf{r}_4^T \mathbf{R}_4 \end{bmatrix}, \quad \mathbf{n} = \begin{bmatrix} \mathbf{b}^T(\mathbf{R}_1 - \mathbf{1})\mathbf{b} - \mathbf{r}_1^T(\mathbf{R}_1 - \mathbf{1})\mathbf{b} - (1/2)\mathbf{r}_1^T \mathbf{r}_1 \\ \mathbf{b}^T(\mathbf{R}_2 - \mathbf{1})\mathbf{b} - \mathbf{r}_2^T(\mathbf{R}_2 - \mathbf{1})\mathbf{b} - (1/2)\mathbf{r}_2^T \mathbf{r}_2 \\ \mathbf{b}^T(\mathbf{R}_3 - \mathbf{1})\mathbf{b} - \mathbf{r}_3^T(\mathbf{R}_3 - \mathbf{1})\mathbf{b} - (1/2)\mathbf{r}_3^T \mathbf{r}_3 \\ \mathbf{b}^T(\mathbf{R}_4 - \mathbf{1})\mathbf{b} - \mathbf{r}_4^T(\mathbf{R}_4 - \mathbf{1})\mathbf{b} - (1/2)\mathbf{r}_4^T \mathbf{r}_4 \end{bmatrix}$$

- Equation (5.8) is bilinear in \mathbf{b}^* and \mathbf{a}_0^* . Once we have \mathbf{a}_0 and \mathbf{b} from eq.(5.9), we can solve eq.(5.8) for \mathbf{a}_0^* and \mathbf{b}^* using dialytic elimination, as we did in the motion-generation case. That is, computing \mathbf{b}^* and \mathbf{a}_0^* leads to the solution of one quartic polynomial. We need not find the roots of this polynomial numerically, if we apply the contour technique introduced in Chapter 4.

Reducing the Degree of the Synthesis Equations of the BA_0R Dyad

Using the definition of \mathbf{Q}_j of eq.(1.6), the first term of eq.(5.7) can be further simplified to

$$\mathbf{b}^T(\mathbf{1} - \mathbf{R}_j)\mathbf{b} = \mathbf{b}^T[(1 - c\beta_j)\mathbf{1} + s\beta_j\mathbf{E}]\mathbf{b} = (1 - c\beta_j)\|\mathbf{b}\|^2, \quad j = 1, \dots, m$$

where we used the identity $\mathbf{b}^T\mathbf{E}\mathbf{b} \equiv 0$, because matrix \mathbf{E} is *skew-symmetric*. Thus, eq.(5.7) reduces to

$$(1 - c\beta_j)\|\mathbf{b}\|^2 + \mathbf{b}^T(\mathbf{R}_j - \mathbf{1})\mathbf{a}_0 + \mathbf{r}_j^T(\mathbf{R}_j - \mathbf{1})\mathbf{b} - \mathbf{r}_j^T \mathbf{R}_j \mathbf{a}_0 + \frac{1}{2}\mathbf{r}_j^T \mathbf{r}_j = 0 \quad (5.11)$$

for $j = 1, \dots, m$.

Let M be $j \in \{1, \dots, m\}$ that maximizes $|1 - c\beta_j|$. Use now the M th equation of eqs.(5.11) as a pivot, to reduce the order of the remaining equations. After a reshuffling of the equations, we let $M = 1$, so that now the pivot equation is the first one of the set. Just as in Gaussian elimination, subtract a “suitable” multiple of the first equation from the remaining ones, so as to eliminate the quadratic term of those equations, which leads, for $j = 2, \dots, m$, to

$$(1 - c\beta_1)\|\mathbf{b}\|^2 + \mathbf{b}^T(\mathbf{R}_1 - \mathbf{1})\mathbf{a}_0 + \mathbf{r}_1^T(\mathbf{R}_1 - \mathbf{1})\mathbf{b} - \mathbf{r}_1^T \mathbf{R}_1 \mathbf{a}_0 + \frac{1}{2}\mathbf{r}_1^T \mathbf{r}_1 = 0 \quad (5.12a)$$

$$\begin{aligned} \mathbf{b}^T[\mathbf{R}_j - \mathbf{1} - q_j(\mathbf{R}_j - \mathbf{1})]\mathbf{a}_0 + [\mathbf{r}_j^T(\mathbf{R}_j - \mathbf{1}) - q_j\mathbf{r}_j^T(\mathbf{R}_1 - \mathbf{1})]\mathbf{b} \\ - (\mathbf{r}_j^T\mathbf{R}_j - q_j\mathbf{r}_1^T\mathbf{R}_1)\mathbf{a}_0 + \frac{1}{2}(\mathbf{r}_j^T\mathbf{r}_j - \mathbf{r}_1^T\mathbf{r}_1) = 0 \quad (5.12b) \\ j = 2, \dots, m \end{aligned}$$

where

$$q_j = \frac{1 - c\beta_j}{1 - c\beta_1}$$

System (5.12) can be cast in linear-homogeneous form in \mathbf{x} , if this vector is defined as $\mathbf{x} = [\mathbf{a}_0^T \quad 1]^T$, thereby obtaining

$$\mathbf{B}\mathbf{x} = \mathbf{0}_4 \quad (5.13a)$$

with

$$\mathbf{B} = \begin{bmatrix} \mathbf{b}^T(\mathbf{R}_1 - \mathbf{1}) - \mathbf{r}_1^T\mathbf{R}_1 & s_1 \\ (1 - q_2)\mathbf{b}^T(\mathbf{R}_2 - \mathbf{1}) - (\mathbf{r}_2^T\mathbf{R}_2 - q_2\mathbf{r}_1^T\mathbf{R}_1) & s_2 \\ (1 - q_3)\mathbf{b}^T(\mathbf{R}_3 - \mathbf{1}) - (\mathbf{R}_3^T\mathbf{r}_3 - q_3\mathbf{r}_1^T\mathbf{R}_1) & s_3 \\ (1 - q_4)\mathbf{b}^T(\mathbf{R}_4 - \mathbf{1}) - (\mathbf{R}_4^T\mathbf{r}_4 - q_4\mathbf{r}_1^T\mathbf{R}_1) & s_4 \end{bmatrix} \quad (5.13b)$$

and

$$\begin{aligned} s_1 &= (1 - c\beta_1)\|\mathbf{b}\|^2 + \mathbf{r}_1^T(\mathbf{R}_1 - \mathbf{1})\mathbf{b} + \frac{1}{2}\mathbf{r}_1^T\mathbf{r}_1 \quad (5.13c) \\ s_j &= [\mathbf{r}_j^T(\mathbf{R}_j - \mathbf{1}) - q_j\mathbf{r}_j^T(\mathbf{R}_1 - \mathbf{1})]\mathbf{b} + \frac{1}{2}(\mathbf{r}_j^T\mathbf{r}_j - \mathbf{r}_1^T\mathbf{r}_1), \quad j = 2, \dots, m \end{aligned}$$

Notice that s_1 is quadratic and $\{s_j\}_2^m$ are all linear in \mathbf{b} . Thus, the corresponding Δ_1 of eq.(5.10) for system (5.13) is quadratic, but $\{\Delta_j\}_2^m$ are all cubic in \mathbf{b} . Consequently, the Bezout number of any pair of equations $(1, j)$, for $j = 2, \dots, m$, is $N_B = 3 \times 4 = 12$.

5.4 Coupler Curves of Planar Four-Bar Linkages

The four-bar linkage of Fig. 5.2 is given in a Cartesian frame \mathcal{F} with origin at B and axes X and Y . The trajectory traced by point R of its coupler link is called the *coupler curve* traced by that point.

Construction of the Coupler Curve

We start by proving a basic result in planar kinematics regarding the nature of the coupler curve of a planar four-bar linkage, namely,

Theorem 5.4.1 (Coupler Curve of a Planar Four-Bar Linkage) *The curve traced by any point of the coupler link of a planar four-bar linkage is algebraic, of sixth degree.*

In general, a curve can be either *algebraic* or *non-algebraic*. A planar curve is algebraic if it is given by an implicit function $F(x, y) = 0$, with $F(x, y)$ being the sum of products

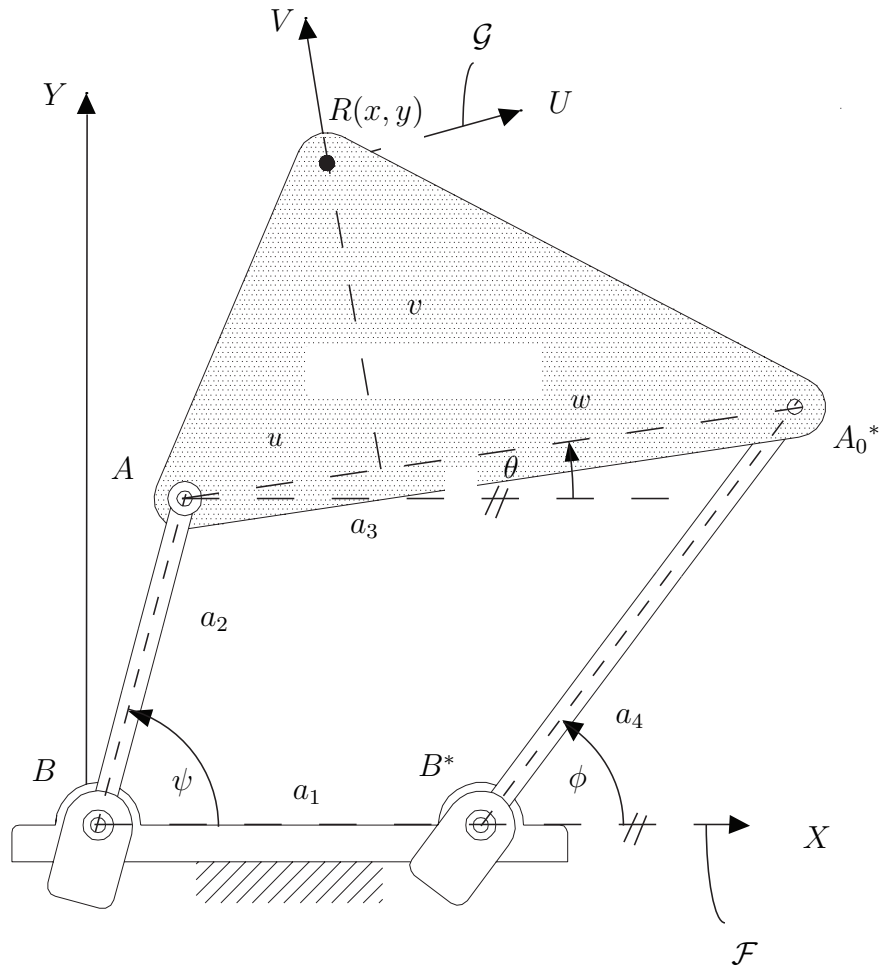


Figure 5.2: Determination of the coupler curve traced by point R of a planar four-bar linkage

of integer powers of x and y . The *degree* of the curve is the highest degree of the various terms making up $F(x, y)$. Moreover, a curve of degree n intersects a straight line at a maximum of n points. Thus, the coupler curve of a four-bar linkage intersects a straight line at a maximum of six points. As a consequence, the coupler curve under discussion *cannot have straight segments of finite length*. There are, however, well-known examples of planar four-bar linkages that trace coupler curves that, to the naked eye, appear as having line segments. The best known of these linkages are those bearing the eponyms of Roberts and Chebyshev. Linkages capable of tracing *exactly* line segments are also known, e.g., those of Peaucellier and Hart (Bricard, 1927; Dudiță et al., 1989; McCarthy, 2000).

The coupler link carries a point $R(x, y)$, which serves as origin of a second Cartesian frame, \mathcal{G} , with origin at R and axes U and V , fixed to this link. What we need now is an implicit function $F(x, y) = 0$, free of any linkage variable, and having as parameters the

link lengths.

The desired function is obtained by first noticing that, irrespective of the linkage posture,

$$\|\overrightarrow{BA_0}\|^2 = a_2^2, \quad \|\overrightarrow{B^*A_0^*}\|^2 = a_4^2 \quad (5.14)$$

Henceforth, we shall use subscripted brackets to indicate the Cartesian frame in which vector components are represented. Thus,

$$[\overrightarrow{RA_0}]_{\mathcal{G}} = \begin{bmatrix} -u \\ -v \end{bmatrix} = \text{const}, \quad [\overrightarrow{RA_0^*}]_{\mathcal{G}} = \begin{bmatrix} w \\ -v \end{bmatrix} = \text{const}, \quad [\overrightarrow{BR}]_{\mathcal{F}} = \begin{bmatrix} x \\ y \end{bmatrix}$$

Note that $\overrightarrow{BA_0} = \overrightarrow{BR} + \overrightarrow{RA_0}$. We have \overrightarrow{BR} in \mathcal{F} , but $\overrightarrow{RA_0}$ in \mathcal{G} . In order to be able to add the two vectors in the above equation, we transform first the components of the second into \mathcal{F} , which is done via the matrix \mathbf{Q} rotating \mathcal{F} into \mathcal{G} , namely,

$$\mathbf{Q} = \begin{bmatrix} \cos \theta & -\sin \theta \\ \sin \theta & \cos \theta \end{bmatrix}$$

Hence,

$$[\overrightarrow{RA_0}]_{\mathcal{F}} = \mathbf{Q}[\overrightarrow{RA_0}]_{\mathcal{G}} = \begin{bmatrix} -u \cos \theta + v \sin \theta \\ -u \sin \theta - v \cos \theta \end{bmatrix}$$

Therefore,

$$[\overrightarrow{BA_0}]_{\mathcal{F}} = \begin{bmatrix} x - u \cos \theta + v \sin \theta \\ y - u \sin \theta - v \cos \theta \end{bmatrix} \quad (5.15)$$

On the other hand,

$$\overrightarrow{B^*A_0^*} = \overrightarrow{BA_0^*} - \overrightarrow{BB^*} = \overrightarrow{BR} + \overrightarrow{RA_0^*} - \overrightarrow{BB^*} \quad (5.16)$$

where

$$[\overrightarrow{BR} - \overrightarrow{BB^*}]_{\mathcal{F}} = \begin{bmatrix} x - a_1 \\ y \end{bmatrix}, \quad [\overrightarrow{RA_0^*}]_{\mathcal{F}} = \mathbf{Q}[\overrightarrow{RA_0^*}]_{\mathcal{G}} = \begin{bmatrix} w \cos \theta + v \sin \theta \\ w \sin \theta - v \cos \theta \end{bmatrix} \quad (5.17)$$

Upon substitution of eqs.(5.17) into eq.(5.16), we obtain

$$[\overrightarrow{B^*A_0^*}]_{\mathcal{F}} = \begin{bmatrix} x - a_1 + w \cos \theta + v \sin \theta \\ y + w \sin \theta - v \cos \theta \end{bmatrix} \quad (5.18)$$

Now, let us substitute eqs.(5.15) and (5.18) into eqs.(5.14), to obtain

$$x^2 + y^2 - 2(ux + vy) \cos \theta + 2(vx - uy) \sin \theta + u^2 + v^2 - a_2^2 = 0 \quad (5.19a)$$

$$\begin{aligned} x^2 + y^2 + 2[w(x - a_1) - vy] \cos \theta + [v(x - a_1) + wy] \sin \theta \\ - 2a_1x + a_1^2 + v^2 + w^2 - a_4^2 = 0 \end{aligned} \quad (5.19b)$$

The above two equations yield the desired implicit function $F(x, y) = 0$, upon elimination of θ from the two of them. While we can do this at this stage, we risk ending up with a

resultant equation of too high a degree, for notice that those two equations are *quadratic* in x and y and linear in $\cos \theta$ and $\sin \theta$. In order to reduce the degree of the resultant equation, let us subtract eq.(5.19b) from eq.(5.19a):

$$\begin{aligned} 2[(u+w)x - a_1w] \cos \theta + 2[2a_1v + (w+u)y] \sin \theta \\ -2a_1x + a_1^2 + a_2^2 - a_4^2 + u^2 + w^2 = 0 \end{aligned} \quad (5.19c)$$

thereby obtaining an alternative equation that is linear in x and y as well as in $\cos \theta$ and $\sin \theta$. Now, we can eliminate θ from any of the two eqs.(5.19a) or (5.19b) and (5.19c). We do this by a) choosing eqs.(5.19b) and (5.19c), and b) using dialytic elimination: First, we introduce the familiar tan-half trigonometric identities, which we reproduce below for θ :

$$\cos \theta \equiv \frac{1 - T^2}{1 + T^2}, \quad \sin \theta \equiv \frac{2T}{1 + T^2}, \quad T \equiv \tan \left(\frac{\theta}{2} \right)$$

Further, we substitute the above expressions for $\cos \theta$ and $\sin \theta$ into eqs.(5.19b) and (5.19c), thereby obtaining

$$A_1T^2 - 2B_1T + C_1 = 0 \quad (5.20a)$$

$$A_2T^2 - 2B_2T + C_2 = 0 \quad (5.20b)$$

with

$$A_1 \equiv x^2 + y^2 + 2(ux + vy) + u^2 - a_2^2$$

$$B_1 \equiv 4(vx - uy)$$

$$C_1 \equiv x^2 + y^2 - 2(ux + vy) + u^2 - a_2^2$$

$$A_2 \equiv -2(a_1 + u + w)x + a_1^2 + a_2^2 + a_4^2 + u^2 + w^2 - 2a_1w$$

$$B_2 \equiv 4[-a_1v + (w + u)y]$$

$$C_2 \equiv -2(a_1 - u - w)x + a_1^2 + a_2^2 + a_4^2 + u^2 + w^2 + 2a_1w$$

In order to eliminate dialytically T from eqs.(5.20a & b), we first multiply both sides of each of these equations by T , thereby obtaining two additional equations, both cubic in T :

$$A_1T^3 - 2B_1T^2 + C_1T = 0 \quad (5.20c)$$

$$A_2T^3 - 2B_2T^2 + C_2T = 0 \quad (5.20d)$$

Equations (5.20a-d) now represent a system of four linear homogeneous equations in T^0 , T^1 , T^2 and T^3 , i.e.,

$$\mathbf{M}\mathbf{x} = \mathbf{0}_4$$

where $\mathbf{0}_4$ is the four-dimensional zero vector, while \mathbf{M} and \mathbf{x} are given below:

$$\mathbf{M} \equiv \begin{bmatrix} A_1 & -2B_1 & C_1 & 0 \\ A_2 & -2B_2 & C_2 & 0 \\ 0 & A_1 & -2B_1 & C_1 \\ 0 & A_2 & -2B_2 & C_2 \end{bmatrix}, \quad \mathbf{x} \equiv \begin{bmatrix} T^3 \\ T^2 \\ T \\ 1 \end{bmatrix}$$

Apparently, the trivial solution $\mathbf{x} = \mathbf{0}$ is not admissible, and hence, \mathbf{M} must be singular, i.e.,

$$F(x, y) \equiv \det(\mathbf{M}) = 0$$

which is the desired implicit function defining the coupler curve sought. It is apparent that the first and third rows of \mathbf{M} are quadratic in x and y , while the second and fourth are linear in the same variables. Consequently, $F(x, y)$ is *sextic* in x and y , q.e.d.

5.5 The Theorem of Roberts-Chebyshev

In the realm of planar linkage synthesis for path generation it is noteworthy that the solution to any problem is not unique. In fact, for every coupler curve generated by a planar four-bar linkage, there exist two more four-bar linkages, called the cognates of the first one, that trace exactly the same coupler curve.

A proof of this result is available in (Bricard, 1927) and (Malik et al., 1994).

Appendix A

A Summary of Dual Algebra

The algebra of dual numbers is recalled here, with extensions to vector and matrix operations. This material is reproduced from a chapter in a NATO Advanced Study Institute book¹

A.1 Introduction

The aim of this Appendix is to outline the applications of dual algebra to kinematic analysis. To this end, the algebra of dual scalars, vectors, and matrices is first recalled. The applications included here refer to the computation of the parameters of the screw of a rigid body between two finitely-separated positions and of the instant screw. However, the applications of dual numbers go beyond that in kinematics. Indeed, the well-known *Principle of Transference* (Dimentberg, 1965; Bottema and Roth, 1978; Rico Martínez and Duffy, 1993) has been found extremely useful in spatial kinematics, since it allows the derivation of spatial kinematic relations by simply *dualizing* the corresponding relations of spherical kinematics.

Dual numbers were first proposed by Clifford (1873), their first applications to kinematics being attributed to both Kotel'nikov (1895) and Study (1903). A comprehensive analysis of dual numbers and their applications to the kinematic analysis of spatial linkages was conducted by Yang (1963) and Yang and Freudenstein (1964). Bottema and Roth(1978) include a treatment of theoretical kinematics using dual numbers. More

¹Angeles, J., 1998, "The Application of Dual Algebra to Kinematic Analysis", in Angeles, J. and Zakhariiev, E. (editors), Computational Methods in Mechanical Systems, Springer-Verlag, Heidelberg, Vol. 161, pp. 3-31.

recently, Agrawal (1987) reported on the application of dual quaternions to spatial kinematics, while Pradeep, Yoder, and Mukundan (1989) used the dual-matrix exponential in the analysis of robotic manipulators. Shoham and Brodsky (1993, 1994) have proposed a dual inertia operator for the dynamical analysis of mechanical systems. A comprehensive introduction to dual quaternions is to be found in (McCarthy, 1990), while an abstract treatment is found in (Chevallier, 1991).

A.2 Definitions

A *dual number* \hat{a} is defined as the sum of a *primal* part a , and a *dual* part a_0 , namely,

$$\hat{a} = a + \epsilon a_0 , \quad (\text{A.1})$$

where ϵ is the dual unity, which verifies $\epsilon \neq 0$, $\epsilon^2 = 0$, and a and a_0 are real numbers, the former being the *primal part* of \hat{a} , the latter its *dual part*. Actually, dual numbers with complex parts can be equally defined (Cheng and Thompson, 1996). For the purposes of this chapter, real numbers will suffice.

If $a_0 = 0$, \hat{a} is called a *real number*, or, correspondingly, a *complex number*; if $a = 0$, \hat{a} is called a *pure dual number*; and if neither is zero \hat{a} is called a *proper dual number*.

Let $\hat{b} = b + \epsilon b_0$ be another dual number. Equality, addition, multiplication, and division are defined, respectively, as

$$\hat{a} = \hat{b} \Leftrightarrow a = b, \quad a_0 = b_0 \quad (\text{A.2a})$$

$$\hat{a} + \hat{b} = (a + b) + \epsilon(a_0 + b_0) \quad (\text{A.2b})$$

$$\hat{a}\hat{b} = ab + \epsilon(ab_0 + a_0b) \quad (\text{A.2c})$$

$$\frac{\hat{a}}{\hat{b}} = \frac{a}{b} - \epsilon \left(\frac{ab_0 - a_0b}{b^2} \right), \quad b \neq 0 . \quad (\text{A.2d})$$

From eq.(A.2d) it is apparent that the division by a pure dual number is not defined. Hence, dual numbers do not form a *field* in the algebraic sense; they do form a *ring* (Simmons, 1963).

All formal operations involving dual numbers are identical to those of ordinary algebra, while taking into account that $\epsilon^2 = \epsilon^3 = \dots = 0$. Therefore, the series expansion of the *analytic function* $f(\hat{x})$ of a dual argument \hat{x} is given by

$$f(\hat{x}) = f(x + \epsilon x_0) = f(x) + \epsilon x_0 \frac{df(x)}{dx} . \quad (\text{A.3})$$

As a direct consequence of eq.(A.3), we have the expression below for the exponential of a dual number \hat{x} :

$$e^{\hat{x}} = e^x + \epsilon x_0 e^x = e^x(1 + \epsilon x_0), \quad (\text{A.4})$$

and hence, *the dual exponential cannot be a pure dual number.*

The *dual angle* $\hat{\theta}$ between two skew lines \mathcal{L}_1 and \mathcal{L}_2 , introduced by Study (1903), is defined as

$$\hat{\theta} = \theta + \epsilon s, \quad (\text{A.5})$$

where θ and s are, respectively, the twist angle and the distance between the two lines. The *dual trigonometric functions* of the dual angle $\hat{\theta}$ are derived directly from eq.(A.3), namely,

$$\cos \hat{\theta} = \cos \theta - \epsilon s \sin \theta, \quad \sin \hat{\theta} = \sin \theta + \epsilon s \cos \theta, \quad \tan \hat{\theta} = \tan \theta + \epsilon s \sec^2 \theta. \quad (\text{A.6})$$

Moreover, all identities for ordinary trigonometry hold for dual angles. Likewise, the square root of a dual number can be readily found by a straightforward application of eq.(A.3), namely,

$$\sqrt{\hat{x}} = \sqrt{x} + \epsilon \frac{x_0}{2\sqrt{x}}, \quad (\text{A.7})$$

A *dual vector* $\hat{\mathbf{a}}$ is defined as the sum of a primal vector part \mathbf{a} , and a dual vector part \mathbf{a}_0 , namely,

$$\hat{\mathbf{a}} = \mathbf{a} + \epsilon \mathbf{a}_0, \quad (\text{A.8})$$

where both \mathbf{a} and \mathbf{a}_0 are Cartesian, 3-dimensional vectors. Henceforth, all vectors are assumed to be of this kind. Further, let $\hat{\mathbf{a}}$ and $\hat{\mathbf{b}}$ be two dual vectors and \hat{c} be a dual scalar. The concepts of dual-vector equality, multiplication of a dual vector by a dual scalar, inner product and vector product of two dual vectors are defined below:

$$\hat{\mathbf{a}} = \hat{\mathbf{b}} \Leftrightarrow \mathbf{a} = \mathbf{b} \quad \text{and} \quad \mathbf{a}_0 = \mathbf{b}_0; \quad (\text{A.9a})$$

$$\hat{c} \hat{\mathbf{a}} = c \mathbf{a} + \epsilon (c_0 \mathbf{a} + c \mathbf{a}_0); \quad (\text{A.9b})$$

$$\hat{\mathbf{a}} \cdot \hat{\mathbf{b}} = \mathbf{a} \cdot \mathbf{b} + \epsilon (\mathbf{a} \cdot \mathbf{b}_0 + \mathbf{a}_0 \cdot \mathbf{b}); \quad (\text{A.9c})$$

$$\hat{\mathbf{a}} \times \hat{\mathbf{b}} = \mathbf{a} \times \mathbf{b} + \epsilon (\mathbf{a} \times \mathbf{b}_0 + \mathbf{a}_0 \times \mathbf{b}). \quad (\text{A.9d})$$

In particular, when $\hat{\mathbf{b}} = \hat{\mathbf{a}}$, eq.(A.9c) leads to the *Euclidean norm* of the dual vector $\hat{\mathbf{a}}$, i.e.,

$$\|\hat{\mathbf{a}}\|^2 = \|\mathbf{a}\|^2 + \epsilon 2\mathbf{a} \cdot \mathbf{a}_0. \quad (\text{A.9e})$$

Furthermore, the six *normalized Plücker coordinates* of a line \mathcal{L} passing through a point P of position vector \mathbf{p} and parallel to the unit vector \mathbf{e} are given by the pair $(\mathbf{e}, \mathbf{p} \times \mathbf{e})$, where the product $\mathbf{e}_0 \equiv \mathbf{p} \times \mathbf{e}$ denotes the *moment* of the line. The foregoing coordinates can be represented by a *dual unit vector* $\hat{\mathbf{e}}^*$, whose six real components in \mathbf{e} and \mathbf{e}_0 are the Plücker coordinates of \mathcal{L} , namely,

$$\hat{\mathbf{e}}^* = \mathbf{e} + \epsilon \mathbf{e}_0, \quad \text{with} \quad \|\mathbf{e}\| = 1 \quad \text{and} \quad \mathbf{e} \cdot \mathbf{e}_0 = 0. \quad (\text{A.10})$$

The reader is invited to verify the results summarized below:

Lemma A.2.1 *For $\hat{\mathbf{e}}^* \equiv \mathbf{e} + \epsilon \mathbf{e}_0$ and $\hat{\mathbf{f}}^* \equiv \mathbf{f} + \epsilon \mathbf{f}_0$ defined as two dual unit vectors representing lines \mathcal{L} and \mathcal{M} , respectively, we have:*

- (i) *If $\hat{\mathbf{e}}^* \times \hat{\mathbf{f}}^*$ is a pure dual vector, then \mathcal{L} and \mathcal{M} are parallel;*
- (ii) *if $\hat{\mathbf{e}}^* \cdot \hat{\mathbf{f}}^*$ is a pure dual number, then \mathcal{L} and \mathcal{M} are perpendicular;*
- (iii) *\mathcal{L} and \mathcal{M} are coincident if and only if $\hat{\mathbf{e}}^* \times \hat{\mathbf{f}}^* = \mathbf{0}$; and*
- (iv) *\mathcal{L} and \mathcal{M} intersect at right angles if and only if $\hat{\mathbf{e}}^* \cdot \hat{\mathbf{f}}^* = 0$.*

Dual matrices can be defined likewise, i.e., if \mathbf{A} and \mathbf{A}_0 are two real $n \times n$ matrices, then the dual $n \times n$ matrix $\hat{\mathbf{A}}$ is defined as

$$\hat{\mathbf{A}} \equiv \mathbf{A} + \epsilon \mathbf{A}_0. \quad (\text{A.11})$$

We will work with 3×3 matrices in connection with dual vectors, but the above definition can be applied to any square matrices, which is the reason why n has been left arbitrary. Equality, multiplication by a dual scalar, and multiplication by a dual vector are defined as in the foregoing cases. Moreover, matrix multiplication is defined correspondingly, but then the order of multiplication must be respected. We thus have that, if $\hat{\mathbf{A}}$ and $\hat{\mathbf{B}}$ are two $n \times n$ dual matrices, with their primal and dual parts self-understood, then

$$\hat{\mathbf{A}}\hat{\mathbf{B}} = \mathbf{A}\mathbf{B} + \epsilon(\mathbf{A}\mathbf{B}_0 + \mathbf{A}_0\mathbf{B}). \quad (\text{A.12})$$

Therefore, matrix $\hat{\mathbf{A}}$ is real if $\mathbf{A}_0 = \mathbf{O}$, where \mathbf{O} denotes the $n \times n$ zero matrix; if $\mathbf{A} = \mathbf{O}$, then $\hat{\mathbf{A}}$ is called a *pure dual matrix*. Moreover, as we shall see below, a square dual matrix admits an inverse if and only if its primal part is nonsingular.

Now we can define the inverse of a dual matrix, if this is nonsingular. Indeed, it suffices to make $\hat{\mathbf{B}} = \hat{\mathbf{A}}^{-1}$ in eq.(A.12) and the right-hand side of this equation equal to the $n \times n$ identity matrix, $\mathbf{1}$, thereby obtaining two matrix equations that allow us to find the primal and the dual parts of $\hat{\mathbf{A}}^{-1}$, namely,

$$\mathbf{A}\mathbf{B} = \mathbf{1}, \quad \mathbf{A}\mathbf{B}_0 + \mathbf{A}_0\mathbf{B} = \mathbf{O},$$

whence

$$\mathbf{B} = \mathbf{A}^{-1}, \quad \mathbf{B}_0 = -\mathbf{A}^{-1}\mathbf{A}_0\mathbf{A}^{-1},$$

which are defined because \mathbf{A} is invertible by hypothesis, and hence, for any nonsingular dual matrix $\hat{\mathbf{A}}$,

$$\hat{\mathbf{A}}^{-1} = \mathbf{A}^{-1} - \epsilon \mathbf{A}^{-1}\mathbf{A}_0\mathbf{A}^{-1}. \quad (\text{A.13})$$

Note the striking similarity of the dual part of the foregoing expression with the time-derivative of the inverse of $\mathbf{A}(t)$, namely,

$$\frac{d}{dt}[\mathbf{A}^{-1}(t)] = -\mathbf{A}^{-1}(t)\dot{\mathbf{A}}(t)\mathbf{A}^{-1}(t).$$

In order to find an expression for the determinant of an $n \times n$ dual matrix, we need to recall the general expression for the dual function defined in eq.(A.3). However, that expression has to be adapted to a dual-matrix argument, which leads to

$$f(\hat{\mathbf{A}}) = f(\mathbf{A}) + \epsilon \operatorname{tr} \left[\mathbf{A}_0 \left(\frac{df}{d\hat{\mathbf{A}}} \right)^T \right] \Big|_{\hat{\mathbf{A}}=\mathbf{A}}. \quad (\text{A.14})$$

In particular, when $f(\hat{\mathbf{A}}) = \det(\hat{\mathbf{A}})$, we have, recalling the formula for the derivative of the determinant with respect to its matrix argument (Angeles, 1982), for any $n \times n$ matrix \mathbf{X} ,

$$\frac{d}{d\mathbf{X}}[\det(\mathbf{X})] = \det(\mathbf{X})\mathbf{X}^{-T},$$

where \mathbf{X}^{-T} denotes the transpose of the inverse of \mathbf{X} or, equivalently, the transpose of \mathbf{X}^{-1} . Therefore,

$$\operatorname{tr} \left[\mathbf{A}_0 \left(\frac{df}{d\hat{\mathbf{A}}} \right)^T \right] \Big|_{\hat{\mathbf{A}}=\mathbf{A}} = \det(\mathbf{A})\operatorname{tr}(\mathbf{A}_0\mathbf{A}^{-1}),$$

and hence,

$$\det(\hat{\mathbf{A}}) = \det(\mathbf{A})[1 + \epsilon \operatorname{tr}(\mathbf{A}_0\mathbf{A}^{-1})]. \quad (\text{A.15})$$

Now we can define the eigenvalue problem for the dual matrix $\hat{\mathbf{A}}$ defined above. Let $\hat{\lambda}$ and $\hat{\mathbf{e}}$ be a dual eigenvalue and a dual (unit) eigenvector of $\hat{\mathbf{A}}$, respectively. Then,

$$\hat{\mathbf{A}}\hat{\mathbf{e}} = \hat{\lambda}\hat{\mathbf{e}}, \quad \|\hat{\mathbf{e}}\| = 1. \quad (\text{A.16a})$$

For the foregoing linear homogeneous equation to admit a nontrivial solution, we must have

$$\det(\hat{\lambda}\mathbf{1} - \hat{\mathbf{A}}) = 0, \quad (\text{A.16b})$$

which yields an n th-order dual polynomial in the dual number $\hat{\lambda}$. Its n dual roots, real and complex, constitute the n *dual eigenvalues* of $\hat{\mathbf{A}}$. Note that, associated with each dual eigenvalue $\hat{\lambda}_i$, a corresponding *dual (unit) eigenvector* $\hat{\mathbf{e}}_i^*$ is defined, for $i = 1, 2, \dots, n$. Moreover, if we recall eq.(A.4), we can write

$$e^{\hat{\mathbf{A}}} = e^{\mathbf{A}} + \epsilon \mathbf{A}_0 e^{\mathbf{A}}. \quad (\text{A.17})$$

Upon expansion, the foregoing expression can be cast in the form

$$e^{\hat{\mathbf{A}}} = (\mathbf{1} + \epsilon \mathbf{A}_0)e^{\mathbf{A}} \neq e^{\mathbf{A}}(\mathbf{1} + \epsilon \mathbf{A}_0), \quad (\text{A.18})$$

the inequality arising because, in general, \mathbf{A} and \mathbf{A}_0 do not commute. They do so only in the case in which they share the same set of eigenvectors. A special case in which the two matrices share the same set of eigenvectors is when one matrix is an *analytic function* of the other. More formally, we have

Lemma A.2.2 *If \mathbf{F} is an analytic matrix function of matrix \mathbf{A} , then the two matrices*

(i) share the same set of eigenvectors, and

(ii) commute under multiplication.

Typical examples of analytic matrix functions are $\mathbf{F} = \mathbf{A}^N$ and $\mathbf{F} = e^{\mathbf{A}}$, for an integer N .

A.3 Fundamentals of Rigid-Body Kinematics

We review in this section some basic facts from rigid-body kinematics. For the sake of conciseness, some proofs are not given, but the pertinent references are cited whenever necessary.

A.3.1 Finite Displacements

A rigid body is understood as a particular case of the continuum with the special feature that, under any given motion, *any* two points of the rigid body remain equidistant. A rigid body is available through a *configuration* or *pose* that will be denoted by \mathcal{B} . Whenever a *reference configuration* is needed, this will be labelled \mathcal{B}^0 . Moreover, the position vector of a point P of the body in configuration \mathcal{B} will be denoted by \mathbf{p} , that in \mathcal{B}^0 being denoted correspondingly by \mathbf{p}^0 .

A rigid-body motion leaving a point O of the body fixed is called a *pure rotation*, and is represented by a *proper orthogonal matrix* \mathbf{Q} , i.e., \mathbf{Q} verifies the two properties below:

$$\mathbf{Q}\mathbf{Q}^T = \mathbf{1}, \quad \det(\mathbf{Q}) = +1. \quad (\text{A.19})$$

According to Euler's Theorem (Euler, 1776), a pure rotation leaves a set of points of the body immutable, this set lying on a line \mathcal{L} , which is termed the *axis of rotation*. If we draw the perpendicular from an arbitrary point P of the body to \mathcal{L} and denote its intersection with \mathcal{L} by P' , the angle ϕ between $P'P^0$ and $P'P$, where, according to our convention, P^0 denotes the point P in the reference configuration \mathcal{B}^0 of the body, is called the *angle of rotation*. Note that a direction must be specified along this line to define the sign of the angle. Furthermore, the direction of the line is specified by the unit vector \mathbf{e} . We term \mathbf{e} and ϕ the *natural invariants* of \mathbf{Q} .

As a result of Euler's Theorem, the rotation \mathbf{Q} can be represented in terms of its natural invariants. This representation takes the form

$$\mathbf{Q} = \mathbf{e}\mathbf{e}^T + \cos \phi(\mathbf{1} - \mathbf{e}\mathbf{e}^T) + \sin \phi \mathbf{E}, \quad (\text{A.20})$$

where \mathbf{E} denotes the *cross-product matrix* of \mathbf{e} , i.e., for any 3-dimensional vector \mathbf{v} ,

$$\mathbf{e} \times \mathbf{v} = \mathbf{E}\mathbf{v}.$$

As a result of the foregoing definition, \mathbf{E} is skew-symmetric, i.e., $\mathbf{E} = -\mathbf{E}^T$ and, moreover, it has the properties below:

$$\mathbf{E}^{2k+1} = (-1)^k \mathbf{E}, \quad \mathbf{E}^{2k} = (-1)^k (\mathbf{1} - \mathbf{e}\mathbf{e}^T), \quad \text{for } k = 1, 2, \dots$$

By virtue of the foregoing properties of the cross-product matrix \mathbf{E} of \mathbf{e} , the rotation matrix \mathbf{Q} can be written in the alternative form

$$\mathbf{Q} = \mathbf{1} + \sin \phi \mathbf{E} + (1 - \cos \phi) \mathbf{E}^2. \quad (\text{A.21})$$

Now, if we recall the *Cayley-Hamilton Theorem* (Halmos, 1974), we can realize that the right-hand side of the foregoing equation is nothing but the exponential of $\phi\mathbf{E}$, i.e.,

$$\mathbf{Q} = e^{\phi\mathbf{E}}, \quad (\text{A.22})$$

which is the *exponential form of the rotation matrix*. Now it is a simple matter to obtain the eigenvalues of the rotation matrix if we first notice that one eigenvalue of \mathbf{E} is 0, the other eigenvalues being readily derived as $\pm\sqrt{-1}$, where $\sqrt{-1}$ is the imaginary unit, i.e., $\sqrt{-1} \equiv \sqrt{-1}$. Therefore, if \mathbf{Q} is the exponential of $\phi\mathbf{E}$, then the eigenvalues of \mathbf{Q} are the exponentials of the eigenvalues of $\phi\mathbf{E}$:

$$\lambda_1 = e^0 = 1, \quad \lambda_{2,3} = e^{\pm\sqrt{-1}\phi} = \cos\phi \pm \sqrt{-1}\sin\phi. \quad (\text{A.23})$$

Moreover, we recall below the *Cartesian decomposition* of an $n \times n$ matrix \mathbf{A} , namely,

$$\mathbf{A} = \mathbf{A}_s + \mathbf{A}_{ss}, \quad (\text{A.24a})$$

where \mathbf{A}_s is symmetric and \mathbf{A}_{ss} is skew-symmetric. These matrices are given by

$$\mathbf{A}_s \equiv \frac{1}{2}(\mathbf{A} + \mathbf{A}^T), \quad \mathbf{A}_{ss} \equiv \frac{1}{2}(\mathbf{A} - \mathbf{A}^T). \quad (\text{A.24b})$$

Any 3×3 skew-symmetric matrix is fully defined by three scalars, which means that such a matrix can then be made isomorphic to a 3-dimensional vector. Indeed, let \mathbf{S} be a 3×3 skew-symmetric matrix and \mathbf{v} be an arbitrary 3-dimensional vector. Then, we have

$$\mathbf{S}\mathbf{v} \equiv \mathbf{s} \times \mathbf{v}. \quad (\text{A.25})$$

When the above items are expressed in a given coordinate frame \mathcal{F} , the components of \mathbf{S} , indicated as $\{s_{i,j}\}_{i,j=1}^3$, and of \mathbf{s} , indicated as $\{s_i\}_1^3$, bear the relations below:

$$\mathbf{S} = \begin{bmatrix} 0 & -s_3 & s_2 \\ s_3 & 0 & -s_1 \\ -s_2 & s_1 & 0 \end{bmatrix}, \quad \mathbf{s} = \frac{1}{2} \begin{bmatrix} s_{32} - s_{23} \\ s_{13} - s_{31} \\ s_{21} - s_{12} \end{bmatrix}. \quad (\text{A.26})$$

In general, we define the *axial vector* of an arbitrary 3×3 matrix \mathbf{A} in terms of the difference of its off-diagonal entries, as appearing in eq.(A.26) for the entries of matrix \mathbf{S} . Apparently, the axial vector of any 3×3 matrix is identical to that of its skew-symmetric component; this vector, represented as $\mathbf{a} \equiv \text{vect}(\mathbf{A})$, is the *vector linear invariant* of \mathbf{A} .

The *scalar linear invariant* of the same matrix is its trace, $\text{tr}(\mathbf{A})$. With this notation, note that

$$\frac{1}{2}(\mathbf{A} - \mathbf{A}^T)\mathbf{v} = \mathbf{a} \times \mathbf{v} .$$

Further, with reference to Fig. A.3.1, let A and P be two points of a rigid body, which is shown in its reference and its current configurations.

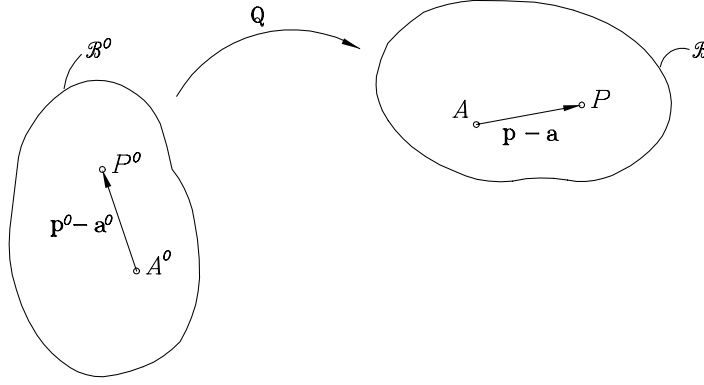


Figure A.1: Displacements of two points of a rigid body in two finitely-separated configurations

We can regard vector $\mathbf{p} - \mathbf{a}$ as the image of $\mathbf{p}^0 - \mathbf{a}^0$ under the rotation \mathbf{Q} , namely,

$$\mathbf{p} - \mathbf{a} = \mathbf{Q}(\mathbf{p}^0 - \mathbf{a}^0) , \quad (\text{A.27})$$

whence an expression for \mathbf{p} can be derived as

$$\mathbf{p} = \mathbf{a} + \mathbf{Q}(\mathbf{p}^0 - \mathbf{a}^0) . \quad (\text{A.28})$$

Furthermore, the *displacement* \mathbf{d}_A of A is defined as the difference $\mathbf{a} - \mathbf{a}^0$, with a similar definition for the displacement \mathbf{d}_P of P . From the above equation, it is now apparent that a linear relation between the two displacements follows:

$$\mathbf{d}_P = \mathbf{d}_A + (\mathbf{Q} - \mathbf{1})(\mathbf{p}^0 - \mathbf{a}^0) . \quad (\text{A.29})$$

Therefore,

Theorem A.3.1 *The displacements of all the points of a rigid body have identical projections onto the axis of the concomitant rotation.*

The proof of the foregoing result follows upon dot-multiplying both sides of eq.(A.29) by \mathbf{e} :

$$\mathbf{e} \cdot \mathbf{d}_P = \mathbf{e} \cdot \mathbf{d}_A .$$

From the previous result it is apparent that $\|\mathbf{d}_P\|$ can attain infinitely large values, depending on $\|\mathbf{p}^0 - \mathbf{a}^0\|$, but, in general, \mathbf{d}_P does not vanish. Hence, a minimum of $\|\mathbf{d}_P\|$ can be found, a result summarized in the Mozzi-Chasles Theorem (Mozzi, 1763;Chasles, 1830). This theorem states that the points of \mathcal{B} of minimum-norm displacement lie in a line \mathcal{M} that is parallel to the axis of the rotation represented by matrix \mathbf{Q} , the minimum-norm displacement being a vector parallel to the same axis. If we recall that \mathbf{e} and ϕ denote the natural invariants of \mathbf{Q} , then the position vector \mathbf{p}^* of the point P^* of \mathcal{M} lying closest to the origin O is given by (Angeles, 1997)

$$\mathbf{p}^* = \frac{(\mathbf{Q} - \mathbf{1})^T(\mathbf{Q}\mathbf{a}^0 - \mathbf{a})}{2(1 - \cos \phi)}, \quad \text{for } \phi \neq 0 , \quad (\text{A.30})$$

the special case in which $\phi = 0$ corresponding to a *pure translation*, whereby all points of \mathcal{B} undergo identical displacements. In this case, then, the axis \mathcal{M} is indeterminate, because all points of the body can be thought of as undergoing minimum-norm displacements. Henceforth, line \mathcal{M} will be termed the *Mozzi-Chasles axis*. Note that the Plücker coordinates of the Mozzi-Chasles axis are given by \mathbf{e} and $\mathbf{e}_0 \equiv \mathbf{p}^* \times \mathbf{e}$. We shall denote with \mathbf{d}^* the minimum-norm displacement, which can be represented in the form

$$\mathbf{d}^* = d^* \mathbf{e}, \quad d^* = \mathbf{d}_P \cdot \mathbf{e} . \quad (\text{A.31})$$

Therefore, the body under study can be regarded as undergoing, from \mathcal{B}^0 to \mathcal{B} , a screw motion, as if the body were rigidly attached to the bolt of a screw of axis \mathcal{M} and *pitch* p given by

$$p = \frac{d^*}{\phi} = \frac{\mathbf{e} \cdot \mathbf{d}_P}{\phi} . \quad (\text{A.32})$$

We list below further results:

Lemma A.3.1 *Let A and P be two points of a rigid body undergoing a general motion from a reference pose \mathcal{B}^0 to a current pose \mathcal{B} . Then, under the notation adopted above, the difference $\mathbf{p} - \mathbf{Q}\mathbf{p}^0$ remains constant and is denoted by \mathbf{d} , i.e.,*

$$\mathbf{p} - \mathbf{Q}\mathbf{p}^0 = \mathbf{a} - \mathbf{Q}\mathbf{a}^0 = \mathbf{d} . \quad (\text{A.33})$$

Proof: If we recall eq.(A.28) and substitute the expression therein for \mathbf{p} in the difference $\mathbf{p} - \mathbf{Q}\mathbf{p}^0$, we obtain

$$\mathbf{p} - \mathbf{Q}\mathbf{p}^0 = \mathbf{a} + \mathbf{Q}(\mathbf{p}^0 - \mathbf{a}^0) - \mathbf{Q}\mathbf{p}^0 = \mathbf{a} - \mathbf{Q}\mathbf{a}^0 = \mathbf{d} ,$$

thereby completing the intended proof.

Note that the kinematic interpretation of \mathbf{d} follows directly from eq.(A.33): \mathbf{d} represents the displacement of the point of \mathcal{B} that coincides with the origin in the reference pose \mathcal{B}^0 .

The geometric interpretation of the foregoing lemma is given in Fig. A.2. What this figure indicates is that the pose \mathcal{B} can be attained from \mathcal{B}^0 in two stages: (a) first, the body is given a rotation \mathbf{Q} about the origin O , that takes the body to the intermediate pose \mathcal{B}' ; (b) then, from \mathcal{B}' , the body is given a pure translation of displacement \mathbf{d} that takes the body into \mathcal{B} .

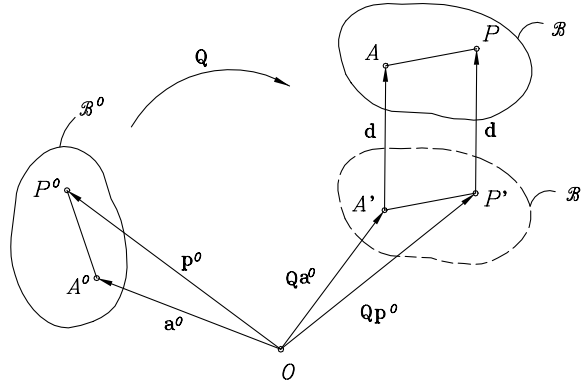


Figure A.2: Geometric interpretation of Lemma 3.1

Therefore, eq.(A.30) for the position vector of the point of the Mozzi-Chasles axis lying closest to the origin can be expressed in terms of vector \mathbf{d} as

$$\mathbf{p}^* = \frac{(\mathbf{1} - \mathbf{Q})^T \mathbf{d}}{2(1 - \cos \phi)}, \quad \text{for } \phi \neq 0 . \quad (\text{A.34})$$

Note that, in general, \mathbf{d} is not of minimum norm. Additionally, \mathbf{d} is origin-dependent, and hence, is not an invariant of the motion under study. Now, if we choose the origin on the Mozzi-Chasles axis \mathcal{M} , then we have the layout of Fig. A.3, and vector \mathbf{d} becomes a multiple of \mathbf{e} , namely, $\mathbf{d} = d^* \mathbf{e}$.

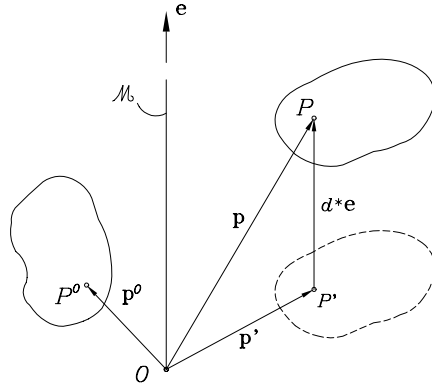


Figure A.3: Rigid-body displacement with origin on the Mozzi-Chasles axis

We can now express the Plücker coordinates of a line \mathcal{L} of a rigid body \mathcal{B} in terms of those of the line in its reference configuration \mathcal{L}^0 (Bottema and Roth, 1978; Pradeep, Yoder, and Mukundan, 1989), as shown in Fig. A.3.1. To this end, we let \mathbf{f} be the unit vector parallel to \mathcal{L} and P be a point of \mathcal{L} , and arrange the Plücker coordinates of \mathcal{L}^0 and \mathcal{L} in the 6-dimensional arrays $\boldsymbol{\lambda}^0$ and $\boldsymbol{\lambda}$, respectively, defined as

$$\boldsymbol{\lambda}^0 \equiv \begin{bmatrix} \mathbf{f}^0 \\ \mathbf{p}^0 \times \mathbf{f}^0 \end{bmatrix}, \quad \boldsymbol{\lambda} \equiv \begin{bmatrix} \mathbf{f} \\ \mathbf{p} \times \mathbf{f} \end{bmatrix}. \quad (\text{A.35})$$

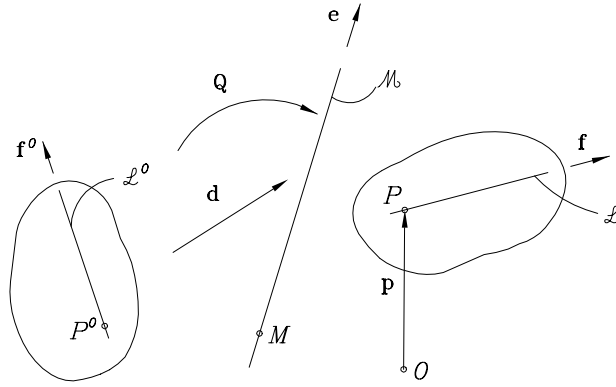


Figure A.4: The reference and the current configurations of a body and one of its lines

We thus have

$$\mathbf{f} = \mathbf{Q}\mathbf{f}^0, \quad \mathbf{p} = \mathbf{Q}\mathbf{p}^0 + \mathbf{d},$$

and hence,

$$\mathbf{p} \times \mathbf{f} = (\mathbf{Q}\mathbf{p}^0 + \mathbf{d}) \times \mathbf{Q}\mathbf{f}^0 = (\mathbf{Q}\mathbf{p}^0) \times \mathbf{Q}\mathbf{f}^0 + \mathbf{d} \times \mathbf{Q}\mathbf{f}^0.$$

Now, the first term of the rightmost-hand side of the above equation can be simplified upon noticing that the cross product of two rotated vectors is identical to the rotated

cross product. Furthermore, the second term of the same side can be expressed in terms of \mathbf{D} , the cross-product matrix of \mathbf{d} , thereby obtaining

$$\mathbf{p} \times \mathbf{f} = \mathbf{Q}(\mathbf{p}^0 \times \mathbf{f}^0) + \mathbf{DQf}^0 .$$

Upon substituting the foregoing expressions for \mathbf{f} and $\mathbf{p} \times \mathbf{f}$ into eq.(A.35), we obtain

$$\boldsymbol{\lambda} = \begin{bmatrix} \mathbf{Qf}^0 \\ \mathbf{DQf}^0 + \mathbf{Q}(\mathbf{p}^0 \times \mathbf{f}^0) \end{bmatrix} ,$$

which can be readily cast in the form of a linear transformation of $\boldsymbol{\lambda}^0$, i.e.,

$$\begin{bmatrix} \mathbf{f} \\ \mathbf{p} \times \mathbf{f} \end{bmatrix} = \begin{bmatrix} \mathbf{Q} & \mathbf{O} \\ \mathbf{DQ} & \mathbf{Q} \end{bmatrix} \begin{bmatrix} \mathbf{f}^0 \\ \mathbf{p}^0 \times \mathbf{f}^0 \end{bmatrix} , \quad (\text{A.36a})$$

where \mathbf{O} denotes the 3×3 zero matrix.

As the reader can readily verify, the inverse relation of eq.(A.36a) takes the form

$$\begin{bmatrix} \mathbf{f}^0 \\ \mathbf{p}^0 \times \mathbf{f}^0 \end{bmatrix} = \begin{bmatrix} \mathbf{Q}^T & \mathbf{O} \\ -\mathbf{Q}^T \mathbf{D} & \mathbf{Q}^T \end{bmatrix} \begin{bmatrix} \mathbf{f} \\ \mathbf{p} \times \mathbf{f} \end{bmatrix} . \quad (\text{A.36b})$$

By inspection of eq.(A.36a), and recalling the dual-unit-vector representation of a line, as given in eq.(A.10), we can realize that the dual unit vector of \mathcal{L} can be expressed as the image of the dual unit vector of \mathcal{L}^0 upon a linear transformation given by a dual matrix $\hat{\mathbf{Q}}$. Moreover, the dual matrix of interest can be readily derived from the real matrix of eq.(A.36a). Indeed, it can be realized from Section 2 that the difference between the primal and the dual parts of a dual quantity is that the units of the dual part are those of the primal part times units of length. Hence, the primal part of the dual matrix sought is bound to be \mathbf{Q} , which is dimensionless, the corresponding dual part being \mathbf{DQ} , which has units of length. A plausible form of the matrix sought is, then,

$$\hat{\mathbf{Q}} = \mathbf{Q} + \epsilon \mathbf{DQ} . \quad (\text{A.37})$$

The correctness of the above expression can be readily realized. Indeed, let $\hat{\mathbf{f}}^* = \mathbf{f} + \epsilon \mathbf{p} \times \mathbf{f}$ and $\hat{\mathbf{f}}^{0*} = \mathbf{f}^0 + \epsilon \mathbf{p}^0 \times \mathbf{f}^0$ be the dual unit vectors of \mathcal{L} and \mathcal{L}^0 , respectively. Then upon performing the product $\hat{\mathbf{Q}}\hat{\mathbf{f}}^{0*}$, we note that the product is rightfully $\hat{\mathbf{f}}^*$, i.e., $\hat{\mathbf{f}}^* = \hat{\mathbf{Q}}\hat{\mathbf{f}}^{0*}$. In the derivations below, we will need expressions for the vector and scalar linear invariants of the product of two matrices, one of which is skew-symmetric. These expressions are derived in detail in (Angeles, 1997). For quick reference, we recall these relations below:

Theorem A.3.2 *Let both \mathbf{A} and \mathbf{S} be 3×3 matrices, the former arbitrary, the latter skew-symmetric. Then,*

$$\text{vect}(\mathbf{SA}) = \frac{1}{2}[\text{tr}(\mathbf{A})\mathbf{1} - \mathbf{A}]\mathbf{s}, \quad (\text{A.38})$$

where $\mathbf{s} \equiv \text{vect}(\mathbf{S})$.

Now, as a direct consequence of the above result, we have

Corollary A.3.1 *If \mathbf{A} in Theorem A.3.2 is skew-symmetric, then the axial vector of the product \mathbf{SA} reduces to*

$$\text{vect}(\mathbf{SA}) = -\frac{1}{2}\mathbf{A}\mathbf{s} = -\frac{1}{2}\mathbf{a} \times \mathbf{s}, \quad (\text{A.39})$$

where $\mathbf{a} \equiv \text{vect}(\mathbf{A})$.

Moreover,

Theorem A.3.3 *Let \mathbf{A} , \mathbf{S} , and \mathbf{s} be defined as in Theorem A.3.2. Then,*

$$\text{tr}(\mathbf{SA}) = -2\mathbf{s} \cdot [\text{vect}(\mathbf{A})]. \quad (\text{A.40})$$

Furthermore, we prove now that $\hat{\mathbf{Q}}$ is proper orthogonal. Indeed, orthogonality can be proven by performing the product $\hat{\mathbf{Q}}\hat{\mathbf{Q}}^T$ and noticing that this product yields the 3×3 identity matrix, i.e., $\hat{\mathbf{Q}}\hat{\mathbf{Q}}^T = \mathbf{1}$. Proper orthogonality is proven, in turn, upon application of formula (A.15) to matrix $\hat{\mathbf{Q}}$, as given by eq.(A.37), namely,

$$\det(\hat{\mathbf{Q}}) = \det(\mathbf{Q})[1 + \epsilon \text{tr}(\mathbf{D}\mathbf{Q}\mathbf{Q}^{-1})] = \det(\mathbf{Q})[1 + \epsilon \text{tr}(\mathbf{D})] = 1,$$

thus completing the proof.

The exponential form of the dual rotation matrix can be obtained if we note that the exponential of a pure dual number $\hat{x} = \epsilon x_0$ reduces to

$$e^{\epsilon x_0} = 1 + \epsilon x_0. \quad (\text{A.41})$$

On the other hand, we can write

$$\hat{\mathbf{Q}} = (\mathbf{1} + \epsilon \mathbf{D})\mathbf{Q}. \quad (\text{A.42})$$

In analogy with eq.(A.41), the foregoing expression takes the form

$$\hat{\mathbf{Q}} = e^{\epsilon \mathbf{D}} \mathbf{Q} .$$

Furthermore, if we recall the exponential form of \mathbf{Q} , as given in eq.(A.22), the foregoing expression simplifies to

$$\hat{\mathbf{Q}} = e^{\epsilon \mathbf{D}} e^{\phi \mathbf{E}} . \quad (\text{A.43})$$

However, since \mathbf{D} and \mathbf{E} are unrelated, they do not share the same set of eigenvectors, and hence, they do not commute under multiplication, the foregoing expression thus not being further reducible to one single exponential. Nevertheless, if the origin is placed on the Mozzi-Chasles axis, as depicted in Fig. A.3, then the dual rotation matrix becomes

$$\hat{\mathbf{Q}} = \mathbf{Q} + \epsilon d^* \mathbf{E} \mathbf{Q} , \quad (\text{A.44})$$

where $d^* \mathbf{E}$ is, apparently, the cross-product matrix of vector $d^* \mathbf{e}$. Furthermore, the exponential form of the dual rotation matrix, eq.(A.43), then simplifies to $\hat{\mathbf{Q}} = e^{(\phi + \epsilon d^*) \mathbf{E}}$ or, if we let $\hat{\phi} = \phi + \epsilon d^*$, then we can write $\hat{\mathbf{Q}} = e^{\hat{\phi} \mathbf{E}}$.

A.3.2 Velocity Analysis

Upon differentiation with respect to time of both sides of eq.(A.27), we obtain

$$\dot{\mathbf{p}} - \dot{\mathbf{a}} = \dot{\mathbf{Q}}(\mathbf{p}^0 - \mathbf{a}^0) ,$$

and, if we solve for $(\mathbf{p}^0 - \mathbf{a}^0)$ from the equation mentioned above, we obtain

$$\dot{\mathbf{p}} - \dot{\mathbf{a}} = \dot{\mathbf{Q}} \mathbf{Q}^T (\mathbf{p} - \mathbf{a}) , \quad (\text{A.45})$$

where $\dot{\mathbf{Q}} \mathbf{Q}^T$ is defined as the angular-velocity matrix of the motion under study, and is represented as $\mathbf{\Omega}$, namely,

$$\mathbf{\Omega} \equiv \dot{\mathbf{Q}} \mathbf{Q}^T . \quad (\text{A.46a})$$

It can be readily proven that the foregoing matrix is skew-symmetric, i.e.,

$$\mathbf{\Omega}^T = -\mathbf{\Omega} . \quad (\text{A.46b})$$

Moreover, the axial vector of $\mathbf{\Omega}$ is the angular-velocity vector $\boldsymbol{\omega}$:

$$\boldsymbol{\omega} = \text{vect}(\mathbf{\Omega}) . \quad (\text{A.46c})$$

We can now write eq.(A.45) in the form

$$\dot{\mathbf{p}} = \dot{\mathbf{a}} + \boldsymbol{\Omega}(\mathbf{p} - \mathbf{a}) = \dot{\mathbf{a}} + \boldsymbol{\omega} \times (\mathbf{p} - \mathbf{a}) , \quad (\text{A.47})$$

whence,

$$\dot{\mathbf{p}} - \boldsymbol{\omega} \times \mathbf{p} = \dot{\mathbf{a}} - \boldsymbol{\omega} \times \mathbf{a} \equiv \mathbf{v}^0 = \text{const} . \quad (\text{A.48})$$

Therefore, the difference $\dot{\mathbf{p}} - \boldsymbol{\omega} \times \mathbf{p}$ is the same for all points of a rigid body. The kinematic interpretation of this quantity is straightforward: If we rewrite \mathbf{v}^0 in the form $\mathbf{v}^0 = \dot{\mathbf{p}} + \boldsymbol{\omega} \times (-\mathbf{p})$, then we can readily realize that, $-\mathbf{p}$ being the vector directed from point P of the rigid body to the origin O , \mathbf{v}^0 represents the velocity of the point of the body that coincides instantaneously with the origin. Furthermore, we express \mathbf{d} , as given by eq.(A.33), in terms of the position vector of an arbitrary point P , \mathbf{p} , thus obtaining

$$\mathbf{d} = \mathbf{p} - Q\mathbf{p}^0 . \quad (\text{A.49})$$

Upon differentiation of the two sides of the above expression with respect to time, we obtain

$$\dot{\mathbf{d}} = \dot{\mathbf{p}} - \dot{Q}\mathbf{p}^0 ,$$

which can be readily expressed in terms of the current value of the position vector of P , by solving for \mathbf{p}^0 from eq.(A.49), namely,

$$\dot{\mathbf{d}} = \dot{\mathbf{p}} - \boldsymbol{\Omega}(\mathbf{p} - \mathbf{d}) \quad \text{or} \quad \dot{\mathbf{d}} - \boldsymbol{\omega} \times \mathbf{d} = \dot{\mathbf{p}} - \boldsymbol{\omega} \times \mathbf{p} , \quad (\text{A.50})$$

and hence, the difference $\dot{\mathbf{d}} - \boldsymbol{\omega} \times \mathbf{d}$ is identical to the difference $\dot{\mathbf{p}} - \boldsymbol{\omega} \times \mathbf{p}$, i.e.,

$$\dot{\mathbf{d}} - \boldsymbol{\omega} \times \mathbf{d} = \mathbf{v}^0 . \quad (\text{A.51})$$

Furthermore, upon dot-multiplying the two sides of eq.(A.48) by $\boldsymbol{\omega}$, we obtain an interesting result, namely,

$$\boldsymbol{\omega} \cdot \dot{\mathbf{p}} = \boldsymbol{\omega} \cdot \dot{\mathbf{a}} , \quad (\text{A.52})$$

and hence,

Theorem A.3.4 *The velocities of all points of a rigid body have the same projection onto the angular-velocity vector of the motion under study.*

Similar to the Mozzi-Chasles Theorem, we have now

Theorem A.3.5 *Given a rigid body \mathcal{B} under general motion, a set of its points, on a line \mathcal{L} , undergoes the identical minimum-magnitude velocity \mathbf{v}^* parallel to the angular velocity $\boldsymbol{\omega}$.*

The Plücker coordinates of line \mathcal{L} , grouped in the 6-dimensional array $\boldsymbol{\lambda}$, are given as

$$\boldsymbol{\lambda} \equiv \begin{bmatrix} \mathbf{f} \\ \boldsymbol{\pi} \times \mathbf{f} \end{bmatrix}, \quad \mathbf{f} \equiv \frac{\boldsymbol{\omega}}{\|\boldsymbol{\omega}\|}, \quad \boldsymbol{\pi} \equiv \frac{\boldsymbol{\omega} \times \mathbf{v}^0}{\|\boldsymbol{\omega}\|^2}, \quad (\text{A.53})$$

where \mathbf{v}^0 was previously introduced as the velocity of the point of \mathcal{B} that coincides instantaneously with the origin. Line \mathcal{L} is termed the *instant screw axis*–ISA, for brevity.

Thus, the instantaneous motion of \mathcal{B} is defined by a screw of axis \mathcal{L} and pitch p' , given by

$$p' = \frac{\dot{\mathbf{p}} \cdot \boldsymbol{\omega}}{\|\boldsymbol{\omega}\|^2}, \quad (\text{A.54})$$

where $\dot{\mathbf{p}}$ is the velocity of an arbitrary point P of \mathcal{B} , the product $\dot{\mathbf{p}} \cdot \boldsymbol{\omega}$ being constant by virtue of Theorem A.3.4. A proof of the foregoing results is available in (Angeles, 1997).

A.3.3 The Linear Invariants of the Dual Rotation Matrix

We start by recalling the *linear invariants* of the real rotation matrix (Angeles, 1997). These are defined as

$$\mathbf{q} \equiv \text{vect}(\mathbf{Q}) = (\sin \phi)\mathbf{e}, \quad q_0 \equiv \frac{\text{tr}(\mathbf{Q}) - 1}{2} = \cos \phi. \quad (\text{A.55a})$$

Note that the linear invariants of any 3×3 matrix can be obtained from simple differences of its off-diagonal entries and sums of its diagonal entries. Once the foregoing linear invariants are calculated, the natural invariants can be obtained uniquely as indicated below: First, note that the sign of \mathbf{e} can be changed without affecting \mathbf{q} if the sign of ϕ is changed accordingly, which means that the sign of ϕ —or that of \mathbf{e} , for that matter—is undefined. In order to define this sign uniquely, we will adopt a positive sign for $\sin \phi$, which means that ϕ is assumed, henceforth, to lie in the interval $0 \leq \phi \leq \pi$.

We can thus obtain the inverse relations of eq.(A.55a) in the form

$$\mathbf{e} = \frac{\mathbf{q}}{\|\mathbf{q}\|}, \quad \phi = \arctan \left(\frac{\|\mathbf{q}\|}{q_0} \right), \quad \mathbf{q} \neq \mathbf{0}, \quad (\text{A.55b})$$

the case $\mathbf{q} = \mathbf{0}$ being handled separately. Indeed, \mathbf{q} vanishes under two cases: (a) $\phi = 0$, in which case the body undergoes a pure translation and the axis of rotation is obviously

undefined; and (b) $\phi = \pi$, in which case \mathbf{Q} is symmetric and takes the form

$$\text{For } \phi = \pi : \quad \mathbf{Q} = -\mathbf{1} + 2\mathbf{e}\mathbf{e}^T, \quad (\text{A.55c})$$

whence the natural invariants become apparent and can be readily extracted from \mathbf{Q} .

Similar to the linear invariants of the real rotation matrix, in the dual case we have

$$\hat{\mathbf{q}} \equiv \text{vect}(\hat{\mathbf{Q}}), \quad \hat{q}_0 \equiv \frac{\text{tr}(\hat{\mathbf{Q}}) - 1}{2}. \quad (\text{A.56})$$

Expressions for the foregoing quantities in terms of the motion parameters are derived below; in the sequel, we also derive expressions for the *dual natural invariants* in terms of the same parameters. We start by expanding the vector linear invariant:

$$\text{vect}(\hat{\mathbf{Q}}) = \text{vect}(\mathbf{Q} + \epsilon \mathbf{DQ}) = \text{vect}(\mathbf{Q}) + \epsilon \text{vect}(\mathbf{DQ}). \quad (\text{A.57a})$$

But, by virtue of eq.(A.20),

$$\text{vect}(\mathbf{Q}) = (\sin \phi)\mathbf{e}. \quad (\text{A.57b})$$

Furthermore, the second term of the rightmost-hand side of eq.(A.57a) can be readily calculated if we recall Theorem A.3.2, with $\mathbf{d} \equiv \text{vect}(\mathbf{D})$:

$$\text{vect}(\mathbf{DQ}) = \frac{1}{2}[\text{tr}(\mathbf{Q})\mathbf{1} - \mathbf{Q}]\mathbf{d}. \quad (\text{A.57c})$$

Now, if we recall expression (A.20), we obtain

$$\text{tr}(\mathbf{Q})\mathbf{1} - \mathbf{Q} = (1 + \cos \phi)\mathbf{1} - \sin \phi \mathbf{E} - (1 - \cos \phi)\mathbf{e}\mathbf{e}^T.$$

Upon substitution of the foregoing expression into eq.(A.57c), the desired expression for $\text{vect}(\mathbf{DQ})$ is readily derived, namely,

$$\text{vect}(\mathbf{DQ}) = \frac{1}{2}[(1 + \cos \phi)\mathbf{d} - \sin \phi \mathbf{e} \times \mathbf{d} - (1 - \cos \phi)(\mathbf{e} \cdot \mathbf{d})\mathbf{e}], \quad (\text{A.57d})$$

and hence,

$$\hat{\mathbf{q}} = (\sin \phi)\mathbf{e} + \epsilon \frac{1}{2}[(\cos \phi)(\mathbf{e} \cdot \mathbf{d})\mathbf{e} + (1 + \cos \phi)\mathbf{d} + (\sin \phi)\mathbf{d} \times \mathbf{e} - (\mathbf{e} \cdot \mathbf{d})\mathbf{e}]. \quad (\text{A.57e})$$

On the other hand, the position vector \mathbf{p}^* of the Mozzi-Chasles axis, given by eq.(A.34), can be expressed as

$$\mathbf{p}^* = \frac{1}{2} \frac{\sin \phi}{1 - \cos \phi} \mathbf{e} \times \mathbf{d} + \frac{1}{2} \mathbf{d} - \frac{1}{2} (\mathbf{e} \cdot \mathbf{d}) \mathbf{e}, \quad (\text{A.58a})$$

and hence,

$$\mathbf{p}^* \times \mathbf{e} = \frac{1}{2} \frac{\sin \phi}{1 - \cos \phi} \mathbf{d} - \frac{1}{2} \frac{\sin \phi}{1 - \cos \phi} (\mathbf{e} \cdot \mathbf{d}) \mathbf{e} + \frac{1}{2} \mathbf{d} \times \mathbf{e}. \quad (\text{A.58b})$$

Moreover, let us recall the identity

$$\frac{1 + \cos \phi}{\sin \phi} = \frac{\sin \phi}{1 - \cos \phi}, \quad (\text{A.58c})$$

which allows us to rewrite eq.(A.58b) in the form

$$\mathbf{p}^* \times \mathbf{e} = \frac{1}{2} \frac{1 + \cos \phi}{\sin \phi} \mathbf{d} - \frac{1}{2} \frac{1 + \cos \phi}{\sin \phi} (\mathbf{e} \cdot \mathbf{d}) \mathbf{e} + \frac{1}{2} \mathbf{d} \times \mathbf{e}, \quad (\text{A.58d})$$

whence,

$$(\sin \phi) \mathbf{p}^* \times \mathbf{e} = \frac{1}{2} [(1 + \cos \phi) \mathbf{d} - (1 + \cos \phi) (\mathbf{e} \cdot \mathbf{d}) \mathbf{e} + (\sin \phi) \mathbf{d} \times \mathbf{e}],$$

and $\hat{\mathbf{q}}$ takes the form

$$\hat{\mathbf{q}} = (\sin \phi) \mathbf{e} + \epsilon [(\cos \phi) (\mathbf{e} \cdot \mathbf{d}) \mathbf{e} + (\sin \phi) \mathbf{p}^* \times \mathbf{e}]. \quad (\text{A.59})$$

If we now recall eqs.(A.31) and (A.32), $\mathbf{d} \cdot \mathbf{e} \equiv d^* = p\phi$, while $\mathbf{p}^* \times \mathbf{e}$ is the moment of the associated Mozzi-Chasles axis, \mathbf{e}_0 , and hence, eq.(A.59) becomes

$$\hat{\mathbf{q}} = (\sin \phi) \mathbf{e} + \epsilon [(\cos \phi) p\phi \mathbf{e} + (\sin \phi) \mathbf{e}_0], \quad (\text{A.60})$$

and hence, $\hat{\mathbf{q}}$ can be further simplified to

$$\hat{\mathbf{q}} = \hat{\mathbf{e}}^* \sin \hat{\phi}, \quad \hat{\phi} \equiv \phi(1 + \epsilon p), \quad (\text{A.61})$$

where $\hat{\mathbf{e}}^*$ is the dual unit vector representing the Mozzi-Chasles axis, i.e., $\hat{\mathbf{e}}^* = \mathbf{e} + \epsilon \mathbf{e}_0$.

Now, such as in the real case, we can calculate the dual natural invariants of the motion under study in terms of the foregoing dual linear invariants. We do this by mimicking eqs.(A.55b), namely,

$$\hat{\mathbf{e}}^* = \frac{\hat{\mathbf{q}}}{\|\hat{\mathbf{q}}\|}, \quad \hat{\phi} = \arctan \left(\frac{\|\hat{\mathbf{q}}\|}{\hat{q}_0} \right), \quad \|\hat{\mathbf{q}}\| \neq 0, \quad (\text{A.62})$$

where $\|\hat{\mathbf{q}}\|$ is calculated from eq.(A.9e), which gives $\|\hat{\mathbf{q}}\|^2$, the square root of the latter then following from eq.(A.7), thus obtaining

$$\|\hat{\mathbf{q}}\| = \sin \hat{\phi} = \sin \phi + \epsilon (\mathbf{e} \cdot \mathbf{d}) \cos \phi, \quad (\text{A.63})$$

and hence, upon simplification,

$$\hat{\mathbf{e}}^* = \mathbf{e} + \epsilon \mathbf{p}^* \times \mathbf{e} = \mathbf{e} + \epsilon \mathbf{e}_0 , \quad (\text{A.64})$$

which is rightfully the dual unit vector of the Mozzi-Chasles axis. Furthermore,

$$\text{tr}(\hat{\mathbf{Q}}) = \text{tr}(\mathbf{Q}) + \epsilon \text{tr}(\mathbf{DQ}) , \quad (\text{A.65a})$$

where, from Theorem A.3.3, $\text{tr}(\mathbf{DQ})$ turns out to be

$$\text{tr}(\mathbf{DQ}) = -2[\text{vect}(\mathbf{Q})] \cdot \mathbf{d} = -2 \sin \phi (\mathbf{e} \cdot \mathbf{d}) , \quad (\text{A.65b})$$

whence,

$$\text{tr}(\hat{\mathbf{Q}}) = 1 + 2 \cos \phi - \epsilon 2(\sin \phi) \mathbf{e} \cdot \mathbf{d} , \quad (\text{A.65c})$$

and so, from the second of eqs.(A.56),

$$\hat{q}_0 \equiv \cos \hat{\phi} = \cos \phi - \epsilon (\sin \phi) (\mathbf{e} \cdot \mathbf{d}) ,$$

which, by virtue of eqs.(A.31), leads to

$$\hat{q}_0 = \cos \phi - \epsilon (\sin \phi) d^* , \quad \hat{\phi} = \phi + \epsilon d^* = \phi(1 + \epsilon p) . \quad (\text{A.65d})$$

In summary, the dual angle of the dual rotation under study comprises the angle of rotation of \mathbf{Q} in its primal part and the axial component of the displacement of all points of the moving body onto the Mozzi-Chasles axis. Upon comparison of the dual angle between two lines, as given in eq.(A.5), with the dual angle of rotation $\hat{\phi}$, it is then apparent that the primal part of the latter plays the role of the angle between two lines, while the corresponding dual part plays the role of the distance s between those lines. It is noteworthy that a pure rotation has a dual angle of rotation that is real, while a pure translation has an angle of rotation that is a pure dual number.

Example 1: Determination of the screw parameters of a rigid-body motion.

We take here an example of (Angeles, 1997): The cube of Fig. A.5 is displaced from configuration $A^0 B^0 \dots H^0$ into configuration $AB \dots H$. Find the Plücker coordinates of the Mozzi-Chasles axis of the motion undergone by the cube.

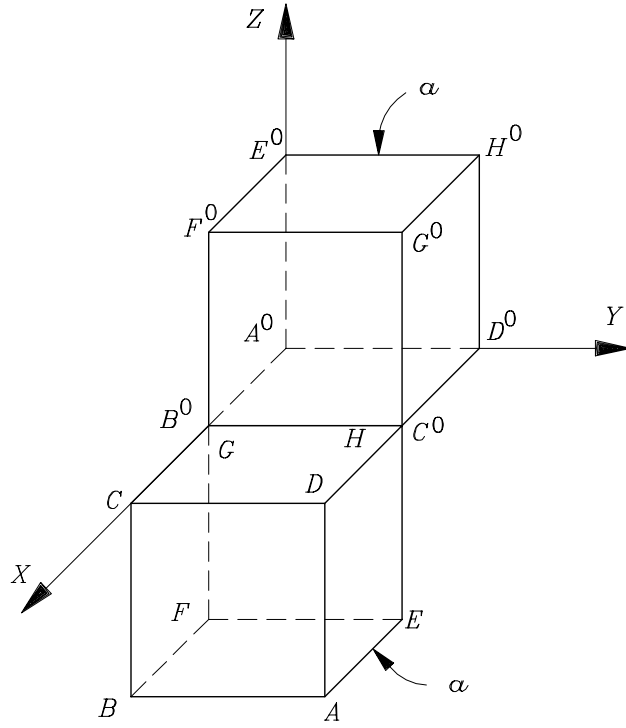


Figure A.5: Motion of a cube

Solution: We start by constructing $\hat{\mathbf{Q}}$: $\hat{\mathbf{Q}} \equiv [\hat{\mathbf{i}}^* \ \hat{\mathbf{j}}^* \ \hat{\mathbf{k}}^*]$, where $\hat{\mathbf{i}}^*$, $\hat{\mathbf{j}}^*$, and $\hat{\mathbf{k}}^*$ are the dual unit vectors of lines AB , AD , and AE , respectively. These lines are, in turn, the images of lines A^0B^0 , A^0D^0 , and A^0E^0 under the rigid-body motion at hand. The dual unit vectors of the latter are denoted by $\hat{\mathbf{i}}^{0*}$, $\hat{\mathbf{j}}^{0*}$, and $\hat{\mathbf{k}}^{0*}$, respectively, and are parallel to the X , Y , and Z axes of the figure. We thus have

$$\hat{\mathbf{i}}^* = -\mathbf{j}^0 + \epsilon \mathbf{a} \times (-\mathbf{j}^0), \quad \hat{\mathbf{j}}^* = \mathbf{k}^0 + \epsilon \mathbf{a} \times \mathbf{k}^0, \quad \hat{\mathbf{k}}^* = -\mathbf{i}^0 + \epsilon \mathbf{a} \times (-\mathbf{i}^0),$$

where \mathbf{a} is the position vector of A , and is given by

$$\mathbf{a} = [2 \quad 1 \quad -1]^T a.$$

Hence,

$$\hat{\mathbf{i}}^* = -\mathbf{j}^0 + \epsilon a(-\mathbf{i}^0 - 2\mathbf{k}^0)$$

$$\hat{\mathbf{j}}^* = \mathbf{k}^0 + \epsilon a(\mathbf{i}^0 - 2\mathbf{j}^0)$$

$$\hat{\mathbf{k}}^* = -\mathbf{i}^0 + \epsilon a(\mathbf{j}^0 + \mathbf{k}^0)$$

Therefore,

$$\hat{\mathbf{Q}} = \begin{bmatrix} -\epsilon a & +\epsilon a & -1 \\ -1 & -\epsilon 2a & +\epsilon a \\ -\epsilon 2a & 1 & +\epsilon a \end{bmatrix},$$

whence,

$$\text{vect}(\hat{\mathbf{Q}}) = \frac{1}{2} \begin{bmatrix} 1 - \epsilon a \\ -1 + \epsilon 2a \\ -1 - \epsilon a \end{bmatrix}, \quad \text{tr}(\hat{\mathbf{Q}}) = -\epsilon(2a),$$

and

$$\|\text{vect}(\hat{\mathbf{Q}})\|^2 = \left\| \frac{1}{2} \begin{bmatrix} 1 \\ -1 \\ -1 \end{bmatrix} \right\|^2 + \epsilon 2 \frac{1}{2} [1 \quad -1 \quad -1] \begin{bmatrix} -1 \\ 2 \\ -1 \end{bmatrix} \frac{a}{2} = \frac{3}{4} - \epsilon a.$$

Thus,

$$\|\text{vect}(\hat{\mathbf{Q}})\| = \frac{\sqrt{3}}{2} + \epsilon \frac{-a}{\sqrt{3}} = \frac{\sqrt{3}}{2} - \epsilon \frac{\sqrt{3}}{3} a.$$

Therefore, the unit dual vector representing the Mozzi-Chasles axis of the motion at hand, $\hat{\mathbf{e}}^*$, is given by $\hat{\mathbf{e}}^* = \text{vect}(\hat{\mathbf{Q}})/\|\text{vect}(\hat{\mathbf{Q}})\|$, i.e.,

$$\hat{\mathbf{e}}^* = \frac{1}{\sqrt{3}/2} \frac{1}{2} \begin{bmatrix} 1 \\ -1 \\ -1 \end{bmatrix} - \epsilon \frac{a}{3/4} \left(\frac{1}{2} \begin{bmatrix} 1 \\ -1 \\ -1 \end{bmatrix} \frac{-\sqrt{3}}{3} - \frac{1}{2} \begin{bmatrix} -1 \\ 2 \\ -1 \end{bmatrix} \frac{\sqrt{3}}{2} \right).$$

After various stages of simplification, the foregoing expression reduces to

$$\hat{\mathbf{e}}^* = \frac{\sqrt{3}}{3} \begin{bmatrix} 1 \\ -1 \\ -1 \end{bmatrix} + \epsilon \frac{\sqrt{3}}{9} \begin{bmatrix} -1 \\ 4 \\ -5 \end{bmatrix} a.$$

Thus, the Mozzi-Chasles axis is parallel to the unit vector \mathbf{e} , which is given by the primal part of $\hat{\mathbf{e}}$, while the dual part of the same dual unit vector represents the moment of the Mozzi-Chasles axis, from which the position vector \mathbf{p}^* of P^* , the point of the Mozzi-Chasles axis closest to the origin, is readily found as

$$\mathbf{p}^* = \mathbf{e} \times \mathbf{e}_0 = \frac{a}{3} [3 \quad 2 \quad 1]^T.$$

A.3.4 The Dual Euler-Rodrigues Parameters of a Rigid-Body Motion

We first recall the definition of the Euler-Rodrigues parameters of a pure rotation, which are isomorphic to the *quaternion* of the rotation (Hamilton, 1844). These are most naturally introduced as the linear invariants of the square root of the rotation at hand, and

represented, paralleling the definition of the linear invariants, as

$$\mathbf{r} \equiv \text{vect}(\sqrt{\mathbf{Q}}), \quad r_0 \equiv \frac{\text{tr}(\sqrt{\mathbf{Q}}) - 1}{2}, \quad (\text{A.66})$$

the *proper orthogonal* square root of \mathbf{Q} being given as (Angeles, 1997):

$$\sqrt{\mathbf{Q}} = \mathbf{1} + \sin\left(\frac{\phi}{2}\right) \mathbf{E} + \left[1 - \cos\left(\frac{\phi}{2}\right)\right] \mathbf{E}^2. \quad (\text{A.67})$$

The *dual Euler-Rodrigues parameters* of a rigid-body motion are thus defined as

$$\hat{\mathbf{r}} \equiv \text{vect}(\sqrt{\hat{\mathbf{Q}}}), \quad \hat{r}_0 \equiv \frac{\text{tr}(\sqrt{\hat{\mathbf{Q}}}) - 1}{2}. \quad (\text{A.68})$$

Below we derive an expression for $\sqrt{\hat{\mathbf{Q}}}$. Prior to this, we introduce a relation that will prove useful:

Lemma A.3.2 *Let \mathbf{a} and \mathbf{b} be arbitrary 3-dimensional vectors, and $\mathbf{c} \equiv \mathbf{a} \times \mathbf{b}$. The cross-product matrix \mathbf{C} of \mathbf{c} is given by*

$$\mathbf{C} = \mathbf{b}\mathbf{a}^T - \mathbf{a}\mathbf{b}^T. \quad (\text{A.69})$$

Proof: This follows by noticing that, for any 3-dimensional vector \mathbf{u} ,

$$\mathbf{c} \times \mathbf{u} = (\mathbf{a} \times \mathbf{b}) \times \mathbf{u} = \mathbf{b}(\mathbf{a}^T \mathbf{u}) - \mathbf{a}(\mathbf{b}^T \mathbf{u}),$$

which readily leads to

$$\mathbf{C}\mathbf{u} = (\mathbf{b}\mathbf{a}^T - \mathbf{a}\mathbf{b}^T)\mathbf{u},$$

thereby completing the proof.

Now we proceed to determine $\sqrt{\hat{\mathbf{Q}}}$. To this end, we regard the motion at hand, from a reference configuration \mathcal{B}^0 to a current configuration \mathcal{B} , as consisting of a rotation \mathbf{Q} about the origin O followed by a translation \mathbf{d} . Then, this motion is decomposed into two parts, as shown in Fig. A.3.4: First, the body is rotated about the origin O by a rotation $\sqrt{\mathbf{Q}}$ and a translation \mathbf{d}_s ; then, from the configuration \mathcal{B}' thus attained, the body is given a new rotation $\sqrt{\mathbf{Q}}$ about O as well, followed by the same translation \mathbf{d}_s .

It is apparent that, from the general expression for the dual rotation matrix, eq.(A.42), $\sqrt{\hat{\mathbf{Q}}}$ can be represented as

$$\sqrt{\hat{\mathbf{Q}}} = (\mathbf{1} + \epsilon \mathbf{D}_s) \sqrt{\mathbf{Q}}, \quad (\text{A.70})$$

the calculation of $\sqrt{\hat{\mathbf{Q}}}$ thus reducing to that of the skew-symmetric matrix \mathbf{D}_s , which is the cross-product matrix of \mathbf{d}_s . This matrix is calculated below in terms of $\sqrt{\mathbf{Q}}$ and \mathbf{D} .

We thus have

$$\mathbf{p}^2 = \sqrt{\mathbf{Q}}\mathbf{p}^0 + \mathbf{d}_s, \quad (\text{A.71})$$

$$\mathbf{p}^4 = \sqrt{\mathbf{Q}}\mathbf{p}^2 + \mathbf{d}_s = \mathbf{Q}\mathbf{p}^0 + (\mathbf{1} + \sqrt{\mathbf{Q}})\mathbf{d}_s. \quad (\text{A.72})$$

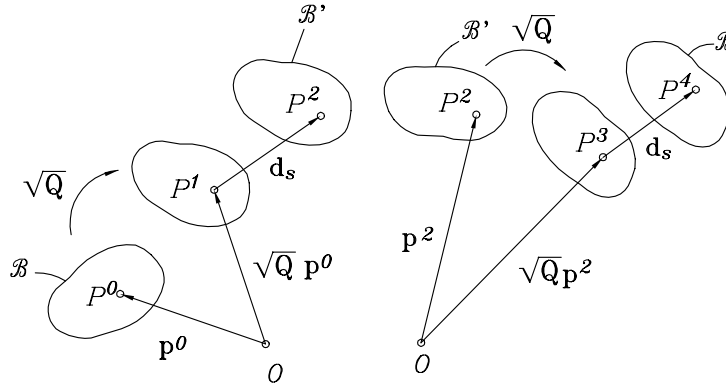


Figure A.6: Decomposition of the motion of a rigid body

But \mathbf{p}^4 is the position vector of point P in \mathcal{B} , which can be attained by a rotation \mathbf{Q} about O followed by a translation \mathbf{d} , i.e.,

$$\mathbf{p}^4 = \mathbf{Q}\mathbf{p}^0 + \mathbf{d}. \quad (\text{A.73})$$

Upon comparing the right-hand sides of eqs.(A.72) and (A.73), we obtain

$$(\mathbf{1} + \sqrt{\mathbf{Q}})\mathbf{d}_s = \mathbf{d},$$

whence,

$$\mathbf{d}_s = (\mathbf{1} + \sqrt{\mathbf{Q}})^{-1}\mathbf{d}. \quad (\text{A.74})$$

An expression for the above inverse can be derived if we realize that this inverse is an analytic function of $\sqrt{\mathbf{Q}}$, which is, in turn, an analytic function of \mathbf{Q} . We can thus conclude that by virtue of the Cayley-Hamilton Theorem, invoked when deriving the exponential

form of the rotation matrix in eq.(A.22), the inverse sought must be a linear combination of the first three powers of \mathbf{E} : $\mathbf{e}^0 \equiv \mathbf{1}$, \mathbf{E} , and \mathbf{E}^2 , namely,

$$(\mathbf{1} + \sqrt{\mathbf{Q}})^{-1} = \alpha \mathbf{1} + \beta \mathbf{E} + \gamma \mathbf{E}^2, \quad (\text{A.75})$$

where α , β , and γ are to be determined. To this end, we write

$$(\mathbf{1} + \sqrt{\mathbf{Q}})^{-1}(\alpha \mathbf{1} + \beta \mathbf{E} + \gamma \mathbf{E}^2) = \mathbf{1}.$$

If we now substitute in the above equation the expression for $\sqrt{\mathbf{Q}}$ displayed in eq.(A.67), we obtain three equations for the three unknowns α , β , and γ , from which it is a simple matter to solve for these unknowns, namely,

$$\alpha = \frac{1}{2}, \quad \beta = -\frac{\sin(\phi/2)}{2[1 + \cos(\phi/2)]}, \quad \gamma = 0, \quad (\text{A.76})$$

the inverse sought thus taking the form

$$(\mathbf{1} + \sqrt{\mathbf{Q}})^{-1} = \frac{1}{2} \left[\mathbf{1} - \frac{\sin(\phi/2)}{1 + \cos(\phi/2)} \mathbf{E} \right]. \quad (\text{A.77})$$

Therefore, eq.(A.74) yields

$$\mathbf{d}_s = (\mathbf{1} + \sqrt{\mathbf{Q}})^{-1} \mathbf{d} = \frac{1}{2} \left[\mathbf{1} - \frac{\sin(\phi/2)}{1 + \cos(\phi/2)} \mathbf{E} \right] \mathbf{d},$$

i.e.,

$$\mathbf{d}_s = \frac{1}{2} \left[\mathbf{d} - \frac{\sin(\phi/2)}{1 + \cos(\phi/2)} \mathbf{e} \times \mathbf{d} \right]. \quad (\text{A.78})$$

Thus, \mathbf{D}_s is the cross-product matrix of the sum of two vectors, and hence, \mathbf{D}_s reduces to the sum of the corresponding cross-product matrices. The cross-product matrix of the first term of the right-hand side of the foregoing equation is apparently proportional to \mathbf{D} , that of the second term being proportional to the cross-product matrix of $\mathbf{e} \times \mathbf{d}$. The latter can be readily obtained by application of Lemma A.3.2, which leads to

$$\mathbf{D}_s = \frac{1}{2} \left[\mathbf{D} - \frac{\sin(\phi/2)}{1 + \cos(\phi/2)} (\mathbf{d}\mathbf{e}^T - \mathbf{e}\mathbf{d}^T) \right]. \quad (\text{A.79})$$

Hence,

$$\sqrt{\hat{\mathbf{Q}}} = \mathbf{1} + \epsilon \frac{1}{2} \left[\mathbf{D} - \frac{\sin(\phi/2)}{1 + \cos(\phi/2)} (\mathbf{d}\mathbf{e}^T - \mathbf{e}\mathbf{d}^T) \right] \sqrt{\mathbf{Q}}. \quad (\text{A.80})$$

Now, the linear invariants of $\sqrt{\hat{\mathbf{Q}}}$ are

$$\text{vect}(\sqrt{\hat{\mathbf{Q}}}) = \text{vect}(\sqrt{\mathbf{Q}}) + \epsilon \text{vect}(\mathbf{D}_s \sqrt{\mathbf{Q}}) \quad (\text{A.81a})$$

and

$$\text{tr}(\sqrt{\hat{\mathbf{Q}}}) = \text{tr}(\sqrt{\mathbf{Q}}) + \epsilon \text{tr}(\mathbf{D}_s \sqrt{\mathbf{Q}}). \quad (\text{A.81b})$$

An expression for $\text{vect}(\sqrt{\mathbf{Q}})$, appearing in the first term of $\text{vect}(\sqrt{\hat{\mathbf{Q}}})$, can be obtained from eq.(A.67), namely,

$$\text{vect}(\sqrt{\mathbf{Q}}) = \sin\left(\frac{\phi}{2}\right) \text{vect}(\mathbf{E}) = \sin\left(\frac{\phi}{2}\right) \mathbf{e}, \quad (\text{A.82})$$

while an expression for the second term of the right-hand side of eq.(A.81b) is obtained by application of Theorem A.3.2:

$$\text{vect}(\mathbf{D}_s \sqrt{\mathbf{Q}}) = \frac{1}{2} [\text{tr}(\sqrt{\mathbf{Q}}) \mathbf{1} - \sqrt{\mathbf{Q}}] \mathbf{d}_s,$$

which can be further expanded without intermediate lengthy derivations if we realize that the above expression is the counterpart of that appearing in eq.(A.57c); the latter is expanded in eq.(A.57d). Thus, all we need now is mimic eq.(A.57d), if with ϕ and \mathbf{d} substituted by their counterparts $\phi/2$ and \mathbf{d}_s , respectively, i.e.,

$$\begin{aligned} \text{vect}(\mathbf{D}_s \sqrt{\mathbf{Q}}) = \frac{1}{2} \left\{ \left[1 + \cos\left(\frac{\phi}{2}\right) \right] \mathbf{d}_s - \sin\left(\frac{\phi}{2}\right) \mathbf{e} \times \mathbf{d}_s \right. \\ \left. - \left[1 - \cos\left(\frac{\phi}{2}\right) \right] (\mathbf{e} \cdot \mathbf{d}) \mathbf{e} \right\}. \end{aligned} \quad (\text{A.83})$$

If we now simplify the above expression for $\text{vect}(\mathbf{D}_s \sqrt{\mathbf{Q}})$, and substitute the simplified expression into eq.(A.81a), along with eq.(A.82), we obtain the desired expression for $\hat{\mathbf{r}}$. Note that the latter is defined in eq.(A.68), and hence,

$$\hat{\mathbf{r}} = \sin\left(\frac{\phi}{2}\right) \mathbf{e} + \epsilon \left[\cos\left(\frac{\phi}{2}\right) p_s \frac{\phi}{2} \mathbf{e} + \sin\left(\frac{\phi}{2}\right) \mathbf{e}_0 \right], \quad (\text{A.84})$$

where p_s is the pitch associated with the motion represented by $\sqrt{\hat{\mathbf{Q}}}$, namely,

$$p_s \equiv \mathbf{d}_s \cdot \mathbf{e} = \frac{1}{2} \mathbf{d}, \quad (\text{A.85})$$

where we have recalled the expression for \mathbf{d}_s displayed in eq.(A.78). Similar to eq.(A.61), then, the dual vector of the Euler-Rodrigues parameters is given by

$$\hat{\mathbf{r}} = \hat{\mathbf{e}}^* \sin\left(\frac{\hat{\phi}}{2}\right), \quad \hat{\phi} \equiv \phi + \epsilon d_s^*, \quad d_s^* \equiv \mathbf{d}_s \cdot \mathbf{e}. \quad (\text{A.86})$$

The scalar of the Euler-Rodrigues parameters under study, \hat{r}_0 , is now found in terms of the trace of $\sqrt{\hat{\mathbf{Q}}}$, which is displayed in eq.(A.81b). In that equation,

$$\text{tr}(\sqrt{\mathbf{Q}}) = 1 + 2 \cos\left(\frac{\phi}{2}\right),$$

the dual part of the right-hand side of eq.(A.81b) being calculated by application of Theorem A.3.3:

$$\text{tr}(\mathbf{D}_s \sqrt{\mathbf{Q}}) = -2\mathbf{d}_s \cdot \text{vect}(\sqrt{\mathbf{Q}}) = -2\mathbf{d}_s \cdot \mathbf{e} \sin\left(\frac{\phi}{2}\right)$$

or, in terms of the corresponding pitch p_s ,

$$\text{tr}(\mathbf{D}_s \sqrt{\mathbf{Q}}) = -2p_s \sin\left(\frac{\phi}{2}\right).$$

Therefore,

$$\text{tr}(\sqrt{\hat{\mathbf{Q}}}) = 1 + 2 \cos\left(\frac{\phi}{2}\right) - \epsilon 2p_s \sin\left(\frac{\phi}{2}\right),$$

and hence,

$$\hat{r}_0 = \cos\left(\frac{\phi}{2}\right) - \epsilon p_s \sin\left(\frac{\phi}{2}\right), \quad (\text{A.87})$$

which is the counterpart of the second of eqs.(A.55a). The set $(\hat{\mathbf{r}}, \hat{r}_0)$ constitutes the *dual quaternion* of the motion under study (McCarthy, 1990).

A.4 The Dual Angular Velocity

Similar to the angular-velocity matrix $\mathbf{\Omega}$ introduced in eq.(A.46a), the *dual angular velocity matrix* $\hat{\mathbf{\Omega}}$ is defined as

$$\hat{\mathbf{\Omega}} \equiv \dot{\hat{\mathbf{Q}}}\hat{\mathbf{Q}}^T. \quad (\text{A.88})$$

Now we differentiate with respect to time the expression for $\hat{\mathbf{Q}}$ introduced in eq.(A.42), which yields

$$\dot{\hat{\mathbf{Q}}} = (\mathbf{1} + \epsilon \mathbf{D})\dot{\mathbf{Q}} + \epsilon \dot{\mathbf{D}}\mathbf{Q}.$$

Upon substitution of the above expression for $\dot{\hat{\mathbf{Q}}}$ and of the expression for $\hat{\mathbf{Q}}$ of eq.(A.42) into eq.(A.88), we obtain

$$\hat{\mathbf{\Omega}} = \mathbf{\Omega} + \epsilon (\mathbf{D}\mathbf{\Omega} - \mathbf{\Omega}\mathbf{D} + \dot{\mathbf{D}}). \quad (\text{A.89})$$

The *dual angular-velocity vector* $\hat{\omega}$ of the motion under study is then obtained as the axial vector of the foregoing expression, namely,

$$\hat{\omega} = \text{vect}(\hat{\Omega}) = \omega + \epsilon [\text{vect}(\mathbf{D}\Omega - \Omega\mathbf{D}) + \dot{\mathbf{d}}] , \quad (\text{A.90})$$

with $\dot{\mathbf{d}}$ being the time-derivative of vector \mathbf{d} , introduced in eq.(A.33). Thus, in order to determine $\hat{\omega}$, all we need is the axial vector of the difference $\mathbf{D}\Omega - \Omega\mathbf{D}$. An expression for this difference can be obtained in various manners, one of which is outlined below: First, note that this difference is skew-symmetric, and hence,

$$\text{vect}(\mathbf{D}\Omega - \Omega\mathbf{D}) = 2 \text{vect}(\mathbf{D}\Omega) .$$

Further, the vector of $\mathbf{D}\Omega$ is computed by means of Corollary A.3.1, eq.(A.39), upon substituting \mathbf{A} by Ω in that expression. Thus,

$$\text{vect}(\mathbf{D}\Omega) = -\frac{1}{2}\omega \times \mathbf{d} . \quad (\text{A.91})$$

Therefore,

$$\hat{\omega} = \omega + \epsilon (\dot{\mathbf{d}} - \omega \times \mathbf{d}) , \quad (\text{A.92})$$

and, if we recall eq.(A.51), the foregoing expression takes the alternative form

$$\hat{\omega} = \omega + \epsilon \mathbf{v}^0 . \quad (\text{A.93})$$

In consequence, the dual angular velocity is the dual representation of the *twist* \mathbf{t} of \mathcal{B} , defined as the 6-dimensional array

$$\mathbf{t} \equiv \begin{bmatrix} \omega \\ \mathbf{v}^0 \end{bmatrix} . \quad (\text{A.94})$$

We can therefore find the angular velocity vector and the moment of the ISA about the given origin—i.e., the *instant screw parameters* of the motion at hand—if we are given enough information as to allow us to compute $\hat{\omega}$. The information required to determine the screw parameters of the motion under study can be given as the position and velocity vectors of three noncollinear points of a rigid body (Angeles, 1997). However, note that the dual rotation matrix was obtained in Example 1 in terms of the dual unit vectors representing three mutually orthogonal lines. Notice that, by virtue of Lemma A.2.1, the three lines of Example 1 were chosen concurrent and mutually orthogonal.

Now, in order to find the instant-screw parameters of interest, we need the time-derivatives of the dual unit vectors representing three concurrent, mutually orthogonal lines, but all we have at our disposal is the position and velocity vectors of three non-collinear points. Nevertheless, once we know three noncollinear points of a rigid body, say A , B , and C , along with their velocities, it is possible to find the position and velocity vectors of three pairs of points defining a triad of concurrent, mutually orthogonal lines, an issue that falls beyond the scope of this chapter. Rather than discussing the problem at hand in its fullest generality, we limit ourselves to the special case in which the position vector \mathbf{p} of a point P of the rigid body under study can be determined so that the three lines PA , PB , and PC are mutually orthogonal. Further, we let the position vectors of the three given points be \mathbf{a} , \mathbf{b} , and \mathbf{c} . Thus, point P of the body in this case forms a rectangular trihedron with vertex at P and edges PA , PB , and PC . We can thus express \mathbf{p} as a nonlinear function of the three position vectors \mathbf{a} , \mathbf{b} , and \mathbf{c} :

$$\mathbf{p} = \mathbf{p}(\mathbf{a}, \mathbf{b}, \mathbf{c}) . \quad (\text{A.95})$$

Moreover, the velocity of point P , $\dot{\mathbf{p}}$, can be calculated now as a linear combination of the velocities of the three given points, by straightforward differentiation of the foregoing expression, namely,

$$\dot{\mathbf{p}} = \mathbf{P}_a \dot{\mathbf{a}} + \mathbf{P}_b \dot{\mathbf{b}} + \mathbf{P}_c \dot{\mathbf{c}} , \quad (\text{A.96})$$

where \mathbf{P}_a , \mathbf{P}_b , and \mathbf{P}_c denote the partial derivatives of \mathbf{p} with respect to \mathbf{a} , \mathbf{b} , and \mathbf{c} , respectively. Once the position and the velocity vectors of point P are known, it is possible to determine the time-rates of change of the dual unit vectors representing the three lines PA , PB and PC , as described below.

Let $\hat{\mathbf{e}}^*$ denote the dual unit vector representing the line determined by points A and P , its primary and dual parts, \mathbf{e} and \mathbf{e}_0 , being given by

$$\mathbf{e} = \frac{\mathbf{a} - \mathbf{p}}{\|\mathbf{a} - \mathbf{p}\|}, \quad \mathbf{e}_0 = \mathbf{p} \times \frac{\mathbf{a} - \mathbf{p}}{\|\mathbf{a} - \mathbf{p}\|} . \quad (\text{A.97})$$

Straightforward differentiation of the foregoing expressions with respect to time leads to

$$\begin{aligned} \dot{\mathbf{e}} &= \frac{1}{\|\mathbf{a} - \mathbf{p}\|} \left(\dot{\mathbf{a}} - \dot{\mathbf{p}} - \mathbf{e} \frac{d}{dt} \|\mathbf{a} - \mathbf{p}\| \right) , \\ \dot{\mathbf{e}}_0 &= \dot{\mathbf{p}} \times \frac{\mathbf{a} - \mathbf{p}}{\|\mathbf{a} - \mathbf{p}\|} + \mathbf{p} \times \frac{1}{\|\mathbf{a} - \mathbf{p}\|} \left(\dot{\mathbf{a}} - \dot{\mathbf{p}} - \mathbf{e} \frac{d}{dt} \|\mathbf{a} - \mathbf{p}\| \right) . \end{aligned}$$

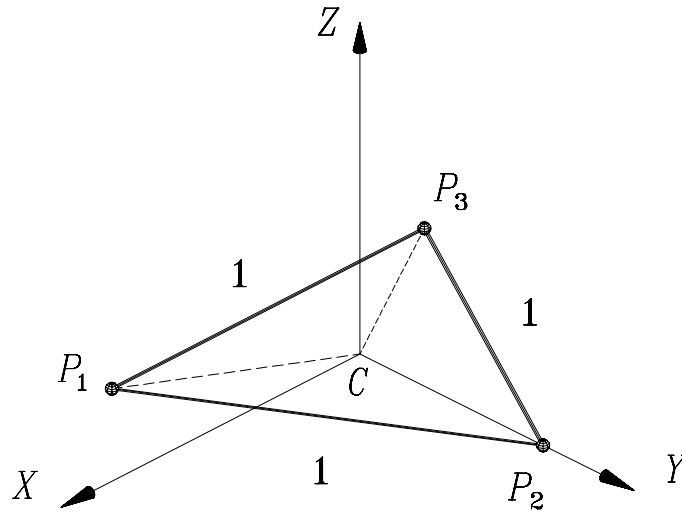


Figure A.7: A rigid triangular plate undergoing a motion given by the velocity of its vertices

Upon simplification, we obtain the desired expression for $\dot{\mathbf{e}}^*$, namely,

$$\dot{\mathbf{e}}^* = \frac{1}{\|\mathbf{a} - \mathbf{p}\|} [\dot{\mathbf{a}} - \dot{\mathbf{p}} + \epsilon(\mathbf{p}\dot{\mathbf{a}} + \dot{\mathbf{p}} \times \mathbf{a})] . \quad (\text{A.98})$$

Therefore, knowing the velocity of two points of a line, we can determine the time-rate of change of the dual unit vector representing the line. The foregoing idea is best illustrated with the aid of the example included below.

Example 2: Determination of the ISA of a rigid-body motion.

For comparison purposes, we take an example from (Angeles, 1997): The three vertices of the equilateral triangular plate of Fig. A.4, which lie in the X - Y plane, $\{P_i\}_1^3$, have the position vectors $\{\mathbf{p}_i\}_1^3$. Moreover, the origin of the coordinate frame X, Y, Z lies at the centroid C of the triangle, and the velocities of the foregoing points, $\{\dot{\mathbf{p}}_i\}_1^3$, are given in this coordinate frame as

$$\dot{\mathbf{p}}_1 = \frac{4 - \sqrt{2}}{4} \begin{bmatrix} 0 \\ 0 \\ 1 \end{bmatrix}, \quad \dot{\mathbf{p}}_2 = \frac{4 - \sqrt{3}}{4} \begin{bmatrix} 0 \\ 0 \\ 1 \end{bmatrix}, \quad \dot{\mathbf{p}}_3 = \frac{4 + \sqrt{2}}{4} \begin{bmatrix} 0 \\ 0 \\ 1 \end{bmatrix} .$$

With the above information, compute the instant-screw parameters of the motion under study.

Solution: Since the centroid C of the triangle coincides with that of the three given points, we have $\mathbf{c} = \mathbf{0}$, where \mathbf{c} is the position vector of C . Moreover,

$$\mathbf{p}_1 = \begin{bmatrix} 1/2 \\ -\sqrt{3}/6 \\ 0 \end{bmatrix}, \quad \mathbf{p}_2 = \begin{bmatrix} 0 \\ \sqrt{3}/3 \\ 0 \end{bmatrix}, \quad \mathbf{p}_3 = \begin{bmatrix} -1/2 \\ -\sqrt{3}/6 \\ 0 \end{bmatrix}.$$

First and foremost, we have to verify the compatibility of the data. To do this, we calculate the component of the relative velocities of two given points onto the line that they define. It can be readily shown that the data are compatible, and hence, the motion is possible. Next, we obtain the position vector of the point P that, along with $\{P_i\}_1^3$, forms an orthogonal trihedron. It is not difficult to realize that the position vector of point P can be expressed as²

$$\mathbf{p} = \mathbf{c} + \frac{\sqrt{2}}{3}(\mathbf{p}_2 - \mathbf{p}_1) \times (\mathbf{p}_3 - \mathbf{p}_1),$$

and hence,

$$\dot{\mathbf{p}} = \dot{\mathbf{c}} + \frac{\sqrt{2}}{3}[(\mathbf{p}_3 - \mathbf{p}_2) \times \dot{\mathbf{p}}_1 + (\mathbf{p}_1 - \mathbf{p}_3) \times \dot{\mathbf{p}}_2 + (\mathbf{p}_2 - \mathbf{p}_1) \times \dot{\mathbf{p}}_3],$$

with the numerical values of \mathbf{p} and $\dot{\mathbf{p}}$ given below:

$$\mathbf{p} = \frac{\sqrt{6}}{6} \begin{bmatrix} 0 \\ 0 \\ 1 \end{bmatrix}, \quad \dot{\mathbf{p}} = \frac{1}{12} \begin{bmatrix} 2\sqrt{3} \\ \sqrt{6} \\ 12 - \sqrt{3} \end{bmatrix}.$$

Now, let $\hat{\mathbf{e}}_i^*$ denote the dual unit vector representing the line that passes through P and P_i , i.e.,

$$\hat{\mathbf{e}}_i^* = \frac{1}{\|\mathbf{p}_i - \mathbf{p}\|}[\mathbf{p}_i - \mathbf{p} + \epsilon \mathbf{p} \times \mathbf{p}_i],$$

where

$$\|\mathbf{p}_i - \mathbf{p}\| = \frac{\sqrt{2}}{2}, \quad i = 1, 2, 3.$$

Next, the three foregoing dual unit vectors are stored columnwise in the dual rotation matrix $\hat{\mathbf{Q}}$, i.e.,

$$\hat{\mathbf{Q}} = [\hat{\mathbf{e}}_1^* \quad \hat{\mathbf{e}}_2^* \quad \hat{\mathbf{e}}_3^*].$$

Upon substitution of the numerical values of these vectors into the above expression, we obtain

$$\hat{\mathbf{Q}} = \frac{\sqrt{12}}{12} \begin{bmatrix} 6 + \epsilon 2 & -\epsilon 2\sqrt{2} & -6 + \epsilon \sqrt{2} \\ -2\sqrt{3} + \epsilon \sqrt{6} & 4\sqrt{3} & -2\sqrt{3} - \epsilon \sqrt{6} \\ -2\sqrt{6} & -2\sqrt{6} & -2\sqrt{6} \end{bmatrix}.$$

²Although $\mathbf{c} = \mathbf{0}$ in this case, $\dot{\mathbf{c}} \neq \mathbf{0}$, and hence, \mathbf{c} must be written explicitly in the expression for \mathbf{p} .

Likewise, the time derivative of $\hat{\mathbf{Q}}$ is computed as

$$\dot{\hat{\mathbf{Q}}} = \frac{\sqrt{2}}{24} \left(\begin{bmatrix} -4\sqrt{3} & -4\sqrt{3} & -4\sqrt{3} \\ -2\sqrt{6} & -2\sqrt{6} & -2\sqrt{6} \\ -6\sqrt{2} + 2\sqrt{3} & -4\sqrt{3} & 6\sqrt{2} + 2\sqrt{3} \end{bmatrix} + \epsilon \begin{bmatrix} -1 + 4\sqrt{3} & 2 - 8\sqrt{3} & -1 + 4\sqrt{3} \\ 12 - \sqrt{3} & 0 & -12 + \sqrt{3} \\ -(2 + \sqrt{6}) & 4 & -2 + \sqrt{6} \end{bmatrix} \right).$$

Therefore,

$$\hat{\mathbf{\Omega}} = \dot{\hat{\mathbf{Q}}}\hat{\mathbf{Q}}^T = \frac{1}{12} \begin{bmatrix} 0 & -\epsilon(12 - \sqrt{3}) & 6\sqrt{2} \\ +\epsilon(12 - \sqrt{3}) & 0 & 6 \\ -6\sqrt{2} & -6 & 0 \end{bmatrix},$$

which, as expected, is a dual skew-symmetric matrix. Hence,

$$\hat{\boldsymbol{\omega}} = \text{vect}(\hat{\mathbf{\Omega}}) = \frac{1}{2} \begin{bmatrix} -1 \\ \sqrt{2} \\ 0 \end{bmatrix} + \epsilon \frac{12 - \sqrt{3}}{12} \begin{bmatrix} 0 \\ 0 \\ 1 \end{bmatrix},$$

from which we can readily identify

$$\boldsymbol{\omega} = \frac{1}{2} \begin{bmatrix} -1 \\ \sqrt{2} \\ 0 \end{bmatrix}, \quad \mathbf{v}^0 = \frac{12 - \sqrt{3}}{12} \begin{bmatrix} 0 \\ 0 \\ 1 \end{bmatrix}.$$

Furthermore, the position vector $\boldsymbol{\pi}^*$ of the point P^* of the ISA lying closest to the origin can be obtained from \mathbf{v}^0 . Indeed, let \mathbf{v}^* be the velocity of P^* , which thus allows us to write

$$\mathbf{v}^0 = \mathbf{v}^* + \boldsymbol{\omega} \times (-\mathbf{p}^*) = \mathbf{v}^* + \mathbf{p}^* \times \boldsymbol{\omega}.$$

Upon cross-multiplying the two sides of the foregoing expression by $\boldsymbol{\omega}$, we obtain

$$\mathbf{v}^0 \times \boldsymbol{\omega} = \mathbf{v}^* \times \boldsymbol{\omega} + (\mathbf{p}^* \times \boldsymbol{\omega}) \times \boldsymbol{\omega},$$

whose first term of the right-hand side vanishes because \mathbf{v}^* and $\boldsymbol{\omega}$ are parallel. Therefore,

$$\mathbf{v}^0 \times \boldsymbol{\omega} = (\mathbf{p}^* \times \boldsymbol{\omega}) \times \boldsymbol{\omega} = (\mathbf{p}^* \cdot \boldsymbol{\omega})\boldsymbol{\omega} - \|\boldsymbol{\omega}\|^2 \mathbf{p}^*.$$

The first term of the rightmost-hand side of the foregoing equation vanishes because \mathbf{p}^* being the position vector of the point of the ISA that lies closest to the origin, and the ISA being parallel to $\boldsymbol{\omega}$, these two vectors are orthogonal. We can thus solve for \mathbf{p}^* from the above expression, which yields

$$\mathbf{p}^* = -\frac{\mathbf{v}^0 \times \boldsymbol{\omega}}{\|\boldsymbol{\omega}\|^2}.$$

The quantities involved in the foregoing expression are now evaluated:

$$-\mathbf{v}^0 \times \boldsymbol{\omega} = \boldsymbol{\omega} \times \mathbf{v}^0 = \frac{12 - \sqrt{3}}{24} \begin{bmatrix} \sqrt{2} \\ 1 \\ 0 \end{bmatrix}, \quad \|\boldsymbol{\omega}\|^2 = \frac{3}{4}.$$

Finally, $\mathbf{p}^* = \{[(12 - \sqrt{3})/18]\sqrt{2} \ 1 \ 0\}^T$, which coincides with the results reported in (Angeles, 1997), obtained by another method.

A.5 Conclusions

We revisited dual algebra in the context of kinematic analysis, which led us to a straightforward introduction of dual quaternions. In the process, we showed that the parameters of both the finite screw and the instant screw of a rigid-body motion can be computed from the sum of the diagonal and the difference of the off-diagonal entries of the dual rotation and, correspondingly, the dual angular-velocity matrices.

Bibliography

AGRAWAL, O.P., 1987, "Hamilton operators and dual-number-quaternions in spatial kinematics," *Mechanism and Machine Theory*, Vol. 22, No. 6, pp. 569–575.

ALTUZARRA, O., SALGADO, O., HERNANDEZ, A. and ANGELES, J., 2009, "Multiobjective optimum design of a symmetric parallel Schönflies-motion generator," *ASME Journal of Mechanical Design*, Vol. 131, No. 3, pp. 031002-1–031002-11.

ANGELES, J., 1982, *Spatial Kinematic Chains. Analysis, Synthesis, Optimization*, Springer-Verlag, Berlin-Heidelberg-New York.

ANGELES, J., 2007, *Fundamentals of Robotic Mechanical Systems. Theory, Methods, and Algorithms*, 3rd ed., Springer, New York.

ANGELES, J. and GOSSELIN, C., 1988, "Détermination du degré de liberté des chaînes cinématiques," *Transactions of the Canadian Society of Mechanical Engineering*, Vol. 12, No. 4, pp. 219–226.

ARAI, T., HERVÉ, J.M. and TANIKAWA, T., 1996, "Development of 3 dof micro finger," *Proc. IROS'96*, Osaka, pp. 981–987.

BAI, S.P. and ANGELES, J., 2008, "A unified input-output analysis of four-bar linkages". *Mechanism and Machine Theory*, Vol. 43, pp. 240–251.

BAI, S., HANSEN, M.R. and ANGELES, J., 2009, "A robust forward-displacement analysis of spherical parallel robots," to appear in *Mechanism and Machine Theory*.

BECK, T., 1859, *Beiträge zur Geschichte des Maschinenbaues*, J. Springer, Berlin.

BJÖRCK, A.A. and DAHLQUIST, G., 1974, *Numerical Methods*, Prentice-Hall, Inc., Upper Saddle River, NJ.

- BOGOLYUBOV, A. N., 1976, *Teoriya mekhanizmov v istoricheskom razvitii (Theory of Mechanisms and its Historical Development)*, Nauka, Moscow (in Russian).
- BORGNIS, G.A., 1818, *Traité Complet de Mécanique Appliquée aux Arts. Traité des Compositions des Machines*, Paris.
- BOTTEMA, O. and ROTH, B., 1978. *Theoretical Kinematics*, North-Holland Publishers Co., North-Holland Publishing Company, Amsterdam.
- BRICARD, R., 1927, *Leçons de Cinématique..* Vols. I & II, Gauthier-Villars et Cie. Publishers, Paris.
- Chen, C. and Angeles, J., 2008, “A novel family of linkages for advanced motion synthesis,” *Mechanism and Machine Theory*, Vol. 43, pp. 882-890.
- CHEN, C., BAI, S.P. and ANGELES, J., 2008, “A comprehensive solution of the classic Burmester problem,” *CSME Transactions*, Vol. 32, No. 2, pp. 137–154.
- CHASLES, M., 1830, “Notes sur les propriétés générales de deux corps semblables entr’eux et placés d’une manière quelconque dans l’espace, et sur le déplacement fini ou infiniment petit d’un corps solide libre,” *Bull. Sci. Math. Ferrusaa*, Vol. 14, pp. 321–32.
- CHENG, H. H. and S. THOMPSON, 1996, “Dual polynomials and complex dual numbers for analysis of spatial mechanisms,” *Proc. ASME Design Engineering Technical Conference and Computers in Engineering Conference*, Irvine, California.
- CHEVALLIER, D.P., 1991, “Lie algebras, modules, dual quaternions and algebraic methods in kinematics,” *Mechanism and Machine Theory*, Vol. 26, No. 6, pp. 613–627.
- CHIANG, C.H., 1988, *Kinematics of Spherical Mechanisms*. Cambridge University Press, Cambridge.
- CLAVEL, R., 1988, “Delta, a fast robot with parallel geometry,” *Proc. 18th Int. Symp. Industrial Robots*, Lausanne, pp. 91–100.

- CLAVEL, R., 1990, *Device for the Movement and Positioning of an Element in Space*, U.S. Patent No. 4,976,582.
- CLIFFORD, W. K., 1873, "Preliminary sketch of bi-quaternions," *London Math. Soc.*, Vol. 4, pp. 381–395.
- COMPANY, O., F. PIERROT, T. SHIBUKAWA, and K. MORITA, March 21, 2001, *Four-degree-of-freedom Parallel Robot*, European Patent No. EP1084802.
- DE LACLOS, C., 1782, *Les liaisons dangereuses ou lettres recueillies dans une société, et publiées pour l'instruction de quelques autres*, Durand Publishers, Paris (the first edition seems to have been published in Amsterdam), 1907 edition by Maurice Bauche Publishers, Paris.
- DENAVID, J. and HARTENBERG, R., 1964. *Kinematic Synthesis of Linkages*, McGraw-Hill Book Company, New York.
- DIETMAIER, P., 1992, "Inverse kinematics of manipulators with 3 revolute and 3 parallelogram joints," *Proc. ASME 22nd Biennial Mechanisms Conference*. Sept. 13–16, Scottsdale, Vol. 45, pp. 35–40.
- DIMENTBERG, F.M., 1965, *The Screw Calculus and Its Applications in Mechanics*, Izdat. Nauka, Moscow.
- DUDIȚĂ, F. and D. DIACONESCU, 1987, *Optimizarea Structurală a Mecanismelor (Optimization of Mechanisms)*, Tehnică Publishers, Bucharest.
- DUDIȚĂ, F. D., *Mecanisme Articulate, Inventica și Cinematica în Abordare Filogenetică*, Tehnică Publishers, Bucharest.
- ERDMAN, A.G. and SANDOR, S.K., 2001, *Mechanism Design Analysis and Synthesis*, Vol. 2, Prentice Hall, Upper Saddle River, N.J.
- EULER, L., 1753, "De machinis in genere," *Novii Comentarum Academiae Scientiarum Petropolitanæ*, III.

- EULER, L., 1775, “Nova methodus motum corporum rigidorum determinandi,” *Novii Comentarum Academiæ Scientiarum Petropolitanæ*, pp. 208–238= *Opera Omnia* (2) 9, Vol. 2, No. 9, pp. 99–125.
- FORSYTHE, G.E., 1970, “Pitfalls in computation, or why a math book isn’t enough” *American Mathematical Monthly*, Vol. 27, pp. 931–956.
- FRENCH, M.E. ,1992, *Form, Structure and Mechanism*, Macmillan, London.
- FREUDENSTEIN, F., 1955, “Approximate synthesis of four-bar linkages” *Trans. ASME*, Vol. 77, pp. 853–861.
- FROLOV, K. V., 1987, *Teoriya Mechanismov i Mashin*, Vyschaya Shkola, Moscow.
- GLEICK, J., 1988, *Chaos. Making a New Science*, Penguin Books, New York.
- GOLUB, G.H. and C.F. VAN LOAN, 1983. *Matrix Computations*, The Johns Hopkins University Press, Baltimore.
- HACHETTE, 1811, *Traité Élémentaire des Machines*, Paris.
- HALMOS, P., 1974, *Finite-Dimensional Vector Spaces*, Springer-Verlag, New York.
- HAMILTON, W.R., 1844, “On quaternions: or a new system of imaginaries in algebra,” *Phil. Mag.*.
- HERVÉ, J, 1978, “Analyse structurelle des mécanismes par groupes de déplacements,” *Mechanism and Machine Theory*, Vol. 13, pp. 437–450.
- HERVÉ, J, 1999, “The Lie group of rigid body displacements, a fundamental tool for mechanism design,” *Mechanism and Machine Theory*, Vol. 34, pp. 719–730.
- HERVÉ, J. and F. SPARACINO, 1992, “Star, a new concept in robotics,” *Proc. 3rd Int. Workshop on Advances in Robot Kinematics*, pp. 176–183, Ferrara.
- IFTOMM PC FOR STANDARDIZATION OF TERMINOLOGY, 2003, *Mechanism and Machine Theory*, Vol. 38, Nos. 7–10.

- KIMBRELL, J.T., 1991, *Kinematic Analysis and Synthesis*, McGraw-Hill, Inc., New York.
- KLEIN, B., 1981, "Zum Einsatz nichtlinearer Optimierungsverfahren zur rechnerunterstützten Konstruktion ebener Koppelgetriebe," *Mechanism and Machine Theory*, Vol. 16, No. 5, pp. 567–576.
- KOENIGS, F., 1901, "Etude critique sur la théorie générale des mécanismes," *Comptes Rendus de l'Académie des Sciences*, Vol. 133.
- KOTEL'NIKOV, A. P., 1895, *Screw calculus and some of its applications to geometry and mechanics*.
- LEUPOLD, J., 1724, *Theatrum Machinarium Generale*, Leipzig.
- MA, O. and ANGELES, J., 1992, "Architecture Singularities of Parallel Manipulators," *Journal of Robotics and Automation*, Vol. 7, No. 1, pp. 23–29.
- MALIK, A.K., GHOSH, A. and DITTRICH, G., 1994, *Kinematic Analysis and Synthesis of Mechanisms*, CRC Press, Boca Raton.
- MANDELBROT, B.B., 1983, *The Fractal Geometry of Nature*, W.H. Freeman and Company, 3rd ed., New York.
- MCAREE, P.R. and DANIEL, R.W., 1996, "A Fast, Robust Solution to the Stewart Platform Kinematics," *Journal of Robotic Systems*, Vol. 13, No. 7, pp. 407–427.
- MCCARTHY, J.M., 1990, *An Introduction to Theoretical Kinematics*, The MIT Press, Cambridge (MA).
- MCCARTHY, J.M., 2000, *Geometric Design of Linkages*, Springer, New York.
- MODLER, K., 1972, "Beitrag zur Theorie der Burmesterschen Mittelpunktcurve," *Maschinenbautechnik*, Vol. 21, No. 5, pp. 98–102.
- MORGAN, A. and WAMPLER, C.W., 1990, "Solving a planar four-bar design problem using continuation," *ASME Journal of Mechanical Design*, Vol. 112, pp. 544–550.

- MOZZI, G., 1763, *Discorso Matematico Sopra il Rotamento Momentaneo dei Corpi*, Stamperia di Donato Campo, Naples.
- PONCELET, J.V., 1824. *Traité de Mécanique Appliquée aux Machines*, Liège.
- PARENTI-CASTELLI, V. and DI GREGORIO, R. , 1995, “A Three-Equation Numerical Method for the Direct Kinematics of the Generalized Gough-Stewart Platform,” *Proc. Ninth World Congress on the Theory of Machines and Mechanisms*, Aug. 29–Sept. 2, Milan, Vol. 2, pp. 837–841.
- PRADEEP, A.K., YODER, P.J. and MUKUNDAN, R., 1989, “On the use of dual matrix exponentials in robot kinematics,” *The Int. J. Robotics Res.*, Vol. 8, No. 5, pp. 57–66.
- REULEAUX, F., 1875, *Theoretische Kinematik*, Braunschweig.
- REULEAUX, F, 1900, *Lehrbuch der Kinematik*, Braunschweig.
- RICO MARTÍNEZ, J.M. and DUFFY, J., 1994, “The principle of transference: History, statement and proof,” *Mechanism and Machine Theory*, Vol. 28, No. 1, pp. 165–177.
- ROBERT, P., 1994, *Le Petit Robert 1. Dictionnaire alphabétique et analogique de la langue française*, Paris.
- SALMON, G., 1964, *Higher Algebra*, Chelsea Publishing Co., New York.
- SANDOR, G.N. and ERDMAN, A.G., 1984, *Advanced Mechanism Design: Analysis and Synthesis*, Vol. 2, Prentice-Hall, Inc., Englewood Cliffs.
- SHOHAM, M. and BRODSKY, V., 1993, “Analysis of mechanisms by the dual inertia operator,” in Angeles, J., Hommel, G. and Kovács, P. (eds.), *Computational Kinematics*, Kluwer Academic Publishers, Dordrecht, pp. 129–138.
- SHOHAM, M. and BRODSKY, V., 1994, “The dual inertia operator and its application to robot dynamics,” *ASME J. Mechanical Design*, Vol. 116, pp. 1089–1095.

- SIMMONS, G.F., 1963, *Introduction to Topology and Modern Analysis*, McGraw-Hill Book Co., New York.
- STEIN, J., 1979, *Random House College Dictionary*, Random House, New York.
- STERNBERG, S., 1994, *Group Theory and Physics*, Cambridge University Press, Cambridge.
- STRANG, G., 1988, *Linear Algebra*, 3rd ed., Harcourt Brace Jovanovich College Publishers, Fort Worth.
- STUDY, E., 1903, *Geometrie der Dynamen*, Leipzig.
- TENG, C.P. and ANGELES, J., 2001, "A sequential-quadratic-programming algorithm using orthogonal decomposition with Gerschgorin stabilization", *ASME J. of Mechanical Design*, Vol. 123, pp. 501–509.
- The Concise Oxford Dictionary of Current English*, 1995, Clarendon Press, Oxford.
- TINUBU, S.O. and GUPTA, K.C., 1984, "Optimal synthesis of function generators without the branch defect," *ASME, J. Mech., Trs., and Auto. in Design*, Vol. 106, pp. 348–354.
- USPENSKY, J., 1948, *Theory of Equations*, McGraw-Hill Book Company, Inc., New York.
- VITRUVIUS, P.M., 28 BCE *De Architectura*, Vol. X.
- WALDRON, K.J. and KINZEL, G.L., 1999, *Kinematics, Dynamics, and Design of Machinery*, John Wiley & Sons, Inc., New York.
- Webster's Collegiate Dictionary, 2003, (on-line).
- WOHLHART, K., 1991, "Der homogene Paralleltrieb-Mechanismus," *Mathematica Pannonica*, Vol. 2, No. 2, pp. 59–76.
- WOHLHART, K., 1992, "Displacement analysis of the general spatial parallelogram manipulator," *Proc. 3rd International Workshop on Advances in Robot Kinematics*, Ferrara, Italy, pp. 104–111.

WRIGHT, D., DESAI S., and HENDERSON, W., 1964, "Action of the subtalar and ankle-joint complex during the stance phase of walking," *The J. Bone and Joint Surgery*, Vol. 46-A, No. 2, pp. 361–382.

YANG, A.T., 1963. *Application of Quaternion Algebra and Dual Numbers to the Analysis of Spatial Mechanisms*, Doctoral Dissertation, Columbia University, New York, No. 64-2803 (University Microfilm, Ann Arbor, Michigan).

YANG, A.T. and FREUDENSTEIN, F., 1964, "Application of dual-number quaternion algebra to the analysis of spatial mechanisms," *J. of Applied Mechanics*, Vol. 31, pp. 300–308.

Index

- II-joint, 44
- algebraic equation
 - degree, 12
- approximate synthesis
 - for function generation, 103
- assemblability, 60
- augmented synthesis equations, 110
- bimodal linkage, 87
- bivariate equations, 12
- branch switching, 122
- chain
 - exceptional, 55
- Chebyshev-Grübler-Kutzbach-Hervé Formula, 53
- chirality, 40
- circularity, 130
- contour-intersection, 74
- cubic of stationary curvature, 128
- damping, 31
- damping factor, 31
- Denavit-Hartenberg
 - frames, 69
 - notation, 69
- Denavit-Hartenberg parameters, 7
- design
 - functions, 5
 - specifications, 6
 - variants, 6
- design vs. structural error, 118
- determined system, 27
- dimensioning, 7
- displacement
 - groups, 39
- dwelling, 127
- eliminant, 12
- engineering design, 5
 - process, 5
- error vector, 20
- exceptional chains, 53
- floating-point operation, 22
- flop, *see* floating-point operation
- four-bar linkage
 - planar, 66
 - spatial, 75
 - spherical, 70
- fractal, 30
- Freudenstein equation
 - for planar linkages, 68
- Freudenstein parameters
 - for the spherical linkage, 72

function generation
 exact synthesis, 78
 exact synthesis for planar four-bar link-
 ages, 78
 exact synthesis for spherical four-bar link-
 ages, 82
 generalized Chebyshev-Grübler-Kutzbach for-
 mula, 54
 generalized CGK formula, 54
 groups of displacements, 53

 Index, 181
 inflection circle, 128
 input-output equation
 for spherical linkages, 73
 input-output functions, 66

 Jacobian matrix, 29

 kinematic bond, 50
 kinematic chain
 architecture, 69
 kinematic chains
 multiloop, 39
 kinematic synthesis, 7
 kinetostatics, 13

 least-square error, 21, 31
 normality condition, 20
 least-square solution, 31
 left Moore-Penrose generalized inverse, 21
 LKP, 39
 lower kinematic pairs, 39

 machine, 5
 function, 5
 mechanical system, 5
 model
 parametric, 6
 monovariate polynomial equation, 12
 motion
 representation, 39
 multiobjective optimization, 6
 multivariable polynomial equations, 12

 nonlinear system, 27
 normality condition, 32

 overdetermined system, 30

 paradoxical chains, 53, 59
 path generation, 127
 with timing, 130
 performance evaluation, 113
 planar four-bar linkage
 coupler curve, 134
 feasibility condition, 80
 Planar Linkages
 transmission angle, quality, 113
 planar linkages
 Bloch synthesis, 80
 planar path-generation, 128
 projection
 theorem, 22

 QR decomposition, 104
 qualitative synthesis, 59

- resolvent, 12
- rigid body, 40
- Roberts-Chebyshev Theorem, 138
- Sarrus mechanism, 55
- semigraphical method, 74
- signum function, 26
- spatial linkages
 - mobility analysis, 101
 - synthesis for function generation, 100
- stationary point, 32
- structure, 5
 - function, 5
- Sylvester's Theorem, 22
- synthesis
 - approximate, 11
 - equations, 12
 - exact, 11
 - qualitative, 7, 39
 - semigraphical methods, 12
- synthesized linkage
 - analysis, 85
 - mobility analysis, 96
- synthesized planar linkage
 - analysis, 85
 - mobility analysis, 91
- synthesized spatial linkage
 - analysis, 96
 - analysis with d_1 as input, 99
- synthesized spherical linkage
 - analysis, 95
- trivial chains, 53
- trivial-chains, 53
- weighting matrix, 31